# ANTI-ANGIOGENIC THERAPY IN NON-SMALL CELL LUNG CANCER: CHARACTERIZING A NEW THERAPY AND INVESTIGATING POTENTIAL MECHANISMS OF RESISTANCE

APPROVED BY SUPERIVISORY COMMITTEE

Rolf A. Brekken, Ph.D. (Mentor)

Robert Bachoo, M.D.,Ph.D. (Chair)

John D. Minna, M.D

Philip Thorpe, Ph.D.

DEDICATION

For Denise, Richard, Sarah, Emily, Adam and James.

# ANTI-ANGIOGENIC THERAPY IN NON-SMALL CELL LUNG CANCER: CHARACTERIZING A NEW THERAPY AND INVESTIGATING POTENTIAL MECHANISMS OF RESISTANCE

by

LAURA ANNE SULLIVAN

DISSERTATION

Presented to the Faculty of the Graduate School of Biomedical Sciences

The University of Texas Southwestern Medical Center at Dallas

In Partial Fulfillment of the Requirements

For the Degree of

DOCTOR OF PHILOSOPHY

The University of Texas Southwestern Medical Center at Dallas

Dallas, Texas

August, 2011

# ACKNOWLEDGEMENTS

The following work described in this dissertation could not have been accomplished without the help of a community of people. I would first like to express my sincerest gratitude and appreciation to my boss and mentor, Dr. Rolf Brekken for his guidance and support and for providing a great scientific home for me the past four years. Thank you for helping me hone my critical thinking and scientific skills and sharing your enthusiasm for science and learning that will serve me well in the future. This work could not have been possible were it not for the support and help I also received from members of the Brekken laboratory. In particular, I would like to acknowledge Juliet Carbon Rivera and Drs. Sean Dineen, Christina Roland, Marie Burdine and Kristi Lynn for their advice, collaborations and great company.

I would also like to thank my committee members Drs. John Minna, Philip Thorpe and Robert Bachoo for their guidance and critical advice throughout my graduate tenure. I have been extremely fortunate to have the collaborative support of Dr. John Minna's laboratory and Dr. Joan Schiller that has fueled the progression of this project. I thank you both for the critical insight, suggestions and funding support that made this work possible. I would also like to thank the CPRIT Training Grant Cancer Intervention and Prevention Discoveries program that has funded my final year as a graduate student.

Finally, I would like to express my gratitude and appreciation for my friends and family for their constant love and encouragement. I would especially like to thank my amazing parents Richard and Denise, my in-laws Tim and Brenda and my best friend and partner James.

ANTI-ANGIOGENIC THERAPY IN NON-SMALL CELL LUNG CANCER: CHARACTERIZING A NEW THERAPY AND INVESTIGATING POTENTIAL MECHANISMS OF RESISTANCE

Publication No. _____

Laura Anne Sullivan, Ph.D.

The University of Texas Southwestern Medical Center at Dallas, 2011

Supervising Professor: Rolf A. Brekken, Ph.D.

**Abstract**

Angiogenesis is the development of blood vessels from a pre-existing vascular network. This process is essential during growth, development and wound healing and plays a critical role in the growth and progression of cancer. Initial tumor size is restricted by the diffusion capacity of oxygen and nutrients

from surrounding blood vessels. Therefore, to progress beyond a volume of several millimeters, a tumor must stimulate angiogenesis to generate a vascular network that will supply the tumor with the necessary blood, oxygen and nutrients that will allow for continued growth, invasion and metastasis.

Over forty years ago, Judah Folkman hypothesized that targeting tumor angiogenesis would be beneficial for cancer patients. One of the first targets for this new class of drugs was vascular endothelial growth factor (VEGF) a predominant mediator of physiological and pathological angiogenesis. Bevacizumab (Avastin®, Genentech/Roche), a humanized monoclonal antibody that recognizes human VEGF and blocks VEGF from binding to VEGF receptor (VEGFR) 1 and 2, was the first anti-angiogenic drug approved by the United States Food and Drug Administration for the treatment of cancer and remains the gold standard for this class of therapeutics. The Brekken laboratory, in collaborations with Peregrine Pharmaceuticals and Affitech A/S has generated a fully human monoclonal antibody, r84 that recognizes mouse and human VEGF and blocks VEGF binding only to VEGFR2. The data presented in the first half of this dissertation demonstrate the specificity of r84 for VEGF *in vitro* and *in vivo*, the efficacy of r84 to control tumor growth and the superior safety profile of r84 as compared to bevacizumab.

Although anti-angiogenic therapy was highly anticipated to have great success in patients, overall results have been somewhat disappointing with modest

improvements in patient progression free survival and few improvements to overall survival. In addition, with the expanding use of anti-angiogenic drugs such as bevacizumab and a host of receptor tyrosine kinase inhibitors in the clinic, it is becoming increasingly apparent that not all tumors respond or maintain sensitivity to treatment. Therefore, it is increasingly important to identify mechanisms of resistance to anti-angiogenic therapy so that new drug targets can be identified and/or patients can be appropriately screened for markers that can predict for resistance or sensitivity to anti-angiogenic therapy de novo. Non-small cell lung cancer (NSCLC), the most common form of lung cancer, claims the most new diagnoses and cancer-related deaths than any other cancer worldwide and the therapeutic options currently available for this disease, including bevacizumab have done little to change this statistic. The latter half of this thesis focuses on the *in vivo* screening of human NSCLC cell lines to identify mechanisms of resistance to the anti-angiogenic monoclonal antibodies bevacizumab and r84 in non-small cell lung cancer.

TABLE OF CONTENTS

PRIOR PUBLICATIONS

1. Sullivan J.P., Spinola M., Dodge M., Raso M.G., Behrens C., Gao B., Schuster K., Shao C., Larsen J.E., **Sullivan L.A.**, Honorio S., Xie Y., Scaglioni P.P., DiMaio J.M., Gazdar A.F., Shay J.W., Wistuba I.I., Minna J.D. Aldehyde dehydrogenase activity selects for lung adenocarcinoma stem cells dependent on notch signaling, Cancer Res, 70(23): 9937-48, 2010.
2. **Sullivan L.A.,** Carbon J.G., Roland C.L., Toombs J.E., Nyquist-Andersen M., Kavlie A., Schlunegger K., Richardson J.A., Brekken R.A. r84, a novel therapeutic antibody against mouse and human VEGF with potent anti-tumor activity and limited toxicity induction. PLoS One, 5(8): e12031, 2010.
3. Korpanty G., **Sullivan L.A.,** Smyth E., Carney D.N., Brekken R.A. Molecular and clinical aspects of targeting the VEGF pathway in tumors. J Oncol, 2010:652320, 2010.
4. Korpanty G., Smyth E., **Sullivan L.A.,** Brekken R.A., Carney D.N. Antiangiogenic therapy in lung cancer: focus on vascular endothelial growth factor pathway. Exp Biol Med, 235(1): 3-9, 2010.
5. **Sullivan L.A.,** Brekken R.A. The VEGF family in cancer and antibody-based strategies for their inhibition. MAbs, 2(2): 165-175, 2010.
6. Roland C.L., Dineen S.P., Lynn K.D., **Sullivan L.A.,** Dellinger M.T., Sadegh L., Sullivan J.P., Shames D.S., Brekken R.A. Inhibition of vascular endothelial growth factor reduces angiogenesis and modulates immune cell

infiltration of orthotopic breast cancer xenografts. Mol Cancer Ther, 8(7): 1761-1771, 2009.

7. Lewis J.D., **Sullivan L.A.,** Byrne J.A., de Riese W., Bright R.K. Memory and cellular immunity induced by a DNA vaccine encoding self antigen TPD52 administered with soluble GM-CSF. Cancer Immunol Immunother, 58 (8): 1337-1349, 2009.
8. Dineen S.P., **Sullivan L.A.,** Beck A.W., Miller A.F., Carbon J.G., Mamluk R., Wong, H., Brekken R.A. The Adnectin CT-322 is a novel VEGF receptor 2 inhibitor that decreases tumor burden in an orthotopic mouse model of pancreatic cancer. BMC Cancer, 8: 352, 2008.
9. **Payton L.A.,** Lewis J.D., Byrne J.A., Bright R.K. Vaccination with metastasis-related tumor associated antigen TPD52 and CpD/ODN induces protective tumor immunity. Cancer Immunol Immunother, 57(6): 799-811, 2008.
10. Lewis J.D., **Payton, L.A.,** Whitford J.G., Byrne J.A., Smith D.I., Yang L., Bright R.K. Induction of tumorigenesis and metastasis by the murine orthologue of tumor protein D52. Mol Cancer Res, 5(2): 133-144, 2007.

LIST OF FIGURES

LIST OF TABLES

LIST OF APPENDICES

LIST OF ABBREVIATIONS

**ALK** — anaplastic lymphoma kinase

**ALT** — alanine aminotransferase

**AMPK** — AMP-activated protein kinase

**AST** — aspartate aminotransferase

**BUN** — blood urea nitrogen

**DAPI** — 4’,6-diamidino-2-phenylindole

**ECM** — extracellular matrix

**ECOG** — Eastern Cooperative Oncology Group

**EGF** — epidermal growth factor

**EGFR** — epidermal growth factor receptor

**ELISA** — enzyme-linked immunosorbent assay

**EML4** — echinoderm microtubule-associated protein-like 4

**EPC** — endothelial progenitor cell

**ERK** — extracellular-signal-related kinase

**Fab** — fragment antigen binding

**FGF** — fibroblast growth factor

**FGFR** — fibroblast growth factor receptor

**Flt** — fms-like tyrosyl kinase

**HDMEC** — human dermal microvascular endothelial cell

**HER2** — human epidermal growth factor receptor 2

**HRP** — horseradish peroxidase

**IFN** — interferon

**IP** — intraperitoneal

**KDR** — kinase domain-containing receptor

**LVD** — lymphatic vessel density

**MAPK** — mitogen-activated protein kinase

**mBC** —metastatic breast cancer

**mcr84** — mouse chimeric r84

**mCRC** — metastatic colorectal cancer

**mRCC** — metastatic renal cell carcinoma

**MVD** — microvessel density

**NOD/SCID** — non-obese diabetic/severe combined immunodeficiency

**Nrp** — neuropilin

**NSCLC** — non-small cell lung cancer

**NTB** — non-tumor bearing

**NTC** — non-targeting control

**OS** — overall survival

**PAE** — porcine aortic endothelial cell

**PBS** — phosphate buffered saline

**PDGFR** — platelet-derived growth factor receptor

**PFS** — progression free survival

**PLCγ** — phospholipase C γ

**PlGF** — placental growth factor

**RET** — rearranged during transfection

**RPMI** — Roswell Park Memorial Institute medium

**RPPA** — reverse-phase protein array

**RTK** — receptor tyrosine kinase

**SCC** — squamous cell carcinoma

**scFv** — single chain variable fragment

**SCLC** — small cell lung cancer

**TB** — tumor bearing

**T/C** — treated/control

**TCI** — tumor cell injection

**TKI** — tyrosine kinase inhibitor

**uPA** — urokinase type of plasminogen activator

**USFDA** — United States Food and Drug Administration

**VEGF** — vascular endothelial growth factor

**VEGFR** — vascular endothelial growth factor receptor

# CHAPTER ONE

# THE VEGF FAMILY IN CANCER AND ANTIBODY-BASED STRATEGIES FOR THEIR INHIBITION


## Abstract

Angiogenesis is required in normal physiological processes, but is also involved in tumor growth, progression and metastasis. Vascular endothelial growth factor (VEGF), a primary mediator of angiogenesis in normal physiology and in disease, and other VEGF family members and their receptors provide targets that have been explored extensively for cancer therapy. Small molecule inhibitors and antibody/protein-based strategies that target the VEGF pathway have been studied in multiple types of cancer. This chapter will focus on VEGF

pathway targeting antibodies that are currently being evaluated in pre-clinical and clinical studies.

Note: The following chapter is in part made up of a review article written by Laura A. Sullivan under the guidance of Rolf A. Brekken.

## 1.1 Introduction

Angiogenesis is a tightly regulated process responsible for the development of new blood vessels from a pre-existing vascular network. During development and normal physiological processes such as wound healing and the menstrual cycle, angiogenesis is regulated by endogenous activators and inhibitors. Within adult animals, the levels of endogenous mediators are balanced and endothelial cells are largely quiescent (Ferrara, 2004; Roskoski, 2007b). In pathological settings, such as age-related macular degeneration, rheumatoid arthritis, diabetic retinopathy and tumor growth and metastasis, angiogenesis is critical for disease progression (Ferrara, 2004; Hoeben et al., 2004). A key step in tumor development, the 'angiogenic switch' occurs when endogenous activators of angiogenesis outweigh endogenous inhibitors, thereby shifting the balance of angiogenic mediators and stimulating angiogenesis. This results in increased blood vessel formation, which supplies growing tumors with necessary oxygen and nutrients for sustained growth (Hanahan and Folkman, 1996); however the resulting vasculature is disorganized and poorly structured, leading to chaotic blood flow and leaky blood vessels (Gerwins et al., 2000; Jain, 2003). Although dysfunctional when compared to the hierarchical, well-structured vascular network found in normal tissue, tumor vasculature is nonetheless essential for continued tumor growth (Dvorak, 2005; Less et al., 1991). In the absence of a blood vascular network, tumors are restrained in size due to limits in the diffusion

of oxygen (Folkman, 1971). In 1971, Judah Folkman was the first to hypothesize the potential therapeutic benefit of targeting tumor angiogenesis (Folkman, 1971). The vascular endothelial growth factor (VEGF) family of proteins are key regulators of normal and tumor angiogenesis, and so provide attractive targets for anti-cancer therapies.

### *1.1.1 The VEGF family*

There are five members of the human VEGF family: VEGF-A (referred to in this chapter as VEGF), VEGF-B, VEGF-C, VEGF-D, and placental growth factor (PlGF) (Ferrara, 2004; Hoeben et al., 2004). In addition, multiple isoforms of VEGF, VEGF-B, and PlGF are generated through alternative splicing of pre-mRNA (Roskoski, 2007b). The VEGF family ligands interact with the receptor tyrosine kinases VEGF receptor-1 (VEGFR1), VEGFR2, and VEGFR3. VEGF family interaction with VEGFRs is also regulated by the non-enzymatic co-receptors neuropilin (Nrp)-1 and Nrp2 (Roskoski, 2007b).

The *VEGF* gene contains eight exons and seven introns (Houck et al., 1991; Tischer et al., 1991). VEGF binds to VEGFR1, VEGFR2, Nrp1 and Nrp2 (Roskoski, 2007b). VEGF induces vascular permeability (Senger et al., 1990) and also functions as an endothelial cell mitogen and survival factor (Alon et al., 1995; Ferrara and Henzel, 1989; Gerber et al., 1998), and an inducer of endothelial cell and monocyte migration (Barleon et al., 1996; Waltenberger et

al., 1994). Alternative splicing of *VEGF* yields nine different isoforms in total and four major isoforms: $VEGF_{121}$, $_{165}$, $_{189}$, and $_{206}$ (Leung et al., 1989). The bioavailability of the different VEGF isoforms is mediated by their expression of heparin sulfate proteoglycan-binding domains, encoded by exons 6a, 6b and 7 (Houck et al., 1992; Park et al., 1993). These domains have strong affinity for proteoglycans found on cell plasma membranes or within the extracellular matrix (ECM), thereby restricting the diffusion of larger isoforms of VEGF (Robinson and Stringer, 2001). Release of VEGF from the ECM and cell membrane allows for VEGF-mediated activity and signaling. Proteolytic release of VEGF is mediated by extracellular proteases plasmin (Keyt et al., 1996), urokinase type of plasminogen activator (Flaumenhaft and Rifkin, 1992) and matrix metalloproteinases (Bergers et al., 2000; Lee et al., 2005; Mignatti and Rifkin, 1993). Proteolytic release of VEGF is induced by remodeling and microenvironment cues elicited during physiological and pathologic angiogenesis (Pepper, 2001).

The *VEGF-B* gene contains seven exons that undergo alternative splicing to produce two isoforms, VEGF-$B_{167}$ and VEGF-$B_{186}$ (Olofsson et al., 1996). VEGF-B binds to VEGFR1 and Nrp1 (Roskoski, 2007b). The overall function of VEGF-B remains unclear, with suggested roles in heart function in adults, but not in developmental angiogenesis or cardiovascular development since *VEGF-B* null

mice are viable despite some abnormalities in cardiac conduction (Aase et al., 2001).

The *VEGF-C* gene is made up of eight exons, but does not undergo alternative splicing. Mature VEGF-C binds to VEGFR2 and VEGFR3 and is involved in developmental lymphangiogenesis and the maintenance of adult lymphatic vasculature (Lymboussaki et al., 1999). *VEGF-C* null mice are embryonic lethal and heterozygous *VEGF-C* loss is characterized by lymphedema from defective development of the lymphatic vasculature (Karkkainen et al., 2004). Interestingly, VEGF-C is not required for blood vessel development since vessels appeared normal in *VEGF-C* null animals (Karkkainen et al., 2004).

*VEGF-D* is composed of seven exons and is found on the X chromosome (Rocchigiani et al., 1998). Mature VEGF-D binds to both VEGFR2 and VEGFR3 as a non-covalent homodimer (Stacker et al., 1999). Knock out studies in mice suggest that VEGF-C, and perhaps other growth factors, are capable of substituting for VEGF-D function, as *VEGF-D* null mice are viable and have a normal lymphatic vasculature during development and in the adult (Baldwin et al., 2005).

The last member of the human VEGF family is PlGF. The *PlGF* gene contains seven exons that generate four different isoforms by alternative splicing (Cao et al., 1997; Maglione et al., 1991; Yang et al., 2003). These isoforms are expressed primarily in the placenta, but are also found within the heart, retina,

skin, and skeletal muscle (Roskoski, 2007b). There is reduced vascularization of the corpus luteum and retina in *PlGF*-null mice, but these animals are viable (Carmeliet et al., 2001).

### *1.1.2 The VEGF receptors*

There are three receptor tyrosine kinases that mediate the angiogenic functions of VEGF family members: VEGFR1, VEGFR2, and VEGFR3. Although these receptors initiate diverse downstream functions, they are structurally very similar. The VEGF receptors each contain a seven member immunoglobulin-like domain extracellular region, a single transmembrane domain segment, a juxtamembrane segment, a split intracellular protein-tyrosine kinase domain, and a carboxyterminal tail (Roskoski, 2007b).

VEGFR1, also known as fms-like tyrosyl kinase-1 (Flt-1), binds VEGF, VEGF-B and PlGF (de Vries et al., 1992; Olofsson et al., 1998; Park et al., 1994; Shibuya et al., 1990). Alternative splicing of *VEGFR1* produces a soluble form of the receptor that contains the first six of the seven immunoglobulin domains, and binds to and inhibits the function of VEGF (Kendall and Thomas, 1993). VEGFR1 can function as a decoy receptor, utilizing its strong affinity for VEGF (approximately 10 times stronger than that of VEGFR2 for VEGF) to sequester the ligand, preventing it from signaling through other receptors (Waltenberger et al., 1994). Despite the strong binding affinity of VEGFR1 to VEGF, the kinase

activity of this receptor is weak making it difficult to evaluate levels of VEGFR1 auto-phosphorylation in cells that have not been engineered to express high levels of the receptor (Waltenberger et al., 1994). VEGFR1 is essential during development. *VEGFR1* null animals are embryonic lethal, characterized by endothelial cells that do not form a structured, organized vascular network (Fong et al., 1995). Interestingly, mice that do not express the tyrosine kinase domain of VEGFR1 but retain the ligand-binding extracellular domains and the transmembrane segment (*VEGFR1-TK*$^{-/-}$) are viable, emphasizing the importance of ligand sequestration in VEGFR1 function (Hiratsuka et al., 1998). The mutant phenotype resulting from *VEGFR1* loss in embryonic stem cell-derived blood vessels can be rescued with VEGFR2 small molecule inhibitors (Roberts et al., 2004). Although VEGFR1 signaling remains unclear, there is support for the involvement of the receptor in hematopoiesis (Gerber et al., 2002; Hattori et al., 2002), the migration of monocytes and the recruitment of bone marrow-derived progenitor cells (Barleon et al., 1996; Luttun et al., 2002). VEGFR1 has also been implicated in the paracrine release of growth factors from endothelial cells (LeCouter et al., 2003) and inducing VEGF-B-mediated endothelial cell expression of matrix metalloproteinase-9, urokinase type of plasminogen activator and plasminogen activator inhibitor-1, molecules important for ECM degradation that can facilitate VEGF release and cell migration (Olofsson et al., 1998). In addition, VEGF binding to VEGFR1 has been shown to induce SHP-1

phosphatase activity that in turn reduced VEGFR2 phosphorylation levels (Nozaki et al., 2006). These data support VEGFR1 functioning to negatively regulate activity of VEGFR2, which could have important implications for targeting the VEGF pathway within tumors.

VEGFR2 (Fetal liver kinase-1 (Flk-1)/Kinase Domain-containing Receptor (KDR)) is the predominant mediator of VEGF-induced angiogenic signaling (Millauer et al., 1993; Quinn et al., 1993; Terman et al., 1992). Functions of VEGFR2 include endothelial cell survival, migration, proliferation and vascular permeability (Bernatchez et al., 1999; Roskoski, 2007b; Takahashi et al., 2001). VEGFR2 binds all VEGF isoforms, VEGF-C and VEGF-D. Although VEGR2 has a lower affinity for VEGF than VEGFR1, it has a stronger kinase activity. When VEGF binds VEGFR2, it induces receptor dimerization and trans auto-phosphorylation (Roskoski, 2007b). The predominant phosphorylation sites on VEGFR2 occur on tyrosine 1175 and 1214, inducing signaling cascades through phosphatidylinosityl 3-kinase (PI3K), AKT, PLCγ, p38 MAPK, and p42/44 MAPK (Bernatchez et al., 1999; Roskoski, 2007b; Shibuya and Claesson-Welsh, 2006). Ebos *et al.* identified a soluble, circulating form of VEGFR2, and Albuquerque *et al.* recently found that this soluble receptor is a distinct splice variant that inhibits lymphangiogenesis (Albuquerque et al., 2009; Ebos et al., 2004). Recently, VEGFR2 expression by macrophages has been demonstrated to mediate macrophage infiltration in tumor-bearing animals (Dineen et al., 2008).

*VEGFR2* null mice are embryonic lethal between day E8.5-9.5. These animals have severe defects in endothelial and hematopoietic cell development with no organized blood vessel found at any point within the developing embryo or the yolk sac (Shalaby et al., 1995).

VEGFR-3 (Flt-4) binds both VEGF-C and VEGF-D and functions in the remodeling of embryonic primary capillary plexus, with sustained roles in adult angiogenesis and lymphangiogenesis (Galland et al., 1993; Kaipainen et al., 1995; Pajusola et al., 1992). *VEGFR3* null mice are embryonic lethal at day E9.5 and display cardiovascular failure as a result of the abnormal structure and organization of large vessels that leads to defective vessel lumens and an accumulation of fluid within the pericardial cavity (Dumont et al., 1998). In humans, inactivating mutations within the catalytic loop of the VEGFR3 kinase domain cause Milroy disease, a hereditary form of lymphedema where defective lymphatic vessels cause chronic swelling of the extremities (Olsson et al., 2006). The lymphatic abnormalities of Milroy disease and the phenotype of *VEGFR3* null mice, suggest that VEGFR3 functions first in the development of the cardiovascular system and later in the lymphatic vasculature in adults (Roskoski, 2007b).

The two non-enzymatic co-receptors for the VEGF family, Nrp1 and Nrp2 were first identified as receptors for semaphorins, which function during neurogenesis (Chen et al., 1997; Roskoski, 2007b; Takagi et al., 1995).

Structurally, the Nrps have a large extracellular region, a transmembrane segment, and a short intracellular domain that apparently does not function catalytically, but may serve as a binding site for other co-receptors or downstream signaling molecules (Mamluk et al., 2002). Nrp1 binds VEGF isoforms with heparin sulfate proteoglycan-binding domains, PlGF and both VEGF-B isoforms and potentiates signaling through VEGFR2 (Makinen et al., 1999; Migdal et al., 1998; Soker et al., 1998). Nrp1 functions during vascular development and in angiogenesis as demonstrated by genetic modifications in mouse models. *Nrp1* over-expressing mice are embryonic lethal due to hemorrhaging and excessive capillary and blood vessel formation (Kitsukawa et al., 1995). *Nrp1* null mice are embryonic lethal between days E10.5-12.5 resulting from nervous system and cardiovascular abnormalities (Kitsukawa et al., 1997). Nrp2 binds to $VEGF_{145, 165}$, VEGF-C and PlGF (Gluzman-Poltorak et al., 2000; Karkkainen et al., 2001). Nrp2 functions during lymphatic development as indicated by *Nrp2* null mice that are normal and display phenotypically normal vasculature but have a severe reduction in small lymphatic vessels (Giger et al., 2000; Yuan et al., 2002). Additional work evaluating the function of Nrp1 and Nrp2 by Takashima *et al.* demonstrated that *Nrp1 Nrp2* double null mice have avascular yolk sacs and are embryonic lethal at day E8.5. Further, $Nrp1^{+/-}$ $Nrp2^{-/-}$ or $Nrp1^{-/-}$ $Nrp2^{+/-}$ mice are embryonic lethal at day E10-10.5 with severe angiogenic abnormalities in both the yolk sac and the embryo and an overall reduction in embryo size (Takashima et al., 2002). These

mutant embryos had a similar phenotype to *VEGF* or *VEGFR2* null mice, highlighting the importance of the Nrps in embryonic blood vessel development.

### *1.1.3 Monoclonal antibodies as therapeutic agents*

The clinical use of monoclonal antibodies (mAbs) to treat cancer and other diseases is well established. There are currently more than 20 mAbs approved by the United States Food and Drug Administration (USFDA) for therapeutic use (Scolnik, 2009). Rituximab (Rituxan®, Genentech), a chimeric mAb directed against CD20 used to treat patients with non-Hodgkin's lymphoma, was the first anti-cancer mAb to gain USFDA approval. Since then, mAbs targeting key pathways in tumor survival have been developed and successfully used clinically to treat patients including trastuzumab (Herceptin®, Genentech) that recognizes the HER2/neu cell surface receptor expressed in 15-20% of breast cancers and cetuximab (Erbitux®, ImClone Systems) that binds epidermal growth factor receptor (EGFR) and is approved for the treatment of metastatic colorectal cancer and head and neck cancer (Scolnik, 2009).

Tumor angiogenesis is a hallmark of cancer, and is required for continued tumor cell growth and metastasis (Hanahan and Weinberg, 2000). VEGF is a major mediator of angiogenesis in normal physiology and in cancer. In many forms of cancer, there is an up-regulation of VEGF family members and the VEGF receptors, providing a target for cancer therapy (Roskoski, 2007b). This

target has been utilized by investigators, leading to the development of anti-angiogenic small molecule tyrosine kinase inhibitors such as sorafenib (Nexavar®, BAY 43-9006, Bayer Pharmaceuticals Corp.) and sunitinib (Sutent®, SU11248, Pfizer, Inc.) as well as a number of mAbs against VEGF ligands and receptors (Roskoski, 2007b). The use of mAbs to target the VEGF pathway will be the focus of the rest of this thesis (refer to Figures 1.1 and Table 1.1 for a summary of the anti-VEGF pathway and the mAbs targeting this pathway discussed here).

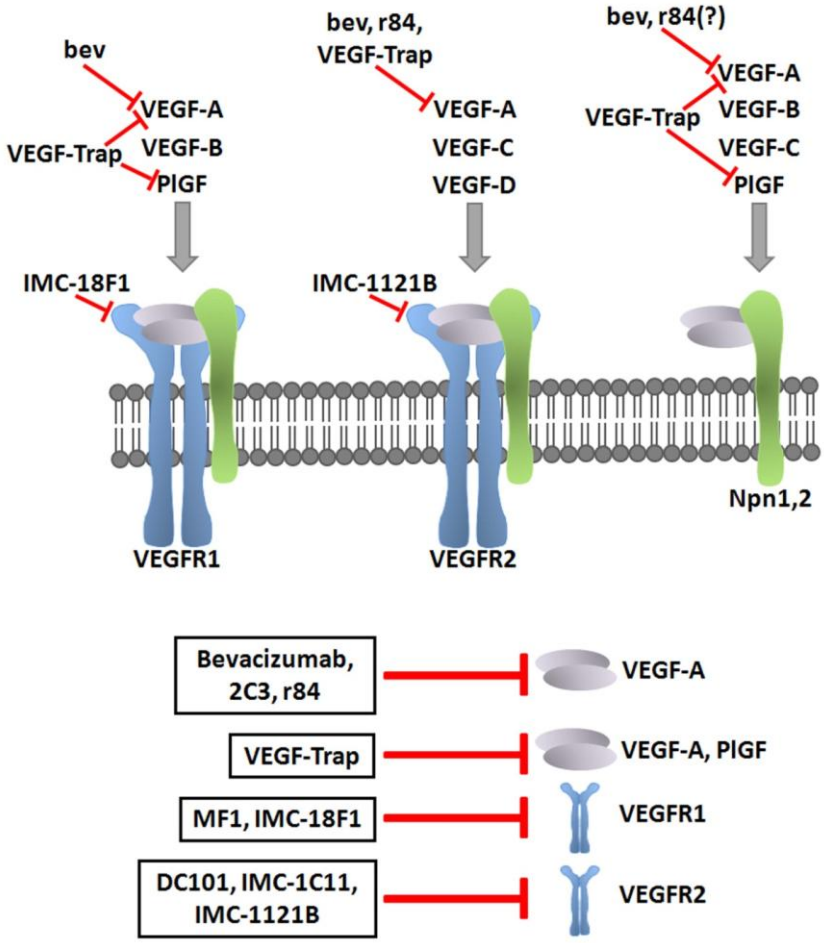


**Figure 1.1: Blockade of the VEGF pathway with mAbs.**

The specificity of the VEGF family ligands for the VEGF receptors and coreceptors are shown. The clinically-relevant mAbs targeting the VEGF pathway discussed in this chapter are placed based on their blockade of VEGF ligand or receptor. The ligand-binding antibodies bevacizumab (bev), r84, and VEGF-Trap inhibit ligand binding to the indicated receptor. IMC-18F1 and IMC-1121B bind VEGFR1 and VEGFR2 respectively, and prevent ligand binding to these receptors.

| Drug | Target | Inhibition | Clinical Status |
|---|---|---|---|
| Bevacizumab hz mAb | hu VEGF | VEGF binding to VEGFR1,R2 | Approved for mCRC, NSCLC, mBC*, mRCC, glioblastoma |
| 2C3 ms mAb | hu VEGF | VEGF binding to VEGFR2 | Effective tool in pre-clinical studies |
| r84 hu mAb | hu,ms VEGF | VEGF binding to VEGFR2 | Effective in pre-clinical studies; clinical trial candidate |
| VEGF-Trap hu Fc fp | hu,ms VEGF PlGF | VEGF,PlGF binding to VEGFR1,R2 | Effective in pre-clinical studies; in clinical trials |
| MF1/IMC-18F1 rt/hu mAb | ms/hu VEGFR1 | VEGFR1 activation by PlGF, VEGF,-B | Effective in pre-clinical studies; in clinical trials |
| DC101/IMC-1C11 rt/hz mAb | ms/hu VEGFR2 | VEGFR2 activation by VEGF,-C,-D | Effective in pre-clinical studies; immunogenic in clinical trials |
| IMC-1121B hu mAb | hu VEGFR2 | VEGFR2 activation by VEGF,-C,-D | Effective in pre-clinical studies; in clinical trials |

**Table 1.1: Current anti-angiogenic mAbs with applications in cancer therapy.**

hz, humanized; hu, human; ms, mouse; rt, rat; fp, fusion protein; mCRC, metastatic colorectal cancer; NSCLC, non-small cell lung cancer; mBC, metastatic breast cancer, *see text for changes to approval status; mRCC, metastatic renal cell carcinoma.

## 1.2 Antibodies and fusion proteins targeting VEGF

### *1.2.1 Bevacizumab (Avastin®, Genentech/Roche)*

In 1993, the Ferrara *et al.* introduced a mouse anti-human VEGF mAb referred to as A.4.6.1 that inhibited the growth of A673 rhabdomyosarcoma, G55 glioblastoma and SK-LMS-1 leyomiosarcoma tumor cell line xenograft models *in vivo* but not *in vitro* (Kim et al., 1993), illustrating an indirect role of VEGF signaling in tumor survival. The efficacy of A.4.6.1 in controlling the growth of a number of tumor cell lines in xenograft models in immunocompromised mice was demonstrated subsequently by a number of publications (Borgstrom et al., 1998; Melnyk et al., 1996; Warren et al., 1995). A.4.6.1 underwent site-directed mutagenesis resulting in the humanized mAb bevacizumab (Avastin®, Genentech/Roche) that binds human VEGF with an affinity similar to A.4.6.1 ($K_d$ ≈ 0.5nM) (Presta et al., 1997). Structural analysis of VEGF bound to bevacizumab Fab gave insight to the specificity and mechanism of the mAb. Gly88 of human VEGF is required for bevacizumab binding. In mouse and rat VEGF this residue is replaced by a serine, disrupting the binding of bevacizumab to rodent VEGF (Muller et al., 1998). Further, bevacizumab Fab bound to VEGF does not induce structural conformational changes in the ligand, suggesting that bevacizumab is effective by sterically disrupting the ability of VEGF to interact with its receptors (Muller et al., 1998; Muller et al., 1997; Wiesmann et al., 1997). Preclinical safety

evaluations of bevacizumab were performed in *Macaca fascicularis*. Some treatment-induced changes were observed, including suppressed angiogenesis within the female reproductive tract, but all adverse effects were reversible with the cessation of bevacizumab treatment (Ferrara et al., 2004).

In 1997, bevacizumab entered Phase I clinical trials and was found to be relatively non-toxic and well-tolerated, without exacerbating toxicities related to patient chemotherapy treatment (Gordon et al., 2001; Margolin et al., 2001). In subsequent Phase II and III trials, the primary toxicities induced following bevacizumab therapy were hypertension, proteinuria, and gastrointestinal perforations, which occurred more frequently in patients with colorectal cancer or metastases within the gastrointestinal tract. Bleeding events are also a concern with bevacizumab therapy and can be fatal with some tumor histologies such as in squamous non-small cell lung cancer (NSCLC) (Grothey and Galanis, 2009). These Phase II and III clinical trials led to the federal approval of bevacizumab, the first anti-angiogenic strategy approved for cancer therapy, for the treatment of five different cancers to date. In metastatic colorectal cancer (mCRC), bevacizumab in combination with chemotherapy (ironotecan, 5-fluorouracil, and leucovorin) significantly increased median duration of patient survival by 4.7 months as compared to chemotherapy treatment alone, leading to the approval of this regimen in 2004 as a first-line treatment for mCRC (Hurwitz et al., 2004). Approval of bevacizumab as a second-line treatment for mCRC in 2006 was the

result of the Eastern Cooperative Oncology Group E3200 (ECOG E3200) study where bevacizumab plus chemotherapy (oxaliplatin, 5-fluororuacil and leucovorin) significantly increased patient overall survival (OS) and progression-free survival (PFS) by 2.1 and 2.6 months, respectively as compared to chemotherapy treatment alone (Giantonio et al., 2007). In 2006, bevacizumab was also approved as a first-line treatment for NSCLC based on the findings of the ECOG E4599 study where bevacizumab in combination with paclitaxel and carboplatin versus chemotherapy alone significantly increased OS by 2 months and PFS by 1.7 months (Sandler et al., 2006). The results of the ECOG E2100 study led to the approval of bevacizumab in 2008 as a first-line therapy for HER2-negative metastatic breast cancer (mBC) where bevacizumab plus paclitaxel failed to increase OS versus paclitaxel alone treatment, but did significantly increase PFS by 5.9 months (Miller et al., 2007). Bevacizumab is not currently recommended for second- or third-line treatment of mBC that has progressed following anthracycline and taxane chemotherapy. This decision was made based on the findings of the AVF2119 study where mBC patients that had previously been treated with anthracycline and taxane had no increased in PFS or OS with bevacizumab in combination with capecitabine versus capecitabine alone (Miller et al., 2005). Analysis of two recent trials using bevacizumab plus chemotherapy in metastatic breast cancer patients have demonstrated small increases in PFS, but no change in OS. As a result of these findings the USFDA voted in late 2010 to

revoke the approval of bevacizumab for breast cancer indications. Repeals of this decision by Genentech/Roche are currently underway (Twombly, 2011). USFDA approval of single agent bevacizumab therapy for second-line treatment of glioblastoma in May 2009 was the result of AVF3708g and NCI 06-C-0064E trial that demonstrated durable, objective response rates (Friedman et al., 2009; Norden et al., 2008). In July 2009, bevacizumab was approved for the treatment of metastatic renal cell carcinoma (mRCC) based on the Hoffmann-La-Roche BO17705 trial where bevacizumab plus interferon (IFN) alfa-2a resulted in a statistically significant 4.8 month increase in PFS versus IFN alfa-2a treatment alone (Escudier et al., 2007), and the Cancer and Leukemia Group B 90206 trial that demonstrated a statistically significant 3.3 month increase in PFS with combination bevacizumab plus IFN alfa therapy versus IFN alfa alone (Rini et al., 2008). Bevacizumab has paved the way for subsequent anti-angiogenic therapies in cancer. A more detailed account of bevacizumab's progress through clinical trials in a number of tumor types is provided in a thorough review by Grothey and Galanis (Grothey and Galanis, 2009). However, the survival benefits of bevacizumab therapy, although reaching statistical significance, are modest and as mentioned above, are measured in months. These somewhat disappointing results of bevacizumab's clinical efficacy in combination with bevacizumab-mediated toxicity highlight the need to re-evaluate how to best utilize anti-angiogenic therapies in the clinic.

### *1.2.2 2C3 and r84 (AT001, Affitech AS)*

2C3 is a murine monoclonal $IgG2_{a,\kappa}$ antibody that binds human VEGF and inhibits VEGF from interacting with VEGFR2, but not VEGFR1. 2C3-mediated blockade of VEGFR2 signaling blocks VEGF-mediated EC growth, VEGFR2 phosphorylation, vascular permeability, and inhibits the growth of established human tumor xenografts in immunocompromised mice (Brekken et al., 1998; Brekken et al., 2000). In addition, 2C3 localizes to pools of VEGF in the tumor stroma and within the perivascular connective tissue of solid human tumors (Brekken et al., 1998). Since its initial identification, 2C3 has been characterized in numerous tumor xenograft models as an effective inhibitor of tumor growth and angiogenesis, and as a modulator of macrophage and immune cell infiltration (Dineen et al., 2008; Holloway et al., 2006; Liang et al., 2006b; Roland et al., 2009a; Stephan et al., 2004).

The success of 2C3 in preclinical models lead to the development of the phenotypically similar, fully human mAb, r84 (AT001, Affitech AS) that was generated by screening a human anti-VEGF single chain variable fragment library for specific 2C3-like properties. 2C3 and r84 crossblock each other in VEGF enzyme-linked immunosorbent assays (ELISAs) indicating that the epitope each mAb binds is very similar; however, the exact epitope on VEGF bound by each mAb has not been determined. Efforts are currently underway to solve the

structure of VEGF bound by the Fab of r84, which is anticipated to uncover the epitope for r84. r84 binds mouse and human VEGF, but not other VEGF family members, and specifically inhibits VEGF from binding to VEGFR2, but allows VEGF to bind and activate VEGFR1. Through specific VEGF blockade, r84 inhibits VEGFR2-mediated endothelial cell migration and phosphorylation cascades *in vitro* and controls tumor growth, angiogenesis, and immune cell infiltration *in vivo* (Roland et al., 2009a; Roland et al., 2009b; Sullivan et al., 2010). Research with 2C3 and r84 demonstrate that inhibition of VEGF-mediated VEGFR2 activation is sufficient to control tumor growth and calls into question the pro-tumorigenic function of VEGFR1. In addition, because r84 binds mouse and human VEGF, it facilitates evaluation of the effects of blocking tumor-derived (human) and stromal (mouse) VEGF in preclinical xenografts models. Therefore r84 should more closely mirror the activity of selective VEGF inhibition in human patients. A mouse chimeric version of r84 (mcr84) has been generated and is a useful tool for studying angiogenesis in immunocompetent animals and in syngenic tumor models (Roland et al., 2009b; Sullivan et al., 2010). To date, treatment of tumor-bearing mice with r84 has not induced anti-VEGF-related toxicities that have been characterized in other preclinical models using different inhibitors of the VEGF pathway (Gerber et al., 2007; Kamba and McDonald, 2007; Kamba et al., 2006). Therefore, the potential efficacy of r84 as a cancer therapeutic for treating cancer patients is highly anticipated.

### *1.2.3 VEGF-Trap (Aflibercept, Regeneron Pharmaceuticals, Inc.)*

The precursor of VEGF-Trap (aflibercept, Regeneron Pharmaceuticals, Inc.), the therapeutic drug currently in Phase II and III clinical trials, was first developed by trying to harness the strong affinity of VEGFR1 for VEGF to inhibit VEGF-mediated angiogenesis within tumors. A soluble decoy receptor was engineered by fusing the first three immunoglobulin domains of VEGFR1 to the Fc constant region of human IgG1 antibody, creating a forced homodimer, mFlt(1-3)-IgG that bound VEGF and PlGF with high affinity (Ferrara et al., 1998; Gerber et al., 1999). However, this fusion protein had poor pharmacokinetic properties *in vivo* that required large, frequent doses for efficacy (Gerber et al., 2000). To improve the half-life without losing affinity, mFlt(1-3)-IgG was modified to contain the second immunoglobulin domain of VEGFR1 and the third immunoglobulin domain of VEGFR2 fused to human IgG1 Fc region, creating the fusion protein known as VEGF-Trap. This fusion protein had improved pharmacokinetics and affinity for VEGF (approximately 1 pM) as compared to the parental mFlt(1-3)-IgG, and effectively inhibited tumor growth and angiogenesis in xenograft models (Holash et al., 2002). Pre-clinical trials demonstrated the efficacy of VEGF-Trap in suppressing tumor growth and angiogenesis through its ability to bind both mouse and human VEGF (Fukasawa and Korc, 2004; Hu et al., 2005; Huang et al., 2003), and supported its entry into

clinical trials were it is being currently evaluated in a number of cancers and in age-related macular degeneration.

## 1.3 Antibodies targeting the VEGF receptors

### *1.3.1 MF1/IMC-18F1 (ImClone Systems)*

The rat anti-mouse VEGFR1 IgG1 mAb, MF1 (ImClone Systems) was first shown to suppress tumor and ischemic retinal angiogenesis, as well as inflammation in an autoimmune arthritis model (Luttun et al., 2002). Kaplan *et al.* used MF1 to demonstrate VEGFR1 participates in the pre-metastatic niche in animal models, and that blockade of VEGFR1 with MF1 more effectively blocked tumor metastases than did inhibition of VEGFR2 (Kaplan et al., 2005). These studies led to the development of a fully human mAb directed against human VEGFR1 (mAb 6.12, IMC-18F1, ImClone Systems) that blocked VEGFR1 signaling in VEGFR1-expressing breast cancer cells lines *in vitro*, and inhibited tumor growth *in vivo* (Wu et al., 2006a). The final characterization of IMC-18F1 came in 2006. IMC-18F1 bound to VEGFR1 with high-affinity and was able to block VEGFR1 from interacting with VEGF, VEGF-B and PlGF, preventing downstream VEGFR1 signaling and breast cancer cell line growth *in vitro* and *in vivo*. Targeting human and mouse VEGFR1 with IMC-18F1 and MF1, respectively, more effectively controlled tumor growth than either agent alone

(Wu et al., 2006b). The safety and dosing of IMC-18F1 is currently being evaluated in a Phase I clinical trial.

### *1.3.2 DC101/IMC-1C11 (ImClone Systems)*

DC101 is a rat anti-mouse VEGFR2 mAb that inhibits ligand-induced activation of VEGFR2 (Rockwell, 1995). *In vivo* syngeneic and xenograft tumor models in mice demonstrated the ability of DC101 to control tumor growth and reduce tumor angiogenesis by targeting EC- or tumor-expressed VEGFR2 (Bruns et al., 2002; Prewett et al., 1999; Shaheen et al., 2001; Skobe et al., 1997; Zhang et al., 2002a). Since DC101 recognizes only mouse VEGFR2 and therefore is not a candidate for clinical trials, a single chain variable fragment with human VEGFR2 reactivity that was also able to block *in vitro* VEGFR2 signaling was isolated from a single chain antibody phage display library (Zhu et al., 1998). This fragment became IMC-1C11 (ImClone Systems), a chimeric mAb that blocked tumor growth and angiogenesis in tumor xenografts and was tested in a Phase I clinical trial in colorectal carcinoma patients with liver metastases (Posey et al., 2003; Zhu and Witte, 1999). Although treatment with IMC-1C11 did not induce grade 3 or 4 toxicities, 50% of treated patients developed anti-chimeric antibodies that impeded the future progression of this antibody in the clinic (Posey et al., 2003).

### *1.3.3 IMC-1121B (ramucirumab, ImClone Systems)*

To develop an anti-human VEGFR2 mAb that would not be immunogenic in clinical trials, ImClone Systems used a human antibody phage display library to isolate VEGFR2-specific human Fab fragments. The resulting best Fab bound to human VEGFR2 with high affinity, and inhibited ligand-induced VEGFR2 activation in endothelial cells (Lu et al., 2002; Lu et al., 2003). Affinity maturation of the best Fab clone and subsequent synthesis of a full length antibody yielded IMC-1121B, a fully human IgG1 mAb with higher affinity for VEGFR2 that was a more potent inhibitor of VEGF-induced VEGFR2 signaling and EC migration *in vitro*. IMC-1121B also increased the survival of murine xenograft models *in vivo* more effectively than other anti-VEGFR2 antibodies, including IMC-1C11 (Miao et al., 2006; Zhu et al., 2003). There are 13 current Phase I or II clinical trials with IMC-1121B to assess the safety and efficacy of this mAb.

## 1.4 The future of mAbs against VEGF

The development of anti-angiogenic therapies was highly anticipated. This therapeutic strategy was hypothesized to avoid the tumor resistance pathways of traditional anti-cancer drugs by targeting the vasculature as opposed to the genetically instable and highly mutagenic tumor cell population. The pre-clinical success of targeting the VEGF pathway using mAb-based therapy further

bolstered this hypothesis. However, clinical studies of anti-VEGF strategies in cancer patients have not delivered the level of efficacy anticipated. To date, bevacizumab is the most developed anti-VEGF pathway mAb. Bevacizumab is currently indicated as a first- or second- line treatment in four different tumor types (not including mBC indications where approval is tenuous), and is being evaluated in many clinical trials. Therefore, experience with bevacizumab in the clinic provides a working model for the benefits and pitfalls of anti-angiogenic mAb therapies as well as a benchmark for other anti-angiogenic mAb discussed in this article.

As discussed previously, the results of bevacizumab in Phase II and III clinical trials have been modest when compared to the success of anti-VEGF therapy in pre-clinical models (Ferrara et al., 2004). In the clinic, responses with bevacizumab as a single agent therapy (in glioblastoma) or in combination with standard chemotherapy (in NSCLC, mCRC, mRCC) is measured in a handful of months correlating with small, albeit statistically significant increases in PFS and rarely in OS (Grothey and Galanis, 2009). This differs from some anti-angiogenic small molecule tyrosine kinase inhibitors (TKIs) that do not display improved efficacy when combined with chemotherapy (Kerbel, 2006). The differences between anti-angiogenic TKIs and mAbs may be due to functional changes occurring within the tumor in response to the different drugs. Treating tumors with bevacizumab or other anti-VEGF pathway mAbs counteracts the inherent

disorganization and abnormalities of the tumor vasculature. This process has been termed “normalization” (Jain, 2005). The pruned, normalized tumor vasculature achieved with anti-angiogenic therapy has increased pericyte coverage and stability and a reduction in vessel leakiness and interstitial fluid pressure, which in combination improves the subsequent delivery of chemotherapy and other drugs. This process allows for cytostatic anti-angiogenic therapy (e.g. bevacizumab and other anti-VEGF pathway mAbs) combined with cytotoxic chemotherapy to have improved clinical response as compared to either agent alone. The absence of synergy with some VEGFR TKIs and chemotherapy is perhaps due to the targeting of other tyrosine kinase receptors such as platelet-derived growth factor receptor (PDGFR) that can disrupt the normalization process (Kerbel, 2006). A better understanding of the normalization process among tumor types would allow for optimization of anti-angiogenic and chemotherapeutic drug delivery schedules, perhaps improving the overall efficacy of these drugs in the clinic.

Bevacizumab therapy is associated with several adverse effects. The most common toxicities are hypertension, proteinuria and bleeding events that result from a loss of homeostatic VEGF signaling and vascular maintenance (Roodhart et al., 2008). Certain histologies, such as squamous NSCLC, were more prone to fatal bleeding events, leading to the exclusion of these patients from future studies (Grothey and Galanis, 2009). In addition, perforations were more frequent in patients with metastatic colorectal cancer, ovarian cancer or metastases within the

gastrointestinal tract. Inhibition of VEGFR signaling with sorafenib and sunitinib therapy is also associated with hypertension, proteinuria, and bleeding events similar to treatment with bevacizumab. However, there are a host of off-target adverse effects with sorafenib and sunitinib therapy, including skin reactions, hand-foot syndrome, fatigue and diarrhea resulting from TKI inhibition of targets other than the VEGFRs (Roodhart et al., 2008). Based on these patterns, specific blockade of VEGF, PlGF, VEGFR1 or VEGFR2 with r84, VEGF-Trap, IMC-18F1 or IMC-1121B might induce toxicities more similar to bevacizumab rather than sorafenib and sunitinib. It is also possible that VEGFR1 signaling is important for maintaining the homeostatic function of VEGF and thus therapies allowing for continued VEGFR1 signaling such as r84 and IMC-1121B may provide a less severe toxicity profile than bevacizumab. In support of this, pre-clinical studies in our lab with extended (12 week) treatment of tumor-bearing and non-tumor bearing mice with r84 failed to induce toxicity (Sullivan et al., 2010). Results from IMC-1121B on-going clinical trials and future studies with r84 in the clinic will ultimately answer these questions about differences in toxicities between the VEGF pathway antibodies. Alternatively, the severity or frequency of toxicities between mAbs targeting the VEGF pathway may depend more on the relative affinity of the drug for its target. In pre-clinical studies with mice engineered to express human VEGF, anti-VEGF antibodies of increasing affinity had a greater toxicity induction (Gerber, 2007). Additionally, chemotherapy

regimens such as carboplatin and paclitaxel, in combination with bevacizumab or VEGFR TKIs can exacerbate the toxicities of these targeted therapies (Chen and Cleck, 2009). Therefore, carefully assessing drug affinity for its target and chemotherapy doses and regimens is required to control toxicity in patients receiving drugs targeting the VEGF pathway. The distribution of toxicities within mAb strategy and patient groups should be taken into consideration as future anti-VEGF pathway therapies are introduced into the clinic to minimize adverse effects and to monitor for new patterns of toxicity.

The opportunity to better understand the function of individual components of the VEGF pathway in the tumor microenvironment is afforded by evaluation of the efficacy and biology of the anti-VEGF strategies outlined in this review. As there are very few studies that directly compare anti-VEGF pathway mAbs, it is difficult to say with certainty that one strategy is best or will work for every patient. All of the mAbs discussed in this chapter target the VEGF pathway; however the specificity of the different mAbs affects the function of these therapies within the tumor microenvironment and provides clues to the potential advantages and disadvantages among the different therapies. It is of particular interest to compare the strategies that are specific to VEGF (bevacizumab and r84) to VEGF-Trap and those that inhibit VEGFR1 (MF1, IMC-18F1) or VEGFR2 (DC101, IMC-1C11, IMC-1121B) directly.

Bevacizumab and r84 are highly specific for VEGF-A and do not directly interfere with other VEGF family members. r84 is even more selective than bevacizumab due to the fact that it only inhibits VEGFR2 activation, leaving intact VEGFR1 signaling. In endothelial cells, VEGFR1 primarily functions as a negative inhibitor of VEGFR2 signaling by acting as a decoy receptor for VEGF and preventing VEGF from binding to and inducing angiogenesis through VEGFR2. This idea is supported by previously mentioned genetic experiments where loss of VEGFR1 leads to embryonic death due to too many endothelial cells, however mice expressing only the extracellular domain of VEGFR1 are viable (Fong et al., 1995; Hiratsuka et al., 1998). Additionally, VEGF binding to VEGFR1 can stimulate SHP-1 phosphatase to actively reduce levels of VEGFR2 phosphorylation (Nozaki et al., 2006). Further, whereas VEGF activation of VEGFR1 does not alter gene expression, PlGF binding to VEGFR1 *in vitro* changes the gene expression of more than 50 genes (Autiero et al., 2003). PlGF may also provide an escape mechanism for anti-VEGF targeted therapy and blocking PlGF directly has been demonstrated to have anti-tumor effects (Fischer et al., 2007). Treatment with r84 would allow for regulatory signaling through VEGFR1 and could reduce PlGF activation of VEGFR1 as a result of competition with PlGF for VEGFR1 binding. Therefore, VEGF binding to VEGFR1 may be an important negative regulator of tumor angiogenesis that could be harnessed with r84, but not with bevacizumab. VEGF-Trap blocks VEGF from binding to

VEGFR1 and VEGFR2 and blocks PlGF from binding to VEGFR1, thereby preventing negative regulation of VEGFR2 activity by VEGFR1 similar to bevacizumab and uniquely controlling VEGFR1 activation by PlGF. Thus the *in vivo* mechanisms of action of VEGF-Trap may fall somewhere between that of r84 and bevacizumab.

Alternatively, blocking VEGFR1 activity with mAbs has been very effective in VEGFR1 expressing tumors (Wu et al., 2006a). VEGFR1 activity has also been linked to tumor metastasis and blocking VEGFR1 with MF1/IMC-18F1 reduces tumor growth, demonstrating the potential importance of this receptor in tumor progression and the need to inhibit its function in patients. Despite these data, the overall functions of VEGFR1 remain unclear and the full effects of VEGFR1 blockade are uncertain. However, there is still a strong possibility that VEGFR1 functions as a negative regulator of VEGFR2 and direct targeting of VEGFR1 with MF1/IMC-18F1 may be in effect, inhibiting an inhibitor of angiogenesis, which may be therapeutically counterproductive. Therefore, the results of on-going IMC-18F1 and IMC-1121B clinical trials and entry of r84 into the clinical arena are highly anticipated to elucidate the importance of VEGFR1 signaling in tumor angiogenesis and progression.

As previously mentioned, VEGFR2 is the predominant mediator of VEGF-induced angiogenesis and consequently, blocking functional signaling of this receptor with neutralizing antibodies such as DC101, IMC-1C11, and IMC-

1121B is effective at reducing angiogenesis and tumor growth. There is increased expression of VEGFR2 in the tumor microenvironment, which in turn increases the potential of anti-VEGFR2 therapies to specifically target the tumor and not normal tissues. Directly targeting VEGFR2 also prevents receptor activation by other VEGF family members (e.g., VEGF-C, -D), which are not blocked by bevacizumab, r84, or VEGF-Trap. Additionally, the anti-VEGFR2 mAbs do not limit VEGFR1 negative regulation of VEGFR2, potentially enhancing blockade of VEGFR2 function. However, the anti-VEGFR2 mAbs will also block soluble VEGFR2, a natural inhibitor of lymphangiogenesis (Albuquerque et al., 2009). This effect is a potential disadvantage of directly targeting VEGFR2, given the importance of the lymphatic vasculature in metastasis (Saharinen et al., 2004). Infiltration immune cells such as macrophages within tumors can promote tumor survival and progression (Murdoch et al., 2008). Macrophages in tumor bearing animals express VEGFR2, and blockade of this receptor has been demonstrated to reduce macrophage migration and infiltration in tumors (Dineen et al., 2008; Roland et al., 2009b). Therefore, targeting VEGFR2 directly can negatively affect tumor growth and metastasis by reducing the population of tumor-promoting immune cells within the tumor microenvironment.

The anti-VEGFR antibodies have a broader specificity profile given that these agents interfere with signaling pathways stimulated by multiple members of the VEGF family. Thus far, it is unclear if a broader specificity anti-VEGF agent

is more effective than bevacizumab or r84. In fact, a recent direct comparison of mouse chimeric r84 with sunitinib and a peptoid that binds and inhibits VEGFR1 and VEGFR2 demonstrated that r84 was as or more effective in controlling tumor growth in two models of breast cancer in immunocompetent mice (Roland et al., 2009b; Sullivan et al., 2010). This study also evaluated the immunological phenotype of tumors under therapy and found that in general, treatment of r84 resulted in fewer immunosuppressive cells (e.g. myeloid-derived suppressor cells, $T_{reg}$, immature dendritic cells) in the tumor microenvironment. These cell-based changes are likely the result of an altered cytokine profile after therapy (Roland et al., 2009b). To our knowledge similar studies have not been performed with the other anti-VEGF agents discussed here. Species specificity issues and other inherent challenges with pharmaceutical-based novel therapies preclude a head to head test of these leading anti-VEGF strategies in pre-clinical models. Thus we are forced to make assumptions regarding the potential superiority of one agent over another based on the efficacy observed in similar models and the biology of the therapy employed.

In reality, arguing the benefits and shortcomings of the individual mAb-based strategies available for targeting the VEGF pathway in cancer may be short-sighted. Selectively targeting angiogenesis in patients will most likely require an arsenal of therapeutics and the best strategy may very well depend upon the tumor type, stage, histology and/or may be entirely patient specific. This highlights the

need for biomarkers that can predict a patient's response to anti-angiogenic therapy (a topic that will be examined more thoroughly in Chapters Four and Five), as well as the need for an array of selective therapies to improve patient survival by inhibiting tumor angiogenesis.

# CHAPTER TWO

# MATERIALS AND METHODS

## 2.1 Construction of human anti-VEGF antibodies

Human anti-VEGF single chain variable fragments (scFvs) were created by Affitech AS (Olso, Norway) and Peregrine Pharmaceuticals, Inc. (Tustin, CA) and screened for specific VEGF binding characteristics. The most desirable scFvs were cloned into full length antibody expression vectors containing the glutamine synthetase gene, transfected into CHO K1SV cells, and selected in a glutamine free cell culture media. The cells were plated into flat bottom 96 well culture plates, and wells with antibody production were diluted and the cells were subcloned. Once subcloned, the high production cells were grown to 500 mL

cultures and the antibody was purified by Protein-A affinity chromatography and size-exclusion chromatography for purities of greater than 90% monomer.

## 2.2 ELISA analysis of r84

To evaluate the binding specificities of r84, a series of enzyme-linked immunosorbent assays (ELISAs) were performed.

### *2.2.1 Determination of r84 specificity*

Relative binding affinity of r84 for mouse and human VEGF was determined by ELISA. Recombinant human VEGF (R&D Systems®, Minneapolis, MN) or mouse VEGF (Sigma-Aldrich®, St. Louis, MO) was coated onto the bottom of 96-well plates at 0.5 µg/mL. Wells were blocked and then incubated with r84 starting at 2 µg/mL with a serial dilution factor of four. Antibody bound to the wells was detected by incubation with anti-human Fc horseradish peroxidise (HRP)-conjugated antibody followed by development with HRP substrate.

### *2.2.2 r84 specificity within VEGF family*

Human VEGF-A, mouse VEGF-A, human VEGF-B, human VEGF-C, human VEGF-D, and human PlGF (R&D Systems®) were coated onto 96-well

ELISA plates at 0.5 µg/mL. Wells were blocked and then incubated with human r84 at 1 µg/mL. Antibody bound to the wells was detected as described above.

### *2.2.3 r84 receptor blocking ELISAs*

Recombinant human VEGFR1/Fc or VEGFR2/Fc (R&D Systems®) was coated onto the bottom of 96-well plates at 1 µg/mL. Wells were blocked and then incubated with 2.38 nM or 4.76 nM biotinylated VEGF for VEGFR1 and VEGFR2, respectively +/- fold the indicated molar excess of antibody. Labelled VEGF bound to the wells was detected by incubation with strepavidin HRP-conjugate, developed as described above, and displayed as a percentage of VEGF binding alone in the absence of antibody.

## 2.3 Endothelial cell *in vitro* assays

The effect of r84 on endothelial cell function and signaling *in vitro* was assessed using human dermal microvascular endothelial cell (HDMEC) (ScienCell™ Research Laboratories, Carlsbad, CA), porcine aortic endothelial cell (PAE)-KDR (Waltenberger et al., 1994), PAE-Flt-1 (Waltenberger et al., 1994) endothelial cell lines.

### *2.3.1 Migration Assays*

A modified Boyden chamber assay was used. 20,000 endothelial cells (ECs) (HDMEC (ScienCell™ Research Laboratories, Carlsbad, CA), PAE-KDR (Waltenberger et al., 1994), PAE-Flt-1 (Waltenberger et al., 1994)) were plated in serum free media on 8.0 µm pore size cell culture inserts (BD Falcon™, San Jose, CA) and allowed to migrate overnight at 37º C. Recombinant human or mouse VEGF (Sigma-Aldrich®) was used as a chemo-attractant at 100 ng/mL, with antibodies added at a 500-fold molar excess. Insert membranes were isolated following migration and stained with 4',6-diamidino-2-phenylindole (DAPI) to allow for quantification of migrated cells (total magnification, 100X).

### *2.3.2 Stimulation Assays*

HDMEC and PAE-KDR, -Flt-1 cell lines were maintained in 100 $mm^2$ tissue culture dishes in MCDB 131 (Gibco®, Carlsbad, CA) media supplemented with 0.4 µg/mL endothelial growth factor and 20% fetal bovine serum (FBS). Following 24 hour serum starvation, cells were stimulated for two minutes with 100 ng recombinant human VEGF or mouse (R&D Systems®) +/- 500-fold molar excess antibody. Cell lysates of stimulated cells were prepared by incubating pelleted cells in M-PER® Mammalian Protein Extraction Reagent (ThermoScientific, Rockford IL) containing freshly added protease and phosphatase inhibitors on ice for 20 minutes with period vortexing followed by centrifugation at 13,500 rpm for 10 minutes. Cleared lysates supernatant was

transferred to a fresh tube and total protein concentration was evaluated using a BCA reaction kit (Pierce Biotechnology, Inc., Rockford, IL). Lysates were analyzed by Western blot using commercially-available antibodies specific for targets of interest (total and phospho- VEGFR2, p38, PLCγ, ERK1/2 (Cell Signaling Technology®, Danvers, MA), and VEGFR1 (Abcam®, Cambridge, MA)).

## 2.4 Animal studies

4-6-week-old NOD/SCID mice were purchased from the breeding core at the University of Texas Southwestern Medical Center. Animals were housed in a pathogen-free facility and all procedures were performed in accordance with a protocol approved by the Institutional Animal Care and Use Committee at the University of Texas Southwestern Medical Center.

### *2.4.1 Tumor cell lines*

All tumor cell lines (with the exception of PANC-1) were generously provided by the Minna and Gazdar laboratories. The human lung cancer cell lines (with the exception of Calu-3, Calu-6 and A549) used in these studies were established by the Minna and Gazdar laboratories. Lung cancer cell lines that were established at the National Cancer Institute or the UTSW Hamon Center for Therapeutic Oncology Research are denoted with the prefix H or HCC,

respectively (Gazdar et al., 2010). All tumor cells lines were cultured in RPMI-1640 medium (HyClone®, Waltham, MA) supplemented with 5% FBS. Cell lines were confirmed to be pathogen free and were authenticated to confirm origin prior to use.

### *2.4.2 Subcutaneous NSCLC xenograft intrinsic resistance to anti-VEGF therapy study*

2.5 million NSCLC cells were injected (in phosphate buffered saline (PBS)) subcutaneously into the right flank of NOD/SCID mice. Mice were treated with 50 mg/kg/week r84 and 25 mg/kg/week bevacizumab/Avastin® (Genentech/Roche) and a control human antibody (palivizumab/Synagis® anti-respiratory syncytial virus or XTL anti-hepatitis C virus supplied by Peregrine Pharmaceuticals, Inc. (Tustin, CA)) via intraperitoneal (IP) injection starting one day post tumor cell injection (TCI) (n = 8-9 per group). Mice were monitored twice a week, recording weights, taking perpendicular tumor measurements, and observing for signs of distress such as weight loss and inactivity. Tumor volume was calculated from perpendicular tumor measurements using the formula $D \times d^2 \times (\pi/6)$, where d = the smaller of the two measurements. Therapy continued until average control-treated tumor volume reached 1500 $mm^3$ or until day 60 post TCI, at which point animals were sacrificed.

### *2.4.3 Toxicity studies*

Five million PANC-1 human pancreatic cancer cells (ATCC, Manassas, VA) (in PBS) were injected subcutaneously into the right flank of NOD/SCID mice. An equal number of NOD/SCID mice were not injected with tumor cells. Therapy began one day post TCI. Tumor bearing (TB) and non-tumor bearing (NTB) mice were treated with 50 mg/kg/week r84 and palivizumab via IP injection. Each group consisted of five mice. Mice were monitored as previously described. All mice were sacrificed following 12 weeks of continuous therapy and evaluated for r84-induced toxicity. Blood was collected from animals at sacrifice; serum was isolated following centrifugation and analyzed by the mouse metabolic phenotyping core at the University of Texas Southwestern Medical Center.

A second toxicity study was performed in immunocompetent mice harbouring spontaneous pancreatic cancer (*p48cre/Kras$^{G12D}$/INK4a*) (Aguirre et al., 2003). Mice were treated with saline (n = 4) or 25 mg/kg/week mouse chimeric r84 (mcr84, n = 3) via IP injection or with 50 mg/kg/week sunitinib (n = 4) by daily oral gavage five days per week. Sunitinib was purchased from LC Laboratories (Woburn, MA). Therapy began when mice reached eight weeks old. Mice were monitored for weight gain as previously described. At weeks two and seven of therapy, tail vein cuff blood pressures of all mice were measured using the Visitech Systems BP-2000 Series II Blood Pressure Analysis System™ through the O'Brien Kidney Research Core Center at the University of Texas

Southwestern Medical Center. To familiarize mice to the procedure, tail cuff blood pressures were measured for five consecutive days, with data collection on the fifth day. Average systolic pressures were calculated from data collected on the last day of measurement (day five). At week six of therapy metabolic cages obtained through the O'Brien Kidney Research Core Center at the University of Texas Southwestern Medical Center were used to collect urine from all animals over a 24-hour collection period. Fresh urine samples were then submitted to the University of Texas Southwestern Medical Center mouse metabolic phenotyping core for analysis of total levels of urine protein and creatine. All mice were sacrificed following eight weeks of continuous therapy and evaluated for mcr84- and sunitinib-induced toxicity. Blood was collected from animals at sacrifice; serum was isolated following centrifugation and analyzed by the mouse metabolic phenotyping core at the University of Texas Southwestern Medical Center.

### *2.4.4 Therapy dose titration*

2.5 million A549 NSCLC cells (in PBS) were injected subcutaneously into the right flank of NOD/SCID mice. Mice were treated with 5, 15, or 50 mg/kg/week r84 and bevacizumab and 15 mg/kg/week control IgG (Peregrine Pharmaceuticals, Inc.) via IP injection starting one day post TCI. Each group consisted of eight mice and were monitored as above. Therapy continued until

average control-treated tumor volume reached 1200 $mm^3$, at which point animals were sacrificed.

### *2.4.5 Generation of Axl knockdown NSCLC lines*

pGIPZ lentiviral shRNAmir Open Biosystems constructs (Thermo Fisher Scientific, Huntsville, AL) targeting human *AXL* were generously provided by the Shay and Wright laboratories at the Univeristy of Texas Southwestern Medical Center. A non-targeting control (NTC) plasmid provided by the Minna laboratory at the Univeristy of Texas Southwestern Medical Center was used as a negative control for gene knockdown. Bacterial production and subsequent purification of construct plasmid DNA together with pMD.G-VSVG and pCMV-ΔR8.91 plasmids were transiently transfected with Fugene® 6 (Roche, Indianapolis, IN) into 293T cells grown in DMEM containing 10% FBS. Resulting virus was harvested and used to infect A549, Calu-3 and Calu-6 NSCLC cells. Stable shRNA expressing cells were generated following two weeks of culture in puromycin. Cell lines were checked for Axl knockdown by qPCR and Western blot analysis.

2.5 million A549 cells stably expressing NTC or *AXL* shRNAmir (A549-NTC or A549-H12, respectively) were injected (in PBS) subcutaneously into the right flank of NOD/SCID mice. Mice were treated with 25 mg/kg/week bevacizumab or saline via IP injection starting one day post TCI (n = 8 per

group). Mice were monitored twice a week, recording weights, taking perpendicular tumor measurements, and observing for signs of distress such as weight loss and inactivity. Therapy continued until average tumor volume in control-treated animals reached 1500 $mm^3$, at which point animals were sacrificed.

### *2.4.6 Subcutaneous NSCLC xenograft combination bevacizumab and 10C9 therapy study*

2.5 million Calu-3, Calu-6 NSCLC cells were injected (in PBS) subcutaneously into the right flank of NOD/SCID mice. Mice were treated with 25 mg/kg/week bevacizumab or saline via IP injection starting one day post TCI (n = 16 per group). Mice were monitored twice a week, recording weights, taking perpendicular tumor measurements, and observing for signs of distress such as weight loss and inactivity. Therapy continued until average tumor volume for each group reached 140 $mm^3$ at which time saline-treated mice were randomized to receive either saline or 25 mg/kg/week anti-human Axl monoclonal antibody10C9 (BerGenBio AS; Bergen, Norway) and bevacizumab-treated mice were randomized to receive bevacizumab or combination bevacizumab and 10C9 (n = 8 per group). Therapy continued until average tumor volume in control-treated animals reached 1500 $mm^3$, at which point animals were sacrificed.

### *2.4.7 Generation and evaluation of NSCLC tumor lines with evasive resistance to anti-VEGF therapy*

2.5 million H1975, H1993, H2073 NSCLC cells that previously displayed intrinsic sensitivity to bevacizumab and r84 therapy were injected (in PBS) subcutaneously into the right flank of NOD/SCID mice. Mice were treated with 50 mg/kg/week r84 and 25 mg/kg/week bevacizumab and saline via IP injection starting one day post TCI (n = 5 per group). Mice were monitored twice a week, recording weights, taking perpendicular tumor measurements, and observing for signs of distress such as weight loss and inactivity. Mice in the control-treated (saline) group were sacrificed when average tumor volume reached 1000 $mm^3$ but therapy continued for r84 and bevacizumab groups. When anti-VEGF-treated individual tumor measurements reached 1500 $mm^3$ mice were sacrificed and tumors were harvested for *ex vivo* culture and subsequent analysis.

To determine the effects of *in vivo* passage and *ex vivo* culture of NSCLC tumor lines on tumorigenicity and resistance to anti-VEGF therapy, 2.5 million H1975, H1993 and H2073 NSCLC cells were injected (in PBS) into the right flank of NOD/SCID mice and received no treatment (n = 5 per group). Mice were monitored as before. When individual tumor measurements reached 1500 $mm^3$ mice were sacrificed and tumors were harvested for *ex vivo* culture and subsequent analysis.

Following approximately 30 days of *ex vivo* culture, 2.5 million H1975, H1993 or H2073 cells generated from tumors that grew out in the face of extended r84 therapy (named H1975-81) or without treatment (named H1975-713, H1993-714 and H2073-712) were injected (in PBS) subcutaneously into the right flank of NOD/SCID mice. Mice were treated with 50 mg/kg/week r84 and 25 mg/kg/week bevacizumab and a control human antibody (XTL anti-hepatitis C virus supplied by Peregrine Pharmaceuticals, Inc. (Tustin, CA) via IP injection starting one day post TCI (n = 3 per group). Mice were monitored twice a week, recording weights, taking perpendicular tumor measurements, and observing for signs of distress such as weight loss and inactivity. Therapy continued until average control-treated tumor volume reached 1500 $mm^3$ at which point animals were sacrificed.

### 2.5 Histology and Immunohistochemical Studies

Formalin-fixed, paraffin-embedded tissues were sectioned and stained with hematoxylin and eosin by the molecular pathology core laboratory at the University of Texas Southwestern Medical Center. Snap frozen tumors were sectioned, blocked with 20% Aquablock (East Coast Biologics, North Berwick, ME) and stained for markers of interest. Primary antibodies used include MECA-32 (DSHB; University of Iowa), endomucin (Santa Cruz Biotechnology®, Inc., Santa Cruz, CA), NG2 (Millipore®, Billerica, MA), smooth muscle actin

(NeoMarkers, Fremont, CA), Lyve1, VEGFR2 (55B11) (Cell Signaling Technology®, Danvers, MA), rabbit anti-VEGFR2 T014 (purified in our laboratory) (Brekken et al., 1998; Huang et al., 1998), rat anti-VEGFR2 RAFL-2 (Ran et al., 2003), and insulin (Dako, Glostrup, Denmark).

### 2.6 Generation of xenograft tumor lysates

Flash frozen tumor tissue was placed in M-PER® Mammalian Protein Extraction Reagent (ThermoScientific, Rockford IL) containing freshly added protease and phosphatase inhibitors and homogenized using a Qiagen TissueLyser at 20 Hz for one minute followed by centrifugation at 13,000 rpm for 10 minutes. Cleared lysates supernatant was moved to a fresh tube. Total protein concentration was evaluated using a BCA reaction kit (Pierce Biotechnology, Inc., Rockford, IL) and samples were stored at -80°C until needed for further analysis. Lysates were analyzed by Western blot using commercially-available antibodies against Axl (Abcam®, Cambridge, MA) and β-actin (Sigma-Aldrich Corp., St. Louis, MO).

### 2.7 SABiosciences angiogenesis growth factors and inhibitors qPCR array

To evaluate the expression of a panel of angiogenesis growth factors and inhibitors in our NSCLC tumors we used SABiosciences $RT^2$ Profiler™ PCR arrays (Catalog number PAHS-072A; Qiagen Inc., Valencia, CA). RNA was

isolated from control-treated Calu-6, A549, Calu-3, H1155, H1395, H2073, H1975 and H1993 tumors (n = 3 per line) using TRIzol® (Invitrogen™, Carlsbad, CA) and Qiagen RNeasy® Mini (Qiagen Inc., Valencia, CA) reagents. RNA quality and concentration was evaluated by spectrophotometry A total of 1 μg of purified RNA was reversed transcribed to cDNA using SABiosciences $RT^2$ First Strand Kit and subsequently loaded with SABiosciences qPCR master mix into plates pre-loaded with 96 human primer sets (84 specific for angiogenesis growth factors and inhibitors, 12 housekeeping genes and RNA and PCR controls) and run on an Applied Biosystems™ 7300 System. A complete list of genes included in this array is provided in Appendix A. For each plate, the threshold cycle (Ct) for all primer sets was calculated using Applied Biosystems™ 7300 software and was uploaded to SABiosciences web-based data analysis to calculate fold changes in gene expression between lines with intrinsic resistance to bevacizumab, r84 or sensitivity to bevacizumab or r84. The raw $C_t$ values from these arrays is included in Appendix B.

### 2.8 MILLIPLEX human and mouse cytokines array

We used the MILLIPLEX® MAP to evaluate expression of 32 mouse and 39 human cytokines in our NSCLC tumors (Catalog numbers MPXMCYTO-70K and MPXHCYTO-60K; Millipore™, Billerica, MA). A complete list of cytokines detected in these arrays is provided in appendix C. Lysates from control-, r84- and

bevacizumab-treated Calu-6, A549, Calu-3, H1155, H1395, H2073, H1975 and H1993 tumors (n = 3 per group) were generated as described previously (Chapter 2.6) and 10 μg of total protein was loaded onto MILLIPLEX MAP kits as per manufacturer's instructions. Concentrations of each cytokine per sample were calculated using MILLIPLEX MAP data analysis software and are provided in Appendix D and Appendix E.

## 2.9 Expression profiling of NSCLC cell lines and tumors by microarray

Dr. Minna's laboratory at the University of Texas Southwestern Medical Center expression profile data generated by Affymetrix (U133 plus 2.0 and U133AB chips) on many lung cancer cell lines, including the 12 NSCLC lines used our studies. This data was collected from lung cancer cell lines grown *in vitro*. To identify genes associated with resistance to anti-VEGF therapy and with the assistance of Dr. Yang Xie's group at the University of Texas Southwestern Medical Center, the T/C ratios calculated for each NSCLC cell line tested were used as a dichotomized variable to find differentially-expressed genes filtered by a false discovery of < 1% and a > 2 fold change in expression. This analysis generated a list of 101 and 86 genes associated with resistance to r84 and bevacizumab therapy, respectively.

To add to Minna laboratory dataset, we harvested tumor RNA using Qiagen RNeasy® Mini (Qiagen Inc., Valencia, CA) kits from control-treated

Calu-6, A549, Calu-3, H2009, H1299, H460, H358, H1155, H1975, H1993, H1395 and H2073 tumors, from H1975, H1993 and H2073 tumors that were untreated or that grew out in the face of extended r84 or bevacizumab therapy, and from control-, r84-, or bevacizumab-treated H1975-81 tumors (n = 3 samples per cell line and treatment group, 72 samples total). RNA quality was verified with capillary electrophoreses using the Experion System (Bio-Rad; Hercules, CA) and subsequently labeled and hybridized on Illumina Human HT-12 V4 array platforms by the University of Texas Southwestern Comprehensive Cancer Center Genomics Core. Completed raw data was imported and analyzed using MATRIX (MicroArray Transformation in Microsoft Excel) software, a Microsoft Visual Basic program created by Dr. Luc Girard in the Minna Laboratory (luc.girard@utsouthwestern.edu). MATRIX was used to normalize median value transcript expression across all samples and to calculate $\log_2$-transformations. Subsequent analysis as previously described was performed to determine *in vivo* NSCLC gene expression associated with resistance to anti-VEGF therapy.

### 2.10 Reverse-phase protein array

Lysates were generated from control-treated Calu-6, A549, Calu-3, H2009, H1299, H460, H358, H1155, H1975, H1993, H1395 and H12073 tumors (n = 3 per line), untreated H1975, H1993, H2073 tumors (n = 3 per line), r84- and bevacizumab-treated H1975, H1993, H2073 following first round of evasive

resistance to therapy (n = 3 per treatment group per line), and control-, r84-, and bevacizumab-treated H1975-81 tumors following second round of evasive resistance to therapy (n = 3 per treatment group per line). Tumor lysates generated as previously described (Chapter 2.6). In addition, *in vitro* lysates were generated from Calu-6, A549, Calu-3, H2009, H1299, H460, H358, H1155, H1975, H1993, H1395 and H12073 as previously described in Chapter 2.3.2. Tumor and cell line lysates were adjusted to a concentration of 1 μg/mL (50 μg total), combined with 4X SDS sample buffer (40% glycerol, 8% SDS, 0.25 M Tris-HCl, 10% 2-mercaptoethanol, pH 6.8) and boiled for five minutes.

Reverse-phase protein array (RPPA) was performed and quantitated as described by Nanjundan et al. (Nanjundan et al.). Briefly, tumor protein lysates were printed on nitrocellulose slides with Aushon 2470 Arrayer (Aushon BioSystems, Inc., Billerica, MA) and stained with antibodies using the Dako Autostainer (Dako Cytomation California, Inc., Capinteria, CA). Following primary and secondary incubation, signal was detected with 3, 3'-diaminobenzidine tetrahydrochloride chromagen for 5 minutes. Following signal quantification, all data were row median normalized for signal intensity for each antibody amongst all samples and were logarithm transformed (base 2) for further analysis. Replicate samples were averaged and classified into groups according to bevacizumab response phenotype. Group 1: bevacizumab resistant tumors Calu-6, A549, Calu-3. Group 2: bevacizumab sensitive tumors H2073, H1395, H1993,

H1975. Fold change in expression between the two groups was calculated by fold change = $2^{(\text{Group 1 average} - \text{Group 2 average})}$ to assess differences in protein regulation.

### 2.11 Quantitative real time PCR analysis

Quantitative real time PCR (qPCR) was performed to evaluate NSCLC *AXL* transcript expression. RNA was harvested from NSCLC tumors using Qiagen RNeasy® Mini (Qiagen Inc., Valencia, CA) kits, assessed for quality and concentration by spectrophotometry and reverse transcribed with iScript cDNA Synthesis kits (Bio-Rad; Hercules, CA). The qPCR was then performed with iQ™ SYBR® Green Supermix reagent (Bio-Rad, Hercules, CA) on an Applied Biosystems™ 7300 System to determine $C_t$ values and calculate $\Delta C_t$ values using β-actin as an internal amplification control. *AXL*: (5'- GAC GGG TCT GTG TCC AAT CT -3'; 5'- ACG AGA AGG CAG GAG TTG AA -3'). *β-ACTIN*: (5'- GAC GAG GCC CAG AGC AAG AGA -3'; 5'- ACG TAC ATG GCT GGG GTG TTG -3').

### 2.12 Detection of Axl in NSCLC tumors by ELISA

Expression levels of human Axl was detected in control-, r84-, and bevacizumab-treated tumors (n = 3 per group) using DuoSet® IC sandwich ELISAs (R&D Systems®; Minneapolis, MN). Briefly, a capture anti-Axl antibody was coated in the wells of a 96-well plate and blocked. Following

incubation with 100 µg of tumor lysates, generated as previously described in Chapter 2.6, captured Axl is detected with a biotinylated anti-Axl antibody and developed using streptavidin-HRP. Concentrations of total Axl within tumor lysates samples is then calculated (at pg/mL) from a standard curve provided in the kit.

## 2.13 Anti-human Axl monoclonal antibody 10C9

### *2.13.1 Purification of anti-Axl monoclonal antibody 10C9*

IgG2bRE hybridoma cells expressing a mouse IgG2 against human Axl named 10C9 were generously provided by BerGenBio AS (Bergen, Norway). Cells were grown in DMEM supplemented with 10% FBS and 10% Hybridoma Cloning Supplement (PAA, Austria). Following one week production incubation medium supernatant was harvested and 10C9 was purified by affinity chromatography using a protein A column. Antibody fractions were eluted from the column using pH 3.5 citrate buffer and dialyzed against four changes of 1X PBS. Purified, dialyzed and sterile filtered antibody fractions were checked for Axl-binding activity by ELISA and structural integrity by Coomassie-stained protein gels prior to use in mice.

### *2.13.2 Detection of active 10C9 from mouse serum by ELISA*

Calu-6 or Calu-3 tumor-bearing NOD/SCID mice were treated with 25 mg/kg/week 10C9 with or without bevacizumab. At sacrifice, blood samples were taken and serum was isolated following centrifugation. To detect 10C9 present in treated mouse sera, 96-well plates were coated with recombinant human Axl (R&D Systems®; Minneapolis, MN), blocked, and incubated with a 1:100 starting dilution of sera from saline-, 10C9- and 10C9 + bevacizumab-treated mice (n = 3 per group) and serially diluted with a dilution factor of five (eight dilutions total). 10C9 bound to human Axl on the plate was detected with HRP-conjugated anti-mouse antibody and developed with HRP substrate.

### 2.14 Statistics

Data were analyzed using GraphPad software (GraphPad Prism version 5.00 for Windows, GraphPad Software). Results are expressed as mean ± SE. Differences are analyzed by *t* test or ANOVA, and results are considered significant at a $p$ value of $< 0.05$.

# CHAPTER THREE

# R84, A NOVEL THERAPEUTIC ANTIBODY AGAINST MOUSE AND HUMAN VEGF WITH POTENT ANTI-TUMOR ACTIVITY AND LIMITED TOXICITY INDUCTION


## Abstract

Vascular endothelial growth factor (VEGF) is critical for physiological and pathological angiogenesis. Within the tumor microenvironment, VEGF functions as an endothelial cell survival factor, permeability factor, mitogen, and chemotactic agent. The majority of these functions are mediated by VEGF-induced activation of VEGF receptor 2 (VEGFR2), a high affinity receptor tyrosine kinase expressed by endothelial cells and other cell types in the tumor microenvironment. VEGF can also ligate other cell surface receptors including

VEGFR1 and neuropilin-1 and -2. However, the importance of VEGF-induced activation of these receptors in tumorigenesis is still unclear. We report the development and characterization of r84, a fully human monoclonal antibody that binds human and mouse VEGF and selectively blocks VEGF from interacting with VEGFR2 but does not interfere with VEGF:VEGFR1 interaction. Selective blockade of VEGF binding to VEGFR2 by r84 is shown through ELISA, receptor binding assays, receptor activation assays, and cell-based functional assays. Furthermore, we show that r84 has potent anti-tumor activity and does not alter tissue histology or blood and urine chemistry after chronic high dose therapy in mice. In addition, chronic r84 therapy does not induce elevated blood pressure levels in some models. The ability of r84 to specifically block VEGF:VEGFR2 binding provides a valuable tool for the characterization of VEGF receptor pathway activation during tumor progression and highlights the utility and safety of selective blockade of VEGF-induced VEGFR2 signaling in tumors.

Note: The following chapter is in part made up of a research article written by Laura A. Sullivan under the guidance of Rolf A. Brekken.

## 3.1 Introduction

Angiogenesis is a tightly regulated process that is essential during growth, wound healing and development, as well as cancer growth, progression and metastasis (Folkman, 1971; Roskoski, 2007b). A key stimulant of angiogenesis is vascular endothelial growth factor-A (VEGF). VEGF induces endothelial cell survival, proliferation, and migration its predominant signaling receptor, VEGF receptor 2 (VEGFR2). Tumor associated macrophages also express VEGFR2 and selective blockade of VEGFR2 is able to decrease macrophage infiltration into tumors (Dineen et al., 2008). VEGF signaling through VEGF receptor 1 (VEGFR1) remains unclear, although it is thought to have effects on hematopoiesis, vascular permeability, and monocyte migration. Importantly, there is elevated expression of VEGF, VEGFR1, and VEGFR2 within tumors, providing a therapeutic target. In fact targeting VEGF has lead to the development of anti-angiogenic therapies such as sunitinib malate (Sutent®, SU11248, Pfizer, Inc.), sorafenib (Nexavar®, BAY 43-9006, Bayer Pharmaceuticals Corp.), bevacizumab (Avastin®, Genentech/Roche), IMC-1121b (ramucirumab, ImClone), VEGF-Trap (aflibercept, Regeneron) and 2C3 (Brekken et al., 1998; Brekken et al., 2000; Grothey and Galanis, 2009; Roskoski, 2007b).

Sunitinib and sorafenib are small molecule inhibitors of multiple receptor tyrosine kinases (RTKs) including the VEGF receptors. Sunitinib inhibits phosphorylation of VEGFR1, VEGFR2, VEGFR3, platelet derived growth factor

receptor (PDGFR) -α and -β, Fms-like tyrosine kinase-3 (Flt-3), glial cell-derived neurotrophic factor receptor and the stem cell factor receptor Kit (Roskoski, 2007a, b). Sorafenib inhibits phosphorylation of VEGFR2, VEGFR3, Kit, PDGFR-β, Raf and Flt-3. (Roskoski, 2007b; Wilhelm et al., 2008; Wilhelm et al., 2004). These drugs have been USFDA-approved for the treatment of renal cell carcinoma (sunitinib and sorafenib), gastrointestinal stromal tumors (sunitinib), pancreatic neuroendocrine tumors (sunitinib; http://www.cancer.gov/cancertopics/druginfo/fda-sunitinib-malate) and unresectable hepatocellular carcinoma (sorafenib) (Raymond et al., 2011; Roskoski, 2007b; Wilhelm et al., 2008; Wilhelm et al., 2004).

Bevacizumab is a humanized monoclonal anti-VEGF antibody that inhibits VEGF from binding to and signaling through VEGFR1 and VEGFR2. Bevacizumab is approved in combination with cytotoxic chemotherapy for the treatment of colorectal cancer and NSCLC, as monotherapy in glioblastoma, and in combination with interferon for renal cell carcinoma (Kamba and McDonald, 2007; Vredenburgh et al., 2009; Yan et al., 2008). Treatment with bevacizumab plus chemotherapy results in a delay of tumor progression and increases in patient survival (Kamba and McDonald, 2007; Roskoski, 2007b). However, treatment with bevacizumab, sorafenib, and sunitinib, is also associated with a number of rare although serious toxicities including gastro-intestinal perforations, bleeding,

proteinurea, and glomerulosclerosis (Gerber et al., 2007; Kamba and McDonald, 2007; Roodhart et al., 2008).

IMC-1121b is a high affinity, fully human IgG1 monoclonal antibody that recognizes VEGFR2. IMC-1121b binding to VEGFR2 inhibits ligand-induced activation of the receptor. There are several on-going Phase I, II, and III clinical trials evaluating the efficacy of IMC-1121b in a number of tumor types (Grothey and Galanis, 2009).

VEGF-Trap is comprised of the second and third extracellular immunoglobulin domains of VEGFR1 and VEGFR2, respectively, joined by an IgG1 Fc region. The resulting fusion protein traps with high affinity multiple VEGF family members including VEGF and PlGF (Holash et al., 2002). Currently, VEGF-Trap is being tested in Phase III clinical trials in a number of tumor types (Grothey and Galanis, 2009).

2C3 is a murine, monoclonal antibody against VEGF that specifically blocks human VEGF binding to VEGFR2 (Brekken et al., 1998). The selective inhibition of VEGF:VEGFR2 signaling by 2C3 reduces vascular permeability, decreases endothelial cell growth, and decreases tumor growth in murine xenograft models. Additionally, 2C3 reduces tumor microvessel density (MVD) and macrophage infiltration and down-regulates VEGFR2 expression on the tumor vasculature (Brekken et al., 1998; Brekken et al., 2000; Dineen et al., 2008;

Zhang et al., 2002b). The desirable anti-angiogenic effects of 2C3 lead to the development of a human antibody that retains 2C3 specificity.

Here we describe a fully human monoclonal antibody, r84 (AT001, Affitech AS) that binds to mouse and human VEGF and specifically inhibits VEGF binding to VEGFR2, while leaving intact VEGF interaction with VEGFR1. Through blockade of VEGFR2 signaling, r84 inhibits the migration of VEGFR2 positive endothelial cells, and blocks VEGFR2 phosphorylation and downstream signaling. In addition, treatment of mice bearing tumor xenografts with r84 controls tumor growth resulting in tumor vascular changes, including reductions in tumor MVD and in tumor lymphatic vessel density (LVD). Furthermore, extended treatment with r84 does not induce significant systemic toxicity in mice.

## 3.2 Results

### *3.2.1 Generation of a fully human monoclonal antibody against VEGF*

The success of 2C3 in preclinical models led to the development of a fully human monoclonal antibody that recognizes VEGF and retains many of the characteristics of 2C3. A number of anti-VEGF human single chain variable fragments (scFv) were screened for several characteristics such as a competition with 2C3 for binding to VEGF, the ability to block VEGF:VEGFR2 binding, and

the ability of the scFv to bind to different VEGF isoforms such as VEGF165 and VEGF121.

### *3.2.2 r84 binds human and mouse VEGF-A and specifically blocks VEGF from binding to VEGFR2*

To determine the binding specificity of r84, a series of ELISAs were performed. A titration of r84 against recombinant human or mouse VEGF demonstrated that r84 binds with equal affinity to both species (Figure 3.1 A). This result established r84 as an important tool in evaluating the contribution of both tumor cell- and host-derived VEGF in tumor progression using xenograft models. The binding specificity of r84 differs from other anti-VEGF antibodies, such as bevacizumab and 2C3 that recognize only human VEGF. Next, the specificity of r84 within the VEGF family was determined. r84 only bound wells coated with recombinant human and mouse VEGF-A (Figure 3.1 B).

The effect of r84 on VEGF binding to VEGFR1 and VEGFR2 was determined using ligand-receptor ELISAs. 2C3 and r84 at increasing fold molar excess significantly reduced biotinylated-VEGF binding to VEGFR2, compared to binding of biotinylated-VEGF alone or in the presence of a non-specific control IgG (Figure 3.2 A). In contrast, neither 2C3 nor r84 inhibited binding of biotinylated-VEGF to VEGFR1 (Figure 3.2 B). However, at a 500-fold molar excess of antibody to biotinylated-VEGF, bevacizumab decreased VEGF binding

to VEGFR1 by approximately 80% (Figure 3.2 C). These blocking ELISAs demonstrate the precise binding of r84 to VEGF to selectively inhibit the VEGF:VEGFR2 interaction.

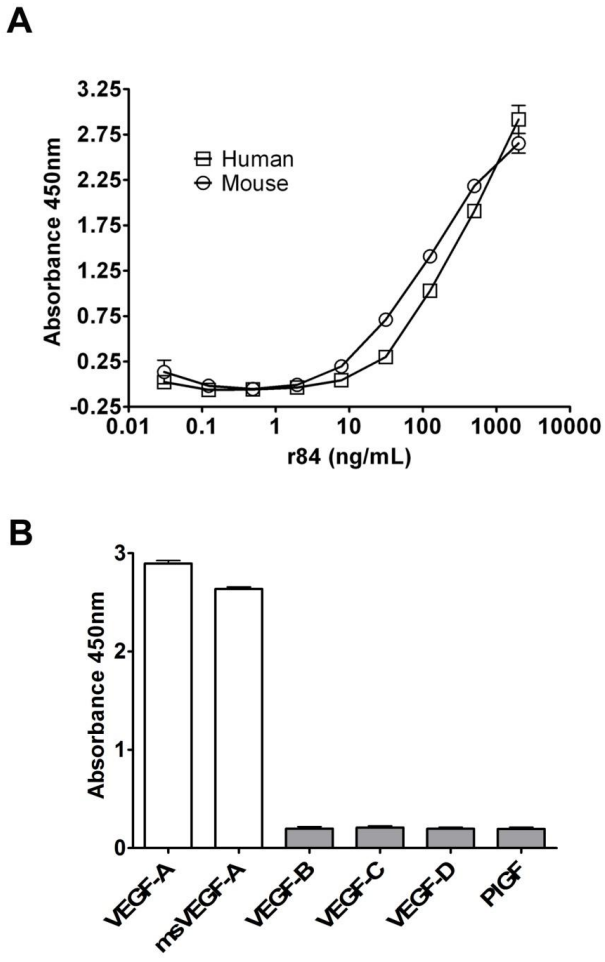


**Figure 3.1: r84 binds human and mouse VEGF-A.**

**A**, Recombinant human VEGF coated at 0.5 mg/mL was detected with a titration of fully human monoclonal antibody r84. r84 bound to VEGF was detected with an anti-human Fc HRP-conjugated antibody, demonstrating r84 binds both human and mouse VEGF-A (open squares and circles, respectively). **B**, Recombinant human and mouse VEGF-A, and human VEGF-B, -C, -D, and PlGF coated at 0.5 mg/mL was detected with r84 at 1 mg/mL. Binding of r84 to VEGF family member was detected as in **A**, demonstrating r84 binds only human and mouse VEGF-A and not other VEGF family members.

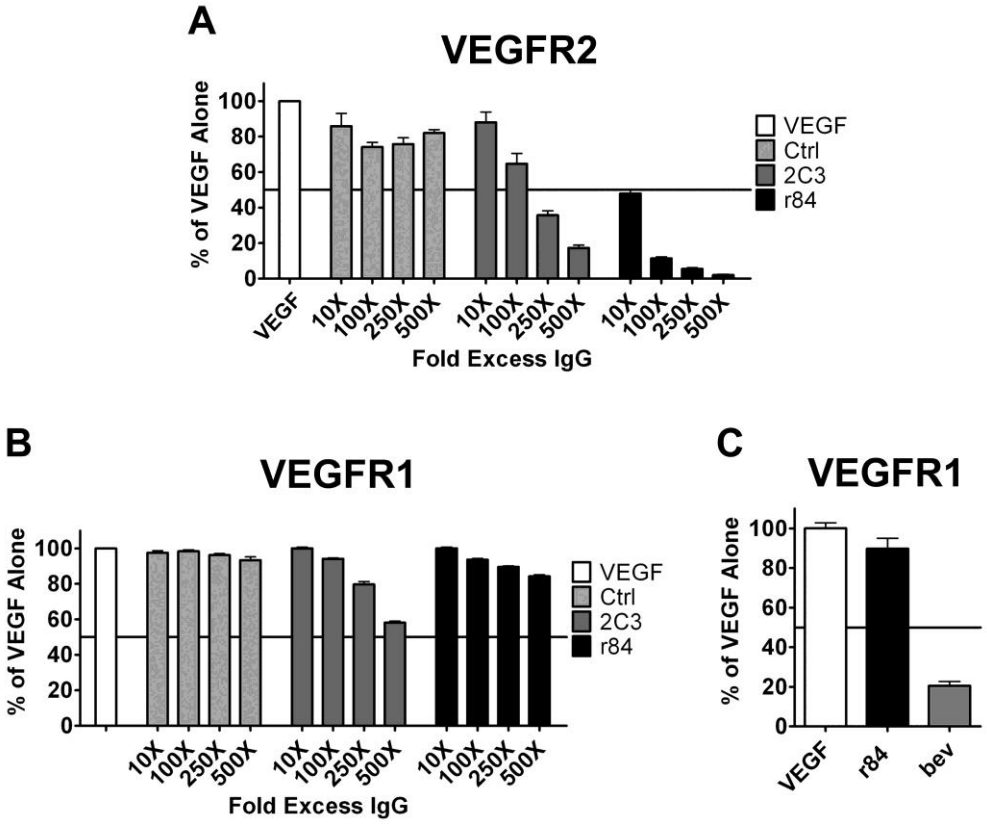


**Figure 3.2: r84 specifically blocks VEGF-A from binding to VEGFR2 but not VEGFR1**.

VEGFR2 (**A**) and VEGFR1 (**B, C**) were coated at 1 mg/mL and incubated with 4.76 nM or 2.38 nM biotinylated VEGF, respectively, +/- the indicated fold excesses of antibody (Control IgG, 2C3, r84). r84 and 2C3 specifically block biotinylated-VEGF binding to VEGFR2 (**A**), but not VEGFR1 (**B**). In contrast, a 500-fold molar excess bevacizumab (bev) reduces biotinylated-VEGF binding to VEGFR1, compared to biotinylated-VEGF alone or plus r84 (**C**).

### *3.2.3 r84 effects VEGFR2-mediated endothelial cell function*

The effect of r84 on endothelial cells was determined using several *in vitro* assays. First, a transwell assay was used to test the effects of anti-VEGF antibodies on VEGF-induced endothelial cell migration. Three different endothelial cell lines, selected for their VEGF receptor expression, were used for the migration assays. Human dermal microvascular endothelial cells (HDMEC) express both VEGFR1 and VEGFR2, porcine aortic endothelial cells (PAE)-KDR and PAE-Flt-1 express high levels of VEGFR2 or VEGFR1, respectively (Waltenberger et al., 1994). Human VEGF significantly induced migration of all three cell types compared to serum free media alone ($p < 0.05$ for HDMEC, $p < 0.001$ for PAE-KDR, -Flt-1), and a non-specific control IgG did not affect VEGF-induced migration (Figure 3.3 A). Both r84 and bevacizumab significantly inhibited VEGF-induced migration of VEGFR2-expressing endothelial cells ($p < 0.001$, Figure 3.3 A, HDMEC, PAE-KDR). However, only bevacizumab was able to decrease the migration of PAE-Flt-1 cells towards VEGF (Figure 3.3 A, PAE-Flt-1). To further evaluate the specificity of r84 to mouse VEGF, migration assays were performed with PAE-KDR cells using mouse VEGF as the chemotactic agent. As seen with human VEGF, mouse VEGF significantly induced the migration of PAE-KDR cells as compared to serum free media alone (Figure 3.3 B). Only r84 was able to significantly inhibit this migration, while bevacizumab and a control IgG had no effect on cell migration ($p < 0.001$, Figure 3.3 B). The

ability of r84 to specifically block both human and mouse VEGF-induced migration of VEGFR2-expressing endothelial cells (HDMEC, PAE-KDR) but not VEGFR1-expressing endothelial cells (PAE-Flt-1) demonstrates the selectivity of r84 to inhibit VEGF-induced VEGFR2 activity.

VEGF binding to VEGFR2 initiates receptor phosphorylation and subsequent phosphorylation of downstream pathway components such as phospholipase C gamma (PLCγ), p38, and the MAP kinase extracellular signal-regulated kinase (ERK1/2). PAE-KDR cells stimulated *in vitro* with human VEGF (100 ng, two minutes) induced phosphorylation of VEGFR2, PLCy, p38, and ERK (Figure 3.4 A). Human VEGF stimulation of HDMECs induced phosphorylation of PLCγ and ERK (Figure 3.4 B). Stimulation of PAE-KDR and HDMEC cells with human VEGF plus 500-fold molar excesses r84 or bevacizumab inhibited phosphorylation of VEGFR2 and downstream targets (Figure 3.4 A, 3.4 B). However, only bevacizumab blocked human VEGF-induced phosphorylation of VEGFR1 in PAE-Flt-1 (Figure 3.4 C). Further, stimulation of PAE-KDR cells with mouse VEGF induced phosphorylation of VEGF2, PLCy, and ERK that was only inhibited by r84 and not by bevacizumab or a control IgG (Figure 3.5). This data shows that r84 selectively inhibits human and mouse VEGF binding and signaling through VEGFR2 without interrupting VEGFR1 signaling. The ability of r84 to bind human and mouse VEGF (Figure 3.1) and block VEGF from binding and signaling through VEGFR2 (Figures 3.2-

3.5) makes r84 a unique tool for studying VEGF inhibition in tumor xenograft models, assessing possible toxicity induction and analyzing the importance of VEGFR1 signaling in these processes.

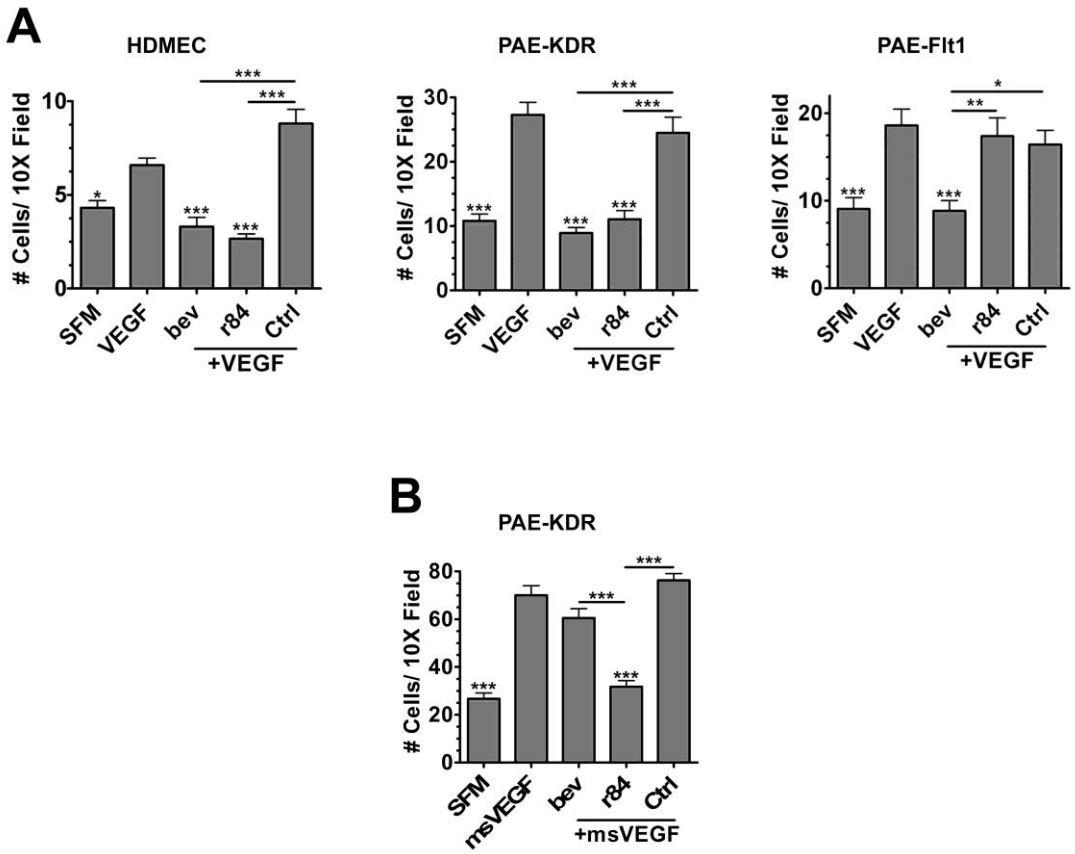


**Figure 3.3: r84 reduces endothelial cell migration *in vitro*.**

**A**, A modified Boyden chamber migration assay was used to assess the effect of r84 and bevacizumab (bev) on VEGF-induced endothelial cell (EC) migration. 20,000 HDMEC, PAE-KDR, PAE-Flt-1 cells were plated on 8.0 mm cell culture inserts and allowed to migrate overnight towards serum free media, human VEGF (**A**, 100 ng/mL), or mouse VEGF (**B**, 100 ng/mL) +/- 500-fold molar excess antibody (bev, r84, control IgG). r84, bev block the human VEGF-induced migration of VEGFR2-expressing ECs (**A**, HDMEC, PAE-KDR). Bev blocks VEGF-induced migration of endothelial cells expressing VEGR1, but r84 does not (**A**, PAE-Flt-1). Only r84 blocks mouse VEGF-induced migration of VEGFR2-expressing PAE-KDR ECs (**B**).
*$p < 0.05$, **$p < 0.01$, ***$p < 0.001$, statistical differences compared to VEGF alone, unless otherwise indicated.

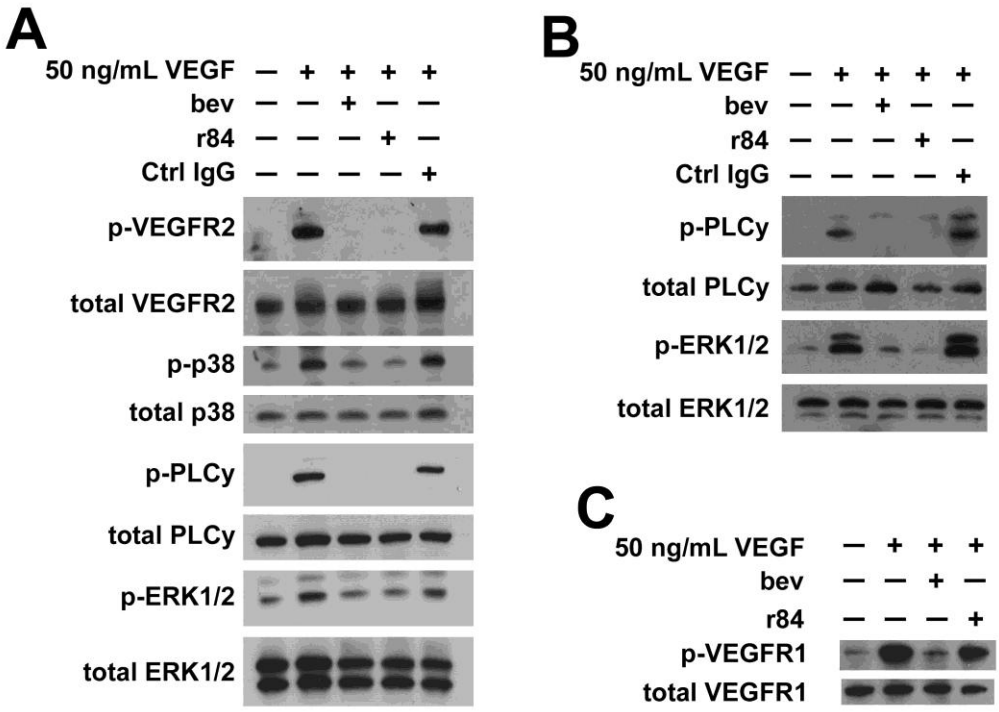


**Figure 3.4: r84 reduces endothelial cell signaling *in vitro*.**

Western blots of VEGF-induced signaling in PAE-KDR (**A**), HDMEC (**B**), and PAE-Flt-1 (**C**) lysates following stimulation of cells with 50 ng/mL human VEGF +/2 500-fold molar excess antibody (bev, r84, control IgG). r84 and bev block VEGFR2 phosphorylation and downstream phosphorylation (p38, PLCc, ERK1/2) (**A**, **B**). Only bev blocks VEGF-induced VEGFR1 phosphorylation in PAE-Flt-1 stimulated cells (**C**).

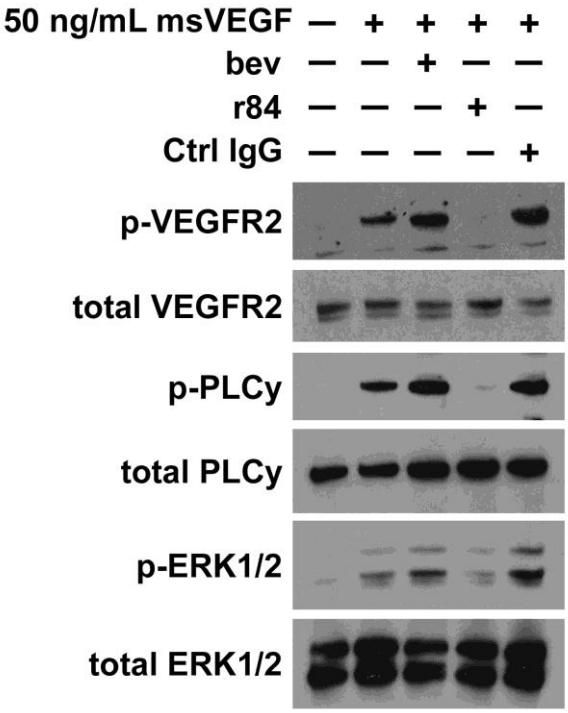


**Figure 3.5: r84 reduces mouse VEGF-induced endothelial cell signaling *in vitro*.**

Western blots of mouse VEGF-induced signaling in PAE-KDR lysates following stimulation of cells with 50 ng/mL mouse VEGF +/- 500-fold molar excess antibody (bev, r84, control IgG). Only r84 blocks VEGFR2 phosphorylation and downstream phosphorylation (PLC-γ, ERK1/2) in mouse VEGF-stimulated cells.

### *3.2.4 r84 controls tumor growth in human xenograft models*

Previous studies in the Brekken laboratory have demonstrated the ability of r84 to control tumor growth and decrease tumor angiogenesis in established models of breast cancer (Roland et al., 2009a; Roland et al., 2009b). The efficacy of r84 as a cancer therapeutic was assessed in tumor xenograft models in NOD/SCID mice. Briefly, four- to six-week old female NOD/SCID mice were implanted subcutaneously with 2.5 million human non-small cell lung cancer (NSCLC) cell lines H460, H1299, or A549. Treatment began one day post TCI and continued until the average tumor volume in control IgG-treated tumors reached 1500 $mm^3$, at which time all animals were sacrificed. Tumor-bearing animals were treated with 50 mg/kg/week r84 and 25 mg/kg/week bevacizumab and control IgG (palivizumab/Synagis®). r84 and bevacizumab similarly controlled H460 and H1299 tumor growth compared to control IgG therapy by both tumor volume and final tumor weights at sacrifice (Figure 3.6, Figure 3.7). In A549 xenografts, r84 controlled tumor growth better than bevacizumab, and the mean final tumor weight at sacrifice of animals treated with r84 was significantly smaller than animals treated with bevacizumab (Figure 3.7 C, $p < 0.05$).

Bevacizumab has a half life in mice of approximately two weeks (Lin et al., 1999). Pharmacokinetic studies (data not shown) determined the half life of r84 in mice to be approximately five days. This difference, along with the fact that

r84 binds both human and mouse VEGF and thus has more target to bind in tumor xenograft models than bevacizumab, led to the differences in antibody doses used in tumor studies. Consequently, this increase in dose could lead to better control of tumor growth as was seen in the A459 model (Figure 3.6 C, Figure 3.7 C).

To evaluate the effect of antibody dose, A549 tumor cells were implanted into mice as previously described. One day post TCI, animals began therapy, receiving 5, 15, or 50 mg/kg/week of r84 or bevacizumab, or 15 mg/kg/week of a non-specific control human IgG. The different doses of bevacizumab had the same effect on tumor growth and final tumor weight (Figure 3.8). In contrast, there was an observable titration of tumor growth control and final tumor weight with r84 therapy, with tighter control seen at higher doses of antibody. In addition, treatment of A549 tumor-bearing animals with 15 and 50 mg/kg/week r84 resulted in smaller tumors as compared to the same dose of bevacizumab (Figure 3.8 B, $p < 0.001$ and $p < 0.01$, respectively). Therefore, these results indicate that r84 may be more effective at controlling tumor growth than bevacizumab independent of dose in certain models. We propose that the appropriate therapeutic antibody dose should be determined independently for different tumor types to maximize therapeutic benefit with minimal induction of toxicity (Dowlati et al., 2005; Jain, 2005; Jayson et al., 2002).

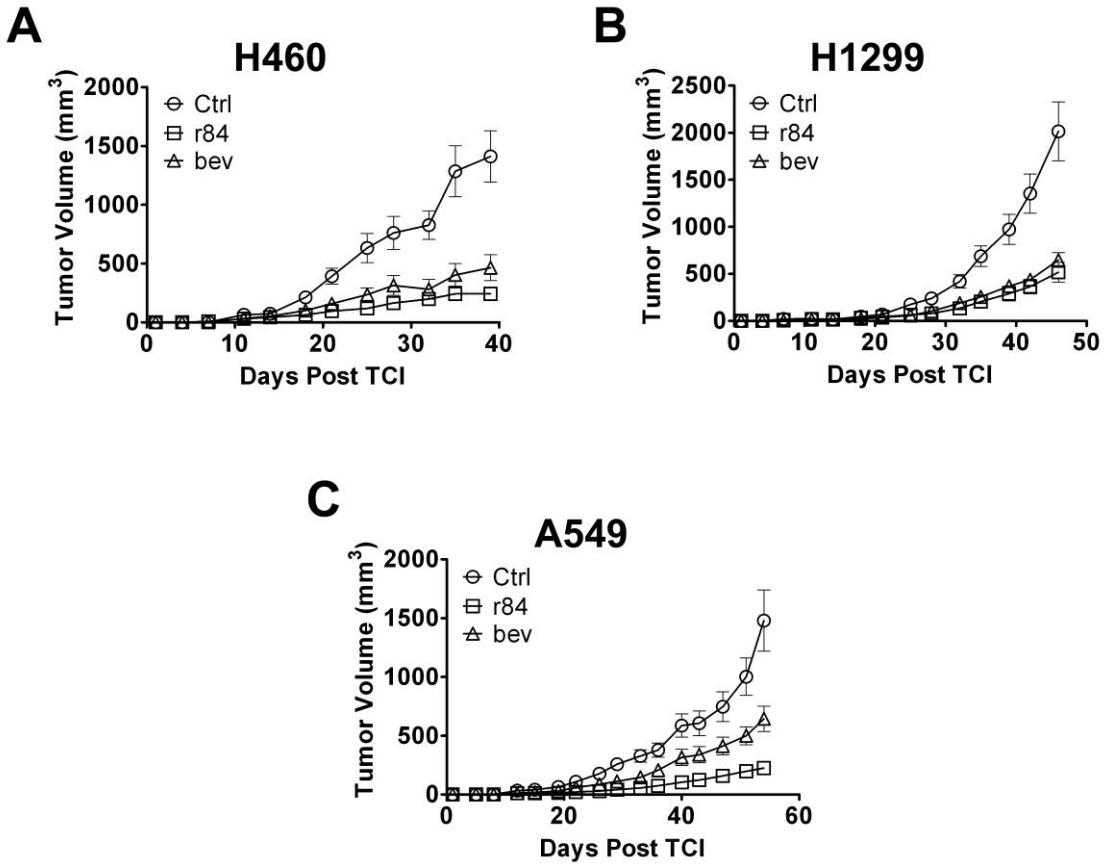


**Figure 3.6: r84 controls tumor growth *in vivo*.**

2.5 million human NSCLC cells were injected subcutaneously into the right flank of NOD/SCID mice. Therapy began one day post tumor cell injection (TCI), and continued for 4-8 weeks. Tumor volumes were measured twice/week. r84 and bevacizumab (bev) similarly control tumor growth as compared to control IgG (Ctrl) treatment in H460, H1299 models (**A**, **B**). **C**, In A549 NSCLC tumor bearing animals, r84 displayed tighter control of tumor growth as compared to bev treatment.

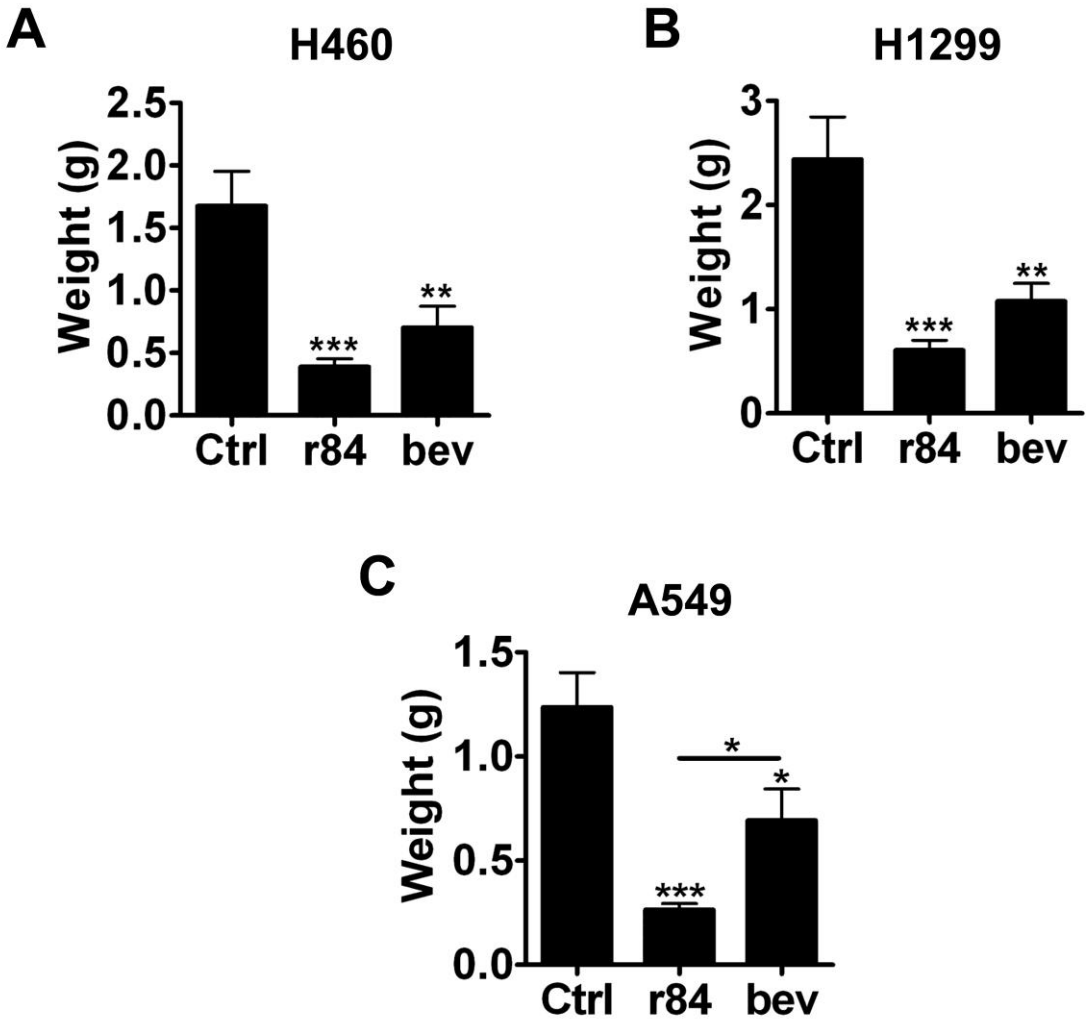


**Figure 3.7: r84 controls final tumor weight *in vivo*.**

2.5 million human NSCLC cells were injected subcutaneously into the right flank of NOD/SCID mice. Therapy began one day post tumor cell injection (TCI), and continued for 4-8 weeks. Final tumor weights were recorded at sacrifice. r84 and bevacizumab (bev) similarly control final tumor weight as compared to control IgG (Ctrl) treatment in H460, H1299 models (**A**, **B**). **C**, In A549 NSCLC tumor bearing animals, r84's control of tumor growth was significantly different from bev ($p < 0.05$) and Ctrl ($p < 0.001$). n = 8 mice per group. *$p < 0.05$, **$p < 0.01$, ***$p < 0.001$, statistical differences compared to Ctrl treatment, unless otherwise indicated.

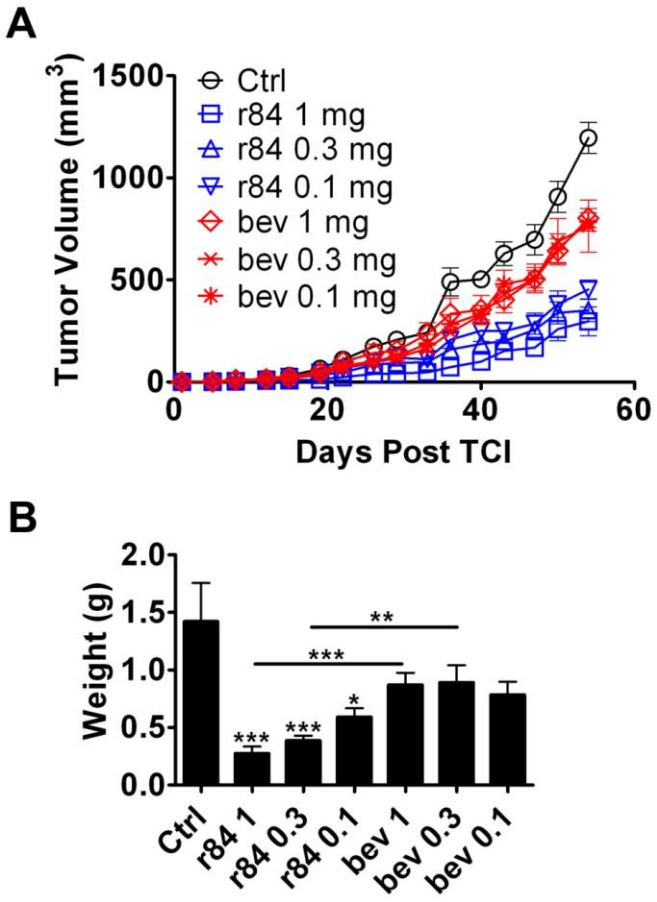


**Figure 3.8: r84 control of final tumor growth *in vivo* is dose dependent.**

2.5 million human A549 NSCLC cells were injected subcutaneously into the right flank of NOD/SCID mice. Therapy began one day post tumor cell injection (TCI), and continued for 4-8 weeks. Tumor volumes (**A**) were measured twice/week and final tumor weights (**B**) were recorded at sacrifice. Titration of antibody dosing in A549 tumor xenografts showed no change in tumor growth and final tumor weight with increasing doses of bev, however there was increasing control of tumor growth with increasing doses of r84, with doses of r84 controlling growth better than bev. n = 6 mice per group. *$p < 0.05$, **$p < 0.01$, ***$p < 0.001$, statistical differences compared to Ctrl treatment, unless otherwise indicated.

### *3.2.5 r84 effects the tumor microenvironment*

The phenotypic effects of r84 therapy within NSCLC tumors were assessed by immunohistochemistry. As was expected for anti-angiogenic therapies, treatment with r84 and bevacizumab resulted in a significant decrease in tumor MVD as demonstrated using two endothelial cell markers, MECA-32 (data not shown) and endomucin (Figure 3.9). There was a trend towards an increase in the number of pericyte-associated blood vessels in r84- and bevacizumab-treated tumors as compared to control IgG, although this increase only reached significance in the H460 model (Figure 3.9, bottom left panel). Treatment of H460 and H1299 xenograft tumors with r84 or bevacizumab also reduced the number of VEGFR2 positive cells, as analyzed by immunohistochemistry (Figure 3.10). Interestingly, VEGFR2 expression in A549 tumors was only decreased following r84 and not bevacizumab (Figure 3.10, bottom right panel, $p < 0.05$) therapy, perhaps reflecting the difference in the efficacy of these two drugs in controlling tumor growth in this model. Additionally, inhibition of VEGF with r84 or bevacizumab decreased tumor LVD as compared to control IgG therapy in both H460 and H1299 models (Figure 3.11). However, bevacizumab therapy failed to reduce LVD in the A549 model. These results suggest that in a model-dependent manner, r84 and bevacizumab may be able to disrupt lymphatic vessel-mediated tumor metastasis.

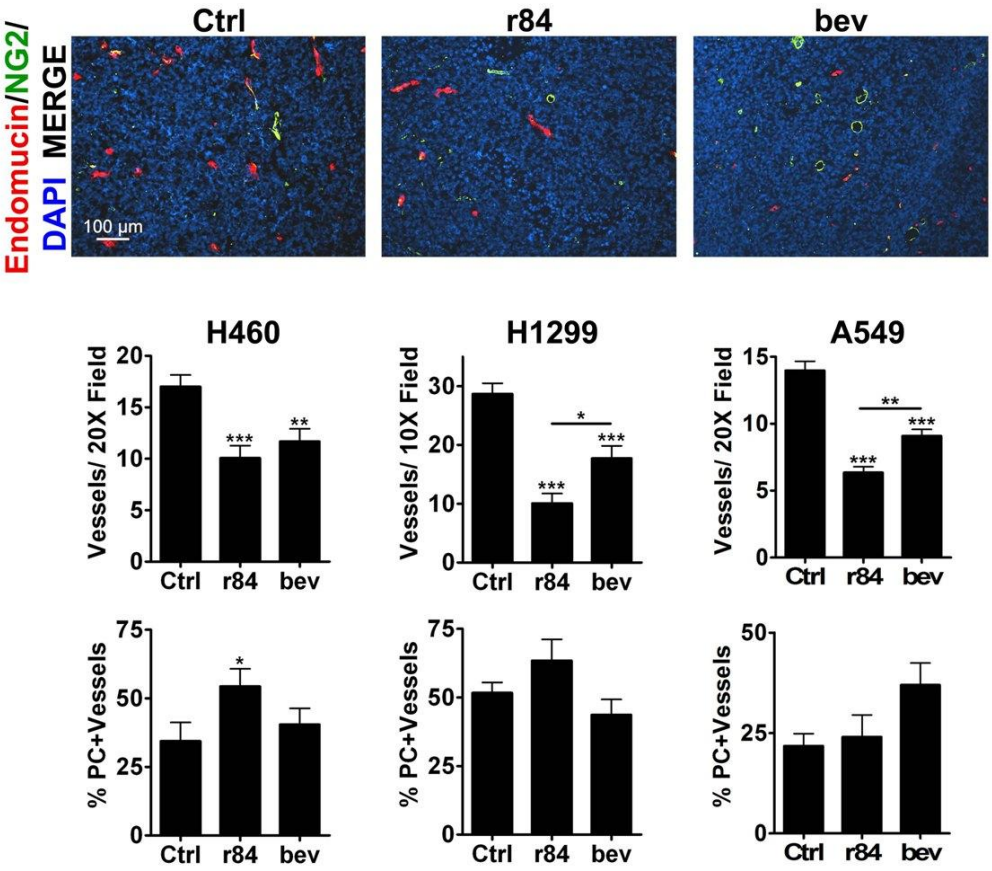


**Figure 3.9: r84 and bevacizumab therapy induces vascular changes within tumors.**

Frozen sections of A549, H460, H1299 tumors treated with control IgG (Ctrl), r84, or bevacizumab (bev) were analyzed by immunofluorescence. Number of positive-staining entities per high powered field was evaluated using Nikon Elements software. r84 and bev treatment significantly decreases tumor microvessel density, shown by a reduction in tumor endomucin positive endothelial cells (red). r84, bev treatment induced a trend towards increased NG2 positive (green) pericyte coverage of vessels as compared to Ctrl. *$p < 0.05$, **$p < 0.01$, ***$p < 0.001$, statistical differences compared to Ctrl, unless otherwise indicated.

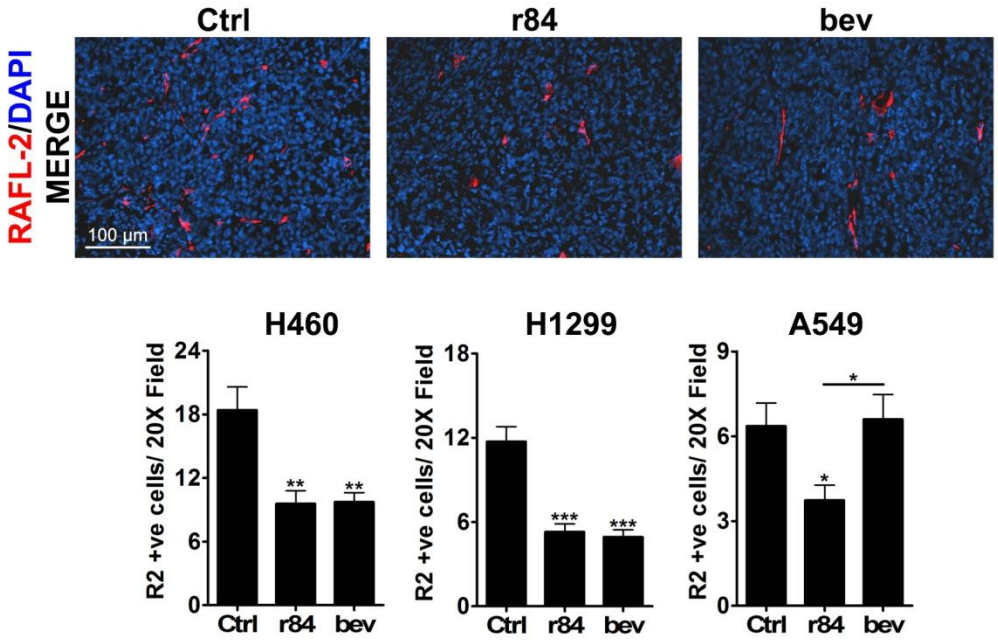


**Figure 3.10: r84 and bevacizumab therapy reduces VEGFR2 expression within tumors.**

Frozen sections of A549, H460, H1299 tumors treated with control IgG (Ctrl), r84, or bevacizumab (bev) were analyzed by immunofluorescence. Number of positive-staining entities per high powered field was evaluated using Nikon Elements software. r84 and bev treatment significantly reduces the number of VEGFR2 positive cells in H460, H1299 tumors as shown by RAFL-2 staining (red). Only r84 treatment significantly reduced VEGFR2 staining in A549 tumors. *$p < 0.05$, **$p < 0.01$, ***$p < 0.001$, statistical differences compared to Ctrl, unless otherwise indicated.

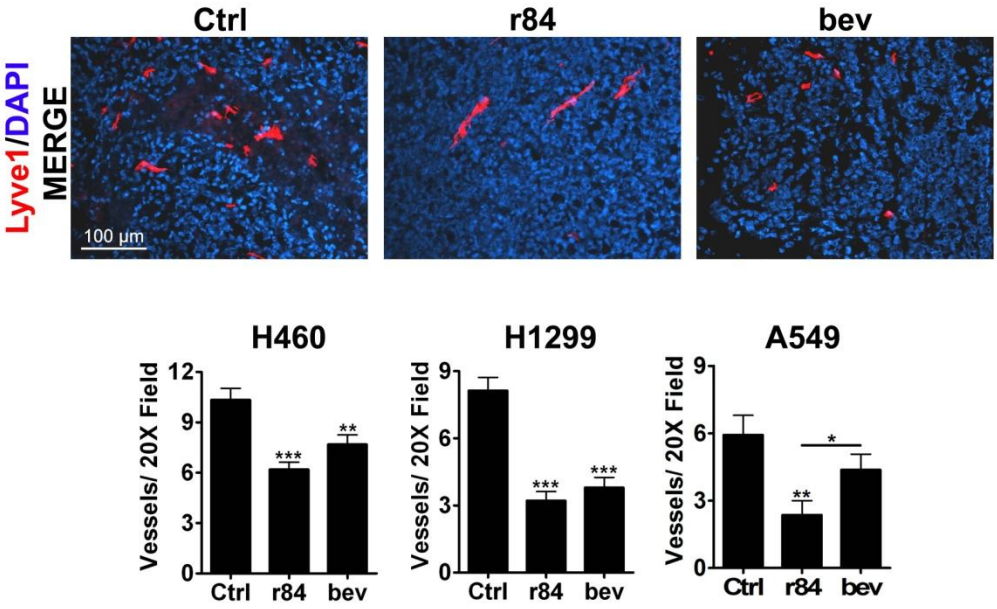


**Figure 3.11: r84 and bevacizumab therapy reduces LVD within tumors.**

Frozen sections of A549, H460, H1299 tumors treated with control IgG (Ctrl), r84, or bevacizumab (bev) were analyzed by immunofluorescence. Number of positive-staining entities per high powered field was evaluated using Nikon Elements software. r84 and bev treatment significantly decreased H460, H1299 tumor lymphatic vessel density (LVD), as indicated by a reduction in lyve1 positive cells (red). Only r84 treatment significantly reduced A549 tumor LVD. *$p < 0.05$, **$p < 0.01$, ***$p < 0.001$, statistical differences compared to Ctrl, unless otherwise indicated.

### *3.2.6 Extended r84 therapy does not induce toxicity*

The use of bevacizumab and other anti-angiogenic therapies in the clinic is associated with a number of toxicities. Toxicity associated with r84 can be evaluated in preclinical mouse xenograft models because of its ability of r84 to bind both human and mouse VEGF. To assess the potential of r84 to induce toxicities, NOD/SCID mice were injected with five million PANC-1 tumor cells (a slow-growing human pancreatic cancer line) subcutaneously. Treatment began one day post TCI, with 50 mg/kg/week r84 or a non-specific control IgG (palivizumab/Synagis®). An equal number of NTB animals received antibody treatment as well. Therapy continued for 12 weeks, at which point animals were sacrificed and tumor, organs and blood were collected for toxicity assessment. Extended r84 therapy had no effect on animal body weight for the duration of the experiment (Figure 3.12 A). As was seen in the NSCLC models, r84 therapy significantly reduced PANC-1 tumor growth and final tumor weight, as compared to control (Figure 3.12 B, Figure 3.12 C, $p < 0.05$). In addition, r84 treatment resulted in decreased tumor MVD (Figure 3.13, $p < 0.001$). r84 did not induce histological changes (as assessed by a pathologist) within the kidney or liver of tumor-bearing (TB) or NTB mice as compared to age-matched naïve animals (Figure 3.14). Blood was collected from all animals at the time of sacrifice, and a serum analysis of 20 metabolic markers was performed at the University of Texas Southwestern Medical Center mouse metabolic phenotyping core (Table 3.1).

There were no significant changes in any of these analytes between treated animals and age-matched naïve animals. This analysis included no observable change in alanine aminotransferase, aspartate aminotransferase, and blood urea nitrogen levels (Figure 3.15), markers of liver and kidney function, respectively. These three markers are elevated in correlation with toxicity in animals treated for 12 weeks with bevacizumab and high-affinity anti-VEGF antibodies (Gerber et al., 2007).

It has been reported that anti-VEGF treatment can reduce pancreatic islet vascular density in adult mice, leaving the supporting pericytes behind (Kamba and McDonald, 2007). In this study, the pancreatic islets of TB and NTB animals treated for 12 weeks with r84 showed a reduction in MVD as compared to control IgG-treated TB and NTB animals ($p < 0.01$), but there was no significant change when compared to naïve animals (Figure 3.16, bottom left panel). Additionally, there was no observable change in the percentage of pericytes without endothelial cell association (Figure 3.16, bottom right panel). Furthermore, there was no change in serum glucose levels, nor was there a change in insulin staining in pancreatic islets of experimental animals (Figure 3.17 A, B). Taken together, long-term therapy with r84 produced no observable toxicity in TB or NTB animals.

Since hypertension and proteinuria are among the most common toxicity-related side effects associated with anti-VEGF therapy and given recent data

suggesting a role for VEGFR2 in controlling blood pressure (Facemire et al., 2009; Roodhart et al., 2008), we investigated the effects of r84 therapy on hypertension and proteinuria in a spontaneous, immunocompetent model of pancreatic cancer. Mice (*p48-Cre:LSL-Kras*$^{G12D}$*:p16*$^{ink4a/arf+/lox}$) expressing a pancreas-specific Cre recombinase activating a constitutively active *Kras* allele (*Kras*$^{G12D}$) and inactivating a single copy of *Ink4a/Arf* that spontaneously develop pancreatic ductal adenocarcinoma (Aguirre et al., 2003) were separated into three groups receiving either saline, mouse chimeric r84 (mcr84 (Roland et al., 2009b)), or sunitinib. Therapy began when mice when mice were eight weeks old, with weekly IP injections of saline 25 mg/kg/week or mcr84, or daily oral gavage of 50 mg/kg/week sunitinib. Therapy continued for a total of eight weeks, at which time all animals were sacrificed. Extended therapy with mcr84 or sunitinib had no effect on animal body weight in this experiment (Figure 3.18 A). Tumor burden, as assessed by final pancreas weight at sacrifice, was reduced in mcr84-treated animals as compared to control- and sunitinib-treated animals, although this trend failed to reach significance (Figure 3.18 B). However, treatment with mcr84 or sunitinib resulted in decreased tumor MVD (Figure 3.18 C, $p < 0.01$ or $p < 0.05$, respectively). Tail cuff blood pressure measurements were gathered during weeks two and seven of therapy. At week two, animals in the mcr84 and sunitinib groups displayed elevated systolic blood pressure as compared to control-treated animals (Figure 3.19 A, left panel, $p < 0.001$). However, at week seven neither mcr84- nor

sunitinib-treated animals displayed elevated systolic blood pressures as compared to control-treated animals although blood pressures were significantly higher in sunitinib-treated animals than in those receiving mcr84 (Figure 3.19 A, right panel, $p < 0.05$). Thus in this model, inhibiting VEGFR2 with mcr84 or multiple receptor tyrosine kinases including both VEGFR1 and VEGFR2 with sunitinib increased systolic blood pressure after acute but not chronic therapy. During week six of therapy, metabolic cages were used to collect urine samples from all mice, which were subsequently analyzed for urine protein and creatine levels by the University of Texas Southwestern Medical Center mouse metabolic phenotyping core to assess possible induction of proteinuria in this model. The urine protein:creatine ratio did not differ between the three treatment groups, suggesting that long term treatment with mcr84 and sunitinib does not induce kidney damage (Figure 3.19 B). Similar to the initial toxicity study in NOD/SCID mice, blood was collected from all animals at sacrifice for analysis by the mouse metabolic phenotyping core, which again yielded no significant changes in any of the 18 tested analytes between mcr84-, sunitinib-, or control-treated animals (Table 3.2). Notably, our immunocompetent model of extended anti-VEGF therapy did not demonstrate any observable change in the metabolic markers of liver and kidney function alanine aminotransferase, aspartate aminotransferase, and blood urea nitrogen (Figure 3.20). Therefore, in a spontaneous tumor model in

immunocompetent animals, chronic treatment with mcr84 failed to produce observable, lasting toxicity.

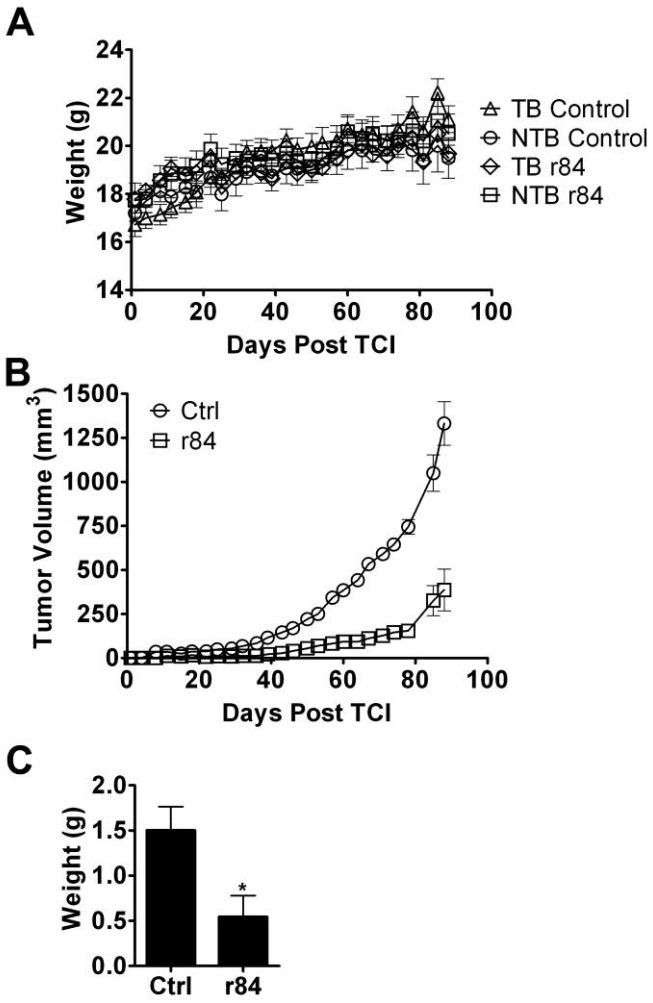


**Figure 3.12: Extended treatment with r84 controls tumor growth.**

r84 was able to control tumor growth in an extended therapy model. NOD/SCID mice with no tumors (non-tumor bearing, NTB) or bearing subcutaneous PANC-1 tumors (tumor bearing, TB) received long-term 12-week therapy with 50 mg/kg/week r84 or a control IgG (Ctrl). Antibody treatment had no effect on animal weight (**A**). r84 therapy significantly controls tumor growth (**B**) and final tumor weight (**C**) compared to control IgG ( $*p < 0.05$).

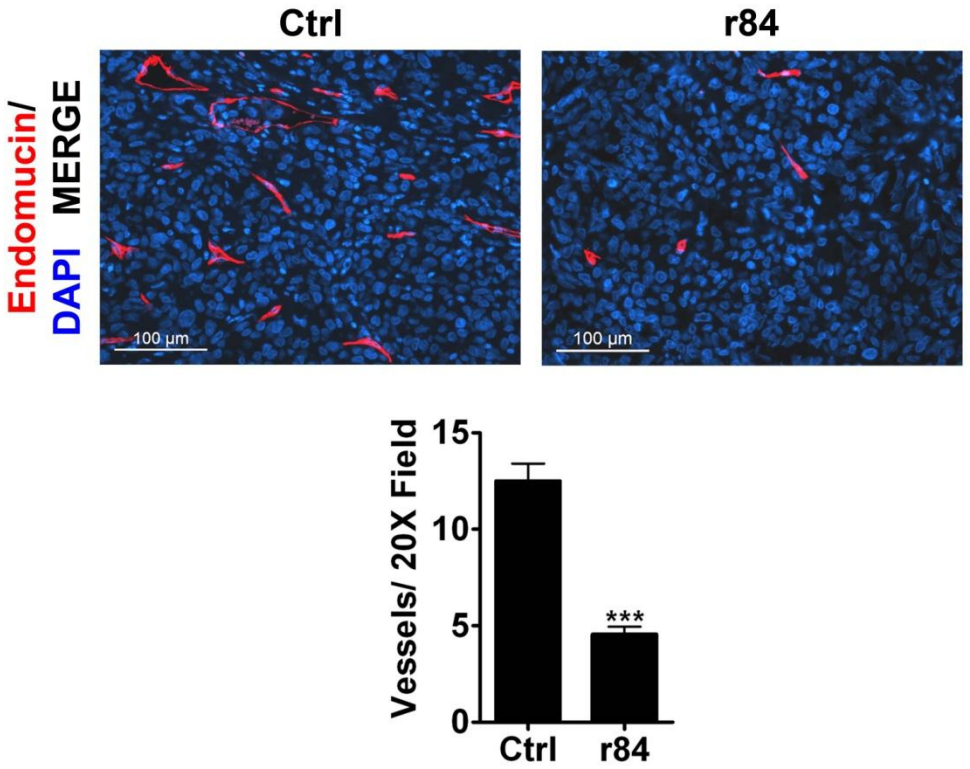


**Figure 3.13: Extended anti-VEGF therapy reduces tumor MVD.**

r84 and mouse chimeric r84 (mcr84) were able to reduce tumor microvessel density in two extended therapy models. NOD/SCID mice bearing subcutaneous PANC-1 tumors received long-term 12-week therapy with 50 mg/kg/week r84 or a control IgG. r84 significantly decreases PANC-1 tumor microvessel density as compared to control IgG (Ctrl) treatment as shown by endomucin staining. ***$p < 0.001$, statistical difference compared to Ctrl treatment.

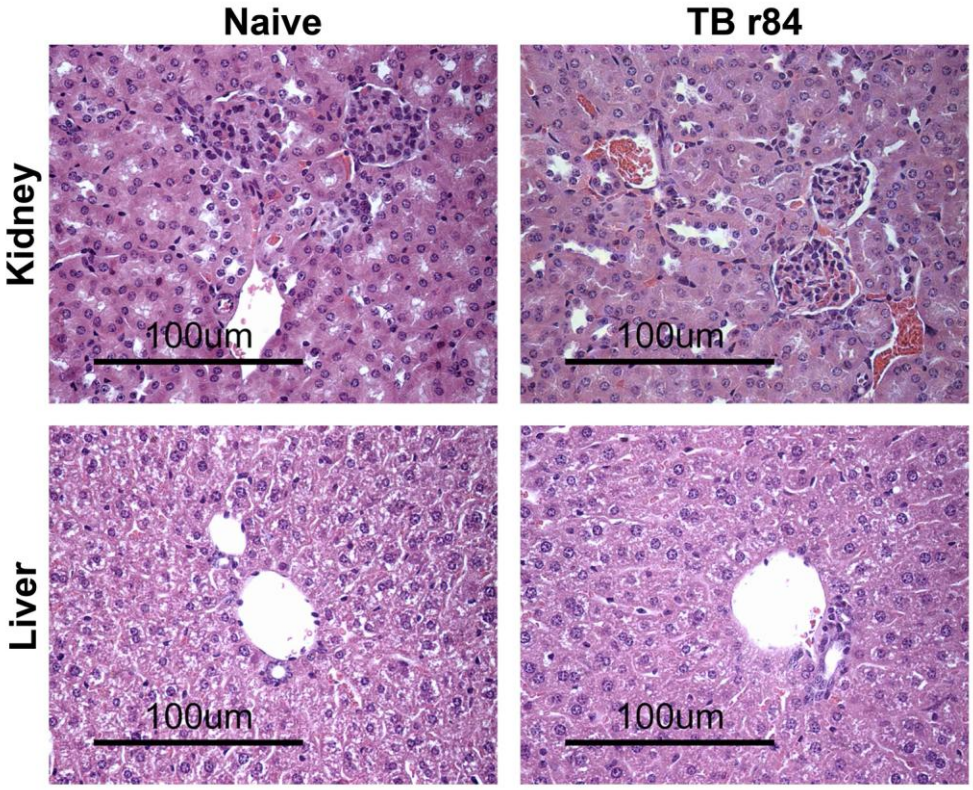


**Figure 3.14: Extended r84 therapy controls tumor growth without inducing histological kidney or liver toxicity.**

Five million PANC-1 tumor cells were injected subcutaneously into NOD/SCID mice. Tumor bearing (TB) and non tumor bearing (NTB) mice received long-term 12-week therapy with 50 mg/kg/week r84 or a control IgG. Following 12-weeks of therapy, animals were sacrificed and organs and blood were collected for toxicity analysis. n = 5 animals per group. Hematoxylin and eosin staining of formalin-fixed, paraffin-embedded kidney and liver sections demonstrated that control of tumor growth is achieved without induction of kidney or liver histopathologic changes.

| Test | TB Ctrl | NTB Ctrl | TB r84 | NTB r84 | Naïve |
|---|---|---|---|---|---|
| Albumin (ALB) g/dL | 2.3+/-0.084 | 2.36+/-0.103 | 2.4+/-0.114 | 2.48+/-0.102 | 2.64+/-0.075 |
| Alkaline Phosphatase (ALKP) U/L | 39.8+/-3.787 | 151.0+/-81.31 | 37.25+/-4.385 | 50.8+/-6.829 | 67+/-4.416 |
| Alanine Aminotransferase (ALT) U/L | 386.8+/-232.4 | 134.6+/-16.56 | 201.8+/-36.36 | 407+/-164.6 | 1523+/-1301 |
| Aspartate Aminotransferase (AST) U/L | 986.8+/-319.9 | 848.4+/-202.1 | 843+/-106.6 | 1166+/-225.4 | 942.3+/-147.9 |
| Unconjugated Bilirubin (Bu) mg/dL | 0.28+/-0.02 | 0.22+/-0.037 | 0.225+/-0.025 | 0.22+/-0.02 | 0.48+/-0.306 |
| Conjugated Bilirubin (Bc) mg/dL | 0.02+/-0.02 | 0.06+/-0.06 | 0.05+/-0.029 | 0.08+/-0.037 | 0.1+/-0.032 |
| Blood Urea Nitrogen (BUN) mg/dL | 21.8+/-0.583 | 21.6+/-1.806 | 21+/-1.095 | 23.6+/-1.03 | 22.8+/-0.49 |
| Calcium (Ca) mg/dL | 8.8+/-0.219 | 8.18+/-0.373 | 8.58+/-0.314 | 7.88+/-0.482 | 6.16+/-1.418 |
| Creatine Kinase (CK) U/L | 22407+/-2419 | 31401+/-7903 | 41325+/-4897 | 43810+/-6519 | 45035+/-9640 |
| Chloride (Cl) mmol/L | 112.6+/-0.51 | 112.6+/-0.678 | 114.6+/-0.812 | 113.6+/-0.678 | 110.6+/-3.473 |
| Creatine (CREA) mg/dL | 0.16+/-0.028 | 0.205+/-0.045 | 0.113+/-0.021 | 0.215+/-0.015 | 0.055+/-0.005 |
| CO2 (ECO2) mmol/L | 17.8+/-1.96 | 17.4+/-2.786 | 11.8+/-1.2 | 13.2+/-1.625 | 11.8+/-0.735 |
| Gamma Glutamyltransferase (GGT) U/L | 10.67+/-3.712 | 14.33+/-6.36 | 19.5+/-4.093 | 20+/-5.759 | 22+/-2.121 |
| Glucose (GLU) mg/dL | 187.4+/-7.139 | 171+/-27.17 | 175+/-12.97 | 169+/-13.85 | 208+/-25.13 |
| Potassium (K) mmol/L | 7.76+/-1.009 | 8.12+/-1.031 | 9.34+/-0.58 | 8.72+/-0.842 | 8.825+/-0.676 |
| Lactate Dehydrogenase (LDH) U/L | 9182+/-2652 | 11714+/-3037 | 10364+/-1841 | 12549+/-1806 | 9491+/-1443 |
| Sodium (Na) mmol/L | 140+/-0.894 | 139+/-1.095 | 136+/-1.049 | 136.2+/-1.281 | 132.2+/-4.104 |
| Phosphorus (PHOS) mg/dL | 7.94+/-0.622 | 9.58+/-0.301 | 11.98+/-0.429 | 11.04+/-0.924 | 9.74+/-0.676 |
| Total Bilirubin (TBIL) mg/dL | 0.86+/-0.136 | 0.94+/-0.216 | 1.44+/-0.181 | 1.34+/-0.289 | 1.6+/-0.0837 |
| Total Protein (TP) g/dL | 4.56+/-0.098 | 4.58+/-0.186 | 4.7+/-0.155 | 4.84+/-0.136 | 5+/-0.105 |

**Table 3.1: Extended r84 therapy does not induce significant changes in blood serum chemistry.**

NOD/SCID mice bearing subcutaneous PANC-1 tumors received long-term 12-week therapy with 50 mg/kg/week r84 or a control IgG. Blood chemistry analysis of serum samples collected from mice at sacrifice indicated that extended r84 treatment does not induce changes in serum levels of 20 different markers, as compared to control-treated (Ctrl) or Naïve animals.

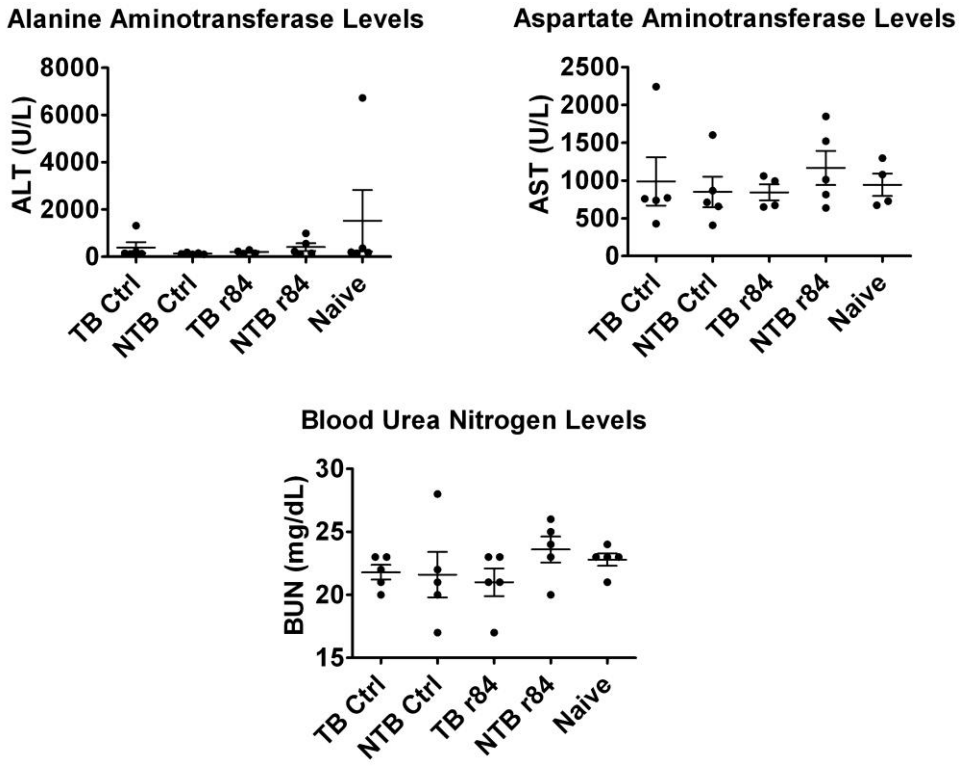


**Figure 3.15: Extended r84 therapy controls tumor growth without induction of liver or kidney toxicity.**

Five million PANC-1 tumor cells were injected subcutaneously into NOD/SCID mice. Tumor bearing (TB) and non tumor bearing (NTB) mice received long-term 12-week therapy with 50 mg/kg/week r84 or a control IgG. Following 12-weeks of therapy, animals were sacrificed and organs and blood were collected for toxicity analysis. n = 5 animals per group. Blood chemistry analysis of serum samples collected from mice at sacrifice indicated that r84 treatment does not induce changes in serum levels of alanine aminotransferase (ALT), aspartate aminotransferase (AST), or blood urea nitrogen (BUN) as compared to control IgG therapy and to age-matched Naïve animals that did not have tumor and never received antibody therapy.

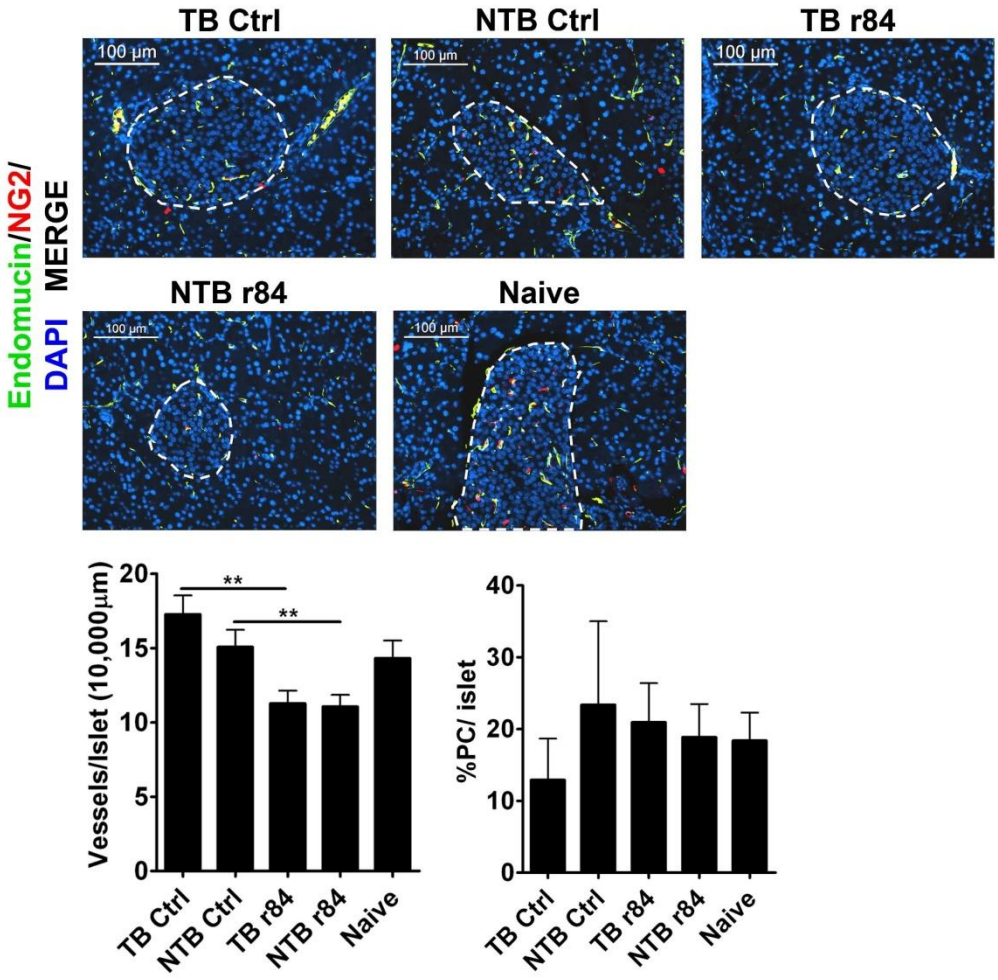


**Figure 3.16: Extended r84 therapy does not induce vascular changes within pancreas islets.**

NOD/SCID mice bearing subcutaneous PANC-1 tumors received long-term 12-week therapy with 50 mg/kg/week r84 or a control IgG. Long-term r84 therapy in TB or NTB animals did not change pancreatic islet vessel density (endomucin, green) or pericyte distribution (NG2, red) as compared to age-matched Naïve animals (**$p < 0.01$).

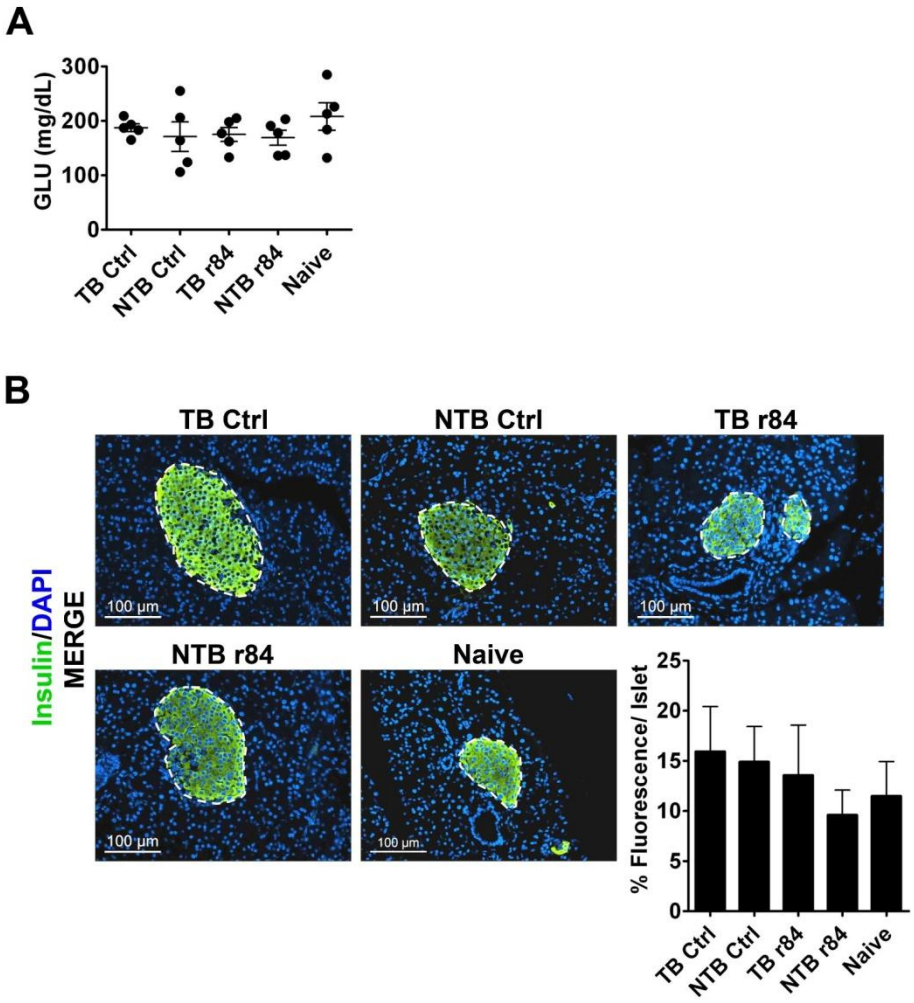


**Figure 3.17: Extended r84 therapy does not damage pancreas function.**

NOD/SCID mice bearing subcutaneous PANC-1 tumors received long-term 12-week therapy with 50 mg/kg/week r84 or a control IgG. Blood chemistry analysis of serum samples collected from mice at sacrifice revealed no change in glucose levels between groups (**A**). Immunohistochemical analysis of pancreas sections revealed no difference in insulin staining intensities (green) within pancreatic islets amongst treatment groups (**B**).

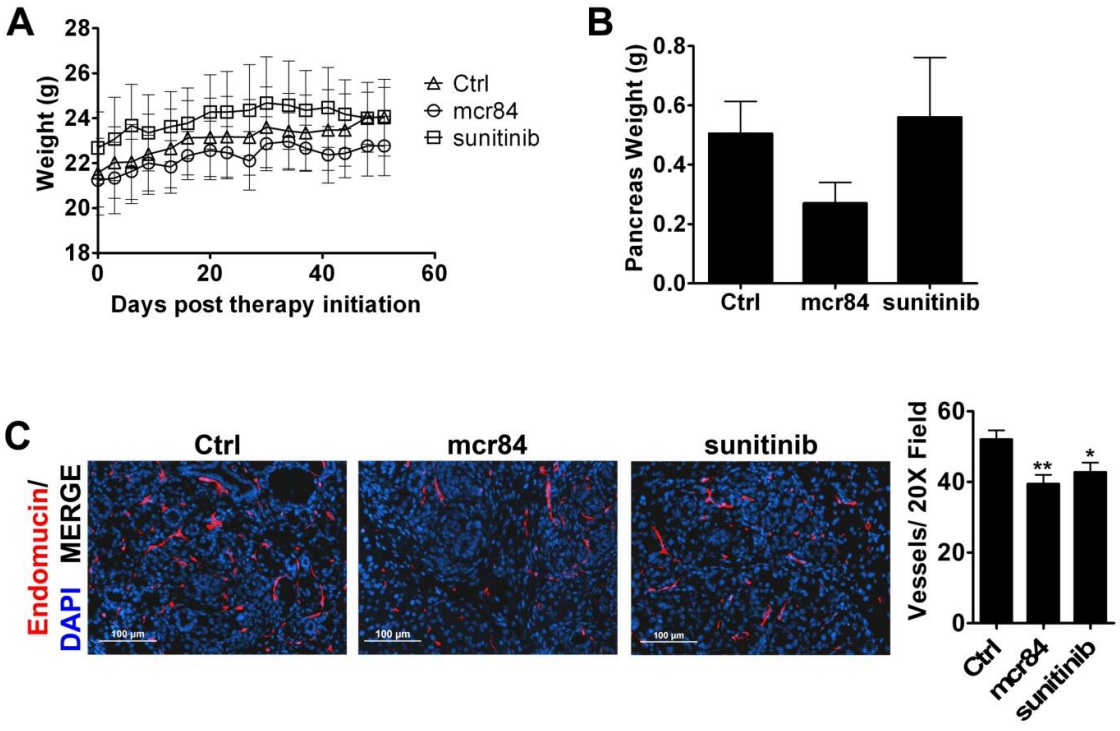


**Figure 3.18: Efficacy of extended mcr84, sunitinib therapy in an immunocompetent mouse model.**

Immunocompetent mice heterozygous for a spontaneous model of pancreatic cancer received extended 8-week therapy with saline, 25 mg/kg/week mouse chimeric r84 (mcr84), or 50 mg/kg/week sunitinib. Anti-VEGF therapy had no effect on animal weight (**A**). There was a trend towards a decrease in final pancreas weight at time of sacrifice in mcr84-treated animals as compared to control, although this decrease failed to reach statistical significance (**B**). **C**, Both mcr84 and sunitinib significantly decreased tumor microvessel density as compared to control treatment (Ctrl) as shown by endomucin staining. *$p < 0.05$, **$p < 0.01$, statistical differences compared to Ctrl treatment.

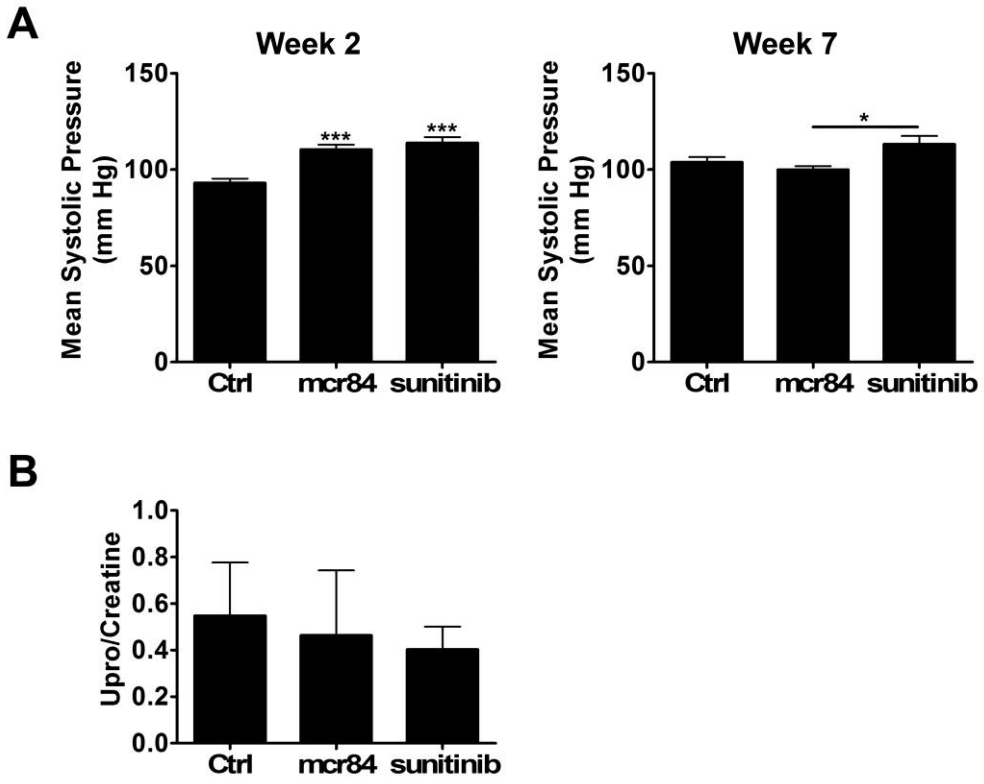


**Figure 3.19: Extended mcr84, sunitinib therapy has minimal effects on blood pressure and proteinuria.**

Immunocompetent Kras/INK4a mice that spontaneously develop pancreatic cancer were treated for eight weeks with saline, 25 mg/kg/week mcr84, or 50 mg/kg/week sunitinib. After 2 weeks of therapy, mcr84 and sunitinib significantly increased mean systolic blood pressure (**A** left panel), but this effect was lost by week 7 of continuous therapy (**A**, right panel). **B**, Urine samples collected during week 6 of therapy and assayed for total levels of urine protein and creatine (Upro/Creatine ratio displayed) showed no significant difference between treated animals as compared to control, indicating that extended therapy with mcr84 and sunitinib did not induce kidney damage in this model. *$p < 0.05$, ***$p < 0.001$, statistical differences compared to control (Ctrl) treatment, unless otherwise indicated.

| Test | Ctrl | mcr84 | sunitinib |
|---|---|---|---|
| Albumin (ALB) g/dL | 2.5+/-0.041 | 2.57+/-0.088 | 2.2+/-0.303 |
| Alkaline Phosphatase (ALKP) U/L | 34.48+/-9.372 | 43.67+/-0.333 | 30.73+/-9.403 |
| Alanine Aminotransferase (ALT) U/L | 103.8+/-21.45 | 155.3+/-82.15 | 61.75+/-4.131 |
| Aspartate Aminotransferase (AST) U/L | 392.8+/-92.68 | 448.7+/-167 | 265.3+/-44.41 |
| Unconjugated Bilirubin (Bu) mg/dL | 0.23+/-0.048 | 0.13+/-0.033 | 0.17+/-0.033 |
| Conjugated Bilirubin (Bc) mg/dL | 0+/-0 | 0.03+/-0.033 | 0+/-0 |
| Blood Urea Nitrogen (BUN) mg/dL | 20.75+/-0.947 | 20+/-1.155 | 20.75+/-2.213 |
| Calcium (Ca) mg/dL | 4.03+/-0.138 | 3.87+/-0.233 | 4.23+/-0.392 |
| Chloride (Cl) mmol/L | 113+/-1.472 | 111+/-0.577 | 114.5+/-3.379 |
| Creatine (CREA) mg/dL | 0.18+/-0.016 | 0.16+/-0.015 | 0.17+/-0.018 |
| Gamma Glutamyltransferase (GGT) U/L | 5+/-0 | 5+/-0 | 5+/-0 |
| Glucose (GLU) mg/dL | 402.3+/-12.53 | 399+/-15.5 | 373+/-47.04 |
| Potassium (K) mmol/L | 5.75+/-0.463 | 5.33+/-0.47 | 5.2+/-0.322 |
| Lactate Dehydrogenase (LDH) U/L | 5649+/-859.7 | 5817+/-1480 | 4201+/-482.2 |
| Sodium (Na) mmol/L | 191+/-2.677 | 187.3+/-2.404 | 185.8+/-3.065 |
| Phosphorus (PHOS) mg/dL | 9.18+/-0.948 | 8.9+/-1.159 | 8.15+/-0.491 |
| Total Bilirubin (TBIL) mg/dL | 0.9+/-0.1 | 1.07+/-0.133 | 0.85+/-0.104 |
| Total Protein (TP) g/dL | 4.35+/-0.104 | 4.43+/-0.088 | 3.9+/-0.303 |

**Table 3.2: Extended mcr84, sunitinib therapy does not induce significant changes in blood serum chemistry.**

Immunocompetent mice heterozygous for a spontaneous model of pancreatic cancer received extended 8-week therapy with saline, 25 mg/kg/week mouse chimeric r84 (mcr84), or 50 mg/kg/week sunitinib. Blood chemistry analysis of serum samples collected from mice at sacrifice indicated that extended mcr84 and sunitinib treatment does not induce changes in serum levels of 18 different markers, as compared to saline-treated animals in this model.

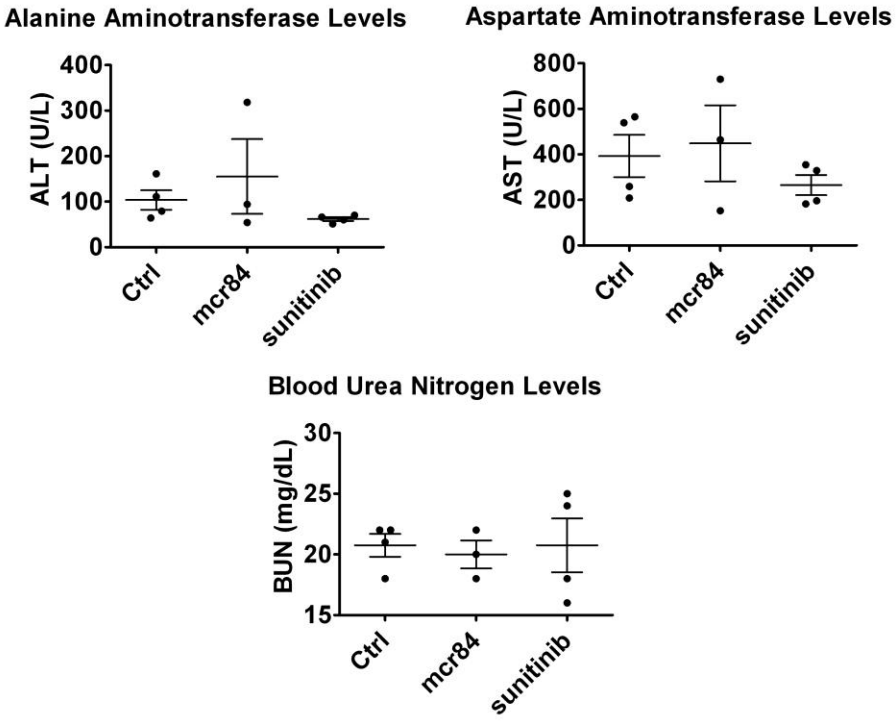


**Figure 3.20: Extended mcr84, sunitinib therapy controls tumor growth without induction of liver or kidney toxicity.**

Immunocompetent mice heterozygous for a spontaneous model of pancreatic cancer received extended 8-week therapy with saline, 25 mg/kg/week mouse chimeric r84 (mcr84), or 50 mg/kg/week sunitinib. Blood chemistry analysis of serum samples collected from mice at sacrifice indicated that extended mcr84 and sunitinib treatment does not induce changes in serum levels of 18 different markers, as compared to saline-treated animals in this model. Blood chemistry analysis of serum samples collected from mice at sacrifice indicated that extended mcr84 or sunitinib treatment does not induce changes in serum levels of alanine aminotransferase (ALT), aspartate aminotransferase (AST), or blood urea nitrogen (BUN) as compared to control (Ctrl) therapy.

### 3.3 Discussion

Angiogenesis is a crucial process during embryonic development and normal physiology, and during tumor development, growth, and progression (Roskoski, 2007b). Anti-angiogenic therapy therefore presents an exciting and rational approach for tumor therapy. However, the clinical efficacy of anti-angiogenic therapies have been mostly disappointing, with modest increases in patient OS (Jain et al., 2006). Therefore, there is still much to learn about angiogenic signaling and angiogenesis dependence within tumors, which can be aided through the development and use of new investigative tools.

Here we describe r84, a fully human monoclonal antibody specific for VEGF, a key mediator of angiogenesis. r84 binds to human and mouse VEGF-A, but not other VEGF family members (VEGF-B, -C, -D, PlGF), and specifically blocks subsequent binding of VEGF to VEGFR2, leaving intact VEGF:VEGFR1 interaction. Through its unique VEGF binding properties, r84 blocked VEGFR2-mediated endothelial cell migration and signaling. *In vivo*, r84 controlled tumor growth in NOD/SCID mice similarly to bevacizumab. r84-treated tumors had reduced MVD, VEGFR2 expression, and LVD as compared to control-treated tumors, and showed a trend towards increased pericyte-associated blood vessels. Importantly, chronic exposure to r84 in tumor bearing and non-tumor bearing NOD/SCID mice and in a spontaneous, immunocompetent model of pancreatic cancer did not induce toxicity.

The discriminating specificity of r84 in that it recognizes one ligand (VEGF) and inhibits binding only to VEGFR2 establishes r84 as a beneficial tool for elucidating VEGFR1 signaling pathways and functional contributions of VEGFR1 and VEGFR2 *in vitro* and *in vivo*. r84 binds both human and mouse VEGF (Figure 3.1 A, B), and a mouse chimeric version of r84 (mcr84) has been developed, thereby obviating the need for complex mouse model systems genetically engineered to express human VEGF (Gerber et al., 2007) to study contributions of host- and tumor-derived VEGF in human xenograft or syngeneic tumor models. Previous work has directly compared the efficacy of r84 with other anti-angiogenic agents in established human tumor xenografts and syngeneic tumor models (Roland et al., 2009a; Roland et al., 2009b). In these studies, r84 has been shown to be more effective than bevacizumab, sunitinib, an anti-VEGFR2 antibody (RAFL-2), and a peptoid against VEGFR1 and VEGFR2 (GU81) in controlling tumor growth and infiltration of immune suppressor cell populations (Ran et al., 2003; Roland et al., 2009b). Functionally, r84 inhibits VEGFR2 activity by specifically blocking only VEGF. This distinguishes r84 from anti-VEGFR2 antibodies such as DC101 that block the activity of all VEGFR2 ligands (Tonra and Hicklin, 2007). The importance of r84's specificity is best observed through direct comparisons where r84 has been shown to outperform less specific anti-VEGFR2 strategies (Roland et al., 2009b). The present study supports previous investigations, highlighting that selective

inhibition of VEGFR2 with r84 can delay tumor take and control tumor growth similar to blockade of both VEGFR1 and VEGFR2 (Figures 3.6-3.8), bringing to question the function of VEGFR1 in tumor angiogenesis and in physiological homeostasis. A caveat to the specificity of r84 is that we have been unable to determine conclusively the effect of r84 on VEGF binding to neuropilin-1 or -2, which might impact the biological effect of r84.

Although the function and signaling pathways of VEGFR1 remain elusive, there is data supporting the concept that VEGFR1 is a negative regulator of VEGFR2 signaling. VEGFR1 deficient mice die *in utero* due to an over abundance of endothelial cells (Fong et al., 1995; Fong et al., 1999), whereas mice expressing on the extracellular domain of VEGFR1 are viable (Hiratsuka et al., 1998). These studies established that VEGFR1 does not need to signal through its cytoplasmic domain and functions during development as a decoy receptor for VEGF, sequestering the ligand and regulating VEGFR2-mediated angiogenesis. Roberts *et al.*, (Roberts et al., 2004) demonstrated that the VEGFR1 mutant phenotype in embryonic stem cell-derived blood vessels could be rescued by incubation with small molecule inhibitors of VEGFR2. These data further supports that VEGFR1 controls blood vessel development by negatively regulating VEGFR2 signaling. In addition, work by Nozaki *et al.*, (Nozaki et al., 2006) demonstrated that VEGF binding to VEGFR1 induced the activity of SHP-1 phosphatase that in turn reduced levels of VEGFR2 phosphorylation. Therefore,

active VEGF binding and signaling through VEGFR1 could potentially negatively regulate tumor angiogenesis, an interesting concept that warrants further investigation. Hypertension is likely caused by decreased levels of nitric oxide (NO) resulting from blockade of VEGF signaling through VEGF2 and VEGF1 by current anti-angiogenic strategies. VEGF activation of VEGFR1 has been demonstrated to induce NO production (Ahmad et al., 2006; Bussolati et al., 2001). Therefore, it is possible that hypertension may be reduced or eliminated following r84 therapy.

Additionally, studies have demonstrated the importance of VEGFR1 function in tumor cell survival. Neutralizing antibodies against VEGFR1 (Wu et al., 2006a; Wu et al., 2006b) and PlGF (Fischer et al., 2007), a VEGFR1 specific ligand, have successfully controlled tumor growth in preclinical models. Adding to the complexity of this pathway, PlGF over expression has also been shown to inhibit tumor growth and angiogenesis through increased levels of functionally inactive VEGF:PlGF heterodimers (Eriksson et al., 2002; Xu et al., 2006). Further, Bais *et al.*, recently demonstrated that although anti-PlGF antibodies were able to inhibit wound healing and cancer cell extravasation, these antibodies only inhibited tumor growth in tumors that over expressed VEGFR1 (Bais et al., 2010). These papers question the importance of directly blocking PlGF or VEGFR1 therapeutically and highlight the potential benefit of anti-angiogenic agents such as r84 that allow for PlGF and VEGFR1 interactions. VEGFR1 has

also been linked to tumor metastasis (Hiratsuka et al., 2002; Kaplan et al., 2005). However, selective blockade of VEGFR2 in our models was sufficient to control tumor growth as compared to simultaneous inhibition of VEGFR1 and VEGFR2 (Figure 3.6 – Figure 3.8). Increased metastasis was not observed from tumor xenografts treated with r84 or the phenotypic precursor of r84, 2C3, in subcutaneous or orthotopic models (Dineen et al., 2008; Roland et al., 2009a). Nevertheless, the effects of anti-angiogenic therapy on tumor progression and metastasis are still being elucidated (Ebos et al., 2009; Paez-Ribes et al., 2009) and could benefit from selective tools, such as r84, to delineate important pathways and mechanisms of action in these processes.

In the present study, control of tumor growth through selective inhibition of VEGFR2 with r84 was associated with several histological changes. r84 reduced tumor MVD similar to bevacizumab treatment (Figure 3.9). Consistent with the concept of anti-angiogenic therapies functioning by pruning nascent tumor vasculature, we observed a trend of increased pericyte association with endothelial cells in r84- and bevacizumab-treated animals, though this only reached statistical significance in the H460 model (Figure 3.9). NSCLC tumors treated with r84 and bevacizumab showed a reduction in VEGFR2 staining (Figure 3.10), with the exception of A549 tumors where bevacizumab had no effect, suggesting specific inhibition of VEGF:VEGFR2 binding by r84 can down regulate receptor expression. As VEGFR2 is considered the predominant

angiogenic signaling receptor, decreasing its expression within tumors could promote the anti-angiogenic effects of r84. Tumor LVD was also decreased in mice treated with r84 and bevacizumab, with the exception of A549 tumors where bevacizumab had no effect (Figure 3.11). In several tumor types, including lung cancer, lymphatic vasculature participates in tumor metastasis (Saharinen et al., 2004). Although predominately mediated by VEGF-C and -D interaction with VEGFR3, recent data demonstrated elevated expression of tumor-derived VEGF-A contributes to pathological lymphangiogenesis (Cursiefen et al., 2004; Hirakawa et al., 2005). In a corneal injury model, Cursiefen *et al.*, (Cursiefen et al., 2004) demonstrated that elevated levels of VEGF-A recruits macrophages and inflammatory cells secreting VEGF-C and -D to the site of injury, thereby inducing lymphangiogenesis. This mechanism may explain the decrease in LVD seen in treated tumors in our studies. Therefore, reduced LVD observed with r84 and bevacizumab therapy is perhaps mechanistically similar to the reduction in LVD observed in 2C3-treated breast cancer xenografts, which correlated with a VEGFR2-mediated down regulation of VEGFR3 in lymphatic endothelial cells and a decrease in angiopoietin-2 expression in endothelial cells and tumor cells (Whitehurst et al., 2007).

Extended therapy with r84 in tumor bearing and non-tumor bearing mice did not induce toxicity, as measured by weight maintenance, blood pressure levels, proteinuria analysis, and preservation of renal, hepatic, and pancreatic

structure and function. Previous studies assessing the safety of anti-VEGF antibodies, including bevacizumab, demonstrated increased hepatic and renal damage with antibodies of increasing affinity to VEGF. Hepatic and renal toxicity produced elevated serum levels of ALT, AST, and BUN as well as glomerulosclerosis and loss of structural integrity seen by hematoxylin and eosin staining (Gerber et al., 2007). These toxicity-inducing antibodies were first characterized in 2006 as cross-reactive antibodies that recognized human and mouse VEGF and highlighted the importance of blocking stromal-derived VEGF in some tumor models (Liang et al., 2006a). Our current work with r84 in the A549 xenograft model (Figure 3.6 C, Figure 3.7 C, Figure 3.8) highlights the importance of host VEGF in the progression of some tumors. However, in our studies, long-term therapy with r84 does not induce renal or hepatic toxicities (Figure 3.14, Table 3.1, Figure 3.15). This separates r84 from previously developed cross-reactive antibodies as a unique therapeutic tool with the potential to answer key questions on the function of stromal VEGF in tumor progression and the importance of VEGFR1 activity in avoiding anti-VEGF induced toxicity. The endocrine pancreas is especially sensitive to VEGF inhibition (Kamba and McDonald, 2007; Kamba et al., 2006). However, extended therapy with r84 did not result in changes in pancreatic islet structure or function (Figure 3.16, Figure 3.17). In an immunocompetent model of spontaneous pancreatic cancer, extended therapy with mcr84 did not induce renal or hepatic toxicities as indicated by urine

analysis and serum metabolic markers (Figure 3.19 B, Table 3.2, Figure 3.20) and acute increases in systolic blood pressure were resolved over time without cessation of therapy (Figure 3.19 A). Thus, we conclude that r84 and mcr84 do not induce significant toxicities in mice perhaps due to the lower affinity of r84 for VEGF as compared to other anti-VEGF antibodies or from a protective function of VEGFR1. Overall, the characteristics of r84 both *in vitro* and *in vivo* establish this antibody as an important tool to further elucidate the importance of VEGF signaling through VEGFR1 and VEGFR2 within tumors and during normal physiology and as a potential adjuvant therapy. At the present time the production of clinical grade r84 is being evaluated and we anticipate that initial safety trials in humans will begin in the near future.

# CHAPTER FOUR

## THE ROLE OF ANTI-ANGIOGENIC THERAPIES IN NSCLC


### Abstract

Worldwide, NSCLC is the most common and deadly cancer despite advances in cancer therapy. Here we describe the pathogenesis and epidemiology of lung cancer and some of the current treatment options for this disease. Several anti-angiogenic strategies have been evaluated in NSCLC, but only the anti-VEGF monoclonal antibody bevacizumab (Genetech/Roche) has gained FDA approval. However, bevacizumab therapy is associated with modest increases in patient survival in NSCLC and its other cancer indications. Therefore, the future of anti-angiogenic therapy in NSCLC and other cancer types is tenuous and may be dependent on a better understanding of how resistance develops and what markers best predict for patient response.

## 4.1 Introduction

Lung cancer has remained the most prevalent and lethal cancer worldwide for the past 26 years (Jemal et al., 2011; Parkin et al., 1993). In 2008, there were more than 1.6 million new cases of lung cancer diagnosed worldwide and an estimated 1.4 million deaths associated with this disease (Jemal et al., 2011). Within the United States, there were more than 220,000 new cases of cancers of the lung and bronchus in 2010 and greater than 157,000 deaths, amounting to 15% and 28% of total cancer incidences and deaths, respectively (Jemal et al., 2010b). If one breaks down cancer incidence by gender, cancers of the lung and bronchus are the second most prevalent cancer type, behind prostate cancer in men and breast cancer in women (Figure 4.1) (Jemal et al., 2010b). However, lung cancer is still the most deadly form of cancer amongst both genders in the United States, representing nearly 1/3 of all cancer-related deaths for each gender (Figure 4.2) (Jemal et al., 2010b).

In general, the prognosis of lung cancer is discouraging. An overwhelming majority of patients with NSCLC, the most prevalent form of lung cancer, have advanced stage disease at the time of their diagnosis (Parkin et al., 2005; Webb and Simon, 2010). Although small cell lung cancer (SCLC) initially responds well to radiation and chemotherapy, NSCLC is not as responsive (Hoffman et al., 2000). Additionally, the highly aggressive and invasive characteristics of NSCLC

often lead to metastasis of the tumor within months to the contralateral lung, bones, liver and brain. The rate and degree of metastatic progression in NSCLC is ultimately the key contributing factor to lung cancer patient death (Hoffman et al., 2000) (Feld et al., 1984; Nguyen et al., 2009). Because of this, the five year survival rates for lung cancer remain dismal at approximately 15% in the United States, 10% across Europe and 9% in developing countries (Parkin et al., 2005; Webb and Simon, 2010). In addition, progress in chemotherapeutic agents has not yielded significant improvements in lung cancer patient survival and many lung cancer patients will recur despite multidisciplinary intervention. Therefore, emerging therapeutic modalities with the potential to improve the prognosis of lung cancer, such as those that inhibit tumor angiogenesis are of special interest.

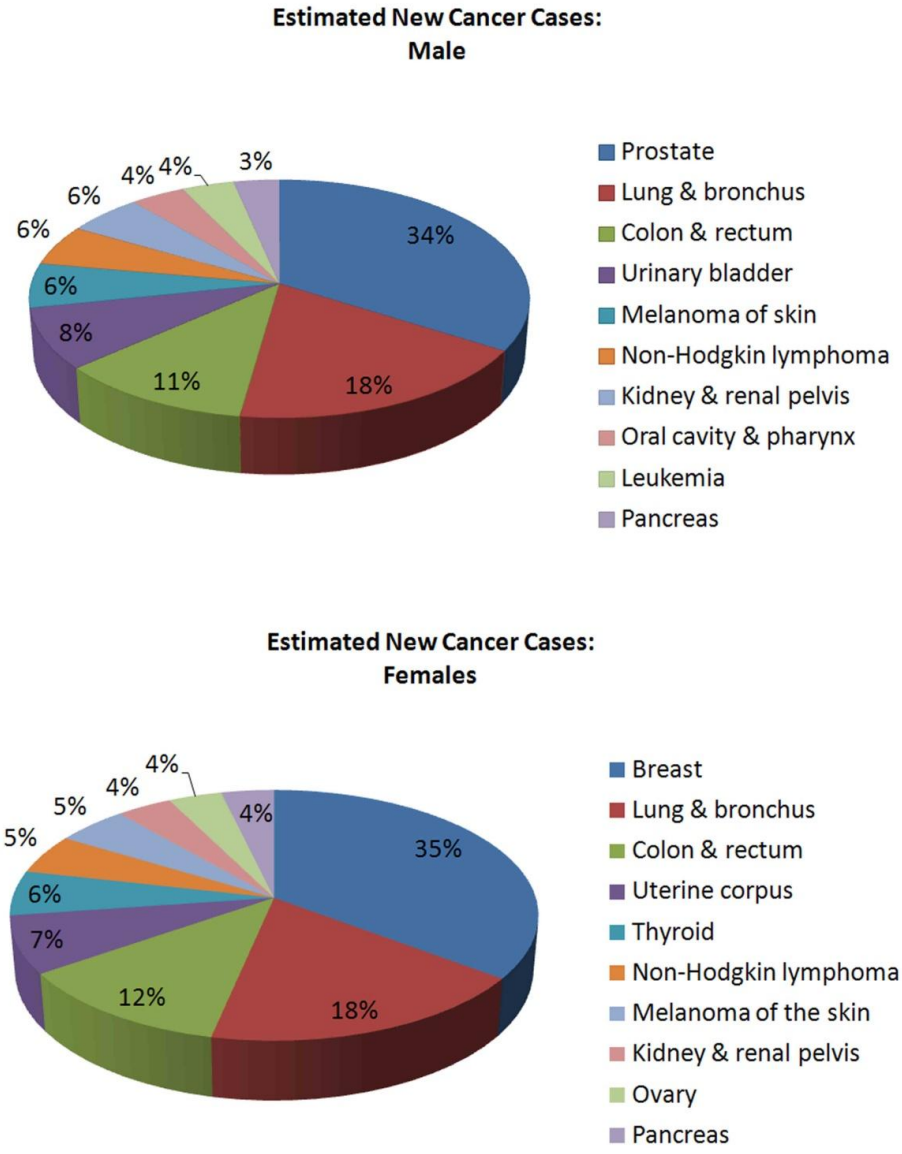


**Figure 4.1: New cancer cases in the United States.**

The distribution of new cases of cancer in men and women in the United States by tumor type is displayed. Cancers of the lung and bronchus are the second most commonly diagnosed cancer among Americans, second only to reproductive cancers in men and women. Data adapted from (Jemal et al., 2010b).

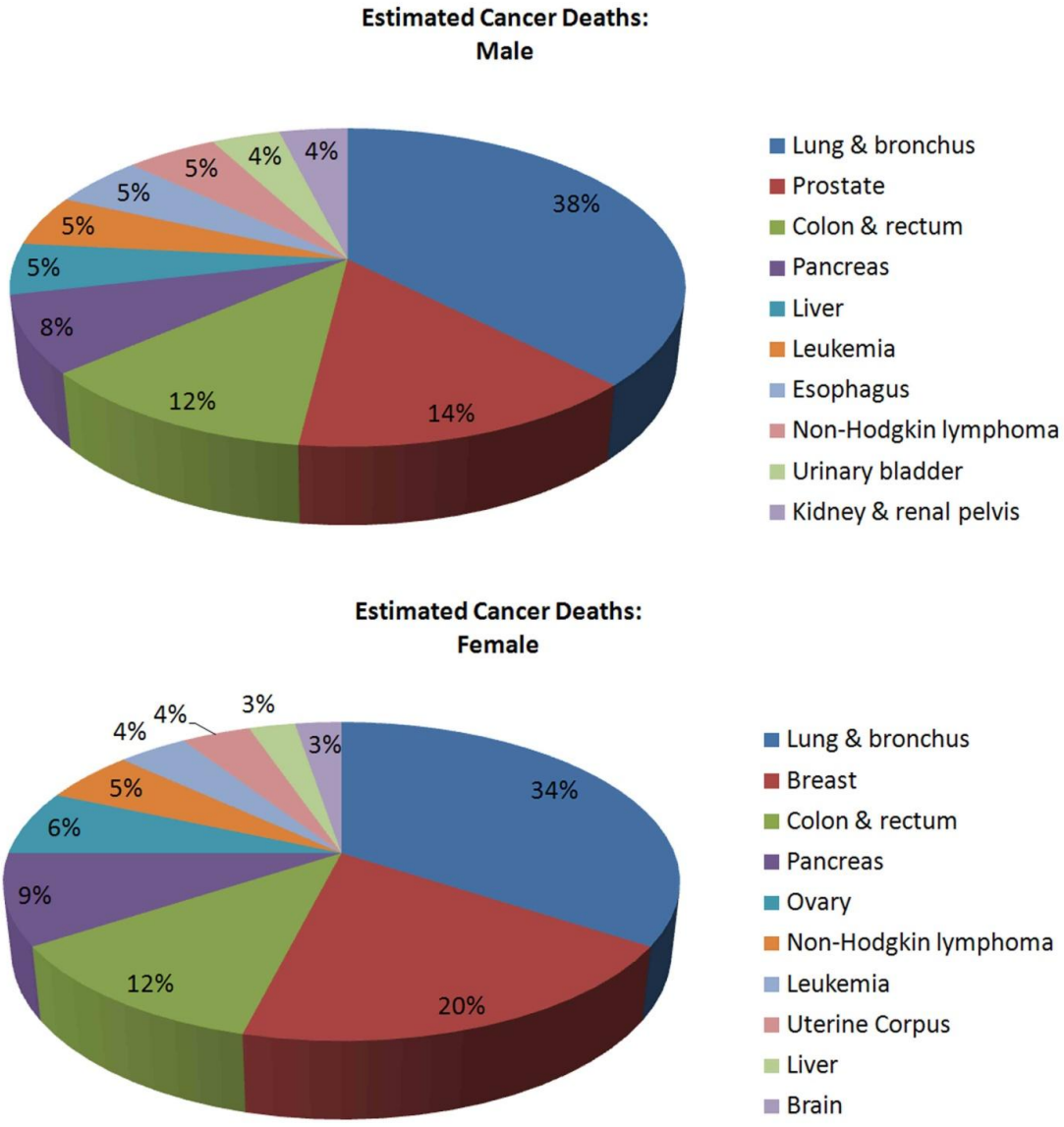


**Figure 4.2: Total cancer deaths in the United States.**

The distribution of annual cancer-related deaths in men and women in the United States is displayed by tumor type. Lung cancer is the most common cause of cancer-related deaths in both genders. Data adapted from (Jemal et al., 2010b).

### *4.1.1 Lung cancer pathogenesis and epidemiology*

There are two broad categories of lung cancer—SCLC and NSCLC. SCLC comprises approximately 15% of all lung cancer diagnoses in the United States. Arising from neuroendocrine cells within the lung, SCLCs tend to be very aggressive and malignant tumors (Herbst et al., 2008). NSCLCs make up the remaining 85% of lung cancer cases. There are three main NSCLC histotypes, squamous cell carcinoma, large cell carcinoma and the most prevalent form of NSCLC, adenocarcinoma (Brambilla et al., 2001; Herbst et al., 2008). The least well-defined of the three NSCLC histotypes is large cell carcinoma, which often includes poorly differentiated or undifferentiated lung cancers that are not readily classified as any of the other histotypes.

Worldwide lung cancer trends are largely dependent on smoking and the use of tobacco products. The patterns of histotype incidence differ between smokers and never-smokers. Smoking is directly related to most lung cancers and is especially correlated with the incidences of squamous cell carcinoma and SCLC (Sun et al., 2007; Toh et al., 2006). Of the thousands of chemicals present in cigarette smoke, the International Agency for Research in Cancer has classified more than 60 as carcinogenic. Among these carcinogens are the highly potent and dangerous polycyclic aromatic hydrocarbons including nitrosamine nicotine-derived nitrosoaminoketone and benzo[a]pyrene (Sun et al., 2007). Metabolism of these carcinogens enhances their ability to form DNA adducts through covalently

binding to DNA, leading to either their removal through nucleotide excision repair or apoptosis of the affected cell (Gazdar, 2007; Sun et al., 2007). The formation and attempted repair of carcinogen-induced adducts can confer mutations in key genes responsible for lung cancer development such as *KRAS* or *TP53*. This process can continue over time, inducing numerous other mutations, both at the genetic and epigenetic levels that escalate tumor progression (Sun et al., 2007). The direct relationship with smoking as the predominant driver of lung cancer pathogenesis is evident from worldwide statistics. In most Western countries, including North America, Europe and Australia, where the tobacco epidemic has peaked over 50 years ago, there are decreasing rates of lung cancer deaths (Bray and Weiderpass, 2010; Jemal et al., 2008; Peto et al., 2006). However, in areas where the epidemic is more recent, such as Asia and Africa where smoking rates are still rising or have not yet become stabilized, there are increasing lung cancer incidence rates (Jemal et al., 2010a; Lam et al., 2004; Youlden et al., 2008). Implementing tobacco intervention programs to control the use of these products by increasing prices, treating tobacco dependence and raising awareness of the harmful consequences of tobacco products has been shown to decrease lung cancer incidence globally (Prevention, 2007). Over the past three decades, increases in public awareness and tobacco control measures have resulted in declining rates of lung cancer incidence and mortality in men and a plateau in women in the United States (Jemal et al., 2001; Jemal et al., 2005).

Similar trends are observed in Europe and other developed regions (Bray et al., 2004). However, in developing countries, the lung cancer epidemic is still on the rise and can be directly associated with the rising use of tobacco products within these regions (Jemal et al., 2011; Parkin et al., 2005). By gender, 80% of lung cancer in men and approximately 50% of lung cancer in women can be contributed to smoking activities (Ezzati et al., 2005; Ezzati and Lopez, 2003). The difference in smoking-related lung cancer incidences between the genders can be attributed to the fact that historically, women have started smoking around 10 years later than their male counterparts (Harris, 1983). Additionally, there is growing data supporting a different set of risk factors for lung cancer in women, a topic that will be further discussed in this chapter. It is important to note that only 10-20% of smokers will develop lung cancer and having a family history or lung cancer confers a 1.5-fold increase in the risk of disease incidence in never-smokers (Matakidou et al., 2005). This association is heightened to a two-fold increase in risk amongst black individuals (Cote et al., 2005). Therefore, genetic differences amongst individual are likely to play large role in determining overall sensitivity to lung cancer carcinogens (Sun et al., 2007).

Although smoking plays a strong role in the majority of lung cancers worldwide, approximately 25% of lung cancers are not attributable to smoking. In fact, 15% of all diagnosed lung cancers in men and 53% in women are not due to smoking exposure (Parkin et al., 2005), highlighting a common public

misconception that lung cancer is solely a self-inflicted disease caused by smoking and the role gender plays in lung cancer development. Patients that are never-smokers, classified as individuals that have smoked fewer than 100 cigarettes, are a growing minority of lung cancer patients. Never-smokers predominantly have adenocarcinoma and account for roughly 10-25% of all lung cancer cases. If this group of patients was evaluated independently from all lung cancer incidences it would represent the seventh most prevalent cancer type in the world (Hecht, 2003; Sun et al., 2007). Studies evaluating mutational status and therapeutic efficacy suggest that lung cancer in never-smokers is a distinct disease from their smoking counterparts (Sun et al., 2007; Toh et al., 2006). A better understanding of genetic and environmental risk factors contributing to lung cancer can provide new information for improving treatment modalities and may help reduce the stigma associated with this disease.

As previously discussed, tobacco product carcinogens are well-known to cause cancer. In never-smokers, the carcinogens are more varied and one predominant factor has not been identified. However, likely suspects include asbestos, arsenic, radon, environmental pollutants and silica (Alberg et al., 2005; Boffetta, 2006; Subramanian and Govindan, 2007). Exposure of never-smokers to environmental tobacco smoke (also known as second hand smoke) has been shown to be causally associated with increased risk of lung cancer incidence (Brown, 1992; Stayner et al., 2007; Vineis et al., 2004). However, environmental

tobacco smoke accounts for less than 10% of total lung cancer cases in never-smokers in the United States and is therefore not the predominant factor influencing this disease (Brown, 1992). Within the global population of never-smokers, lung cancer incidence is more common in females. The frequency of lung cancer in women never-smokers varies dramatically by region (Sun et al., 2007). In the United States, approximately 15% of women with lung cancer are never-smokers (Cerfolio et al., 2006; Visbal et al., 2004; Wakelee et al., 2007). This proportion increases to over 80% in South Asia (Badar et al., 2006; Jindal et al., 1982), illustrating the strong influence of genetic and/or environmental factors contributing to lung cancer epidemiology in never-smokers. For example, in China the high rates of lung cancer in female never-smokers has been linked to exposure of Chinese women to vapors from poorly-ventilated indoor coal burning and cooking oils (Sun et al., 2007). During traditional Chinese cooking, the heated cooking oils produce volatile mutagenic and carcinogenic substances including aldehydes and polycyclic aromatic hydrocarbons. Long-term exposure to these risk factors is strongly associated with lung cancer in these populations (Kleinerman et al., 2002; Wu-Williams et al., 1990; Xu et al., 1989).

In cancer oncogene addiction can occur where certain mutations can drive tumor progression (Fisher et al., 2001; Weinstein, 2002). These genes are typically involved in cell proliferation and survival and can be successfully combated with targeted therapies. Several genetic mutations driving lung cancer

progression and pathogenesis have been identified and well studied including, *EGFR, KRAS* and *TP53*. EGFR is a RTK activated by extracellular growth factors and is over expressed in many cancer types, including approximately 50% of lung cancers (Sharma et al., 2007). Growth factor binding to EGFR induces receptor homo- or heterodimer formation with other RTKs and induces downstream signaling pathways that mediate numerous effects (Sharma et al., 2007). EGFR activation can lead to downstream signaling affecting apoptosis inhibition, increased cellular proliferation, and increased invasion, metastasis and angiogenesis through phosphatidylinosityl 3-kinase (PI3K) and AKT, Ras-Raf-Mek-Erk and STAT signaling cascades, respectively (Sun et al., 2007). More than 60% of NSCLCs have *EGFR* over expression and the prognosis of this patient population is poor (Hirsch et al., 2003; Nicholson et al., 2001; Ohsaki et al., 2000). In addition, enhanced autocrine activation of EGFR signaling can occur in tumors over expressing the EGFR ligands epidermal growth factor (EGF) and transforming growth factor α (TGFα) (Putnam et al., 1992; Rusch et al., 1993). The identification of EGFR mutations in cancer led to the development and clinical use of two FDA-approved small molecule tyrosine kinase inhibitors (TKIs) targeting EGFR, gefitinib (Iressa, AstraZeneca) and erlotinib (Tarceva, OSI Pharmaceuticals, Genetech) for use in chemotherapy refractory advanced NSCLC (Blackhall et al., 2006; Herbst et al., 2005; Shepherd et al., 2005; Thatcher et al., 2005). A small population of patients treated in early clinical trials

with EGFR TKIs showed a striking response to therapy (Fukuoka et al., 2003; Kris et al., 2003; Perez-Soler et al., 2004; Shepherd et al., 2005). Further investigation of this group of patients led to the discovery that sensitivity to these drugs was due to mutations within EGFR's tyrosine kinase domain (Lynch et al., 2004; Paez et al., 2004). Interestingly, these mutations are predominantly found in adenocarcinomas from never-smoker females of East Asian descent (Ciardiello and Tortora, 2008; Kim et al., 2008; Sharma et al., 2007; Shigematsu and Gazdar, 2006). In fact, increased exposure to tobacco smoke is inversely correlated with *EGFR* mutation frequency (Kosaka et al., 2004; Pham et al., 2006). Despite the initial success of EGFR inhibitors, the majority of these responders will eventually become resistant to erlotinib and gefitinib therapy (Pao et al., 2005a; Sequist et al., 2007). The resistance mechanisms and new therapeutic approaches to overcome resistance are being actively researched and developed (Webb and Simon, 2010).

Downstream of EGFR, the Ras family of proteins are small GTPases that primarily function in regulating cell proliferation (Downward, 2003). When the GTPase activity of KRAS is lost following missense mutations, these proteins lose the ability to switch back to their inactive GDP-bound state and therefore remain constitutively active and contribute to the development of tumors (Downward, 2003; Sun et al., 2007). The most common Ras pathway mutations are found in *KRAS*. Activating mutations in *KRAS* are found in up to half of all

lung adenocarcinomas (Herbst et al., 2008; Webb and Simon, 2010). Oncogenic *KRAS* mutations are never found in SCLC, but are exclusively found within adenocarcinoma histotypes of NSCLC (Shigematsu and Gazdar, 2006; Shigematsu et al., 2005; Tam et al., 2006). The highly carcinogenic substances nitrosoaminoketone and BAP that are found in tobacco smoke have the ability to induce oncogenic, constitutively active KRAS by forming DNA adducts within codon 12 (Sun et al., 2007). Consequently, KRAS mutations are more prevalent in smokers than never-smokers, are not frequently found in East Asian populations and are primarily mutually exclusive to EGFR mutations (Pao et al., 2005b; Shigematsu et al., 2005). Additionally, these mutations are associated with poor prognosis and survival and resistance to conventional chemotherapy and TKIs (Eberhard et al., 2005; Mascaux et al., 2005; Pao et al., 2005b; Riely et al., 2008). Currently there is a paucity of efficacious therapeutic options for lung cancers harboring *KRAS* mutations, although research is actively underway to remedy this.

Within human cancers, one of the most commonly found mutations involves the *TP53* gene encoding the tumor suppressor p53 (Sun et al., 2007). As a transcription factor, p53 affects many important pathways including maintenance of the DNA damage response and control of apoptosis (Sengupta and Harris, 2005). Mutations within *TP53* predominantly affect the ability of the protein to recognize and bind to DNA, reducing its functionality as a transcription

factor (Sun et al., 2007). Although mutations in *TP53* are found in lung cancers of smokers and never-smokers, they are more common within smoker populations (Le Calvez et al., 2005; Vahakangas et al., 2001).

During cancer progression, tumor suppressor genes are frequently inactivated by chromatin remodelling occurring following aberrant methylation of CpG islands within the promoter region of these genes (Sharma et al., 2007). Although further studies are required to disseminate methylation patterns and frequency, there appears to be selective differences within this process between smokers and never-smokers (Sun et al., 2007).

### *4.1.2 Current treatment modalities for NSCLC*

Lung cancer development, like other tumor types, occurs via stepwise progression of malignant transformation within normal respiratory epithelium (Noguchi, 2010). Tobacco smoke carcinogens drive the genetic alterations and progression of 85% of all lung cancers in developed countries (Ramalingam et al., 2011). There has been much progress in our comprehension of the biological mechanisms governing the development and progression of lung cancer. This has led to the discovery of new therapeutic targets in lung cancer and the development of drugs to combat them. As the understanding of molecular drivers of lung cancer improved, so has the ability for using personalized therapy to treat a patient's lung cancer based on their specific mutations and phenotypes.

Each year there are more than 25,000 new cases of SCLC diagnosed in the United States (Govindan et al., 2006). There are a limited number of therapeutic options for SCLC. For the past 30 years, platinum-based chemotherapy and etoposide have been the most efficacious regimens of systemic therapy for SCLC patients (Ramalingam et al., 2011). Studies evaluating varying doses, combinatorial strategies with topoisomerase, mTOR or Bcl-2 inhibitors have failed to improve SCLC patient survival (Hanna et al., 2006a; Lara et al., 2009; Pandya et al., 2007; Rudin et al., 2008). A recent study suggested prophylactic cranial irradiation can increase OS (Slotman et al., 2007), although follow up studies will be necessary to evaluate efficacy of this strategy in larger patient populations.

One third of all NSCLC patients are diagnosed with early stage disease. Although surgical resection is the best standard care for stage I, II and some IIIA lung cancer patients, approximately 40% will have a comorbid illness that precludes surgery (Ramalingam et al., 2011). Surgery in lung cancer involves the removal of the entire afflicted lobe or lung, as there is a higher incidence of local recurrence following sublobar resections (Ramalingam et al., 2011). Recurrence of lung cancer following surgery is predominantly at distant sites, highlighting the need for systemic therapies to combat this disease (Ramalingam et al., 2011). However, post-operative radiation therapy is generally not used for lung cancer patients since historical data indicated this can negatively impact survival

(NSCLCCollaborativeGroup, 1995; PORTMeta-analysisTrialistsGroup, 1998). Alternatively, for early stage NSCLC patients that are not surgical candidates, stereotactic body radiotherapy (SBRT) is a new therapeutic option that has been recently shown to confer a 97% three-year primary tumor control rate (Timmerman et al., 2010). Clinical studies are currently evaluating the efficacy of SBRT compared to surgery in early stage NSCLC patients in Europe (Ramalingam et al., 2011). Additionally, non-surgical early stage NSCLC patients with smaller peripheral tumors can achieve high local control rates with radiofrequency ablation therapy (Pennathur et al., 2007).

For patients with locally advanced disease that cannot be surgically removed, systemic and radiation therapy is used. Tumors are considered unresectable if they have invaded directly into major blood vessels, the mediastinum, heart or the vertebral body or if the tumor has spread to the mediastinal lymph nodes on the same side of the body as the initial tumor (Ramalingam et al., 2011). Studies in the early 1990s demonstrated increased OS with combination chemotherapy and radiation therapy as compared to radiation alone in stage III NSCLC patients (Dillman et al., 1990; Le Chevalier et al., 1991). Later studies demonstrated increased efficacy with concurrent chemotherapy and radiation (Curran et al., 2000; Furuse et al., 1999). However, this approach also has increased toxicities and is therefore only used in patients that have a good performance status. Locally advanced NSCLC can be treated

with radiation therapy and full doses of cisplatin and etoposide (Albain et al., 2002), or weekly "radiosensitizing" doses followed by two full doses of carboplatin and paclitaxel (Belani et al., 2005a). The traditional dose of radiation for locally advanced NSCLC patients is 60 gray, but ongoing studies are evaluating the safety and efficacy of increasing doses to 74 gray (Perez et al., 1980; Ramalingam et al., 2011).

Over the past 16 years, numerous studies have identified platinum-based chemotherapy (generally with three to four cycles of cisplatin-based chemotherapy) as the most effective option for early stage NSCLC patients (Ramalingam et al., 2011). Chemotherapy is given as adjuvant therapy following surgery in early stage NSCLC patients. Treatment options for advanced stage NSCLC relies heavily on patient performance status, with the overall goals to maintain or enhance quality of life, improve symptoms and prolong survival (Ramalingam et al., 2011). Females have been recently shown to have improved survival versus their male counterparts, making gender a prognostic factor in advanced stage NSCLC (Batevik et al., 2005; Harichand-Herdt and Ramalingam, 2009; Siddiqui et al., 2010; Visbal et al., 2004). Standard treatment involves systemic platinum-based therapy regimens as this strategy proved more efficacious to supportive care alone in clinical trials conducted in the late 1980s (Bunn, 2002; Rapp et al., 1988). Although cisplatin-based regimes provide the best response rates, regimens with carboplatin are more tolerable and are routinely

used in the clinic (Kelly et al., 2001; Schiller et al., 2002). Two-drug combinations of platinum-containing chemotherapy regimens have demonstrated improved progression free survival (PFS), OS and response rate when compared to single agent therapy and have become the standard of care for advanced NSCLC patients (Lilenbaum et al., 2005; Sandler et al., 2000; Wozniak et al., 1998). Commonly used, efficacious combination drugs include paclitaxel, docetaxel, vinorelbine, gemcitabine, pemetrexed and ironotecan (Belani et al., 2005b; Ohe et al., 2007; Schiller et al., 2002; Wozniak et al., 1998). In a large randomized study of more than 1200 NSCLC patients performed by the Eastern Cooperative Oncology Group (ECOG), there was no difference in efficacy (median survival of eight months) between four different platinum-based chemotherapy regimens. However, the combination of paclitaxel and carboplatin had the fewest toxicities (Schiller et al., 2002). Trials evaluating three-drug cytotoxic combinations in advanced NSCLC patients did not show improved efficacy as compared to two-drug regimens, but did induce higher toxicities and have therefore not been implemented in standards of care (Alberola et al., 2003; Stinchcombe and Socinski, 2009). The platinum-based two-drug regimens use in good performance status advanced NSCLC patients confer an 8-11 month median survival and 30-40% one-year survival rates (Ramalingam and Belani, 2004).

40-80% of NSCLC cases express *EGFR* (Ramalingam et al., 2011). In general, EGFR TKIs are well-tolerated and the most common toxicities are

diarrhea and skin rash. Mutations in *EGFR* occur in 10-15% of Caucasian patients and are found in up to 40% of Asian patients (Paez et al., 2004). Treatment of resected, early stage NSCLC patients with the EGFR inhibitors gefitinib and erlotinib has yet to demonstrate any survival or progression advantages (Goss et al., 2010; Ramalingam et al., 2011). Further studies are underway to elucidate potential efficacies of other targeted therapies in this patient population. In a Phase III trial in inoperable stage III NSCLC patients, targeting EGFR signaling with maintenance gefitinib therapy after chemotherapy and radiation failed to increase survival over placebo (Kelly et al., 2008). However, use of the anti-EGFR monoclonal antibody cetuximab (IMC-C225/Erbitux, ImClone) demonstrated a two-fold improvement in OS when combined with radiation therapy in a Phase III trial in head and neck cancer patients (Bonner et al., 2006). This treatment strategy is now being evaluated in a Phase III trial in locally advanced NSCLC patients (Ramalingam et al., 2011). Clinical studies performed within the last decade have demonstrated a striking response of mutant *EGFR* NSCLC to small molecule EGFR TKIs, leading to the use of these agents as first-line therapy in advanced NSCLC patients with a known *EGFR* sensitizing mutation (Maemondo et al., 2010; Mitsudomi et al., 2010; Mok et al., 2009; Rosell et al., 2009). Use of these drugs in this patient population produces a 60-80% response rate, 10-12 month PFS and 24-30 month OS (Ramalingam et al., 2011). Interestingly, there are no survival advantages with combination

chemotherapy and EGFR TKIs in general or selected NSCLC patients (Giaccone et al., 2004; Herbst et al., 2004). Similar efficacies to the TKIs are not seen when the external domain of EGFR is targeted by cetuximab, suggesting that a different mechanism of action is at play (Hanna et al., 2006b; Mukohara et al., 2005). As previously mentioned, although there is great efficacy of EGFR TKIs in a subset of NSCLC, most patients will eventually become resistant to therapy. The best understood mechanisms of resistance include gain of a second *EGFR* mutation (T790M; happens in 50-60% of patients) occurring in exon 20 that alters the binding site for the TKIs, rendering them useless (Inukai et al., 2006; Kobayashi et al., 2005; Pao et al., 2005a), amplification of the proto-oncogene *MET*, activation of additional RTKs, or the initiation of epithelial to mesenchymal transition within tumors (Herbst et al., 2008; Webb and Simon, 2010). To combat these effects, second-generation EGFR inhibitors are under development and are currently at different stages of clinical evaluation (Ramalingam et al., 2011). Some of the strategies being investigated include irreversible inhibitors of EGFR as well as inhibitors of c-Met and downstream mediators of EGFR signalling such as heat shock protein 90 (Ramalingam et al., 2011).

A recent success story in personalized therapy in NSCLC involves a small subset of lung cancers driven by an inversion translocation of echinoderm microtubule-associated protein-like 4 (*EML4*) and anaplastic lymphoma kinase (*ALK*) genes (Shaw et al., 2009; Soda et al., 2007; Soda et al., 2008). The

resultant *EML4/ALK* fusion gene occurs in approximately five percent of NSCLC patients predominantly in younger, never-smoker patients that have adenocarcinoma with signet cell features (Pao and Girard, 2011; Shaw et al., 2009). Interestingly the *EML4/ALK* translocation is mutually exclusive with mutations in *KRAS* and *EGFR* and do not respond to the EGFR inhibitors erlotinib and gefitinib (Horn and Pao, 2009; Ramalingam et al., 2011). Pfizer's small molecule TKI crizotinib (PF-02341066, Pfizer) inhibits c-Met and ALK. A Phase IB trial of crizotinib in NSCLC patients with an *ALK* translocation demonstrate a 66% response rate and an 87% disease control rate characterized by tumor shrinkage (Bang et al., 2010). A Phase III study is currently underway to evaluate the efficacy of crizotinib in this cohort of NSCLC patients and is expected to gain FDA approval.

### 4.2 Anti-angiogenic therapy in NSCLC

Lung microvascular endothelial cells produce significant amounts of VEGF, which contributes to endothelial maintenance and homeostasis within the lungs in an autocrine manner (Voelkel et al., 2006). Finely tuned interactions between endothelial cells, VEGF and the lung embryonic mesenchyma are critical to the formation and maturation of the lung (Akeson et al., 2003; Majka et al., 2006).

Tumor angiogenesis is functionally and structurally abnormal and is characterized by poorly organized and hyperpermeable tortuous dilated vessels (Blau and Banfi, 2001; Folkman, 2007; Jain, 2001). Therefore, the tumor microenvironment is characterized by hypoxia, acidosis and interstitial hypertension, which increases VEGF production and decreases cytotoxic chemotherapy efficacy (Carmeliet, 2005; Carmeliet and Jain, 2000). Tumor angiogenesis can be targeted therapeutically through blockade of the VEGF pathway at various molecular levels. Currently, there are two major concepts being studied in the clinical setting: blocking VEGF from binding to its extracellular receptors with VEGF or VEGFR antagonists or inhibiting VEGF signalling with TKIs.

### *4.2.1 Bevacizumab (Avastin®, Genentech/Roche)*

Bevacizumab is currently the only anti-angiogenic drug FDA-approved for use in lung cancer patients. In 2004, Johnson et al first demonstrated the efficacy of bevacizumab (15 mg/kg) in combination with paclitaxel and carboplatin in providing increased patient response rate, time to progression and a non-significant trend towards OS increases in a randomized Phase II trial in 99 patients with advanced NSCLC (Johnson et al., 2004). In this trial, approximately six percent of patients that received bevacizumab and had tumors located close to major vessels and with squamous cell histology suffered fatal hemoptysis. Due to this finding, patients with brain metastases or squamous histology tumors were

excluded from future studies with bevacizumab in NSCLC. As previously mentioned in Chapter One, the Phase III ECOG 4599 trial of 878 patients with advanced or recurrent non-squamous NSCLC evaluated the efficacy of combination carboplatin and paclitaxel chemotherapy versus chemotherapy plus 15 mg/kg bevacizumab. The triple combination was associated with small, yet statistically significant gains in OS (12.3 months versus 10.3 months with chemotherapy alone) and PFS (6.2 months versus 4.5 months with chemotherapy alone) and led to the approval of this regimen in NSCLC in 2006 (Sandler et al., 2006). This was the first report of an anti-angiogenic agent in the advanced NSCLC population demonstrating a survival benefit when used as first-line treatment in combination with standard doublet chemotherapy (Ramalingam and Belani, 2010). There were increased toxicities observed in the bevacizumab-treated group including hypertension, proteinuria, bleeding and febrile neutropenia (Sandler et al., 2006). A subsequent Phase III randomized AVAiL trail in advanced non-squamous NSCLC assessed response to cisplatin and gemcitabine with or without two doses of bevacizumab. Although the addition of bevacizumab failed to improve OS, there was a statistically significant increase in the primary endpoint of PFS versus the control chemotherapy alone arm (Reck et al., 2009). Several studies have evaluated the potential utility of targeting both VEGF and EGFR signaling. Combinations of bevacizumab and docetaxel or pemetrexed or bevacizumab and erlotinib as second-line therapy were

demonstrated to have superior gains in PFS and OS versus chemotherapy alone in a 120 patient Phase II trial in advanced non-squamous NSCLC. There was no observed difference between the bevacizumab containing arms, prompting further research into the efficacy of erlotinib and bevacizumab combinations in NSCLC (Herbst et al., 2007). The Phase II BeTA trial evaluated the efficacy of erlotinib with or without bevacizumab in advanced NSCLC patients that had failed standard first-line therapy. Again, this trial found combination therapy yielded increases in PFS, but failed to meet its primary endpoint of OS (Hainsworth and Herbst, 2008). In a separate Phase IIIb trial (ATLAS) using a different dosing strategy, combination of bevacizumab and erlotinib demonstrated an increase in PFS versus single agent bevacizumab in advanced NSCLC patients (Miller et al., 2009). A small Phase II trial in advanced NSCLC demonstrated promising OS and PFS results using combination pemetrexed, carboplatin and bevacizumab followed by pemetrexed and bevacizumab maintenance therapy (Patel et al., 2009b). Based on these results, a large Phase III Pointbreak trial comparing the efficacy of pemetrexed, carboplatin and bevacizumab with pemetrexed and bevacizumab or bevacizumab alone maintenance therapy is ongoing (Patel et al., 2009a). Second-line therapy with pemetrexed and bevacizumab in advanced NSCLC was shown to have encouraging OS and PFS outcomes and had a tolerable toxicity profile in a small Phase II trial (Adjei et al., 2010). Overall, bevacizumab therapy in NSCLC is associated with statistically significant, but

small increases in OS and PFS, suggesting we have not yet identified the optimal therapeutic combinations or patient subpopulations to benefit most from these regimens. There are currently 69 ongoing trials with bevacizumab in NSCLC listed on the National Cancer Institute website evaluating the efficacies of different combination strategies with bevacizumab that will hopefully contribute to the elucidation of the best regimens for bevacizumab in this indication (NationalCancerInstitute, 2011).

### *4.2.2 Anti-angiogenic receptor tyrosine kinase inhibitors*

Numerous studies have evaluated the utility of VEGFR targeting TKIs in NSCLC. These agents have potential benefits including their oral administration, ability to hit multiple targets and acceptable toxicity profiles. A selective list of the anti-angiogenic TKIs discussed in this chapter, detailing their respective targets is included in Table 4.1.

| Inhibitor | VEGFR1/2/3 | PDGFR-α/-β | c-kit | RET | Other |
|---|---|---|---|---|---|
| Sorafenib | —/+/+ | —/+ | + | — | Raf |
| Sunitinib | +/+/+ | +/+ | + | + | Flt3 |
| Cediranib | +/+/+ | +/— | + | — | |
| Vandetanib | +/+/+ | —/— | — | + | EGFR |
| Pazopanib | +/+/+ | +/+ | + | — | |
| Axitinib | +/+/+ | +/+ | + | — | |

**Table 4.1: Receptor tyrosine kinase inhibitors evaluated therapeutically in NSCLC**

The targets of six anti-angiogenic receptor tyrosine kinase inhibitors that have been tested in NSCLC are listed. Of these inhibitors, none are currently approved for the treatment of NSCLC, although sorafenib, sunitinib, vandetanib and pazopanib are have approval in other cancer indications (see text). VEGFR, vascular endothelial growth factor receptor; PDGFR, platlet-derived growth factor receptor; RET, rearranged during transfection.

#### *4.2.2.1 Sorafenib Tosylate (Nexavar®, BAY 43-9806, Bayer Pharmaceuticals Corp.)*

Sorafenib targets VEGFR2, VEGFR3, PDGFR-β, c-kit and Raf, and as previously mentioned, has FDA approval for the treatment of advanced renal cell carcinoma and unresectable hepatocellular carcinoma (Wilhelm et al., 2008; Wilhelm et al., 2004), but has not yet been demonstrated as an effective regimen in NSCLC. A small Phase I/II trial in advanced NSCLC assessed the safety and preliminary efficacy of carboplatin and paclitaxel in combination with sorafenib. This study demonstrated a PFS of 104 days and had a reasonable toxicity profile with common TKI adverse events such as hand-foot syndrome, rash and gastrointestinal side effects (Flaherty et al., 2008). The ESCAPE trial was a large, randomized Phase III trial evaluating carboplatin and paclitaxel alone or in combination with sorafenib for advanced NSCLC patients in a first-line setting. Unfortunately, this trial was stopped early as there were no differences between the treatment arms in terms of response rate, PFS or OS. In addition, patients receiving sorafenib had more toxicities and infection rates (Scagliotti et al., 2010). Further studies evaluating sorafenib as monotherapy or in combination with other drugs are ongoing in NSCLC (Ulahannan and Brahmer, 2011).

#### *4.2.2.2 Sunitinib Malate (Sutent®, SU11248, Pfizer, Inc.)*

Sunitinib inhibits all three VEGFRs, PDGFR-α and –β, fms-like TK-3 (Flt3), c-kit and rearranged during transfection (RET) and is FDA approved for the treatment of gastrointestinal stromal tumors after disease progression on or resistance to imatinib, advanced renal cell carcinoma, and most recently in progressive well-differentiated pancreatic neuroendocrine tumors (Raymond et al., 2011; Roskoski, 2007a; Socinski, 2008) (http://www.cancer.gov/cancertopics/druginfo/fda-sunitinib-malate). In a Phase II multicenter trial evaluating single-agent sunitinib efficacy in advanced NSCLC as second- or third-line therapy, there were encouraging data on sunitinib in terms of response rate, PFS and OS as compared with other agents approved for this advanced setting patient population (Socinski et al., 2008). A second Phase II study using continuous sunitinib monotherapy in advanced NSCLC supported these findings and both studies had acceptable toxicity profiles (Novello et al., 2009). Two Phase I trials have assessed the safety of sunitinib in combination with chemotherapy (docetaxel or cisplatin and gemcitabine) and have observed manageable profiles and several partial responses (Reck et al., 2010; Robert et al., 2010). More trials are needed to establish sunitinib as a beneficial treatment option as a single agent or in combination with chemotherapy in NSCLC.

#### *4.2.2.3 Cediranib (Recentin, AZD2171, AstraZeneca)*

Cediranib inhibits VEGFR1, VEGFR2, VEGFR3, PDGFR-α and c-kit and has not yet gained approval for any disease indication (Nikolinakos and Heymach, 2008; Wedge et al., 2005). Cediranib was shown to have single agent anti-tumor activity in Phase I trials, and like other anti-angiogenic TKIs, has manageable toxicity profiles containing common adverse events for this class of drugs such as diarrhea, hypertension and fatigue (Drevs et al., 2007; Yamamoto et al., 2009). Several small Phase I trials have assessed the safety of combination cediranib and chemotherapy regimens in advanced NSCLC. In these trials, the toxicity profiles were manageable and in some instances combination therapy demonstrated improved efficacy (LoRusso et al., 2006). A Phase II/III randomized, double-blind, placebo-controlled BR.24 trial evaluated combination carboplatin, paclitaxel and cediranib first-line treatment in NSCLC patients. Although some initial clinical efficacy was observed, excessive toxicity forced the trial to be terminated early and prevented its progression to a full Phase III study (Goss et al., 2010; Ulahannan and Brahmer, 2011). Further evaluation is needed for cediranib, especially in combination therapy regimens to determine its utility in NSCLC.

#### *4.2.2.4 Vandetanib (Zactima, ZD6474, AstraZeneca)*

Vandetanib is an orally-available TKI that inhibits VEGFR1, VEGFR2, VEGFR3, rearranged during transfection (RET) and EGFR (Ciardiello et al.,

2003; Herbst et al., 2010; Wedge et al., 2002). Recently, vandetanib gained FDA approval for the treatment of advanced thyroid cancer (http://www.cancer.gov/cancertopics/druginfo/fda-vandetanib). The large Phase III, double-blind, randomized ZODIAC trial evaluating second-line treatment of advanced NSCLC with combination docetaxel and vandetanib demonstrated a modest improvement in PFS, but no increase in OS (Herbst et al., 2010). The ZEST Phase III trial assessed the efficacies of single agent vandetanib or erlotinib therapy in previously treated advanced NSCLC patients. Although similar OS and PFS were observed with both drugs, there were greater toxicities with vandetanib (Natale et al., 2009). Preliminary analysis on the efficacy of vandetanib in advanced NSCLC patients that have progressed on combination EGFR TKI and chemotherapy has revealed that the primary endpoint of OS was not reached (Ulahannan and Brahmer, 2011). Overall, the potential of vandetanib as an efficacious therapeutic for NSCLC is disappointing. In regimens with vandetanib and combination chemotherapy there are changes in response rate and PFS, but no advantages are seen in OS and minimal efficacy is seen when combined with another targeted therapy (Ramalingam and Belani, 2010; Ulahannan and Brahmer, 2011).

#### *4.2.2.5 Pazopanib Hydrochloride (Votrient™, GW786034, GlaxoSmithKline)*

The TKI pazopanib inhibits all three VEGFRs, PDGFR and c-kit and has FDA approval for the treatment of advanced renal cell carcinoma (Hutson, 2011; Kumar et al., 2007; Sternberg et al., 2010). In a small Phase II trial in early stage NSCLC patients, pazopanib neoadjuvant monotherapy yielded partial responses in 11.5% of patients. There were the typical toxicities seen with anti-angiogenic TKIs, including hypertension, rash and elevations in alanine aminotransferase levels (Altorki et al., 2010). Further studies are needed to assess the efficacy and safety of pazopanib as single agent therapy or in combination with chemotherapy in NSCLC.

#### *4.2.2.6 Axitinib (AG-013736, Pfizer, Inc.)*

Axitinib is very similar to pazopanib and also inhibits VEGFR1, VEGFR2, VEGFR3, PDGFR and c-kit (Choueiri, 2008). A small Phase I trial demonstrated safety and there was observed anti-tumor activity with single agent therapy (Rugo et al., 2005). First-line axitinib therapy in advanced NSCLC in a Phase II trial showed promising results for PFS and OS (Schiller et al., 2009). In both of these trials, observed adverse events were similar to those seen with other anti-angiogenic TKIs, such as hypertension, nausea, diarrhea and vomiting. Similar response rates among solid tumors, including NSCLCs were seen in a small Phase I trial testing combination paclitaxel, carboplatin and axitinib or gemcitabine, cisplatin and axitinib therapy (Martin et al., 2009). More single and

combination axitinib studies are needed to delineate the potential efficacy of this drug.

The current data available on VEGFR TKIs have been mostly disappointing, with minimal efficacies observed with these drugs as single agents or in combination with chemotherapy in lung cancer clinical trials. Overall, further studies are needed to determine potential efficacies of anti-angiogenic TKIs.

### 4.3 Resistance to anti-angiogenic therapy

When analyzing the available data on clinical use of anti-angiogenic therapies, the results are underwhelming. There are some modest gains seen in PFS, tumor regression and stabilization of disease and minimal changes in OS that are measured in weeks or months. However, these modest effects are temporary and expensive to obtain. This has made many, including the FDA as represented in their recent removal of bevacizumab's approval in breast cancer, question if the high costs of these drugs that do not provide impressive benefit to treated patients are really worth it. Analyses done in our lab and by other investigators have demonstrated that anti-angiogenic drugs are hitting their designed target and result in decreases in tumor microvessel density (see Chapter Three, Figures 3.9, 3.13, and 3.18). Therefore, these drugs are not inherently

faulty and their relative failure in patients can instead be correlated with the tumor's ability to resist the drug's action. Indeed, with the expanding use of anti-angiogenic therapies in the clinic, it has become apparent that not all tumors respond or will remain responsive to anti-angiogenic treatment. The inherent non-responsiveness of certain tumor and the development of acquired resistance to therapy following an initial response, has been termed intrinsic and evasive resistance, respectively (Figure 4.3) (Bergers and Hanahan, 2008). Patients with intrinsically resistant tumors would have no clinical benefit from anti-angiogenic therapy and therefore should be excluded from these treatments; however, we currently lack effective biomarkers that would allow for the stratification of intrinsically resistant or sensitive tumors, or for the monitoring of tumor response and the development of resistance to therapy (Sessa et al., 2008). Research from a number of investigators has identified several mechanisms mediating resistance to anti-angiogenic therapy, including a switch to growth factors other than VEGF, vessel mimicry, genetic instability of tumor endothelial cells, and tumor invasion occurring independently of angiogenesis (Bergers and Hanahan, 2008; Mitchell and Bryan, 2010).

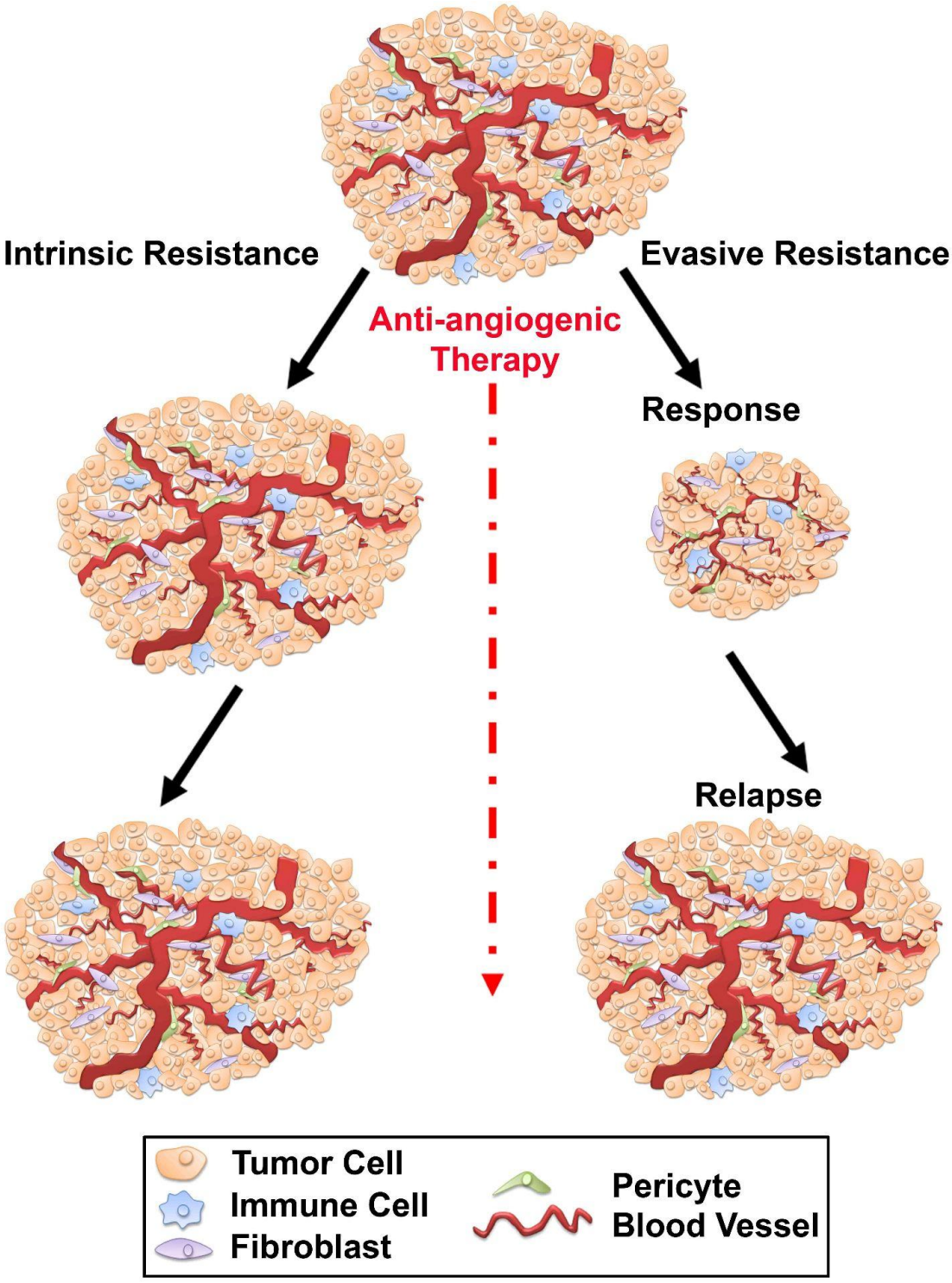
Intrinsic Resistance
Evasive Resistance
Anti-angiogenic Therapy
Response
Relapse
Tumor Cell
Immune Cell
Fibroblast
Pericyte
Blood Vessel

**Figure 4.3: Tumor resistance to anti-angiogenic therapy *in vivo*.**

There are two broad classes of resistance to anti-angiogenic therapies *in vivo*. The first is intrinsic resistance where a tumor shows no response over time in the face of anti-angiogenic therapy (left panel). The second is evasive resistant where there is an initial response to anti-angiogenic therapy that is lost over time (right panel). Adapted from (Bergers and Hanahan, 2008).

### *4.3.1 Growth factor switching*

The tumor microenvironment is hypoxic and the use of anti-angiogenic drugs to target and reduce the tumor vasculature increases this stress. This can lead to signaling to increase expression of pro-angiogenic growth factors. Several studies have demonstrated that blocking VEGF *in vivo* in mice or humans can result in the increased expression of pro-angiogenic growth factors such as VEGF, PlGF, fibroblast growth factor (FGF), FGF-2 (also known as basic FGF), angiopoietin-1, and stromal derived factor 1 (SDF-1) (Batchelor et al., 2007; Casanovas et al., 2005; Ebos et al., 2007; Fisher et al., 2007; Motzer et al., 2006). The milieu of pro-angiogenic factors that become expressed following increased tumor microenvironmental stress brought on by anti-angiogenic therapy can result in the formation of a vascular network that is poorly constructed and functionally inefficient. This can in turn increase hypoxia, inducing more stress and growth factor release as well as impairing drug delivery to tumors (Mitchell and Bryan, 2010). Alternatively, advanced stage cancers can express numerous angiogenic growth factors rendering them capable of continuing angiogenesis in the face of inhibitors of VEGF, such as bevacizumab. In support of this idea, Relf et al found that while VEGF is preferentially expressed in early-stage human breast cancers, there are a multitude of pro-angiogenic factors including FGF-2, PlGF, and transforming growth factor-β (TGF-β) found in advanced stage cancers (Relf et al., 1997).

### *4.3.2 Vessel mimicry*

Vessel mimicry can occur as an alternative process through which blood vessels can be formed without undergoing the process of angiogenesis or vasculogenesis by the differentiation of endothelial progenitor cells (EPCs) into endothelial cells and their subsequent incorporation into new blood vessels. Several studies have demonstrated the ability of bone marrow derived EPCs to differentiate into endothelial cells and become part of the tumor endothelium, promote tumor growth and metastasis and occur in response to chemotherapy (Gao et al., 2008; Lyden et al., 2001; Nolan et al., 2007; Shaked et al., 2006; Shaked and Kerbel, 2007). Studies performed in the last decade have illustrated the ability of several cell types to give rise to EPCs, as characterized by their ability to function as endothelial cells and the secretion of pro-angiogenic factors such as VEGF, stromal derived factor 1 (SDF-1) and angiopoietin-1 and -2 (Pomyje et al., 2003; Yamazaki et al., 2008). This includes mesenchymal stem cells, dendritic progenitor cells, vascular leukocytes, monocyte-derived multipotent cells and tumor stem cells (Annabi et al., 2004; Bussolati et al., 2008; Conejo-Garcia et al., 2005; Kuwana et al., 2008). Recent work has shown that glioblastoma stem-like cells can imitate endothelial cells, comprise the tumor endothelium and harbour the same mutations as the surrounding/parental tumor (Ricci-Vitiani et al., 2010; Wang et al., 2010). Interestingly, tumor cells can

directly participate in vessel mimicry by de-differentiating or trans-differentiating into endothelial or endothelial-like cells. These cells can form channels that do not contain endothelial cells, but have basement membranes and epithelial linings (Mitchell and Bryan, 2010). This concept has been illustrated in sarcomas and carcinomas that are not responsive to anti-angiogenic therapy (Zhang et al., 2007).

### *4.3.3 Tumor endothelial cell genetic instability*

One of the early hypothesized advantages of anti-angiogenic therapy targeting tumor vasculature was the relative genetic stability of endothelial cells as compared to tumor cells. Whereas tumor cells are known to harbour many mutations and can acquire new mutations under the stress of drug therapy to evolve resistance, it was hoped that endothelial cells are more genetically stable and would not evolve mechanisms of resistance to targeted therapies. However, several studies performed in the last decade have chipped away at these ideas and have demonstrated that tumor endothelial cells do acquire mutations and genomic instability. For example, *ex vivo* culture of endothelial cells taken from tumors has demonstrated that these cells have altered cellular morphologies and ECM components, are resistant to apoptosis and serum starvation, do not senesce in culture and have increased expression of oncogenes and decreases expression of tumor suppressor genes (Allport and Weissleder, 2003; Bussolati et al., 2008). In addition, tumor endothelial cells have been found to be cytogenetically abnormal,

containing non-reciprocal translocations, aneuploidy, multiple centromeres and can have missing chromosomes (Hida et al., 2008). The exact mechanism(s) through which genetic instability occurs in tumor endothelial cells is not precisely understood and warrants further investigation. Since tumor endothelial cells are genetically different from normal endothelial cells, they in turn behave differently, which can possibly explain why they do not respond as well as originally hypothesized to anti-angiogenic therapies.

### *4.3.4 Angiogenesis-independent tumor invasion*

There is growing evidence that the use of anti-angiogenic drugs can contribute to mechanisms of tumor escape and progression. The tumor microenvironment following treatment with anti-angiogenic drugs has fewer blood vessels than were present before therapy. This results in drastic reduction of oxygen and nutrients and thus an increase in hypoxia, creating an overall more hostile environment for tumors. Additionally, as anti-angiogenic therapy prunes and decreases tumor vasculature tracts of basement membrane are left behind. These residual tumor vasculature basement membrane tracts can in turn be utilized by the tumor to invade or metastasize to a more conducive environment for their continued growth (Bergers and Hanahan, 2008; Mitchell and Bryan, 2010). In support of this idea, recent studies in glioblastoma demonstrated that VEGF inhibition was associated with continued cell growth, increased matrix

metalloproteinase activity and tumor cell migration occurring along normal blood vessels (Bergers and Hanahan, 2008; Lucio-Eterovic et al., 2009). Hypoxia levels can also mediate tumor signaling and promote migration in multiple tumor types though notch in breast cancer, the MAPK pathway in melanoma and markers of epithelial to mesenchymal transition and extracellular matrix proteins in prostate cancer (Chen et al., 2010; Luo et al., 2006; Mills et al., 2009; Mitchell and Bryan, 2010). Further, increased hypoxia following sunitinib treatment in mouse tumor models was shown to promote increased tumor invasiveness and metastasis even though there were observed improvements in OS and tumor shrinkage (Ebos et al., 2009; Paez-Ribes et al., 2009).

As discussed in this chapter, NSCLC is a deadly disease with dismal survival rates. Therapeutic advances over the past 15 years have done little to improve patient prognosis. In addition, anti-angiogenic therapy in NSCLC and in other cancer types has not had the dramatic clinical impact initially hypothesized. More research is needed on the mechanisms of resistance of NSCLC to anti-angiogenic therapy to better understand why not all tumors respond to treatment. Further, elucidation of resistance pathways could lead to the identification of patient biomarkers that could predict for therapy response thereby segmenting the patient population that received anti-angiogenic therapy and improving the overall efficacy of these drugs in the appropriate subset of patients.

### 4.4 Reliable biomarkers of tumor response to anti-angiogenic therapy

There are currently three USFDA-approved drugs targeting angiogenesis for the treatment of cancer, bevacizumab, sorafenib and sunitinib. In addition, there are numerous other anti-angiogenic drugs at various stages of clinical development (as discussed in Chapter One and Four). To date, there is a lack of reproducible, consistent biomarkers for predicting anti-angiogenic drug efficacy in cancer patients. This makes it impossible to distinguish patient populations that stand to benefit the most from treatment with this class of drugs. As a result, treatment with anti-angiogenic therapies in the whole patient population has had limited success. The identification of reliable biomarkers would enhance the utility of anti-angiogenic agents and could lead to a better understanding of how these drugs work, why they fail and to the development of new strategies to improve therapy. There are several important characteristics necessary for a useful biomarker. A good biomarker needs to be a measurable cellular, molecular or functional factor that represents the epigenetic, genetic or functional status of a biological system (Ludwig and Weinstein, 2005). In addition, to be clinically valuable, a biomarker needs to be able to be measured through a minimally invasive procedure, and be repeatable and consistently reproducible. A prognostic biomarker is indicative of disease course and outcome independent of the therapy used. The expression of a predictive biomarker is directly correlated to the

response seen following treatment with a specific drug or class of drugs (Gerger et al., 2011). Pharmacodynamic markers provide information on the effects of a drug on the target tissue (i.e. the tumor) or the host, but are independent of the overall efficacy of the drug. If the presence of the drug *in vivo* is associated with clinical response, than a pharmacodynamic marker can become a potentially useful surrogate marker of drug activity (Sessa et al., 2008).

Although there have been some studies providing evidence for some prognostic or pharmacodynamic biomarkers for anti-angiogenic agents in cancer, there is no consensus for one reliable marker (DePrimo and Bello, 2007; Gerger et al., 2011; Murukesh et al., 2010). VEGF expression levels within tumors or in circulation, although initially hypothesized to be useful biomarkers of responsiveness to anti-angiogenic therapies, have not been consistently validated in cancer patients (Gerger et al., 2011). A retrospective analysis of metastatic colorectal cancer patients that received bevacizumab did not show any correlation between response to drug and VEGF or thrombospondin (an endogenous anti-angiogenic factor) expression levels (Jubb et al., 2006). In glioblastoma mulitforme patients, expression of angiogenesis and hypoxia signaling pathways had no predictive value as to whether or not a patient would benefit from ironotecan therapy plus bevacizumab (Hasselbalch et al., 2010). However, in metastatic renal cell carcinoma patients, expression of carbonic anhydrase IX, an enzyme involved in mediating hypoxia-induced cellular proliferation, was directly

correlated with a decrease in tumor size following sorafenib treatment (Choueiri et al., 2010). In breast cancer, higher expression of CD31 and PDGF-β within tumor vasculature by Immunohistochemistry staining was associated with improved response rates (Yang et al., 2008). However, within this same study, there was only a non-significant trend for enhanced response rate with baseline expression levels of VEGF (Yang et al., 2008). In rectal cancer patients receiving bevacizumab, there was a significant increase in VEGF and PlGF plasma levels (Willett et al., 2009). This increase was not seen in patients that received fluorouracil and radiation therapy without bevacizumab. Additionally, the expression of interleukin-6 and soluble VEGFR1 was negatively associated with tumor regression (Willett et al., 2009). However, when plasma samples from colon cancer patients treated with bevacizumab were immunodepleted of all immunoglobulins to distinguish overall levels of bevacizumab-bound and free circulating VEGF, biologically active levels of VEGF were greatly depleted by bevacizumab treatment (Loupakis et al., 2007). A subsequent study in bevacizumab-treated colorectal cancer patients has confirmed this result (Brostjan et al., 2008). In studies performed in our lab, treatment with the anti-VEGF therapeutic antibody r84 was shown to increase the circulation time of drug-bound VEGF, but immunodepletion of the serum removed all detectable levels of VEGF (Roland et al., 2009a). However, illustrating the lack of reproducibility of VEGF as a biomarker, Kopetz et al did not find a pattern between VEGF plasma

expression levels and response in bevacizumab-treated metastatic colorectal patients, but did find that circulating interleukin-8 levels were inversely correlated with PFS (Kopetz et al., 2010). Although studies in bevacizumab-treated breast cancer populations have shown changes in expression levels of angiogenesis associated factors PlGF, VEGF, soluble VEGFR2 and intercellular adhesion molecule 1, there have been no clear associations between expression levels and patient response (Baar et al., 2009; Denduluri et al., 2008; Gerger et al., 2011; Kopetz et al., 2010). The Phase III ECOG 2100 trial evaluated paclitaxel versus paclitaxel plus bevacizumab as first-line therapy in metastatic breast cancer. Evaluation of polymorphisms between VEGF and VEGFR2 in this study identified VEGF-2578 AA and VEGF-1154 AA genotypes as a predictive marker for OS in patients receiving combination therapy (Schneider et al., 2008). This study also demonstrated a significant reduction in grade three or four hypertension in patients with VEGF-634 CC and VEGF-1498 TT genotypes, however there was no difference in overall VEGF and VEGFR2 expression amongst all patients (Schneider et al., 2008). In NSCLC patients, the VEGF-2578 CC and VEGF 1154 AA genotypes were strongly associated with low levels of VEGF expression (Koukourakis et al., 2004). A systematic increase in blood pressure has potential as a pharmacodynamic biomarker of the efficacy of VEGF signaling blockade by bevacizumab and VEGFR TKIs. Recent studies have implicated the degree of hypertension in patients as an indicator of response to

VEGF targeted therapy, although this has yet to be validated in large studies (Jain et al., 2009). Overall, the utility of circulating growth factors and genetic polymorphism expression varies depending on tumor type and therapy regimen and is thus a convoluted predictor of tumor response to anti-angiogenic therapy.

In practice, we still lack biomarkers predictive of response to therapy that exist for other targeted drugs such as the over expression of human epidermal growth factor receptor 2 (HER2/*neu*) in BC or mutated *EGFR* in lung cancer as a predictive marker of response to trastuzumab or EGFR TKI therapy, respectively. Similarly, predictive markers of response to anti-angiogenic therapy may be tumor-dependent. Our lab and others are currently assessing tumor-specific factors in xenograft models while others are evaluating patient samples for potential biomarkers of response. Further studies are required to identify and validate predictive versus prognostic biomarkers and may require carefully designed clinical trials and more frequent collection of patient tumor and serum samples throughout treatment. A better understanding of what dictates patient response and how to monitor resistance could lead to improved efficacy of monoclonal antibodies targeting the VEGF pathway.

# CHAPTER FIVE

# INVESTIGATING TUMOR-DERIVED FACTORS THAT PREDICT RESPONSE OF NSCLC TO ANTI-VEGF MONOCLONAL ANTIBODIES IN VIVO


## Abstract

Anti-angiogenic therapies are a rapidly-growing class of drugs used for the treatment of lung cancer. This category of drugs works by targeting blood vessels in a tumor in an effort to prevent the expansion of the tumor by shutting off the supply of nutrients and oxygen provided by the vascular tree. VEGF is critical in the growth and maintenance of tumor vasculature. The FDA has recently approved anti-VEGF monoclonal antibody bevacizumab (Avastin®, Genentech/Roche) for the treatment of NSCLC, however, there has been limited

clinical success with anti-VEGF therapy and data now suggest that a significant portion of patients are resistant to bevacizumab treatment. The variation of tumor response to anti-angiogenic therapy suggests a complex mechanism of drug action within lung tumors. Therefore, the success of anti-VEGF therapy for the treatment of cancer may rely on a better understanding of genes associated with responsiveness or resistance. We have completed a robust effort to explore differences in NSCLC cell expression patterns that determine intrinsic resistance or sensitivity to anti-VEGF therapies bevacizumab and r84 *in vivo*. Results from these studies demonstrate that NSCLC cell lines can be grouped based on response *in vivo* to anti-VEGF treatment. Expression of angiogenic growth factors and inhibitors, cytokines, microarray and reverse-phase protein array in sensitive and resistant tumor cell lines has been analyzed in an effort to elucidate pathways involved in resistance to anti-VEGF therapy. From these analyses, the receptor tyrosine kinase Axl was identified as having increased expression NSCLC lines intrinsically resistance to bevacizumab therapy compared to those sensitive to bevacizumab therapy, but subsequent analysis failed to confirm this correlation. However, the databases generated on NSCLC genomic and proteomic expression and responses to anti-VEGF therapy *in vivo* provide an extensive source of information that can be utilized to better understand mechanisms of resistance to therapy.

## 5.1 Introduction

Tumors are required to initiate angiogenesis, the formation of new blood vessels from a pre-existing vascular network, to provide oxygen and nutrients needed for continued growth and development beyond the limits of their diffusion from neighboring vessels. Anti-angiogenic therapy targeting the development and maintenance of tumor blood vessels was highly anticipated as an innovative and promising strategy, however its use clinically has been somewhat disappointing, with minimal observed gains in progression free survival (PFS) and overall survival (OS) (Jain et al., 2006). There are three anti-angiogenic drugs currently approved by the FDA for use in cancer patients, sunitinib malate (Sutent®, SU11248, Pfizer, Inc.), sorafenib (Nexavar®, BAY 43-9006, Bayer Pharmaceuticals Corp.), and bevacizumab (Avastin®, Genentech/Roche) (Roskoski, 2007b). These agents target the vascular endothelial growth factor (VEGF) pathway, the predominant mediator of physiological and pathological angiogenesis. Sunitinib and sorafenib are small molecule receptor tyrosine kinase inhibitors (RTKis). Sunitinib inhibits all three VEGF receptors (VEGFRs), platelet-derived growth factor receptor (PDGFR) –α and –β, fms-like TK-3 (Flt3), c-kit and rearranged during transfection (RET) and is FDA approved for the treatment of gastrointestinal stromal tumors after disease progression on or resistance to imatinib, advanced renal cell carcinoma and most recently in progressive well-differentiated pancreatic neuroendocrine tumors (Raymond et

al., 2011; Roskoski, 2007a; Socinski, 2008) (http://www.cancer.gov/cancertopics/druginfo/fda-sunitinib-malate). Sorafenib inhibits VEGFR2, VEGFR3, PDGFR-β, c-kit and Raf and has FDA approval for the treatment of advanced renal cell carcinoma and unresectable hepatocellular carcinoma (Wilhelm et al., 2008; Wilhelm et al., 2004). Bevacizumab is a humanized monoclonal antibody that recognizes human VEGF and blocks VEGF from binding to VEGFR1 and VEGFR2 and has FDA approval for colorectal cancer, non-small cell lung cancer (NSCLC), glioblastoma and renal cell carcinoma (Kamba and McDonald, 2007; Vredenburgh et al., 2009; Yan et al., 2008). Although in the early stages of clinical development, r84 (AT001, Affitech A/S) is a fully human monoclonal antibody that recognizes mouse and human VEGF and prevents ligand interaction to VEGFR2 that shows great clinical promise. Pre-clinically, r84 has been demonstrated to inhibit VEGFR2-induced endothelial cell signaling and migration *in vitro*, to control tumor growth in multiple models and to reduce tumor angiogenesis and immune cell infiltration (Roland et al., 2009a; Roland et al., 2009b; Sullivan and Brekken, 2010; Sullivan et al., 2010). Additional studies with r84 are currently underway and clinical trials are anticipated to begin in early 2012.

NSCLC is the most prevalent and deadly form of cancer worldwide (Jemal et al., 2011). This statistic holds true despite recent therapeutic advances including the anti-angiogenic therapy bevacizumab. Although bevacizumab gained FDA

approval in NSCLC by demonstrating gains in OS and PFS, these are small increases, indicating that the optimal therapeutic combinations or patient populations most likely to benefit from therapy have not been adequately identified (Miller et al., 2009; Reck et al., 2009; Sandler et al., 2006). There is a growing body of evidence indicating that some tumors may be intrinsically resistant to anti-angiogenic therapy, or will develop evasive resistance after a brief period of response (Bergers and Hanahan, 2008; Mitchell and Bryan, 2010). We hypothesized that differentially expressed tumor-derived factors are predictive and functionally related to response to anti-angiogenic therapy *in vivo*. Here we present the largest data set to date on *in vivo* response and molecular characterization of twelve NSCLC cell line xenografts to bevacizumab and r84. We demonstrated that response to anti-VEGF monoclonal antibody therapy varies by cell line and treatment strategy and have identified NSCLC lines with intrinsic resistance and sensitivity to bevacizumab or r84. Further, response to therapy is characterized by changes genomic and proteomic expression patterns. Based on expression analysis of NSCLC lines that were resistant versus sensitive to bevacizumab therapy, we identified a potential role for the RTK Axl in mediating resistance. Although subsequent analysis failed to validate this connection, we feel that the databases generated through these studies provide an excellent source of information on NSCLC signaling *in vivo* and can help elucidate why some tumors do or do not respond to anti-VEGF therapy.

## 5.2 Results

### *5.2.1 Response to anti-angiogenic therapy is dependent on NSCLC line*

We set out to identify factors mediating intrinsic resistance to anti-VEGF monoclonal antibody therapy by testing 12 NSCLC cell lines *in vivo* since these drugs primarily function within the tumor microenvironment, which cannot be adequately recapitulated or targeted *in vitro*. Briefly, 2.5 million NSCLC cells were injected subcutaneously into mice and treated, as described in Chapter Three, starting one day post tumor cell injection with 25 mg/kg/week bevacizumab, and 50 mg/kg/week r84 or a control IgG. Treatment continued until average tumor volume in control-treated animal reached approximately 1200 $mm^3$, at which time all animals were sacrificed and tumor and organs were harvested for subsequent analysis. We tested a total of 12 NSCLC cell lines (A549, Calu-3, Calu-6, H1975, H1993, H2073, H1155, H1395, H358, H460, H1299 and H2009) as tumor xenografts. Tumor growth curves and final tumor weights are displayed in Figure 5.1 and Figure 5.2, respectively. To normalize tumor response to bevacizumab or r84 therapy amongst all cell lines and to illustrate overall sensitivity of a cell line to anti-VEGF therapy, we calculated treated/control (T/C) ratios by dividing the average final tumor weight of anti-VEGF-treated animals (with bevacizumab or r84) by the average final tumor

weight of control-treated animals (Figure 5.3 and Figure 5.4). We found that response to anti-VEGF therapy varied by tumor line and by the anti-VEGF monoclonal antibody used. For example, Calu-6, A549 and Calu-3 displayed intrinsic resistance to bevacizumab therapy as illustrated by their tumor growth curves (Figure 5.1), final tumor weights (Figure 5.2) and their T/C ratios of 0.60, 0.56 and 0.55, respectively (Figure 5.3). However, these same tumors responded very well to r84 treatment (Figure 5.1, Figure 5.2) and had T/C ratios of 0.26, 0.21 and 0.28, respectively (Figure 5.4). In contrast to bevacizumab, the majority of tumor lines tested displayed great sensitivity to r84, with the exception of H1155 and H1395 that had T/C ratios of 0.54 and 0.40, respectively (Figure 5.4). It should be noted however, that these two cell lines are also the most inconsistent in terms of *in vivo* growth reproducibility of all 12 tested, which could make it difficult to replicate these results and be able to confidently classify these lines as resistant to r84 therapy. Further, the enhanced sensitivity of NSCLC lines to r84 therapy versus bevacizumab could be related to the ability of r84 to bind both the mouse and human VEGF present in this model. To assess this possibility, H1395 and H1155 animal experiments were repeated and mice were treated with 50 mg/kg/week r84, control IgG, 25 mg/kg/week bevacizumab or 2C3. As previously mentioned in Chapter One and Three, 2C3 is a murine anti-human VEGF monoclonal antibody developed by Rolf Brekken at the University of Texas Southwestern Medical Center that blocks VEGF binding only to VEGR2, has

effective anti-tumor activity in a number of cancer models *in vivo* and was the basis behind the development of r84 (Brekken et al., 1998; Brekken et al., 2000). We found that blockade of mouse and human VEGF binding to VEGFR2 with r84 resulted in larger tumors as illustrated by tumor growth curves, final tumor weights and T/C ratios than in animals treated with bevacizumab or 2C3 that blocked only human VEGF from binding to VEGFR1 and VEGFR2 or only VEGFR2, respectively (Figure 5.5). These preliminary results are somewhat paradoxical and at this time suggest that stromal VEGF may play an inhibitory role in H1155 and H1395 tumor progression, although further investigation is necessary.

Immunohistochemical analysis of treated tumors demonstrated that our dosing strategies with bevacizumab and r84 were effectively hitting their target, as illustrated by reductions in tumor microvessel density (MVD) (Figure 5.6). There is a slight trend in MVD reduction correlating with sensitivity to bevacizumab, with a greater percentage of MVD reduction seen in tumors more sensitive to bevacizumab (Figure 5.6, H1975 and H2073). The common oncogenotype status, tumor histotypes, gender and *in vivo* response to anti-VEGF therapy of the 12 tested NSCLC lines are displayed in Table 5.1 and Table 5.2. However, no clear patterns that could predict responsiveness of lines to therapy can be determined from this information. Therefore, we further probed the genomic and proteomic expression profiles of these lines with a series of arrays,

generating a large database of information on these 12 NSCLC lines and how they respond to anti-angiogenesis monoclonal antibody therapy *in vivo*.

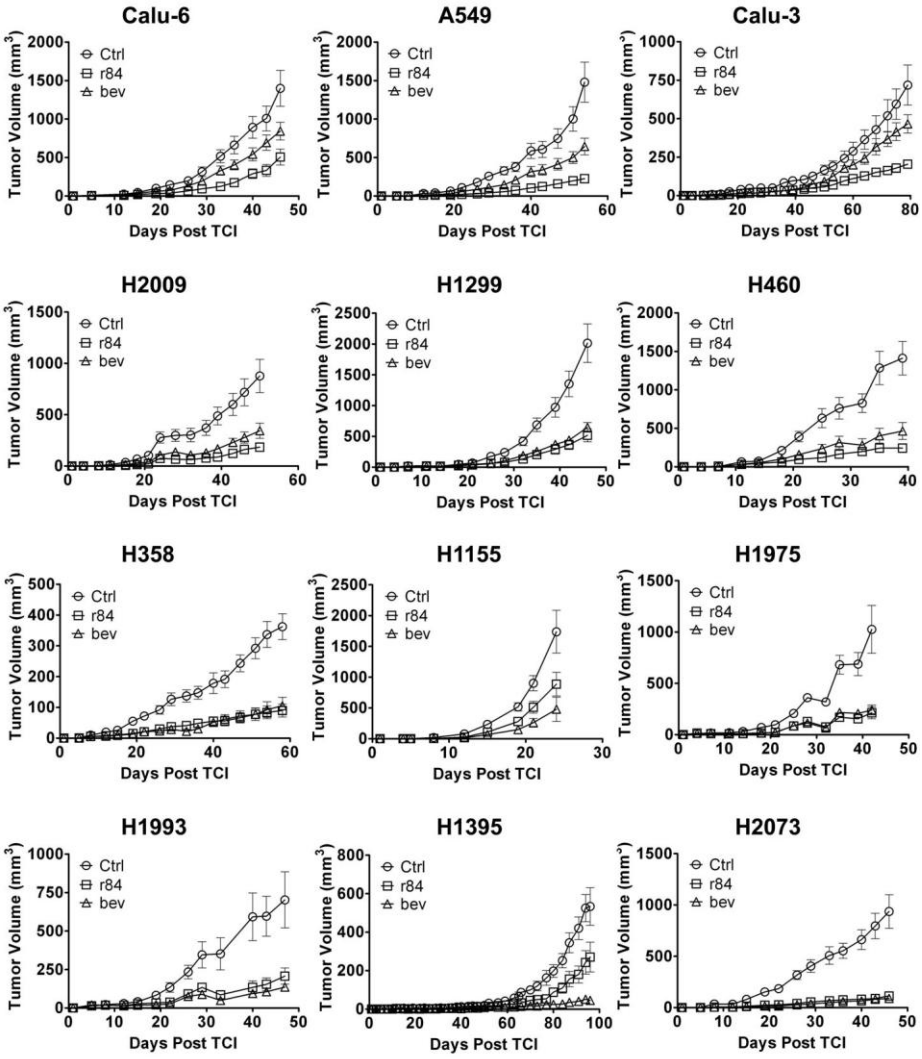


**Figure 5.1: NSCLC xenograft tumor growth in response to anti-angiogenesis therapy varies by cell line.**

Twelve NSCLC tumor cell lines were implanted subcutaneously in NOD/SCID mice (2.5 million cells/mouse) and treated with the anti-VEGF monoclonal antibodies r84 and bevacizumab (bev). Tumor volumes were monitored and recorded throughout the course of the experiment. All mice were sacrificed when average control-treated tumor volumes exceeded ~1000 $mm^3$.

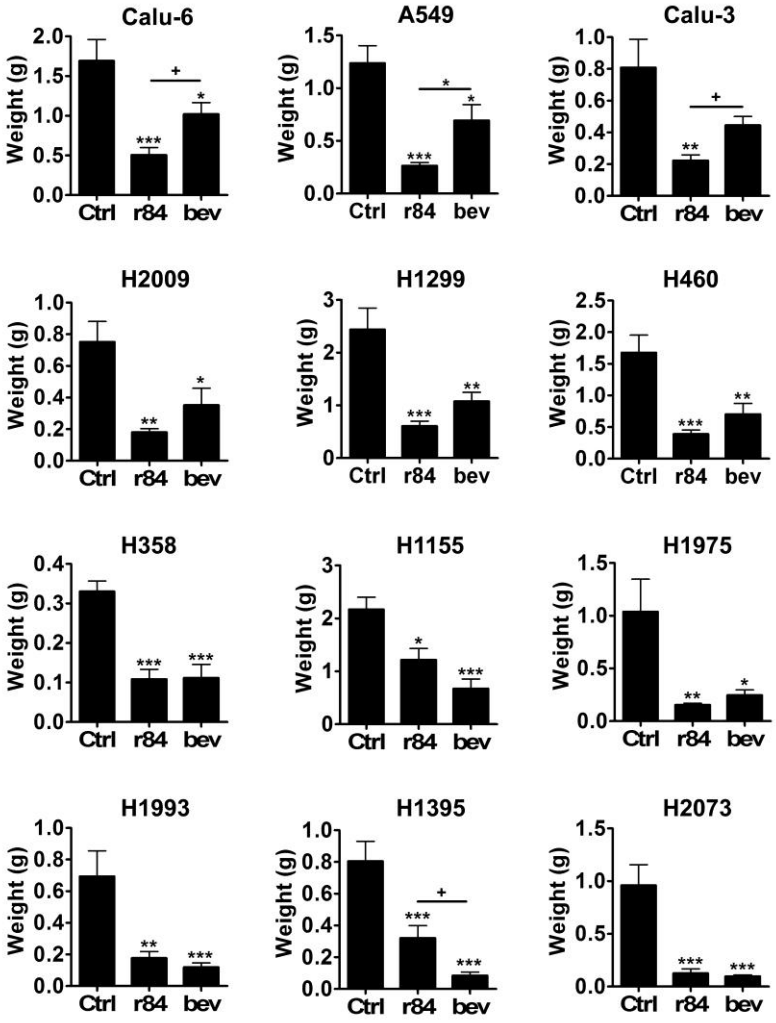


**Figure 5.2: NSCLC xenograft final tumor weight following anti-angiogenesis therapy varies by cell line.**

Twelve NSCLC tumor cell lines were implanted subcutaneously in NOD/SCID mice (2.5 million cells/mouse) and treated with the anti-VEGF monoclonal antibodies r84 and bevacizumab (bev). Tumor volumes were monitored and recorded throughout the course of the experiment. All mice were sacrificed when average control-treated tumor volumes exceeded ~1000 $mm^3$ and final tumor weights were measured and recorded. *$p < 0.05$, **$p < 0.01$, ***$p < 0.001$ statistical differences compared to control (Ctrl) treatment, unless otherwise indicated.

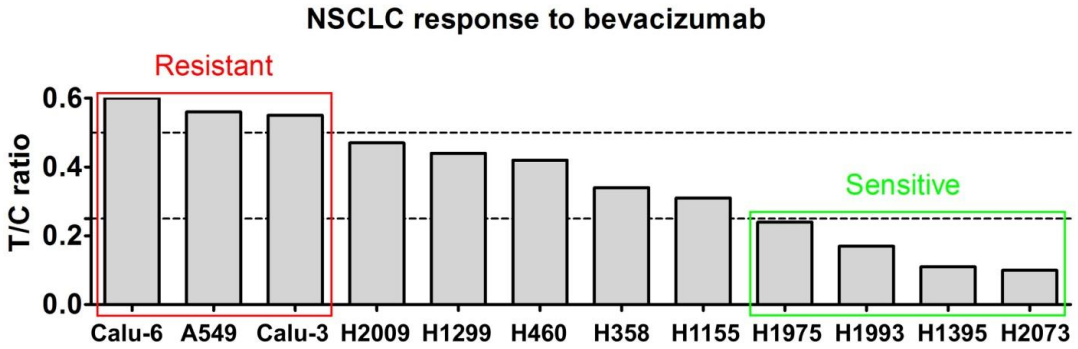


**Figure 5.3: Response of NSCLC lines to bevacizumab therapy *in vivo* varies by cell line.**

Twelve NSCLC tumor cell lines were implanted subcutaneously in NOD/SCID mice (2.5 million cells/mouse) and treated with the anti-VEGF monoclonal antibodies r84 and bevacizumab (bev). Tumor volumes and final tumor weights were monitored and recorded. To normalize the responsiveness of each cell line to bev therapy *in vivo*, the T/C ratio was calculated by dividing the average final tumor weight of bev-treated animals by the average final tumor weight of control-treated animals. Preliminary restrictions were set so that a T/C ratio > 0.5 or < 0.25 represented resistant or sensitive NSCLC lines, respectively.

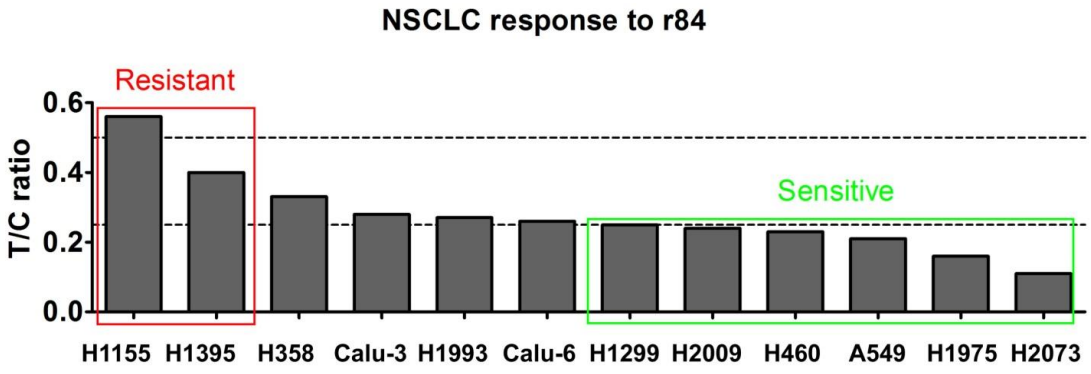


**Figure 5.4: Response of NSCLC lines to r84 therapy *in vivo* varies by cell line.**

Twelve NSCLC tumor cell lines were implanted subcutaneously in NOD/SCID mice (2.5 million cells/mouse) and treated with the anti-VEGF monoclonal antibodies r84 and bevacizumab (bev). Tumor volumes and final tumor weights were monitored and recorded. To normalize the responsiveness of each cell line to r84 therapy *in vivo*, the T/C ratio was calculated by dividing the average final tumor weight of r84-treated animals by the average final tumor weight of control-treated animals. Preliminary restrictions were set so that a T/C ratio > 0.4 or < 0.25 represented resistant or sensitive NSCLC lines, respectively.

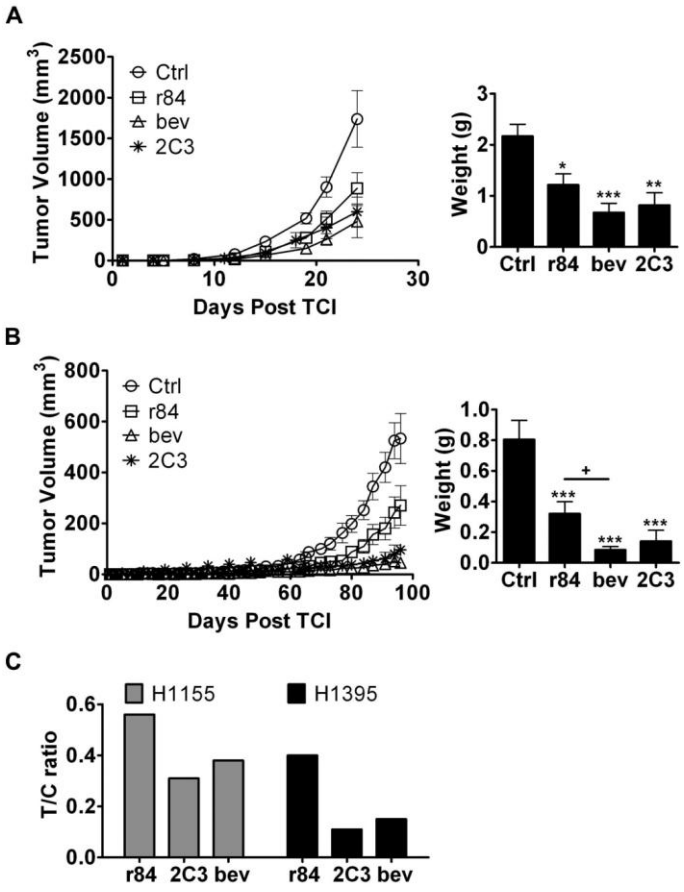


**Figure 5.5: Blockade of stromal VEGF enhances NSCLC resistance to r84.**

H1155 (**A**) and H1395 (**B**) NSCLC tumor cell lines were implanted subcutaneously in NOD/SCID mice (2.5 million cells/mouse) and treated with the anti-VEGF monoclonal antibodies r84, bevacizumab (bev) and 2C3 and sacrificed when average control-treated tumor volumes exceeded ~1000 $mm^3$. Tumor volumes and final tumor weights were monitored and recorded. To normalize the responsiveness of each cell line to bev therapy *in vivo*, the T/C ratio was calculated by dividing the average final tumor weight of r84-treated animals by the average final tumor weight of control-treated animals (**C**). *$p < 0.05$, **$p < 0.01$, ***$p < 0.001$ by ANOVA, +$p < 0.05$ by t-test, statistical differences compared to Ctrl treatment, unless otherwise indicated.

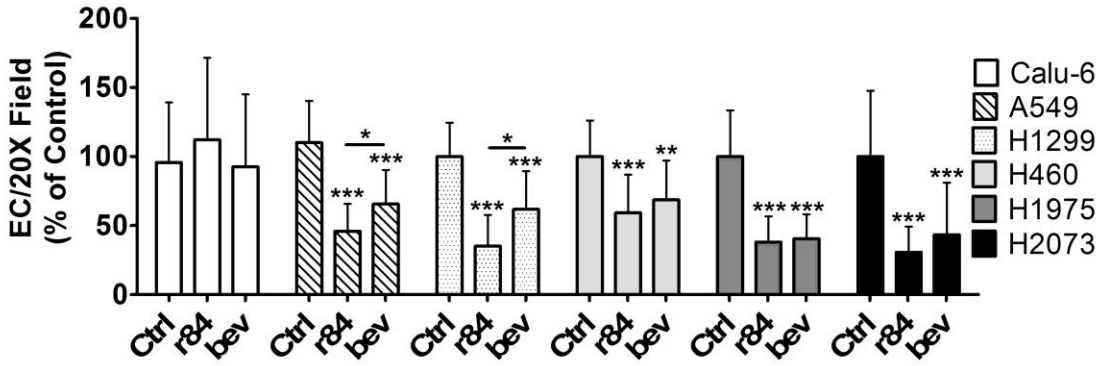


**Figure 5.6: Treatment of NSCLC xenografts with anti-VEGF monoclonal antibodies reduces tumor microvessel density.**

Frozen sections of NSCLC tumors treated with control IgG (Ctrl), r84, or bevacizumab (bev) were analyzed by immunofluorescence. Number of positive-staining entities per high powered field was evaluated using Nikon Elements software. Data is displayed as the number of positive-staining endothelial cells (ECs) per 20X field as a percent of ECs in control-treated tumors. r84 and bev treatment significantly decreases tumor microvessel density. *$p < 0.05$, **$p < 0.01$, ***$p < 0.001$ statistical differences compared to Ctrl, unless otherwise indicated.

| | | | | Mutation Status | | | | | | | | |
|---|---|---|---|---|---|---|---|---|---|---|---|---|
| Cell Line | Source | Gender | T/C Ratio | TP53 | KRAS | PTEN | PIK3CA | EGFR | MET | ERBB2 | KDR | ALK |
| Calu-6 | Primary | F | 0.60 | | | | | | | | | |
| A549 | Primary | M | 0.56 | | | | | | | | | |
| Calu-3 | Metastasis | M | 0.55 | | | | | | | | | |
| H2009 | Metastasis | F | 0.47 | | | | | | | | | |
| H1299 | Metastasis | M | 0.44 | | | | | | | | | |
| H460 | Metastasis | M | 0.42 | | | | | | | | | |
| H358 | Primary | M | 0.34 | | | | | | | | | |
| H1155 | Metastasis | M | 0.31 | | | | | | | | | |
| H1975 | Primary | F | 0.24 | | | | | | | | | |
| H1993 | Metastasis | F | 0.17 | | | | | | | | | |
| H1395 | Primary | F | 0.11 | | | | | | | | | |
| H2073 | Primary | F | 0.10 | | | | | | | | | |

Adenocarcinoma
Large Cell Neuroendocrine
Large Cell

Wild type
Mutant

**Table 5.1: Characteristics of NSCLC lines studied displayed by sensitivity to bevacizumab *in vivo*.**

The tumor histology, source, gender, mutation status of common oncogenotypes, and bevacizumab T/C ratio for 12 NSCLC cell lines are given. No obvious patterns are identified based on these characteristics that could predict for tumor responsiveness to bevacizumab therapy.

| | | | | Mutation Status | | | | | | | | |
|---|---|---|---|---|---|---|---|---|---|---|---|---|
| Cell Line | Source | Gender | T/C Ratio | TP53 | KRAS | PTEN | PIK3CA | EGFR | MET | ERBB2 | KDR | ALK |
| H1155 | Metastasis | M | 0.54 | | | | | | | | | |
| H1395 | Primary | F | 0.40 | | | | | | | | | |
| H358 | Primary | M | 0.33 | | | | | | | | | |
| Calu-3 | Metastasis | M | 0.28 | | | | | | | | | |
| H1993 | Metastasis | F | 0.27 | | | | | | | | | |
| Calu-6 | Primary | F | 0.26 | | | | | | | | | |
| H1299 | Metastasis | M | 0.25 | | | | | | | | | |
| H2009 | Metastasis | F | 0.24 | | | | | | | | | |
| H460 | Metastasis | M | 0.23 | | | | | | | | | |
| A549 | Primary | M | 0.21 | | | | | | | | | |
| H1975 | Primary | F | 0.16 | | | | | | | | | |
| H2073 | Primary | F | 0.11 | | | | | | | | | |

Adenocarcinoma
Large Cell Neuroendocrine
Large Cell

Wild type
Mutant

**Table 5.2: Characteristic of NSCLC lines studied displayed by sensitivity to r84 *in vivo*.**

The tumor histology, source, gender, mutation status of common oncogenotypes, and r84 T/C ratio for 12 NSCLC cell lines are given. No obvious patterns are identified based on these characteristics that could predict for tumor responsiveness to r84 therapy.

### *5.2.2 Analysis of intrinsically resistant and sensitive NSCLC phenotypes*

To further evaluate differences in gene expression among the 12 NSCLC cell lines tested *in vivo* for response to the anti-angiogenic monoclonal antibodies r84 and bevacizumab, a series of assays were performed, including qPCR arrays, cytokine arrays, microarrays, and reverse-phase protein array (RPPA). We believe these data sets offer an abundant source of information that can be used to identify distinguishing factors or pathways that are important in mediating response of NSCLC to anti-VEGF therapy.

#### *5.2.2.1 Tumor qPCR array of angiogenesis growth factors and inhibitors*

To evaluate the expression of angiogenesis mediators in our NSCLC tumors, we utilized the commercially-available SABiosciences angiogenesis growth factors and inhibitors human qPCR array (PAHS-072, Qiagen). This assay provides quantitative real-time PCR (qPCR) expression analysis of 84 genes run in a 96-well format. Briefly, RNA was isolated from control-treated NSCLC xenograft tumors and reverse transcribed to generate cDNA that was then evaluated by qPCR for the expression of angiogenesis growth factors and inhibitors. A total of three tumors per NSCLC line was used for lines that displayed intrinsic resistance to bevacizumab (Calu-6, A549, Calu-3) or r84 (H1155, H1395) or were intrinsically sensitive to bevacizumab and r84 (H1993, H1975, H2073). Raw cycle threshold values were uploaded to SABiosciences

web-based data analysis software to calculate fold changes in gene expression among our response phenotypes (resistant to bevacizumab, resistant to r84, sensitive to bevacizumab and r84) and are included in Appendix B. There are nearly 30 genes with a greater than four-fold increase in gene expression in tumors intrinsically resistant versus sensitive to bevacizumab therapy (Table 5.3) including platelet-derived growth factor D, angiopoietin-1, fibroblast growth factor-2 (FGF-2, also known as basic FGF) and FGF-13. When r84 intrinsically resistant versus sensitive tumors are compared, there are almost 50 genes with differential expression including interleukin-8 (IL-8), fibronectin-1 and FGF-13 (Table 5.4). There are 15 genes with increased expression in bevacizumab resistant versus r84 resistant tumors (Table 5.5). Although there are differences in the degree of change between groups, the majority of the differentially expressed genes are repeated.

## Bevacizumab Resistant vs. Sensitive

| | Gene Symbol | Gene Name | Fold Regulation | | Gene Symbol | Gene Name | Fold Regulation |
|---|---|---|---|---|---|---|---|
| 1*+ | CXCL5 | Chemokine (C-X-C motif) ligand 5 | 41.9202 | 15* | CHGA | Chromogranin A | 5.0652 |
| 2* | PF4 | Platelet factor 4 | 32.6703 | 16* | IL10 | Interleukin 10 | 4.8785 |
| 3+ | CXCL6 | Chemokine (C-X-C motif) ligand 6 | 28.3696 | 17* | CXCL9 | Chemokine (C-X-C motif) ligand 9 | 4.7938 |
| 4* | AMOT | Angiomotin | 21.984 | 18* | LEP | Leptin | 4.7683 |
| 5* | CCL15 | Chemokine (C-C motif) ligand 15 | 9.4759 | 19+ | SERPINF1 | Serpin peptidase inhibitor, clade F | 4.6514 |
| 6+ | COL4A3 | Collagen, type IV, alpha 3 | 8.5995 | 20* | IFNB1 | Interferon beta 1 | 4.6352 |
| 7+ | COL18A1 | Collagen, type XVIII, alpha 1 | 8.2435 | 21* | KLK3 | Kallikrein-related peptidase 3 | 4.5698 |
| 8 | ANGPT1 | Angiopoietin 1 | 8.0093 | 22* | CCL2 | Chemokine (C-C motif) ligand 2 | 4.3185 |
| 9* | CXCL14 | Chemokine (C-X-C motif) ligand 14 | 7.2159 | 23 | FGF2 | Fibroblast growth factor 2 (basic) | 4.2911 |
| 10* | GRP | Gastrin-releasing peptide | 6.3218 | 24* | PLG | Plasminogen | 4.2868 |
| 11* | IL17F | Interleukin 17F | 5.7098 | 25* | TIMP3 | TIMP metallopeptidase inhibitor 3 | 4.2763 |
| 12* | CXCL13 | Chemokine (C-X-C motif) ligand 13 | 5.1996 | 26 | IFNA1 | Interferon alpha 1 | 4.0560 |
| 13* | PDGFD | Platelet derived growth factor D | 5.1397 | 27* | FGF13 | Fibroblast growth factor 13 | 4.0319 |
| 14* | PRL | Prolactin | 5.0749 | | | | |

**Table 5.3: Panel of angiogenesis growth factors and inhibitors over expressed in tumors resistant versus sensitive to bevacizumab therapy *in vivo*.**

The SABiosciences angiogenesis growth factors and inhibitors qPCR array was run on a panel of NSCLC tumors with differential response to bevacizumab therapy *in vivo*. The displayed panel of genes had a greater than four-fold change in gene expression in bevacizumab resistant versus sensitive tumors. *, + genes shared amongst r84 resistant vs. sensitive, bevacizumab resistant vs. r84 resistant, respectively.

# r84 Resistant vs. Sensitive

| | Gene Symbol | Gene Name | Fold Regulation | | Gene Symbol | Gene Name | Fold Regulation |
|---|---|---|---|---|---|---|---|
| 1+ | SERPINE1 | Serpin peptidase inhibitor, clade E | -69.2818 | 24* | PDGFD | Platelet derived growth factor D | 7.6200 |
| 2+ | THBS1 | Thrombospondin 1 | -47.3422 | 25* | CCL2 | Chemokine (C-C motif) ligand 2 | 9.7442 |
| 3+ | FN1 | Fibronectin 1 | -35.5877 | 26 | NPPB | Natriuretic peptide precursor B | 9.8295 |
| 4 | BMP2 | Bone morphogenetic protein 2 | -13.8778 | 27* | FGF13 | Fibroblast growth factor 13 | 11.1180 |
| 5 | FGFBP1 | Fibroblast growth factor binding protein 1 | -13.5891 | 28 | PROK1 | Prokineticin 1 | 12.5468 |
| 6+ | TGFA | Transforming growth factor, alpha | -12.4485 | 29 | IL12B | Interleukin 12B | 15.2749 |
| 7+ | EREG | Epiregulin | -9.7985 | 30*+ | CXCL5 | Chemokine (C-X-C motif) ligand 5 | 16.9163 |
| 8+ | CXCL3 | Chemokine (C-X-C motif) ligand 3 | -7.9555 | 31* | PLG | Plasminogen | 17.7027 |
| 9*+ | PDGFB | Platelet-derived growth factor beta | -7.612 | 32* | IL17F | Interleukin 17F | 21.1318 |
| 10+ | RUNX1 | Runt-related transcription factor 1 | -6.0739 | 33* | CXCL13 | Chemokine (C-X-C motif) ligand 13 | 21.2523 |
| 11 | IL8 | Interleukin 8 | -5.6921 | 34* | LEP | Leptin | 22.0881 |
| 12* | CXCL2 | Chemokine (C-X-C motif) ligand 2 | -5.3565 | 35* | AMOT | Angiomotin | 22.3456 |
| 13+ | TGFB1 | Transforming growth factor, beta 1 | -4.9411 | 36* | PRL | Prolactin | 25.8908 |
| 14 | RHOB | Ras homolog gene family, member B | -4.4207 | 37* | TIMP3 | TIMP metallopeptidase inhibitor 3 | 26.3982 |
| 15 | CD59 | CD59 molecule, complement regulatory | -4.2231 | 38* | CXCL9 | Chemokine (C-X-C motif) ligand 9 | 27.4616 |
| 16 | ANG | Angiogenin | 4.0664 | 39* | KLK3 | Kallikrein-related peptidase 3 | 30.6671 |
| 17 | FIGF | C-fos induced growth factor (vascular | 5.0796 | 40 | BAI1 | Brain-specific angiogenesis inhibitor 1 | 33.2037 |
| 18 | PTN | Pleiotrophin | 5.6166 | 41* | IL10 | Interleukin 10 | 35.3728 |
| 19* | IFNB1 | Interferon beta 1 | 5.7139 | 42* | PF4 | Platelet factor 4 | 42.0205 |
| 20 | TIE1 | Tyrosine kinase with immunoglobulin-like | 5.7530 | 43* | CXCL14 | Chemokine (C-X-C motif) ligand 14 | 49.1083 |
| 21 | SERPINC1 | Serpin peptidase inhibitor clade C | 7.1074 | 44* | GRP | Gastrin-releasing peptide | 53.7967 |
| 22 | HGF | Hepatocyte growth factor | 7.1239 | 45* | CHGA | Chromogranin A | 60.3046 |
| 23 | IFNG | Interferon gamma | 7.1296 | 46* | CCL15 | Chemokine (C-C motif) ligand 15 | 65.2619 |

**Table 5.4: Panel of angiogenesis growth factors and inhibitors over expressed in tumors resistant versus sensitive to r84 therapy *in vivo*.**

The SABiosciences angiogenesis growth factors and inhibitors qPCR array was run on a panel of NSCLC tumors with differential response to r84 therapy *in vivo*. The displayed panel of genes had a greater than four-fold change in gene expression in r84 resistant versus sensitive tumors. *, + genes shared amongst bevacizumab resistant vs. sensitive, bevacizumab resistant vs. r84 resistant, respectively.

## Bevacizumab Resistant vs. r84 Resistant

| | Gene Symbol | Gene Name | Fold Regulation |
|---|---|---|---|
| 1+ | FN1 | Fibronectin 1 | 23.0743 |
| 2+ | CXCL6 | Chemokine (C-X-C motif) ligand 6 | 22.2382 |
| 3+ | THBS1 | Thrombospondin 1 | 18.8681 |
| 4+ | COL18A1 | Collagen, type XVIII, alpha 1 | 15.3673 |
| 5+ | EREG | Epiregulin | 10.9544 |
| 6+ | CXCL3 | Chemokine (C-X-C motif) ligand 3 | 10.8893 |
| 7+ | TGFB1 | Transforming growth factor beta 1 | 10.4071 |
| 8+ | PDGFB | Platelet-derived growth factor beta | 8.7397 |
| 9+ | TGFA | Transforming growth factor, alpha | 8.4115 |
| 10+ | CXCL5 | Chemokine (C-X-C motif) ligand 5 | 7.3543 |
| 11+ | COL4A3 | Collagen, type IV, alpha 3 | 6.8886 |
| 12+ | RUNX1 | Runt-related transcription factor 1 | 6.5617 |
| 13+ | SERPINE1 | Serpin peptidase inhibitor, clade E | 5.7483 |
| 14+ | SERPINF1 | Serpin peptidase inhibitor, clade F | 4.4524 |
| 15 | MDK | Midkine | 4.0740 |

**Table 5.5: Panel of angiogenesis growth factors and inhibitors over expressed in tumors resistant to bevacizumab versus resistant to r84 therapy *in vivo*.**

The SABiosciences angiogenesis growth factors and inhibitors qPCR array was run on a panel of NSCLC tumors with differential response to bevacizumab and r84 therapy *in vivo*. The displayed panel of genes had a greater than four-fold change in gene expression in bevacizumab resistant versus r84 resistant tumors. + genes shared amongst bevacizumab resistant vs. sensitive or r84 resistant vs. sensitive.

#### *5.2.2.2 Tumor cytokine array*

Human and mouse cytokines expressed in control-, r84- and bevacizumab-treated NSCLC xenograft tumors were evaluated using the MILLIPLEX MAP (multi-analyte panel) Multiplex Assay kits from Millipore. This technology uses distinctly colored beads conjugated to species-specific antibodies to detect multiple analytes in protein lysate within a single well of a 96-well plate. Using these assays, we were able to screen tumor lysate samples for the expression of 39 human and 32 mouse cytokines, generating a large data base of information on tumor expression of these molecules by NSCLC line and treatment group. The complete results from these assays are included in Appendix D and Appendix E. Interestingly, there was differential expression of pro-angiogenic (Figure 5.7 A, B and Figure 5.8 A, B) and anti-angiogenic (Figure 5.7 C, Figure 5.8 C) cytokines as well as cytokines involved in recruitment of tumor associated macrophages (Figure 5.7 D and Figure 5.8 D). For example, sensitive tumors expressed significantly higher levels ($p < 0.05$ by t-test) of human VEGF than bevacizumab resistant tumors (Figure 5.7 A). In addition, there was higher expression of human FGF-2 in tumors that were resistant to bevacizumab therapy as compared to sensitive tumors (Figure 5.7 A). This increase in FGF-2 expression correlated with our SABiosciences qPCR data in bevacizumab resistant versus sensitive tumors (Table 5.3). As previously mentioned in Chapter Four, FGF-2 has been implicated as a growth factor involved in resistance of tumors to anti-angiogenic

therapies (Bergers and Hanahan, 2008; Casanovas et al., 2005; Mitchell and Bryan, 2010). Therefore, differences in cytokine expression may play a role in mediating tumor response to anti-angiogenic therapy *in vivo*.

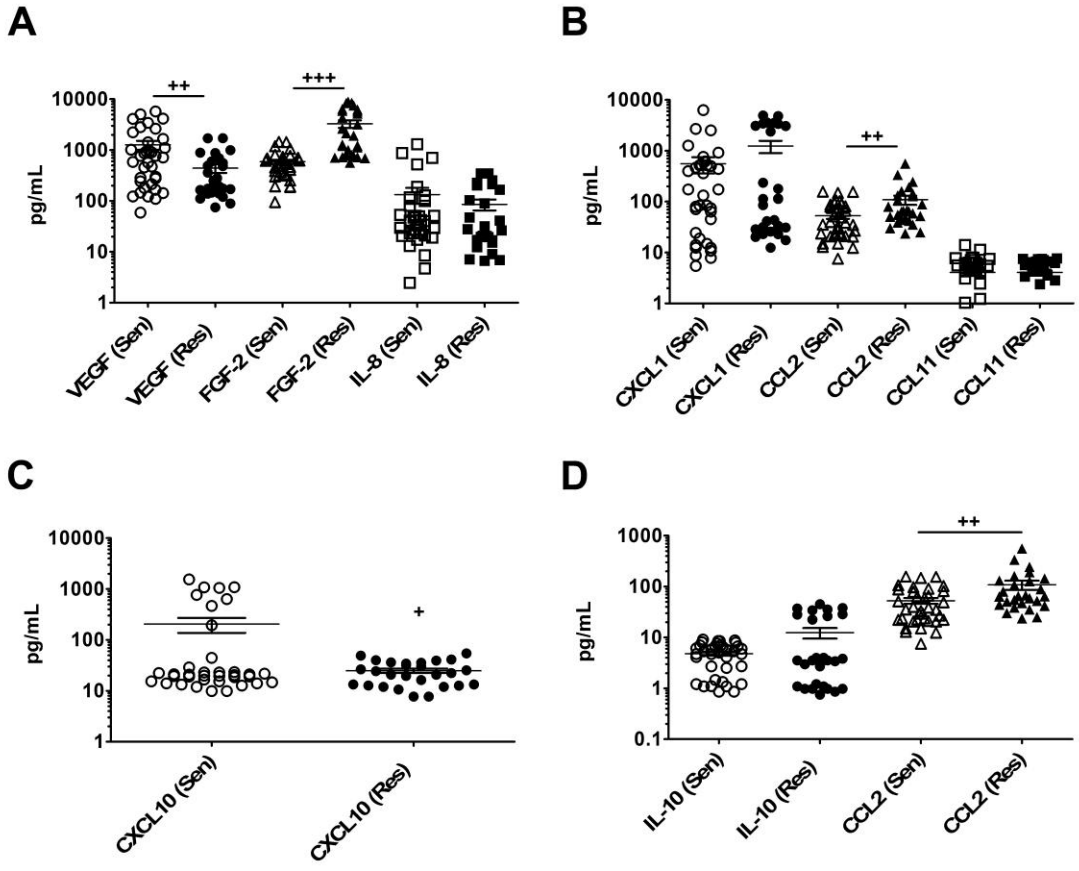


**Figure 5.7: Expression of human cytokines varies between bevacizumab resistant and sensitive xenograft tumors.**

A subset of human tumor cytokine expression as determined through MILLIPLEX MAP multiplex assays are displayed. There are differences in the expression of pro-angiogenic (**A**, **B**), anti-angiogenic (**C**) and pro-tumor associated macrophage recruitment (**D**) cytokines between bevacizumab resistant (Res) and sensitive (Sen) samples.

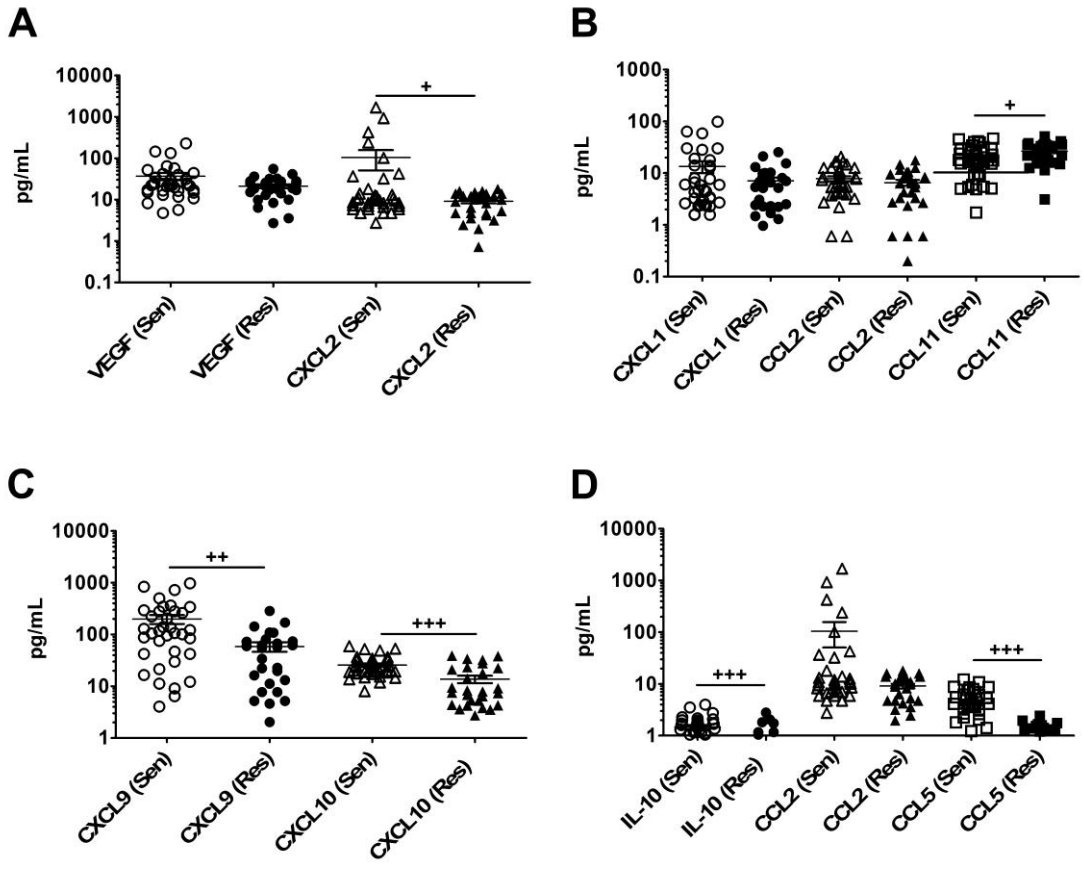


**Figure 5.8: Expression of mouse cytokines varies between bevacizumab resistant and sensitive xenograft tumors.**

A subset of mouse tumor cytokine expression as determined through MILLIPLEX MAP multiplex assays are displayed. There are differences in the expression of pro-angiogenic (**A**, **B**), anti-angiogenic (**C**) and pro-tumor associated macrophage recruitment (**D**) cytokines between bevacizumab resistant (Res) and sensitive (Sen) samples.

#### *5.2.2.3 NSCLC tumor and cell line microarray*

Through collaborations with Dr. John Minna's and Dr. Adi Gazdar's laboratories at the University of Texas Southwestern Medical Center, we had access to *in vitro* gene expression microarray data from the 12 NSCLC cell lines we evaluated as xenografts. With the help of Dr. Yang Xie's group (also at the University of Texas Southwestern Medical Center) the T/C ratios calculated following treatment of xenograft tumors with either r84 or bevacizumab were used as a continuous dichotomized variable to weigh NSCLC cell line gene expression based on *in vivo* response to anti-VEGF therapy. Filtering with cut-offs of a less than 1% false discovery rate and greater than two-fold change in expression, we were able to identify 86 and 101 differentially expressed genes based on responsiveness to bevacizumab and r84, respectively. There are 14 differentially expressed genes that have a greater than three-fold change in gene expression in NSCLC cell lines that have intrinsic resistance to bevacizumab therapy as compared to cell lines that are sensitive to therapy (Table 5.6). A subsequent microarray database was generated using RNA harvested from control-treated NSCLC xenografts (n = 3 tumors per NSCLC line, 12 lines total) run on Illumina Human HT-12 V4 arrays. Similar statistical analyses were performed to generate of list of differentially-expressed genes weighted based on response to r84 or bevacizumab therapy *in vivo*. This *in vivo* NSCLC microarray yielded fewer gene hits than the previous array and did not include any of the

same genes as the *in vitro* analysis, with the exception of pleckstrin homology domain containing A5 (Table 5.7).

| Name | Function | Fold Δ |
|---|---|---|
| Axl | RTK; Angiogenesis, survival, tumorigenesis | 7.35 |
| SLC7A11 (Solute Carrier Family 7-11) | Cystine/glutamate transporter | 4.13 |
| Caprin 2 | Cytoplasmic activation/ proliferation-associated | 4.06 |
| Pleckstrin Homology Domain Containing A5 | Signaling, cell structure | 3.85 |
| Supervillin | Cell structure | 3.8 |
| NEDD4-like binding protein | Ubiquitination | 3.47 |
| C15orf52 | Unknown | 3.26 |
| Far Upstream Element (FUSE) Binding Protein 1 | ATP-dependent DNA helicase; c-myc activation | 3.14 |
| PC4 and SFRS1 interacting protein 1 (PSIP1) | Transcription co-activator | 3.11 |
| N-myc downstream regulated 1 | p53 signaling | 0.28 |
| C10orf116 | Unknown | 0.24 |
| ISG15 ubiquitin-like modifier | Activated by interferon-alpha/-beta | 0.22 |
| RasGEF1A | Ras-like GTPase | 0.20 |

**Table 5.6: Differential gene expression in bevacizumab resistant tumors by *in vitro* microarray.**

Existing microarray data from the Minna and Gazdar laboratories on NSCLC cell lines grown *in vitro* was analyzed using the T/C ratios calculated following *in vivo* treatment of 12 NSCLC lines with bevacizumab to weight gene expression based on sensitivity to therapy. The above list of genes had a greater than three-fold change in expression between NSCLC lines resistant versus sensitive to bevacizumab.

| Name | Function | Fold Δ |
|---|---|---|
| Epithelial Membrane Protein 1 | Tumor suppressor in oral squamous cell carcinoma | 13.579 |
| Epithelial Membrane Protein 1 | Tumor suppressor in oral squamous cell carcinoma | 11.262 |
| WD Repeat Domain 11 | Cell cycle progression, signal transduction, apoptosis, | 7.078 |
| Pleckstrin Homology Domain Containing A5 | Signaling, cell structure | 4.199 |
| Zinc finger, MYND-type containing 11 | Transcriptional repressor | 2.126 |
| CWC22 spliceosome-associated protein | Precursor mRNA splicing | 0.469 |
| Zinc Finger protein 550 | Transcription factor | 0.423 |
| LOC100131551 | Unknown | 0.351 |
| Jagged 2 | Notch signaling pathway | 0.133 |
| Jagged 2 | Notch signaling pathway | 0.104 |
| Zinc Finger Protein 3 | Transcription factor | 0.060 |
| RAS dexamethasone-induced 1 | Regulation of cell morphology, growth, | 0.036 |

**Table 5.7: Differential gene expression in bevacizumab resistant tumors by *in vivo* microarray.**

Microarray data from NSCLC cell lines grown as xenografts *in vivo* and treated with a control IgG was analyzed using the T/C ratios calculated following *in vivo* treatment of 12 NSCLC lines with bevacizumab to weight gene expression based on sensitivity to therapy. The above list of genes had a greater than two-fold change in expression between NSCLC lines resistant versus sensitive to bevacizumab.

#### *5.2.2.4 NSCLC tumor and cell line reverse-phase protein array*

Tumor lysates from control-treated NSCLC xenografts were prepared from flash frozen tumor tissue or *in vitro* cell lines and sent to the laboratory of Dr. John Heymach at the University of Texas MD Anderson Cancer Center to be analyzed by RPPA for the expression of 125 proteins and phosphoproteins. An unsupervised hierarchical clustering analysis demonstrated differential protein expression between NSCLC tumors that are intrinsically resistant versus sensitive to bevacizumab therapy. In addition, tumors sensitive to bevacizumab therapy cluster closely together, independent of treatment (Figure 5.9). Samples were separated into groups based on *in vivo* response to bevacizumab therapy and the fold change in protein expression was calculated for bevacizumab resistant versus sensitive tumors (Appendix F). Proteins with a greater than 1.5-fold change in expression are displayed in Table 5.8. Interestingly, there were a number of proteins associated with tumorigenesis that had differential expression.

At the top of the differential expression lists generated from the *in vitro* microarray and RPPA data was the receptor tyrosine kinase Axl, with a 7.35-fold increase in gene expression and a 2.36-fold increase in protein expression in bevacizumab resistant versus sensitive lines (Table 5.6 and Table 5.8). Axl functions in angiogenesis, cell survival, proliferation, migration and in the release of inflammatory cytokines (Linger et al., 2008). Axl is over expressed in many cancers, including NSCLC (Shieh et al., 2005; Wimmel et al., 2001). The appeal

of Axl as a therapeutic target in cancer is supported by several recent publications. In primary breast cancer, Axl expression was demonstrated to be driven by epithelial to mesenchymal transition and is correlated with a worse prognosis (Gjerdrum et al., 2010). Knockdown of Axl using shRNA in the breast cancer cell line MDA-MB-231 prevented tumor metastases and increased overall survival in xenograft mouse models (Gjerdrum et al., 2010). Blockade of Axl signaling with the small molecule inhibitor R428 (Rigel, Inc.) reduced metastases and improved overall survival in two models of breast cancer (Holland et al., 2010). In NSCLC and breast cancer xenograft models, shRNA mediated knockdown of Axl decreased tumor growth and metastasis of breast cancer to the lung (Li et al., 2009). The use of therapeutic anti-Axl monoclonal antibodies in NSCLC xenografts decreased tumor growth by down regulating Axl expression, reducing tumor proliferation and increasing apoptosis (Li et al., 2009). In addition, the treatment of A549 and MDA-MB-231 xenografts with the monoclonal antibody YW327.6S2 (Genentech) that recognizes mouse and human Axl decreases tumor growth, microvessel density, inflammatory cytokine production and enhances the activity of chemotherapy and VEGF inhibition (Ye et al., 2010). However, there are no publications to date suggesting that Axl expression may be correlated with *in vivo* resistance of NSCLC or other cancers to anti-VEGF therapy. Thus, we were excited to explore the potential of Axl as a mediator of resistance to bevacizumab therapy *in vivo*.

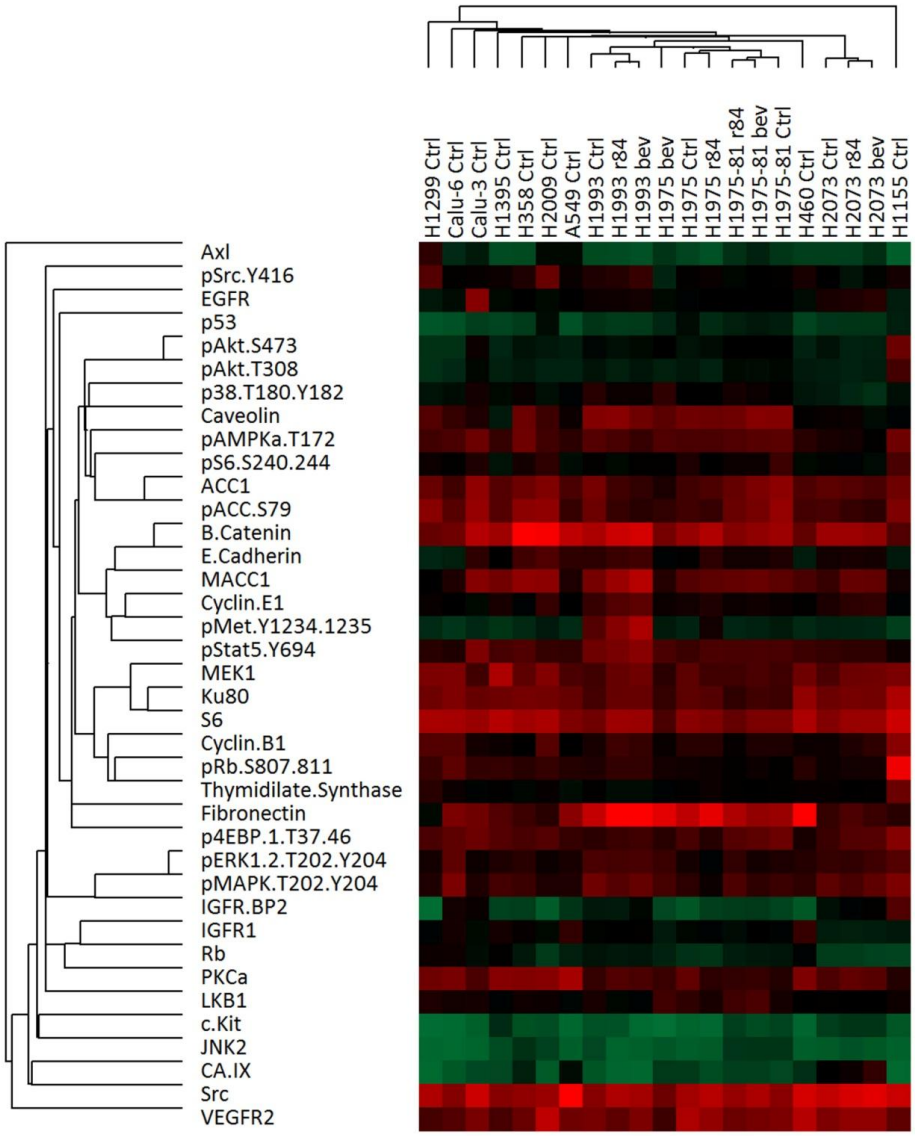


**Figure 5.9: Cluster analysis of NSCLC tumor RPPA.**

Unsupervised clustering analysis of control (Ctrl)-, r84- or bevacizumab-treated NSCLC tumors where shades of red and green denote high and low levels of protein expression, respectively.

| Name | Function | Fold Δ |
|---|---|---|
| Axl | Angiogenesis, survival, tumorigenesis | 2.36 |
| Insulin-like growth factor-binding protein 2 (IGFBP2) | Growth factor signaling; tumorignesis | 2.00 |
| Src | Proto-oncogene | 1.72 |
| Protein kinase C α (PKCα) | Cell signaling, adhesion, cycle, transformation | 1.65 |
| Retinoblastoma (Rb) | Tumor suppressor, cell cycle regulation | 1.62 |
| Insulin-like growth factor receptor 1 (IGFR1) | Development, cell survival, tumorigenesis | 1.57 |
| phospho-Retinblastoma (Rb) (S807/811) | Tumor suppressor, cell cycle regulation | 1.55 |
| Epidermal growth factor receptor (EGFR) | Cell proliferation, migration, adhesion, tumorigenesis | 1.51 |
| Caveolin | Endocytosis, migration | 0.63 |
| Cyclin.E1 | Cell cycle, tumorigenesis | 0.59 |
| c.Kit | Proto-oncogene | 0.59 |
| Tumor protein 53 (p53) | Tumor suppressor | 0.54 |
| pMet (Y1234/1235) | Proto-oncogene | 0.50 |

**Table 5.8: Differential protein expression in bevacizumab resistant tumors by reverse-phase protein array.**

Reverse-phase protein lysates array data from NSCLC cell lines grown as xenografts *in vivo* and treated with a control IgG was evaluated for proteins displaying a greater than 1.5 fold change in expression between bevacizumab sensitive and resistant tumors.

### *5.2.3 The receptor tyrosine kinase Axl as a potential marker for resistance to bevacizumab therapy*

#### *5.2.3.1 Axl expression is increased in NSCLC lines resistant to bevacizumab therapy*

Given the increase in Axl expression in bevacizumab resistant tumors as compared to sensitive tumors by *in vitro* microarray and RPPA and known roles for Axl in tumor angiogenesis, progression and metastasis, we wanted to investigate the role of Axl in mediating resistance to bevacizumab therapy *in vivo*. To validate expression in NSCLC tumors, we evaluated mRNA expression levels in control-treated NSCLC xenograft tumors using qPCR. Although *AXL* expression varied amongst NSCLC line, there was a trend towards higher levels of Axl expression in tumors with resistance to bevacizumab therapy (Figure 5.10 A). Combining data for bevacizumab resistant (T/C > 0.40) and sensitive (T/C < 0.40) tumors demonstrated a significant increase in *AXL* expression in resistant tumors ($p < 0.01$) (Figure 5.10 B). Protein expression of Axl in control-treated NSCLC xenograft tumor lysates was evaluated using a commercially-available total Axl ELISA (R&D Systems). Similar to the qPCR results, there was a trend of increased Axl expression in bevacizumab resistant tumors as compared to sensitive tumors (Figure 5.11 A), which reached significance ($p < 0.0001$) when samples were combined based on *in vivo* response phenotype (Figure 5.11 B).

Control-treated NSCLC xenograft tumor lysates were also evaluated for Axl expression by Western blot (Figure 5.12 A). However, in this assay Axl expression (normalized to actin expression levels) was not enhanced in bevacizumab resistant samples (Figure 5.12 B). It is unclear at this time why there is a discrepancy between qPCR, ELISA and Western blot detection levels of Axl transcript and protein expression. The Western blot analysis of Axl in tumor lysates has been repeated multiple times with different lysate samples and has generated similar results to those shown in Figure 5.12. Despite these differences, we felt that Axl expression was indeed correlating with resistance to bevacizumab therapy *in vivo* and set out to validate this relationship.

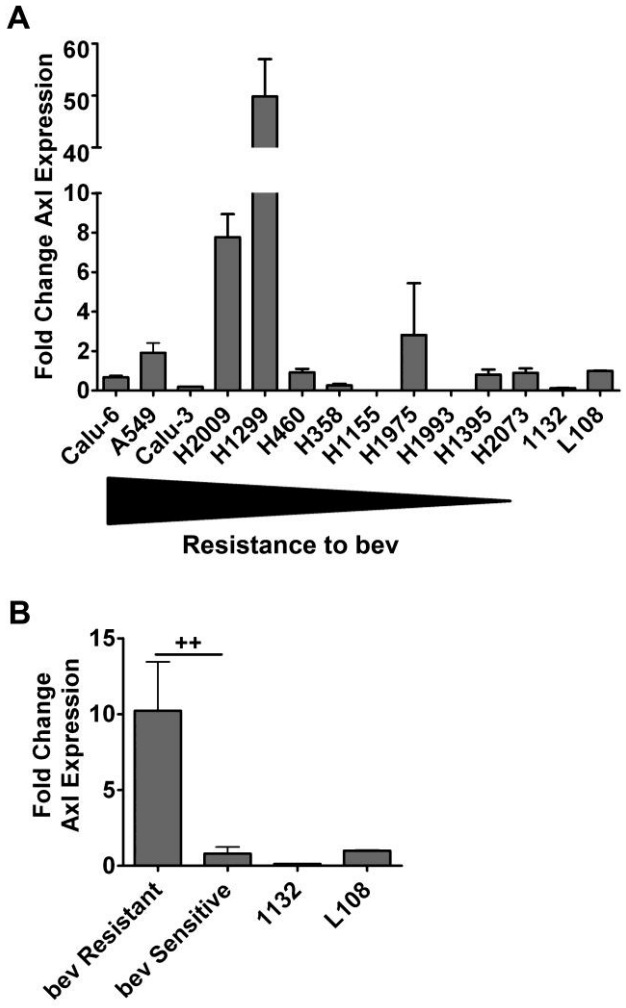


**Figure 5.10: Detection of *AXL* expression in NSCLC tumors by qPCR.**

RNA was harvested from control-treated NSCLC xenografts (n = 3 tumors per NSCLC line, assayed in duplicate), reversed transcribed to generate cDNA and analyzed for expression of *AXL* by quantitative PCR (qPCR). *AXL* expression was normalized to L108 MiaPaca sample. Expression of *AXL* varies amongst the NSCLC tumors (**A**), and is more highly expressed in bevacizumab (bev) resistant versus sensitive tumors. Data normalized to *AXL*-low expressing MiaPaca2-1132 (1132) sample. ++ $p < 0.01$ by t-test.

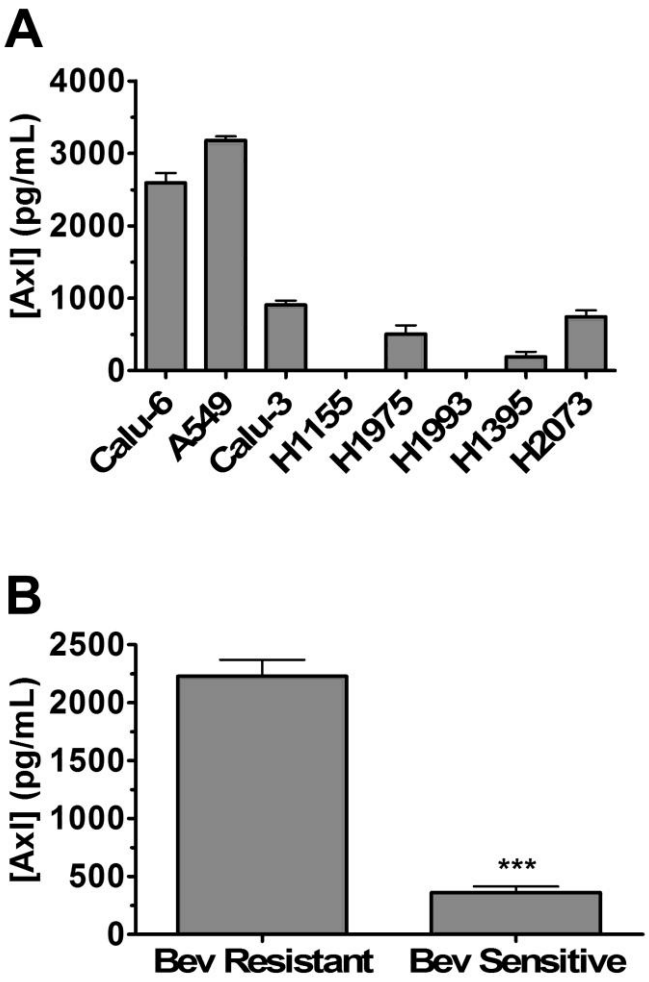


**Figure 5.11: The receptor tyrosine kinase Axl is expressed at higher levels in tumor resistant to bevacizumab therapy.**

The commercially-available R&D Systems Axl ELISA kit was performed with tumor lysates from NSCLC xenograft tumors that displayed *in vivo* resistance or sensitivity to treatment with bevacizumab. Axl expression within these tumor lysates was much higher in bevacizumab resistant versus sensitive samples. *** $p < 0.001$.

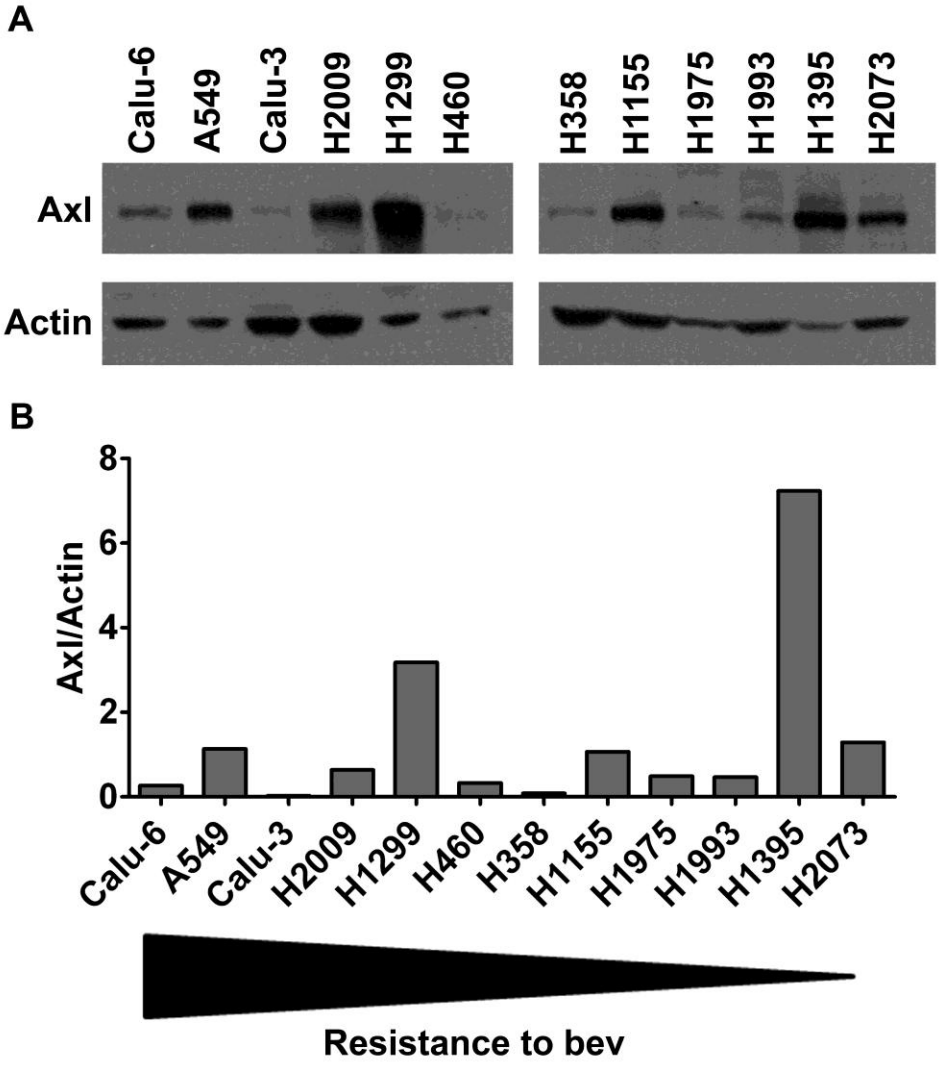


**Figure 5.12: Detection of Axl expression in NSCLC tumors by Western blot.**

Lysates generated from control-treated NSCLC xenografts and analyzed for expression of Axl by Western blot. Although Axl expression varies by NSCLC tumor line, there is no observable correlation between expression and sensitivity to bevacizumab (bev).

#### *5.2.3.2 Targeting Axl signaling in vivo does not enhance response of NSCLC lines to bevacizumab therapy*

Stable knockdown of Axl in bevacizumab resistant cell lines A549, Calu-3 and Calu-6 was achieved using viral infection of *AXL* specific shRNAmir Open Biosystems constructs (designated B4, H12) followed by two weeks of selection in puromycin. Cells were also infected with a non-targeting control (NTC) shRNAmir construct as a negative control. A549 cells responded best to viral infection and Axl knockdown and were thus selected to go forward with subsequent experiments. Validation of Axl transcript and protein knockdown was assessed by qPCR and Western blot (Figure 5.13). In both assays, a greater reduction in Axl expression was observed in cells with stable expression of H12 shRNAmir as compared to B4 (Figure 5.13).

To evaluate the role of Axl in mediating resistance to bevacizumab therapy *in vivo*, 2.5 million A549-NTC or A549-H12 cells were injected subcutaneously into NOD/SCID mice and treated with 25 mg/kg/week with a control IgG or bevacizumab (n = 8 per group) starting one day post tumor cell injection and continuing until control-treated A549-NTC tumors reached approximately 1200 $mm^3$, at which time all animals were sacrificed and tumors were harvested, weighed and stored for further analysis. Similar to results seen by other investigators following Axl knockdown (Li et al., 2009), A549-H12 tumors grew much slower than A549-NTC tumors (Figure 5.14). However, loss of Axl

did not significantly increase sensitivity to bevacizumab therapy as indicated by tumor growth curves (Figure 5.14 A) or final tumor weights (Figure 5.14 B, top panel). Further, T/C ratios for parental A549 and bevacizumab-treated A549-NTC tumors were essentially the same (Figure 5.14 B, bottom panel) and indicated a high level of resistance of each tumor line to bevacizumab. Although the T/C ratio of bevacizumab-treated A549-H12 tumors (as compared to control-treated A549-NTC) was reduced, final tumor weights were not significantly different from bevacizumab-treated A549-NTC or control-treated A549-H12 (Figure 5.14 B). It is possible that the lack of increased sensitivity to bevacizumab in A549-H12 tumors could be the result of loss of Axl shRNAmir expression *in vivo*. To test this possibility, control- and bevacizumab-treated A549-NTC and A549 H12 tumor lysates were evaluated for expression of Axl by Western blot. Axl knockdown was maintained *in vivo* and was significantly reduced in A549-H12 control- and bevacizumab-treated tumors (Figure 5.15 A and B, respectively). Further, treatment with bevacizumab had no effect on Axl expression in either A549-NTC or A549-H12 tumors. Therefore, the lack of enhanced sensitivity of A549-H12 tumors to bevacizumab was not the result of inadequate reduction of Axl expression.

A second set of experiments was performed to independently evaluate the effect of therapeutic blockade of Axl in sensitizing bevacizumab resistant NSCLC tumors to therapy. 2.5 million Calu-6 or Calu-3 cells were injected

subcutaneously into NOD/SCID mice and treated with saline or 25 mg/kg/week bevacizumab (n = 18 per group) starting one day post tumor cell injection and continuing until tumors reached approximately 140 $mm^3$. Saline-treated animals were then randomized to receive continued saline or 25 mg/kg/week anti-human Axl monoclonal antibody 10C9 (BerGen Bio AS) and bevacizumab-treated animals were randomized to receive continued bevacizumab or combination bevacizumab plus 10C9 (n = 8 per group). Therapy continued for 14 days post randomization for Calu-6 tumors and for 32 days post randomization for Calu-3 tumors, at which time all animals were sacrificed and tumors were harvested, weighed and stored for further analysis. Inhibition of Axl with 10C9 as single agent therapy had no effect on Calu-6 or Calu-3 tumor growth, final tumor weight or T/C ratios and did not sensitize tumors to bevacizumab (Figure 5.16 and Figure 5.17). These results differ from those seen by Ye et al, who demonstrated single agent efficacy with anti-mouse and human Axl monoclonal antibody therapy and enhanced tumor growth control when combined with anti-VEGF treatment in A549 and MDA-MB-231 xenografts (Ye et al., 2010). However, these differences could be related to the different cell lines used (A549 versus Calu-6 and Calu-3) or the specificity and function of their anti-Axl monoclonal antibody as compared to 10C9. Western blot analysis from Calu-6 and Calu-3 tumor lysates demonstrated that Axl is indeed expressed in these tumors, and expression does not change following treatment with 10C9, bevacizumab or combination therapy

(Figure 5.18). To test *in vivo* availability and function of 10C9, serum was collected from animals at sacrifice and evaluated for binding activity to recombinant human Axl by ELISA. Serum from animals receiving 10C9 monotherapy or in combination with bevacizumab had strong anti-Axl activity, indicating that the lack of tumor response to therapy was not due to antibody degradation or lack of binding activity (Figure 5.19 and Figure 5.20).

Although Axl expression initially appeared to be related to intrinsic resistance of NSCLC tumors to bevacizumab therapy *in vivo*, subsequent experiments have not been able to validate this relationship. This could be the result of sub-optimal reagents used to block Axl function *in vivo*. Alternatively, even though Axl expression has been demonstrated to play important roles in tumor progression and metastasis by a number of investigators, this protein may have little to no function in mediating resistance to anti-VEGF therapy. Further investigation of *AXL* and other gene targets generated from our array datasets are warranted to identify mechanisms of intrinsic resistance to bevacizumab and r84 therapy.

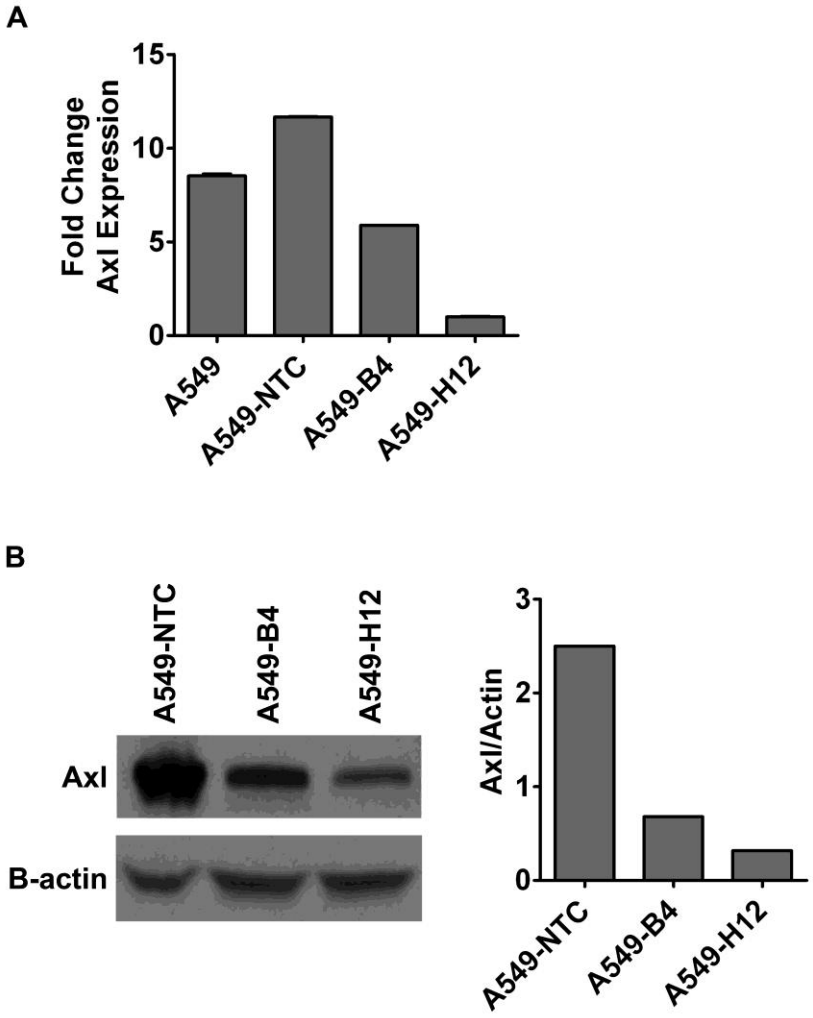


**Figure 5.13: Generation of A549 NSCLC cell line stably expression *AXL* shRNAmir.**

Knockdown of Axl in A549 cell line was generated through infection of lentivirus containing shRNAmir specific to human *AXL* (A549-B4, A549-H12; see Chapter Three, Materials and Methods). A non-targeting control (NTC) vector was used as a negative control. Following two weeks of selection, Axl knockdown was confirmed by qPCR (**A**) and Western blot (**B**).

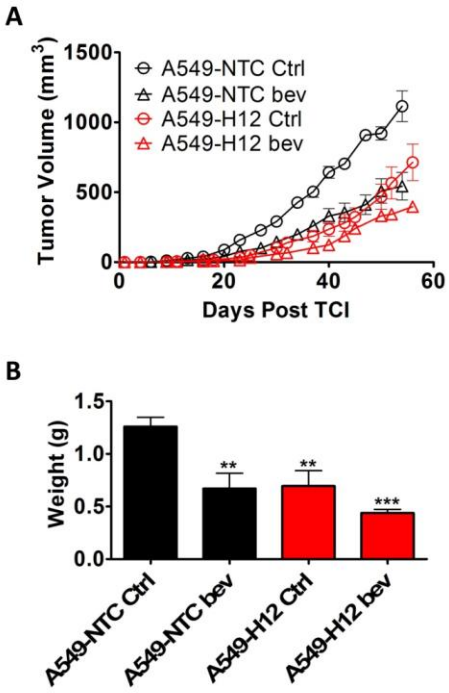


| Cell Line | Therapy | T/C Ratio |
|---|---|---|
| A549 | bev | 0.56 |
| A549-NTC | bev | 0.53 |
| A549-H12 | bev | 0.35 |

**Figure 5.14: Knockdown of Axl in A549 NSCLC tumors does not increase sensitivity to bevacizumab.**

2.5 million A549-H12 cells stably expressing shRNAmir to human *AXL* that confers knockdown of Axl expression were injected subcutaneously (s.c.) into NOD/SCID mice and treated with 25 mg/kg/week control IgG (Ctrl) or bevacizumab (bev) beginning one day post tumor cell injection (TCI) (n = 8 per group). Knockdown of Axl resulted in slower tumor growth in A549-H12 tumors versus A549-NTC (non-targeting control) tumors (**A**) but did not confer significantly increased sensitivity to bev by tumor growth curves (**A**) or final tumor weight (**B**). T/C ratios of bev-treated A549-NTC tumors were similar to historical A549 with a slight improvement in A549-H12 tumors. **p < 0.01, ***p < 0.001 versus A549-NTC Ctrl.

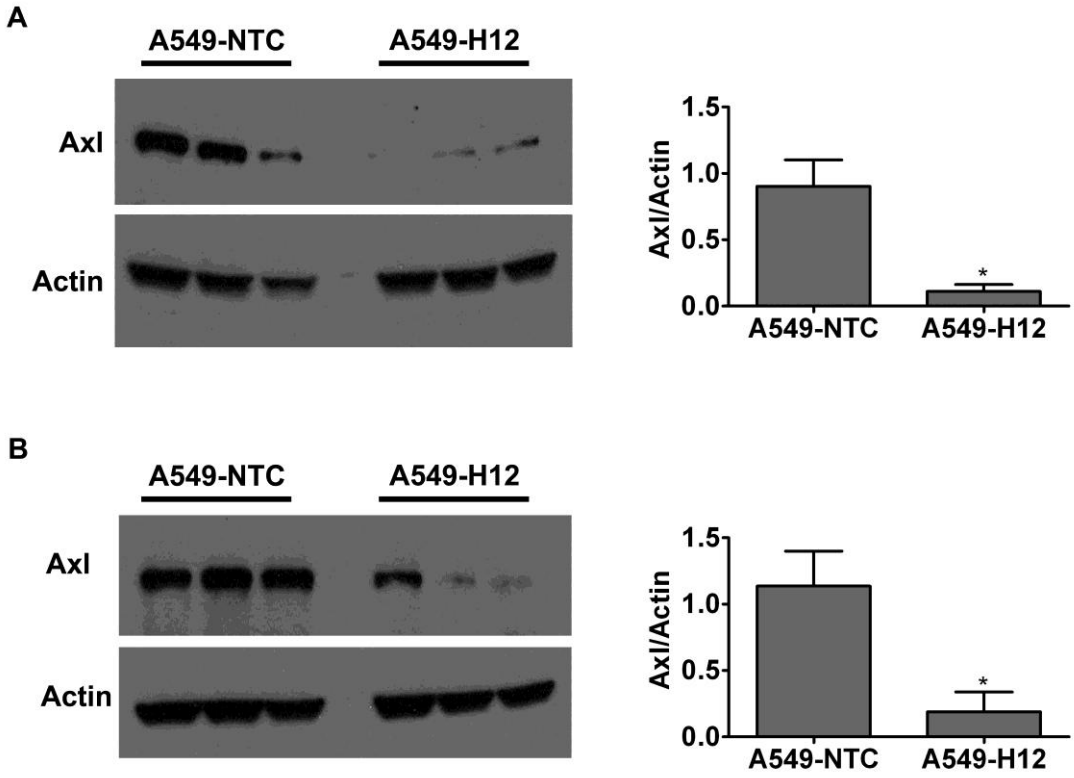


**Figure 5.15: Knockdown of Axl with shRNAmir is stable *in vivo*.**

Tumor lysates were generated from control-treated (**A**) or bevacizumab-treated (**B**) A549-NTC and A549-H12 xenografts that stably express shRNAmir non-targeting control or *AXL* constructs, respectively. Western blot analysis demonstrates Axl knockdown is maintained *in vivo* and that control or bevacizumab therapy does not alter Axl expression. Axl expression is significantly reduced in A549-H12 tumors as compared to A549-NTC tumors (**A** and **B**, right panel for quantification). *$p < 0.05$.

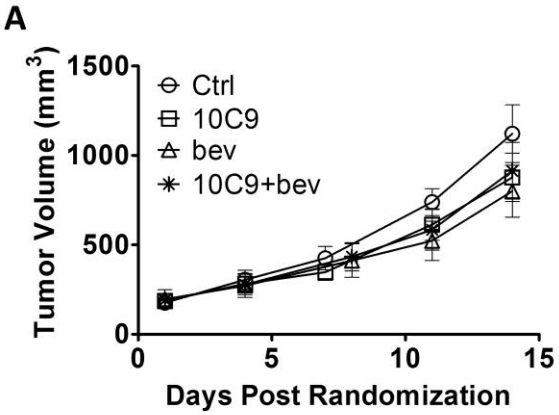


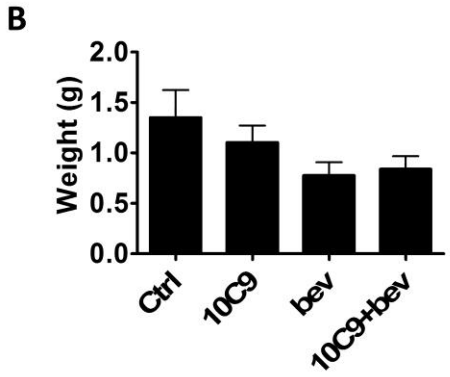


| Cell Line | Therapy | T/C Ratio |
|---|---|---|
| Calu-6 | 10C9 | 0.81 |
| Calu-6 | bev | 0.57 |
| Calu-6 | bev+10C9 | 0.61 |

**Figure 5.16: Therapeutic targeting of Axl does not affect Calu-6 tumor growth or response to bevacizumab.**

2.5 million Calu-6 NSCLC cells were injected subcutaneously (in PBS) into NOD/SCID mice. Starting one day post tumor cell injection (TCI), mice were treated IP. with saline or bevacizumab (bev) at 25 mg/kg/week (n = 16 per group). When average tumor volume of the saline group reached 140 $mm^3$, animals were randomized to receive saline or the anti-human Axl monoclonal antibody 10C9 at 25 mg/kg/week (n = 8 per group). Similarly, when average tumor volume of the bev group reached 140 $mm^3$, animals were randomized to receive bev or combination bev+10C9 at 25 mg/kg/week (n = 8 per group). Therapy continued for 14 days post randomization, at which time animals were sacrificed and tumors were collected. None of the treatment groups had any inhibitory effect on Calu-6 tumor growth (**A**) or final tumor weight and T/C ratios (**B**).

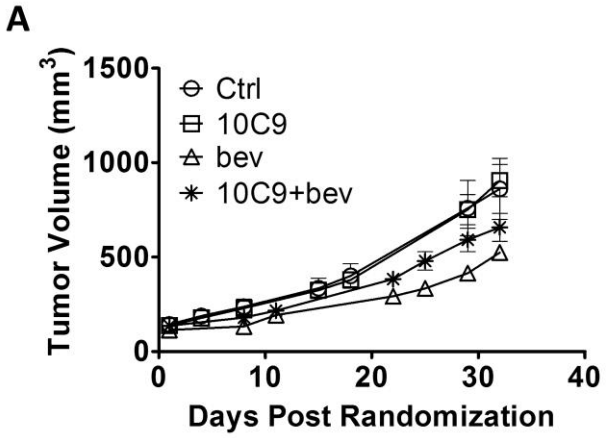


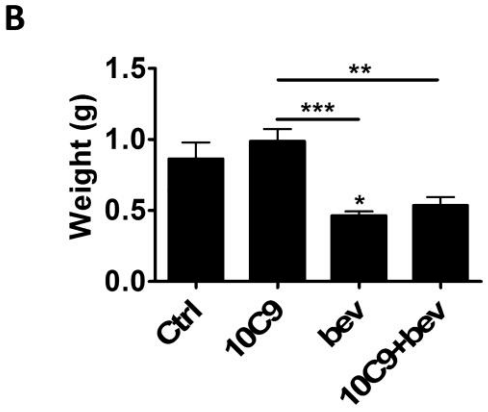


| Cell Line | Therapy | T/C Ratio |
|---|---|---|
| Calu-3 | 10C9 | 1.15 |
| Calu-3 | bev | 0.54 |
| Calu-3 | bev+10C9 | 0.62 |

**Figure 5.17: Therapeutic targeting of Axl does not affect Calu-3 tumor growth or response to bevacizumab.**

2.5 million Calu-3 NSCLC cells were injected subcutaneously (in PBS) into NOD/SCID mice. Starting one day post tumor cell injection (TCI), mice were treated IP with saline or bevacizumab (bev) at 25 mg/kg/week (n = 16 per group). When average tumor volume of the saline group reached 140 $mm^3$, animals were randomized to receive saline or the anti-human Axl monoclonal antibody 10C9 at 25 mg/kg/week (n = 8 per group). Similarly, when average tumor volume of the bev group reached 140 $mm^3$, animals were randomized to receive bev or combination bev+10C9 at 25 mg/kg/week (n = 8 per group). Therapy continued for 32 days post randomization, at which time animals were sacrificed and tumors were collected. None of the treatment groups had any inhibitory effect on Calu-3 tumor growth (**A**) or final tumor weight and T/C ratios (**B**).

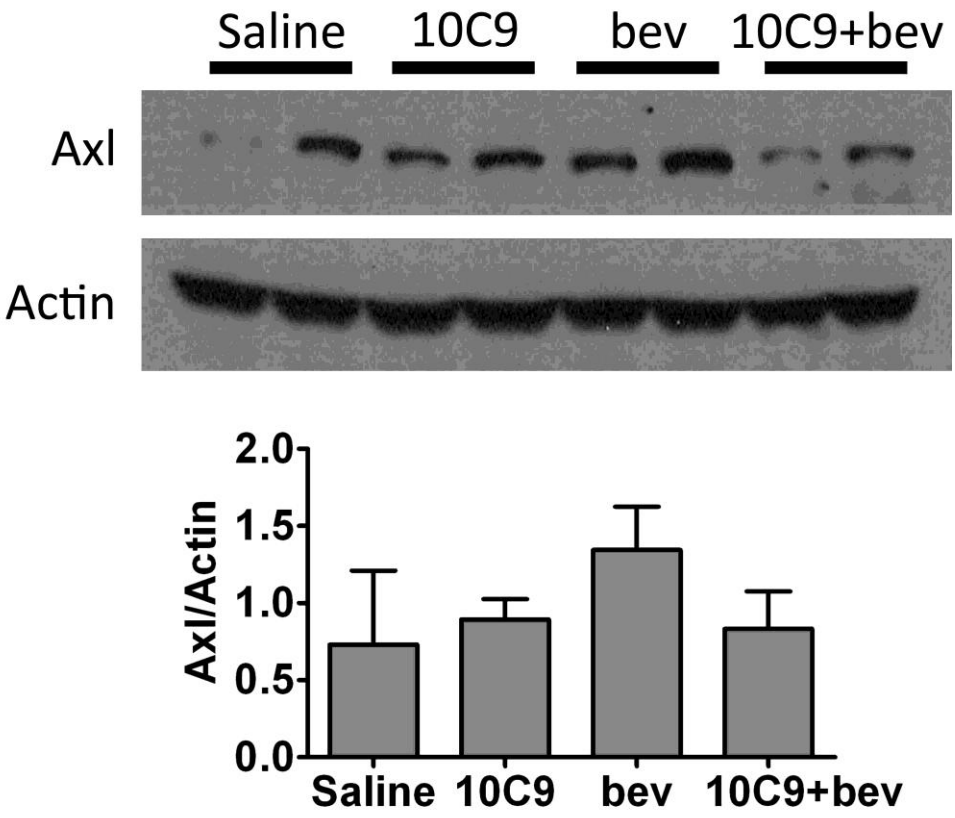


**Figure 5.18: Targeting Axl with the monoclonal antibody 10C9 does not alter Axl expression.**

Lysates were generated from Calu-6 and Calu-3 tumor xenografts treated with saline, bevacizumab (bev), 10C9, and 10C9 + bev and analyzed by Western blot for Axl expression. Calu-6 and Calu-3 tumors express Axl, but expression is not altered by 10C9 and/or bev therapy.

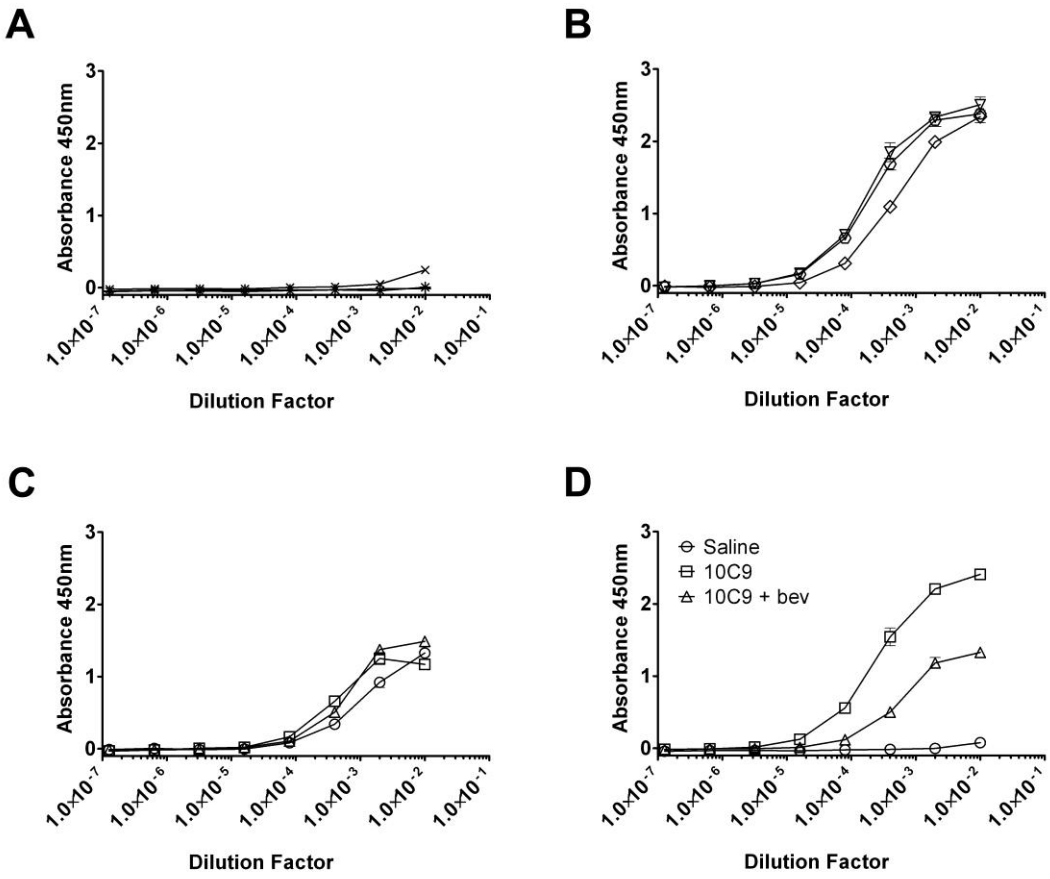


**Figure 5.19: Active 10C9 is detected in serum of treated animals with Calu-6 tumors.**

Serum was collected from NOD/SCID mice bearing Calu-6 tumors and receiving treatment with saline (**A**), 10C9 (**B**; 24 hours post last therapy), bevacizumab (bev) or 10C9 + bev (**C**; 72 hours post last therapy) and tested for binding activity to recombinant human Axl by ELISA. Animals that received 10C9 therapy have strong Axl binding activity that is not seen in animals that received saline (**D**).

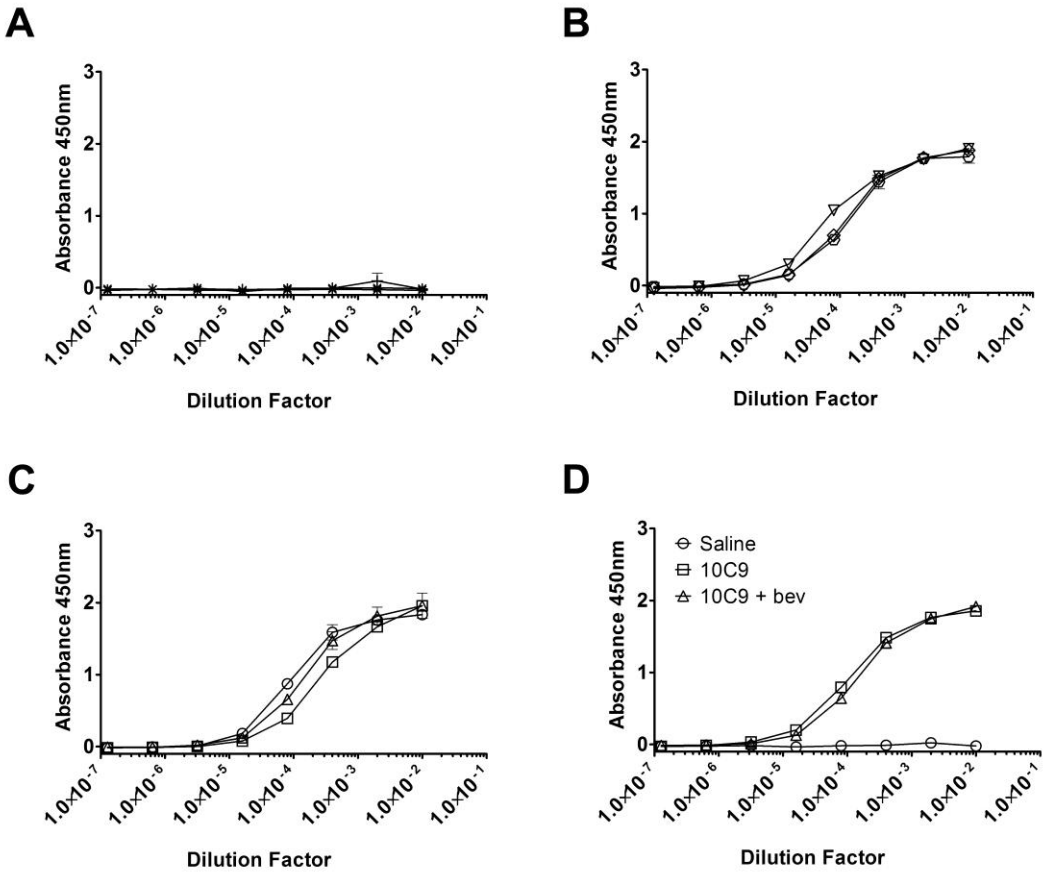


**Figure 5.20: Active 10C9 is detected in serum of treated animals with Calu-3 tumors.**

Serum was collected from NOD/SCID mice bearing Calu-3 tumors and receiving treatment with saline (**A**), 10C9 (**B**), bevacizumab (bev) or 10C9 + bev (**C**) (all collected 24 hours post last therapy) and tested for binding activity to recombinant human Axl by ELISA. Animals that received 10C9 therapy have strong Axl binding activity that is not seen in animals that received saline (**D**).

## 5.3 Discussion

Anti-angiogenic therapy has failed to deliver substantial gains in cancer patient survival and with expanded use of anti-angiogenic agents in the clinic it has become increasingly apparent that this strategy is not immune to the development of resistance, as was initially hypothesized. There are two broad categories of resistance to anti-angiogenic therapy, intrinsic resistance where a tumor never responds to therapy or evasive resistance where treatment stops being effective after a brief period of responsiveness (See Chapter Four and Figure 4.3) (Bergers and Hanahan, 2008; Mitchell and Bryan, 2010). However, the patterns and mechanisms of NSCLC resistance to anti-angiogenic therapies are not well defined and require further investigation. The ability to predict *de novo* if a patient will respond to a specific anti-angiogenic therapy is critical to improve the overall success of these drugs and to avoid treating patients that will receive no benefit from therapy. In addition, understanding the mechanisms through which resistance occurs can identify new targets that could be used effectively as monotherapy or combined to improve the efficacy of anti-angiogenic drugs.

NSCLC is the most common and deadliest cancer worldwide despite therapeutic advances (Jemal et al., 2011). Bevacizumab is approved for the treatment of NSCLC, but has not produced long-term survival advantages for these patients (Reck et al., 2009; Sandler et al., 2006). Therefore, there is the need to improve the efficacy of NSCLC treatments. We set out to identify tumor-

derived factors that mediate intrinsic resistance of NSCLC tumors to the anti-VEGF therapeutic monoclonal antibodies bevacizumab and r84. Since the primary effects of these agents are on the tumor vasculature and microenvironment, treating NSCLC cell lines *in vitro* with bevacizumab and r84 has no effect on cell proliferation or viability (data not shown), thus resistance to therapy must be evaluated *in vivo*. We evaluated the response of a total of 12 NSCLC cell lines, grown as xenografts in mice, and found that response varied by line and therapy (Figure 5.1 – Figure 5.4). Three of the 12 lines tested (Calu-6, A549, Calu-3) displayed intrinsic resistance to bevacizumab and sensitivity to r84 therapy. Two lines (H1395, H1155) displayed intrinsic resistance to r84 therapy and sensitivity to bevacizumab therapy. Interestingly, none of the 12 lines we tested displayed intrinsic resistance to both anti-VEGF therapies; however there were common lines with sensitivity to bevacizumab and r84. This is the largest publically-available dataset of *in vivo* response of NSCLC to anti-VEGF to our knowledge and provides an excellent source of information to evaluate mechanisms of resistance.

There are no obvious patterns of tumor histotypes, gender, source (primary tumor or metastasis) of the original tumor sample or mutation status of common tumorigenesis genes that predict for NSCLC response to anti-VEGF therapy (Table 5.1 and Table 5.2). Therefore, we investigated the genetic and proteomic expression profiles of our 12 NSCLC tumor lines to identify key mediators of

response to bevacizumab and r84 therapy. There are several proposed mechanisms through which tumors can become resistant to anti-angiogenic therapy, including the deregulation of growth factor and cytokine expression (Bergers and Hanahan, 2008; Mitchell and Bryan, 2010). To evaluate these possible changes in our tumors, we performed qPCR and MILLIPLEX MAP arrays. We observed very few changes in the expression of growth factors between intrinsically resistant and sensitive tumor lines. For example, switching from VEGF to alternative growth factors such as FGF, platelet-derived growth factor (PDGF) and PlGF can compensate for therapeutic blockade of VEGF (Bergers and Hanahan, 2008). We observed a slight reduction in human VEGF and an increase in FGF-2 expression in tumors intrinsically resistant to bevacizumab versus sensitive by the MILLIPLEX MAP array (Figure 5.7 A). Using the SABiosciences qPCR arrays, we found a greater than four-fold increase in the expression of PDGF-D and FGF-13 in bevacizumab and r84 intrinsically resistant versus sensitive tumor lines (Table 5.3 and Table 5.4). However, we have no evidence that these alternative growth factors are driving continued tumor angiogenesis as we still have significant reductions in tumor microvessel density with bevacizumab and r84 treatment that is independent of response to anti-VEGF therapy (Figure 5.6). Therefore, these models do not support the idea of alternative growth factor switching as a mode of NSCLC resistance to anti-VEGF

therapy and suggest that other mechanisms may be responsible for intrinsic resistance.

Cancer is a disease of chronic inflammation and the inflammatory cytokines expressed in the tumor microenvironment can regulate cell proliferation, angiogenesis, metastasis and the maintenance of pro-tumorigenic inflammation (Grivennikov et al., 2010). Although smoking is known to drive inflammation in NSCLC, the relationship between inflammation and patient prognosis remains unclear (O'Callaghan et al., 2010). Chemotactic cytokines, or chemokines, can have direct effects such as induction of apoptosis, proliferation or angiogenesis on cells expressing the appropriate chemokine receptors. Additionally, chemokines can recruit other cell types such as leukocytes and stromal cells to the tumor to influence tumor growth and progression (Garin and Proudfoot, 2011). Thus the expression patterns of cytokines and chemokines can have pro- or anti-tumor effects. We evaluated tumor cytokine expression with SABiosciences qPCR and MILLIPLEX MAP arrays and observed some interesting patterns in intrinsically resistant and sensitive tumors. There are a number of pro- and anti-angiogenic cytokines evaluated in these arrays, including pro-angiogenic CXCL1, CXCL2, CXCL3, CXCL5, CXCL6, CCL2, CCL11 and IL-8 and anti-angiogenic CXCL4, CXCL9, CXCL10 AND CXCL11 (Keeley et al., 2011). We observed statistically significant increases in pro-angiogenic human CCL2, mouse CCL11 and CXCL6 in bevacizumab resistant versus

sensitive tumors (Figure 5.7, Figure 5.8 and Table 5.3). In addition, the expression of anti-angiogenic CXLC4 and CXCL9 cytokines was increased in bevacizumab resistant versus sensitive tumors by SABiosciences qPCR array (Table 5.3). However, protein levels of CXLC9 and CXCL10 expression were decreased in bevacizumab resistant versus sensitive tumors (Figure 5.7 and Figure 5.8). The significance of these changes is not fully understood at this time. When assessing only the protein expression data provided by the MILLIPLEX MAP assays, the increases in pro-angiogenic cytokines and reductions in anti-angiogenic cytokines in bevacizumab resistant versus sensitive tumors may work together to generate tumors that are actively undergoing angiogenesis and are thus good candidates for anti-VEGF therapy. However, although the expression of pro-angiogenic cytokines may play a role in tumor angiogenesis, we again do not see a change in the ability of anti-VEGF antibodies to reduce tumor microvessel density, again suggesting a muted, if any role for alternative growth factor switching in our model.

Although tumor associated macrophages have been demonstrated to have pro-tumorigenic effects in multiple cancer types, their role in NSCLC remains controversial (Grivennikov et al., 2010; O'Callaghan et al., 2010). Attempts by our lab to detect significant populations of macrophages within NSCLC xenograft tumors have been unsuccessful. Several cytokines detected by the MILLIPLEX MAP assay have roles in mediating the recruitment and function of pro-

tumorigenic tumor associated macrophages, such as IL-10, CCL2 and CCL5 (Allavena et al., 2011; Garin and Proudfoot, 2011). In bevacizumab resistant versus sensitive tumors, there were increases in human CCL2 and IL-10 expression but a significant decrease in mouse CCL5 and IL-10 (Figure 5.7 and Figure 5.8), adding to the controversy of this cell type in lung cancer. However, given that there was significant expression of tumor associated macrophage recruiting cytokines, further investigation on the presence and function of macrophages in our NSCLC may be worthwhile.

To identify other key signaling pathways involved in mediating resistance to anti-VEGF therapy we analyzed existing microarray data from *in vitro* NSCLC cell lines, generated new microarray data from our control-treated NSCLC tumors *in vivo* and performed a RPPA on NSCLC tumor lysates (Table 5.6 – Table 5.8). These datasets generated a great source of information of NSCLC expression profiles *in vitro*, *in vivo* and how expression correlates with response to anti-VEGF therapy. From these arrays, we identified that the receptor tyrosine kinase *AXL* transcript was increased in tumors intrinsically resistant to bevacizumab and performed subsequent experiments to validate this connection (Table 5.6 and Table 5.8). By qPCR and ELISA, Axl is expressed at much higher levels in bevacizumab resistant tumors as compared to sensitive tumors (Figure 5.10 and Figure 5.11); however this relationship was not seen by Western blot (Figure 5.12). The Axl ELISA used different anti-Axl antibodies and did not test

expression in H2009, H1299, H460 and H358 tumor samples, which were evaluated by Western blot. These differences may account for the difference in Axl association to intrinsic bevacizumab resistance between the two assays. Regardless, we relied on the data from our microarrays, RPPA, qPCR and ELISA and further evaluated the role of Axl in mediating resistance to bevacizumab by targeting Axl signaling *in vivo*. First, we generated A549 cells expressing a shRNAmir construct targeted to the *AXL* transcript (A549-H12) that significantly reduced *AXL* expression (Figure 5.13). These cells, along with A549-NTC (non-targeting shRNAmir control line) were injected into NOD/SCID mice and evaluated for response to bevacizumab. Although A549-H12 tumors grew more slowly than A549-NTC, there was not increased sensitivity to bevacizumab therapy (Figure 5.14) although there was significant knockdown of Axl within these tumors (Figure 5.15). Previous experiments from other investigators also investigated the efficacy of Axl knockdown in controlling tumor growth. In those experiments, A549, H1299 and the breast cancer cell line MDA-MB-231 expressing a doxycycline-inducible shRNA to *AXL* were grown in mice and treated with sucrose of doxycycline (Li et al., 2009). Similar to our results, significant control of tumor growth was seen following Axl knockdown, however they did not evaluate the efficacy of anti-VEGF therapy in the face of Axl knockdown (Li et al., 2009). In the future, it could be useful to verify the results we observed with A549-H12 using the Calu-6 and Calu-3 tumor cell lines we

have generated that also have Axl knockdown to see if reduced Axl expression can sensitize other intrinsically bevacizumab resistant tumors to therapy. In our second set of Axl experiments, we used the anti-Axl monoclonal antibody 10C9 (BerGen Bio A/S) in bevacizumab resistant Calu-6 and Calu-3 tumors. 10C9 therapy either alone or in combination with bevacizumab had no effect on tumor growth, final tumor weight or tumor expression of Axl (Figure 5.16 – Figure 5.18) although there was active 10C9 in serum collected from treated mice at sacrifice (Figure 5.19 and Figure 5.20). These results differ from other investigators who demonstrated that targeting Axl *in vivo* with anti-human or anti-mouse and anti-human specific Axl antibodies controlled A549 and MDA-MB-231 tumor growth similar to anti-VEGF therapy alone and that combination therapy greatly reduced tumor growth (Li et al., 2009; Ye et al., 2010). In addition, treatment with anti-Axl antibody also reduced tumor expression of Axl (Ye et al., 2010). In these studies, antibody that recognized human and mouse Axl was more effective at controlling tumor growth than antibody specific to only human Axl. 10C9 recognizes human Axl, and thus its lack of activity may be due to stromal Axl activity. However, other anti-human Axl antibodies have demonstrated modest reductions in tumor growth (Li et al., 2009) and our experiments with 10C9 failed to show any therapeutic benefit, indicating that 10C9 is not an effective anti-Axl therapeutic. Therefore, it would be interesting to repeat these combination

experiments with better anti-Axl drugs to see if tumors that are intrinsically resistant to bevacizumab can become sensitive following anti-Axl blockade.

Two recently published papers have identified novel pathways that may be important for NSCLC resistance to anti-VEGF monoclonal antibody therapy. Nardo et al., recently described a role for AMP-activated protein kinase (AMPK) in mediating a poorly glycolytic phenotype associated with resistance of ovarian tumors to anti-VEGF monoclonal antibody therapy (Nardo et al., 2011). In NSCLC H1975 and A549 tumors, stromal activation of FGF receptor (FGFR) and EGFR conferred resistance to bevacizumab (Cascone et al., 2011). Preliminary analysis of our tumor RPPA data demonstrate a greater than 1.2-fold increase in phospho-AMPK (T172) and phosphorylation of its downstream target acetyl-coenzyme A carboxylase (ACC; S72) in bevacizumab resistant versus sensitive tumors (Appendix F), which correlates with increased activation of these proteins observed in poorly glycolytic ovarian tumors (Nardo et al., 2011) and suggests metabolic characterization of our NSCLC panel may be important in elucidating mechanisms of anti-VEGF resistance. Although we have not yet evaluated mouse levels of FGFR and EGFR, we do see elevated human FGF-2 levels by MILLIPLEX array in bevacizumab resistant versus sensitive tumors (Figure 5.7). There is a 1.51 fold increase in EGFR expression in bevacizumab resistant versus sensitive tumors by RPPA, but levels of phospho-EGFR (Y1173, Y992) are reduced (Table 5.8 and Appendix F). Therefore, further investigation into stromal

activation of the FGFR and EGFR pathway in our tumors could determine whether or not these pathways are important mediators of resistance to bevacizumab in a larger panel of NSCLC tumors.

At this time, our data suggest that although Axl may play important roles in tumor growth and progression, it does not appear to mediate resistance to bevacizumab. However, there are many other interesting proteins and pathways that have been identified by the many datasets generated by our lab that need further investigation. Hopefully some of these targets will be directly involved in NSCLC response to anti-VEGF therapy and will help elucidate novel drug targets or patient populations that will benefit from treatment.

# CHAPTER SIX

# CONCLUSIONS AND FUTURE DIRECTIONS

## 6.1 Conclusions

Tumor angiogenesis is critical for tumor growth, development and metastasis and has been the studied by numerous investigators and pharmaceutical companies to identify the best method to target this process in patients. Although initially highly anticipated as a universal cancer drug that would be immune to the resistance seen by other therapies, the overall clinical results are disappointing. At best, anti-angiogenic therapies only modestly improve patient overall survival or progression free survival and are associated with numerous toxicities. In addition, it is now obvious that patients can be either intrinsically resistant to anti-angiogenic therapy or will develop resistance over time. The objectives of this

thesis were to characterize a new, efficacious anti-angiogenic therapy and to investigate mediators of intrinsic resistance of NSCLC to anti-angiogenic monoclonal antibodies.

VEGF is a primary mediator of physiological and pathological angiogenesis. There are several monoclonal antibodies targeting VEGF or the VEGF pathway that have been evaluated for efficacy in cancer, including the only anti-angiogenic monoclonal antibody approved by the FDA, bevacizumab (Genentech/Roche) (See Chapter One or (Sullivan and Brekken, 2010)). Here we characterized r84 (AT001, Affitech A/S), a fully human monoclonal antibody that recognizes mouse and human VEGF and blocks VEGF from binding and signaling through VEGFR2. r84 can block VEGF induced signaling and migration of endothelial cells through VEGFR2 and controls tumor growth, angiogenesis and lymphangiogenesis *in vivo*. Importantly, r84 does not induce the significant liver, kidney or heart toxicities that are seen with bevacizumab, rendering r84 as a safe and highly efficacious therapy that has great clinical potential.

To evaluate tumor-derived mediators of resistance to anti-VEGF monoclonal antibodies, we treated 12 NSCLC cell lines with bevacizumab or r84 *in vivo*. From these animal experiments, we discovered that NSCLC response to anti-VEGF is dependent on cell line and therapy. Three lines displayed intrinsic resistance to bevacizumab (Calu-6, A549, Calu-3), two lines expressed intrinsic

resistance to r84 (H1155, H1395). Although there were no cell lines that were intrinsically resistant to bevacizumab and r84, there were lines with sensitivity to both therapies. There were no obvious relationships between oncogenotype, histology, source or gender of our 12 NSCLC cell lines and resistance to therapy; therefore we performed a number of arrays to gather more information on the genetic and proteomic signatures of these lines. We have compiled the largest dataset to our knowledge on *in vivo* response of NSCLC to anti-VEGF monoclonal antibodies, tumor expression of angiogenic growth factors, angiogenic inhibitors and cytokines, microarray and RPPA of the 12 lines grown *in vitro* and as xenografts. These datasets are an excellent source of information and can continue to be analyzed in the future to identify mediators of resistance to therapy and other pathways involved in NSCLC tumor growth and progression.

Using these datasets, we identified that the receptor tyrosine kinase Axl has increased expression in tumors that are intrinsically resistant as compared to sensitive to bevacizumab therapy. Although knockdown of Axl expression by shRNAmir controls A549 tumor growth *in vivo*, it does not increase sensitivity of tumors to bevacizumab. In addition, treatment with the anti-human Axl monoclonal antibody 10C9 does not control Calu-6 or Calu-3 tumor growth as a single agent therapy or in combination with bevacizumab. Although there are remaining questions on the efficacy of 10C9 at functionally blocking Axl activity, at this time it appears that Axl does not play a significant role in mediating

intrinsic resistance to bevacizumab. Even so, this finding does not detract from the immense source of data we have generated and that is available for further studies.

## 6.2 Future directions

We initially designed our *in vivo* tumor experiments to identify tumors that had intrinsic resistance or sensitivity to r84 or bevacizumab. However, the development of evasive resistance is a critical problem of anti-angiogenic therapies in the clinic and warrants future investigation. To this end, we have begun to develop models of evasive resistance of NSCLC to bevacizumab and r84. Briefly, we injected NOD/SCID mice with 2.5 million NSCLC cells subcutaneously that were previously identified to have intrinsic sensitivity to bevacizumab and r84, H1975, H1993 and H2073. As done in our previous experiments, animals were treated starting one day post tumor cell injection with 50 mg/kg/week control IgG, r84 or 25 mg/kg/week bevacizumab. When the tumors in control-treated animals reached approximately 1000 $mm^3$, this group was sacrificed, but therapy continued in r84 and bevacizumab groups. As individual anti-VEGF-treated tumors reached 1000 $mm^3$, they were sacrificed and their tumors were harvested and cultured *ex vivo* to generate tumor cell lines that were evasively resistant to therapy (Figure 6.1 – Figure 6.3). We have created at least three cell lines with evasive resistance to bevacizumab or r84 for H1975,

H1993 and H2073. One of these lines, H1975-81 was generated following extended r84 therapy and was subsequently re-injected into NOD/SCID mice and treated as indicated previously. Interestingly, tumor growth was accelerated as compared to parental H1975 and tumors had lost their sensitivity to r84 and to a lesser extent, bevacizumab (Figure 6.4, T/C 0.66 and 0.38, respectively).

To determine if enhanced growth and resistance was due to extended therapy or *ex vivo* culture, we treated H1975-, H1993- and H2073-tumor bearing mice with saline until tumors reached 1000 $mm^3$, at which time mice were sacrificed and their tumors harvested and cultured *ex vivo*. Subsequent re-injection demonstrated similar growth curves and anti-VEGF sensitivity to parental lines (Figure 6.5 – Figure 6.7). Therefore, the changes we observed in H1975-81 tumor growth appear to be as a direct result of extended r84 therapy. Further analysis of other *ex vivo* cultured cell lines is required to verify these findings and molecular and genetic profiling of these tumors could help identify mediators of resistance. H1975-81 control IgG-, r84- and bevacizumab-treated tumors were included in the *in vivo* microarray and RPPA described in Chapter Five and although this dataset is small, can be analyzed for preliminary expression differences. In addition, it would be interesting to evaluate if tumor microvessel density is reduced and if angiogenic growth factor switching is occurring in this model. It would be very exciting if either of these parameters were similar to our intrinsic resistance model, where we observe that we are

hitting the target therapeutically (as indicated by a reduction in tumor microvessel density) but have little evidence to suggest that the angiogenic driver in our tumors has switched from VEGF to another growth factor. Thus the results of these experiments could potentially change one mechanism of anti-angiogenic resistance in NSCLC and could lead to the elucidation of novel ways that tumors can defy anti-angiogenic treatment.

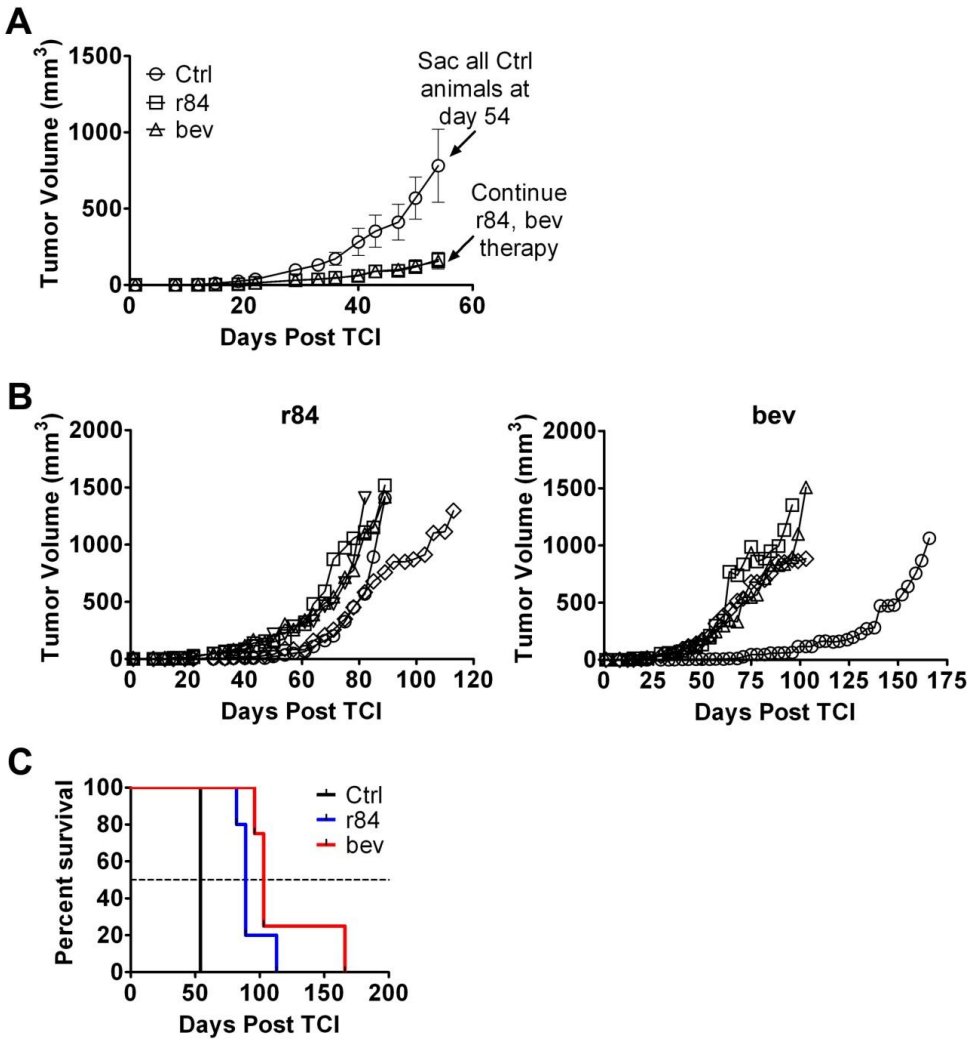


**Figure 6.1: Generation of evasive resistance of H1975 tumors to r84 and bevacizumab.**

Similar to previous experiments, NOD/SCID mice were injected subcutaneously with 2.5 million H1975 tumor cells and treated with control IgG, r84 or bevacizumab. Control-treated tumors were sacrificed when average tumor volume reached ~1000 $mm^3$. Therapy continued with r84 and bev and tumors were individually sacrificed once they reached tumor volumes of 1500 $mm^3$ and were cultured *ex vivo* to generate separate lines representing evasively-resistant tumors.

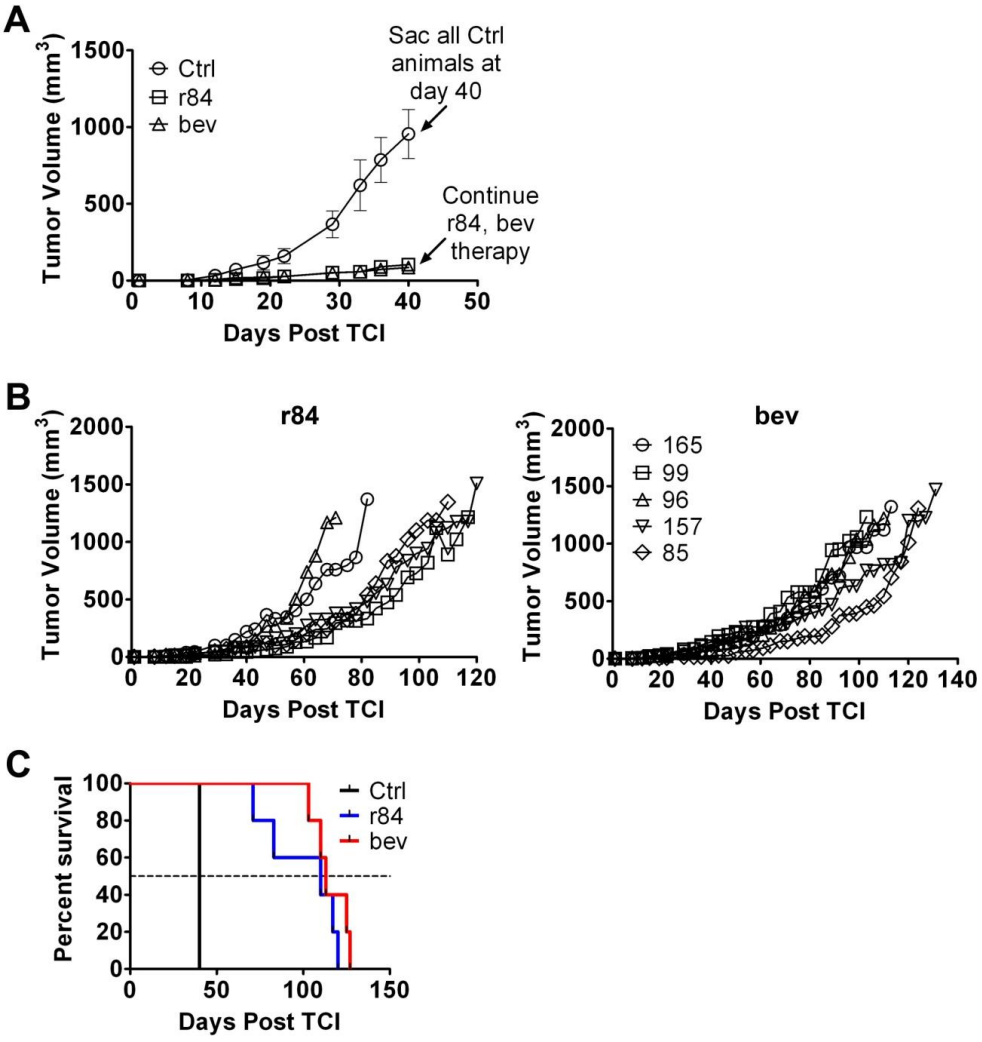


**Figure 6.2: Generation of evasive resistance of H1993 tumors to r84 and bevacizumab.**

Similar to previous experiments, NOD/SCID mice were injected subcutaneously with 2.5 million H1993 tumor cells and treated with control IgG, r84 or bevacizumab. Control-treated tumors were sacrificed when average tumor volume reached ~1000 $mm^3$. Therapy continued with r84 and bev and tumors were individually sacrificed once they reached tumor volumes of 1500 $mm^3$ and were cultured *ex vivo* to generate separate lines representing evasively-resistant tumors.

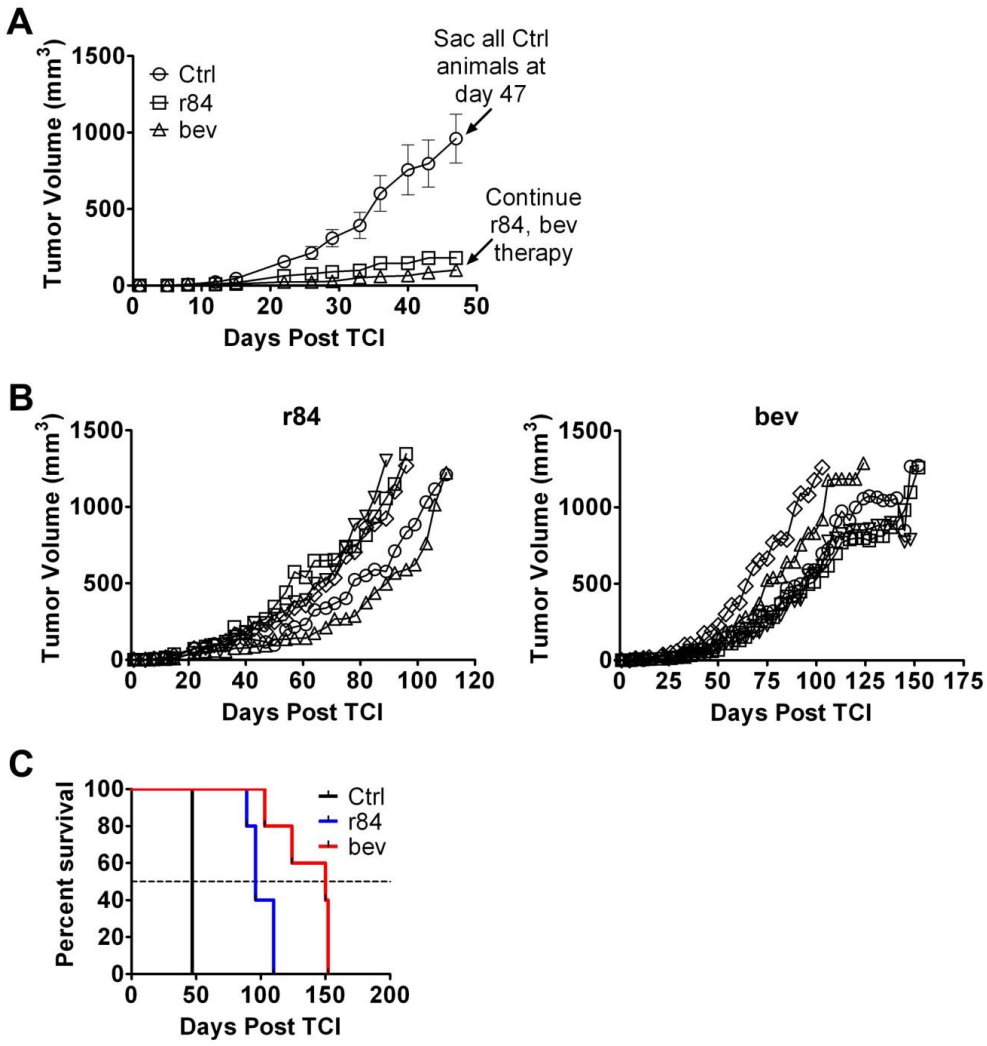


**Figure 6.3: Generation of evasive resistance of H2073 tumors to r84 and bevacizumab.**

Similar to previous experiments, NOD/SCID mice were injected subcutaneously with 2.5 million H2073 tumor cells and treated with control IgG, r84 or bevacizumab. Control-treated tumors were sacrificed when average tumor volume reached ~1000 $mm^3$. Therapy continued with r84 and bev and tumors were individually sacrificed once they reached tumor volumes of 1500 $mm^3$ and were cultured *ex vivo* to generate separate lines representing evasively-resistant tumors.

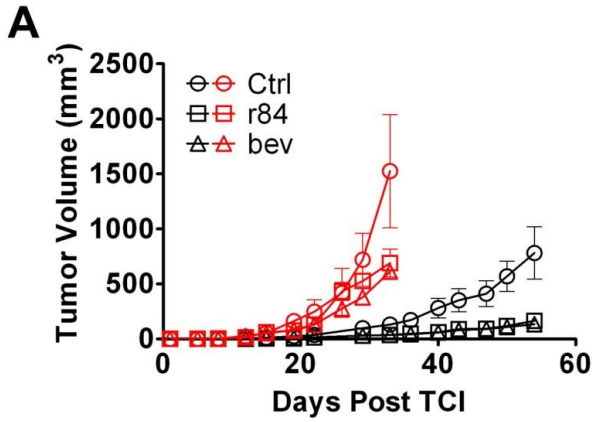


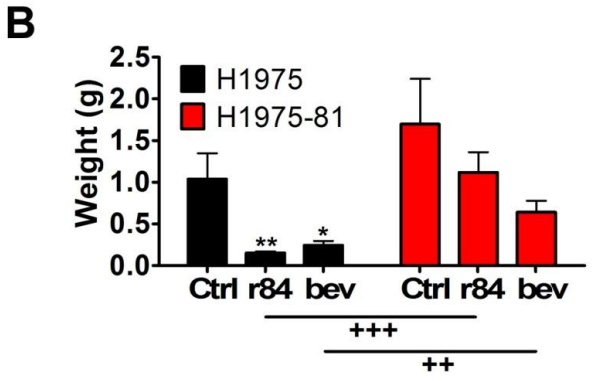


| Cell Line | Therapy | T/C Ratio |
|---|---|---|
| H1975 | r84 | 0.16 |
| | bev | 0.24 |
| H1975-81 | r84 | 0.66 |
| | bev | 0.38 |

**Figure 6.4: Extended r84 therapy in H1975 tumor bearing mice can generate a cell line that displays enhanced resistance to r84 and bevacizumab**.

*Ex vivo* cultured H1975 tumors that grew out following extended therapy (H1975-81) with r84 were re-implanted into NOD/SCID mice (2.5 million cells/ mouse) and treated with control IgG, r84 or bevacizumab. Unlike parental H1975 cells, H1975-81 displays enhanced resistance to both r84 and bevacizumab as indicated by tumor growth curves (**A**) and final tumor weights (**B**).

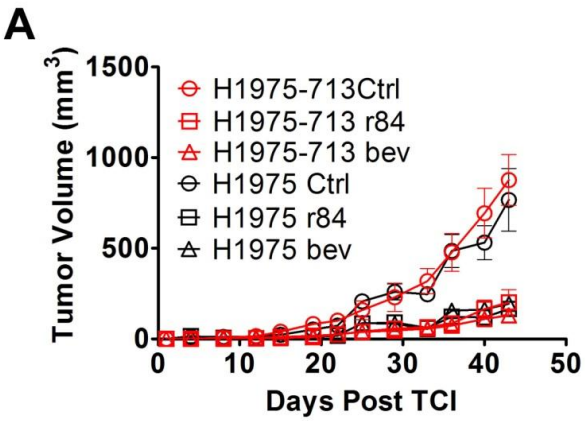


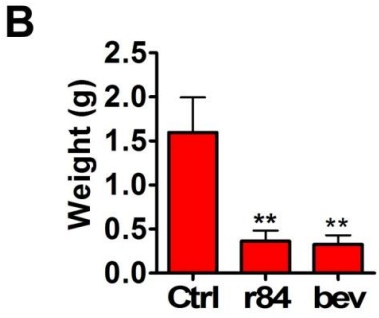


C

| Cell Line | Therapy | T/C Ratio |
|---|---|---|
| H1975 | r84 | 0.16 |
| | bev | 0.24 |
| H1975-713 | r84 | 0.23 |
| | bev | 0.20 |

**Figure 6.5:** ***Ex vivo*** **culture of H1975 does not enhance tumorigenicity or anti-VEGF resistance.**

*Ex vivo* culture of saline-treated H1975 tumor (H1975-713) was re-implanted into NOD/SCID mice (2.5 million cells/ mouse) and treated with control IgG, r84 or bevacizumab. H1975-713 grew similarly to parental H1975 cells and did not display enhanced resistance to r84 or bevacizumab as indicated by tumor growth curves (**A**), final tumor weights (**B**) or T/C ratios (**C**).

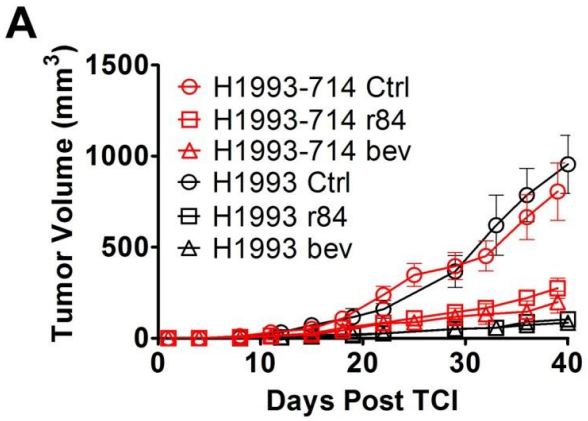


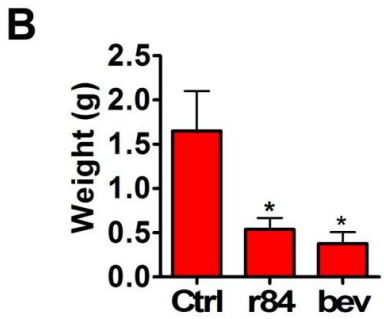


C

| Cell Line | Therapy | T/C Ratio |
|---|---|---|
| H1993 | r84 | 0.27 |
| | bev | 0.17 |
| H1993-714 | r84 | 0.33 |
| | bev | 0.23 |

**Figure 6.6:** ***Ex vivo*** **culture of H1993 does not enhance tumorigenicity or anti-VEGF resistance.**

*Ex vivo* culture of saline-treated H1993 tumor (H1975-714) was re-implanted into NOD/SCID mice (2.5 million cells/ mouse) and treated with control IgG, r84 or bevacizumab. H1993-714 grew similarly to parental H1993 cells and did not display enhanced resistance to r84 or bevacizumab as indicated by tumor growth curves (**A**), final tumor weights (**B**) or T/C ratios (**C**).

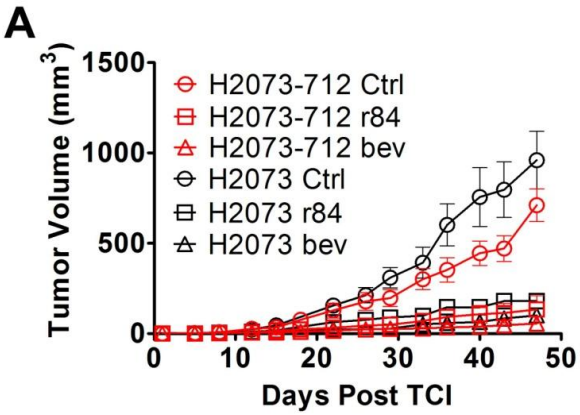


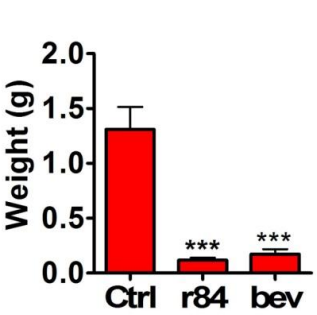


C

| Cell Line | Therapy | T/C Ratio |
|---|---|---|
| H2073 | r84 | 0.11 |
| | bev | 0.10 |
| H2073-712 | r84 | 0.10 |
| | bev | 0.15 |

**Figure 6.7:** ***Ex vivo*** **culture of H2073 does not enhance tumorigenicity or anti-VEGF resistance.**

*Ex vivo* culture of saline-treated H2073 tumor (H2073-712) was re-implanted into NOD/SCID mice (2.5 million cells/ mouse) and treated with control IgG, r84 or bevacizumab. H2073-712 grew similarly to parental H2073 cells and did not display enhanced resistance to r84 or bevacizumab as indicated by tumor growth curves (**A**), final tumor weights (**B**) or T/C ratios (**C**).

# Appendix A: List of SABiosciences qPCR primer sets

| Position | Unigene | GeneBank | Symbol | Description | Gene Name |
|---|---|---|---|---|---|
| A01 | Hs.634849 | NM_018046 | AGGF1 | Angiogenic factor with G patch and FHA domains 1 | FLJ10283, GPATC7, GPATCH7, HSU84971, HUS84971, VG5Q |
| A02 | Hs.528051 | NM_133265 | AMOT | Angiomotin | KIAA1071 |
| A03 | Hs.283749 | NM_001145 | ANG | Angiogenin, ribonuclease, RNase A family, 5 | ALS9, HEL168, MGC22466, MGC71966, RNASE4, RNASE5 |
| A04 | Hs.369675 | NM_001146 | ANGPT1 | Angiopoietin 1 | AGP1, AGPT, ANG1 |
| A05 | Hs.583870 | NM_001147 | ANGPT2 | Angiopoietin 2 | AGPT2, ANG2 |
| A06 | Hs.591474 | NM_004673 | ANGPTL1 | Angiopoietin-like 1 | ANG3, ANGPT3, ARP1, AngY, KIAA0351, UNQ162, dJ595C2.2 |
| A07 | Hs.194654 | NM_001702 | BAI1 | Brain-specific angiogenesis inhibitor 1 | FLJ41988, GDAIF |
| A08 | Hs.73853 | NM_001200 | BMP2 | Bone morphogenetic protein 2 | BMP2A |
| A09 | Hs.255935 | NM_001731 | BTG1 | B-cell translocation gene 1, anti-proliferative | |
| A10 | Hs.272493 | NM_032965 | CCL15 | Chemokine (C-C motif) ligand 15 | HCC-2, HMRP-2B, LKN1, Lkn-1, MIP-1d, MIP-5, NCC-3, NCC3, SCYA15, SCYL3, SY15 |
| A11 | Hs.303649 | NM_002982 | CCL2 | Chemokine (C-C motif) ligand 2 | GDCF-2, HC11, HSMCR30, MCAF, MCP-1, MCP1, MGC9434, SCYA2, SMC-CF |
| A12 | Hs.126517 | NM_000574 | CD55 | CD55 molecule, decay accelerating factor for complement (Cromer blood group) | CR, CROM, DAF, TC |

| Position | Unigene | GeneBank | Symbol | Description | Gene Name |
|---|---|---|---|---|---|
| B01 | Hs.278573 | NM_000611 | CD59 | CD59 molecule, complement regulatory protein | 16.3A5, 1F5, EJ16, EJ30, EL32, FLJ38134, FLJ92039, G344, HRF-20, HRF20, MAC-IP, MACIF, MEM43, MGC2354, MIC11, MIN1, MIN2, MIN3, MIRL, MSK21, p18-20 |
| B02 | Hs.150793 | NM_001275 | CHGA | Chromogranin A (parathyroid secretory protein 1) | CGA |
| B03 | Hs.517356 | NM_030582 | COL18A1 | Collagen, type XVIII, alpha 1 | FLJ27325, FLJ34914, KNO, KNO1, MGC74745 |
| B04 | Hs.570065 | NM_000091 | COL4A3 | Collagen, type IV, alpha 3 (Goodpasture antigen) | |
| B05 | Hs.2233 | NM_000759 | CSF3 | Colony stimulating factor 3 (granulocyte) | G-CSF, GCSF, MGC45931 |
| B06 | Hs.632586 | NM_001565 | CXCL10 | Chemokine (C-X-C motif) ligand 10 | C7, IFI10, INP10, IP-10, SCYB10, crg-2, gIP-10, mob-1 |
| B07 | Hs.632592 | NM_005409 | CXCL11 | Chemokine (C-X-C motif) ligand 11 | H174, I-TAC, IP-9, IP9, MGC102770, SCYB11, SCYB9B, b-R1 |
| B08 | Hs.522891 | NM_000609 | CXCL12 | Chemokine (C-X-C motif) ligand 12 (stromal cell-derived factor 1) | PBSF, SCYB12, SDF-1a, SDF-1b, SDF1, SDF1A, SDF1B, TLSF-a, TLSF-b, TPAR1 |
| B09 | Hs.100431 | NM_006419 | CXCL13 | Chemokine (C-X-C motif) ligand 13 | ANGIE, ANGIE2, BCA-1, BCA1, BLC, BLR1L, SCYB13 |
| B10 | Hs.483444 | NM_004887 | CXCL14 | Chemokine (C-X-C motif) ligand 14 | BMAC, BRAK, KS1, Kec, MGC10687, MIP-2g, NJAC, SCYB14, bolekine |
| B11 | Hs.590921 | NM_002089 | CXCL2 | Chemokine (C-X-C motif) ligand 2 | CINC-2a, GRO2, GROb, MGSA-b, MIP-2a, MIP2, MIP2A, SCYB2 |
| B12 | Hs.89690 | NM_002090 | CXCL3 | Chemokine (C-X-C motif) ligand 3 | CINC-2b, GRO3, GROg, MIP-2b, MIP2B, SCYB3 |

| Position | Unigene | GeneBank | Symbol | Description | Gene Name |
|---|---|---|---|---|---|
| C01 | Hs.89714 | NM_002994 | CXCL5 | Chemokine (C-X-C motif) ligand 5 | ENA-78, SCYB5 |
| C02 | Hs.164021 | NM_002993 | CXCL6 | Chemokine (C-X-C motif) ligand 6 (granulocyte chemotactic protein 2) | CKA-3, GCP-2, GCP2, SCYB6 |
| C03 | Hs.77367 | NM_002416 | CXCL9 | Chemokine (C-X-C motif) ligand 9 | CMK, Humig, MIG, SCYB9, crg-10 |
| C04 | Hs.592212 | NM_001953 | TYMP | Thymidine phosphorylase | ECGF1, MNGIE, PDECGF, TP, hPD-ECGF |
| C05 | Hs.482730 | NM_005711 | EDIL3 | EGF-like repeats and discoidin I-like domains 3 | DEL1, MGC26287 |
| C06 | Hs.115263 | NM_001432 | EREG | Epiregulin | ER |
| C07 | Hs.483635 | NM_000800 | FGF1 | Fibroblast growth factor 1 (acidic) | AFGF, ECGF, ECGF-beta, ECGFA, ECGFB, FGF-alpha, FGFA, GLIO703, HBGF1 |
| C08 | Hs.6540 | NM_004114 | FGF13 | Fibroblast growth factor 13 | FGF2, FHF-2, FHF2 |
| C09 | Hs.284244 | NM_002006 | FGF2 | Fibroblast growth factor 2 (basic) | BFGF, FGFB, HBGF-2 |
| C10 | Hs.1690 | NM_005130 | FGFBP1 | Fibroblast growth factor binding protein 1 | FGFBP, HBP17 |
| C11 | Hs.11392 | NM_004469 | FIGF | C-fos induced growth factor (vascular endothelial growth factor D) | VEGF-D, VEGFD |
| C12 | Hs.203717 | NM_002026 | FN1 | Fibronectin 1 | CIG, DKFZp686F10164, DKFZp686H0342, DKFZp686I1370, DKFZp686O13149, ED-B, FINC, FN, FNZ, GFND, GFND2, LETS, MSF |

| Position | Unigene | GeneBank | Symbol | Description | Gene Name |
|---|---|---|---|---|---|
| D01 | Hs.9914 | NM_006350 | FST | Follistatin | FS |
| D02 | Hs.514220 | NM_002087 | GRN | Granulin | GEP, GP88, PCDGF, PEPI, PGRN |
| D03 | Hs.153444 | NM_002091 | GRP | Gastrin-releasing peptide | BN, GRP-10, preproGRP, proGRP |
| D04 | Hs.396530 | NM_000601 | HGF | Hepatocyte growth factor (hepapoietin A; scatter factor) | F-TCF, HGFB, HPTA, SF |
| D05 | Hs.37026 | NM_024013 | IFNA1 | Interferon, alpha 1 | IFL, IFN, IFN-ALPHA, IFNA13, IFNA@, MGC138207, MGC138505, MGC138507 |
| D06 | Hs.93177 | NM_002176 | IFNB1 | Interferon, beta 1, fibroblast | IFB, IFF, IFNB, MGC96956 |
| D07 | Hs.856 | NM_000619 | IFNG | Interferon, gamma | IFG, IFI |
| D08 | Hs.193717 | NM_000572 | IL10 | Interleukin 10 | CSIF, IL-10, IL10A, MGC126450, MGC126451, TGIF |
| D09 | Hs.673 | NM_000882 | IL12A | Interleukin 12A (natural killer cell stimulatory factor 1, cytotoxic lymphocyte maturation factor 1, p35) | CLMF, IL-12A, NFSK, NKSF1, P35 |
| D10 | Hs.674 | NM_002187 | IL12B | Interleukin 12B (natural killer cell stimulatory factor 2, cytotoxic lymphocyte maturation factor 2, p40) | CLMF, CLMF2, IL-12B, NKSF, NKSF2 |
| D11 | Hs.272295 | NM_052872 | IL17F | Interleukin 17F | IL-17F, ML-1, ML1 |
| D12 | Hs.654458 | NM_000600 | IL6 | Interleukin 6 (interferon, beta 2) | BSF2, HGF, HSF, IFNB2, IL-6 |

| Position | Unigene | GeneBank | Symbol | Description | Gene Name |
|---|---|---|---|---|---|
| E01 | Hs.624 | NM_000584 | IL8 | Interleukin 8 | CXCL8, GCP-1, GCP1, LECT, LUCT, LYNAP, MDNCF, MONAP, NAF, NAP-1, NAP1 |
| E02 | Hs.1048 | NM_003994 | KITLG | KIT ligand | DKFZp686F2250, KL-1, Kitl, MGF, SCF, SF, SHEP7 |
| E03 | Hs.171995 | NM_001648 | KLK3 | Kallikrein-related peptidase 3 | APS, KLK2A1, PSA, hK3 |
| E04 | Hs.194236 | NM_000230 | LEP | Leptin | FLJ94114, OB, OBS |
| E05 | Hs.82045 | NM_002391 | MDK | Midkine (neurite growth-promoting factor 2) | FLJ27379, MK, NEGF2 |
| E06 | Hs.584654 | NM_005938 | FOXO4 | Forkhead box O4 | AFX, AFX1, MGC120490, MLLT7 |
| E07 | Hs.219140 | NM_002521 | NPPB | Natriuretic peptide precursor B | BNP |
| E08 | Hs.490330 | NM_000906 | NPR1 | Natriuretic peptide receptor A/guanylate cyclase A (atrionatriuretic peptide receptor A) | ANPRA, ANPa, GUC2A, GUCY2A, NPRA |
| E09 | Hs.1976 | NM_002608 | PDGFB | Platelet-derived growth factor beta polypeptide (simian sarcoma viral (v-sis) oncogene homolog) | FLJ12858, PDGF2, SIS, SSV, c-sis |
| E10 | Hs.352298 | NM_025208 | PDGFD | Platelet derived growth factor D | IEGF, MGC26867, MSTP036, SCDGF-B, SCDGFB |
| E11 | Hs.81564 | NM_002619 | PF4 | Platelet factor 4 | CXCL4, MGC138298, SCYB4 |
| E12 | Hs.252820 | NM_002632 | PGF | Placental growth factor | D12S1900, PGFL, PLGF, PlGF-2, SHGC-10760 |

| Position | Unigene | GeneBank | Symbol | Description | Gene Name |
|---|---|---|---|---|---|
| F01 | Hs.143436 | NM_000301 | PLG | Plasminogen | DKFZp779M0222 |
| F02 | Hs.2164 | NM_002704 | PPBP | Pro-platelet basic protein (chemokine (C-X-C motif) ligand 7) | B-TG1, Beta-TG, CTAP-III, CTAP3, CTAPIII, CXCL7, LA-PF4, LDGF, MDGF, NAP-2, PBP, SCYB7, TC1, TC2, TGB, TGB1, THBGB, THBGB1 |
| F03 | Hs.1905 | NM_000948 | PRL | Prolactin | |
| F04 | Hs.514793 | NM_032414 | PROK1 | Prokineticin 1 | EGVEGF, PK1, PRK1 |
| F05 | Hs.371249 | NM_002825 | PTN | Pleiotrophin | HARP, HBGF8, HBNF, NEGF1 |
| F06 | Hs.502876 | NM_004040 | RHOB | Ras homolog gene family, member B | ARH6, ARHB, MST081, MSTP081, RHOH6 |
| F07 | Hs.530687 | NM_002939 | RNH1 | Ribonuclease/angiogenin inhibitor 1 | MGC18200, MGC4569, MGC54054, RAI, RNH |
| F08 | Hs.149261 | NM_001754 | RUNX1 | Runt-related transcription factor 1 | AML1, AML1-EVI-1, AMLCR1, CBFA2, EVI-1, PEBP2aB |
| F09 | Hs.75599 | NM_000488 | SERPINC1 | Serpin peptidase inhibitor, clade C (antithrombin), member 1 | AT3, ATIII, MGC22579 |
| F10 | Hs.414795 | NM_000602 | SERPINE1 | Serpin peptidase inhibitor, clade E (nexin, plasminogen activator inhibitor type 1), member 1 | PAI, PAI-1, PAI1, PLANH1 |
| F11 | Hs.532768 | NM_002615 | SERPINF1 | Serpin peptidase inhibitor, clade F (alpha-2 antiplasmin, pigment epithelium derived factor), member 1 | EPC-1, PEDF, PIG35 |
| F12 | Hs.331555 | NM_006846 | SPINK5 | Serine peptidase inhibitor, Kazal type 5 | DKFZp686K19184, FLJ21544, FLJ97536, FLJ97596, FLJ99794, LEKTI, LETKI, NETS, NS, VAKTI |

| Position | Unigene | GeneBank | Symbol | Description | Gene Name |
|---|---|---|---|---|---|
| G01 | Hs.301989 | NM_015136 | STAB1 | Stabilin 1 | CLEVER-1, FEEL-1, FELE-1, FEX1, KIAA0246, STAB-1 |
| G02 | Hs.170009 | NM_003236 | TGFA | Transforming growth factor, alpha | TFGA |
| G03 | Hs.645227 | NM_000660 | TGFB1 | Transforming growth factor, beta 1 | CED, DPD1, TGFB, TGFbeta |
| G04 | Hs.164226 | NM_003246 | THBS1 | Thrombospondin 1 | THBS, THBS-1, TSP, TSP-1, TSP1 |
| G05 | Hs.78824 | NM_005424 | TIE1 | Tyrosine kinase with immunoglobulin-like and EGF-like domains 1 | JTK14, TIE |
| G06 | Hs.522632 | NM_003254 | TIMP1 | TIMP metallopeptidase inhibitor 1 | CLGI, EPA, EPO, FLJ90373, HCI, TIMP |
| G07 | Hs.633514 | NM_003255 | TIMP2 | TIMP metallopeptidase inhibitor 2 | CSC-21K |
| G08 | Hs.644633 | NM_000362 | TIMP3 | TIMP metallopeptidase inhibitor 3 | HSMRK222, K222, K222TA2, SFD |
| G09 | Hs.241570 | NM_000594 | TNF | Tumor necrosis factor (TNF superfamily, member 2) | DIF, TNF-alpha, TNFA, TNFSF2 |
| G10 | Hs.523403 | NM_003282 | TNNI2 | Troponin I type 2 (skeletal, fast) | AMCD2B, DA2B, FSSV, fsTnI |
| G11 | Hs.644596 | NM_000363 | TNNI3 | Troponin I type 3 (cardiac) | CMD2A, CMH7, MGC116817, RCM1, TNNC1, cTnI |
| G12 | Hs.73793 | NM_003376 | VEGFA | Vascular endothelial growth factor A | MGC70609, MVCD1, VEGF, VEGF-A, VPF |

| Position | Unigene | GeneBank | Symbol | Description | Gene Name |
|---|---|---|---|---|---|
| H01 | Hs.534255 | NM_004048 | B2M | Beta-2-microglobulin | |
| H02 | Hs.412707 | NM_000194 | HPRT1 | Hypoxanthine phosphoribosyltransferase 1 | HGPRT, HPRT |
| H03 | Hs.523185 | NM_012423 | RPL13A | Ribosomal protein L13a | |
| H04 | Hs.592355 | NM_002046 | GAPDH | Glyceraldehyde-3-phosphate dehydrogenase | G3PD, GAPD, MGC88685 |
| H05 | Hs.520640 | NM_001101 | ACTB | Actin, beta | PS1TP5BP1 |
| H06 | N/A | SA_00105 | HGDC | Human Genomic DNA Contamination | HIGX1A |
| H07 | N/A | SA_00104 | RTC | Reverse Transcription Control | RTC |
| H08 | N/A | SA_00104 | RTC | Reverse Transcription Control | RTC |
| H09 | N/A | SA_00104 | RTC | Reverse Transcription Control | RTC |
| H10 | N/A | SA_00103 | PPC | Positive PCR Control | PPC |
| H11 | N/A | SA_00103 | PPC | Positive PCR Control | PPC |
| H12 | N/A | SA_00103 | PPC | Positive PCR Control | PPC |

## Appendix B: SABiosciences qPCR raw $C_t$ values

| | H1993 T653 | H1993 T449 | H1975 T314 | H1975 T453 | H1975 T671 | H2073 449 | H2073 370 | H2073 266 | Calu-6 265 | Calu-6 270 | Calu-6 397 |
|---|---|---|---|---|---|---|---|---|---|---|---|
| AGGF1 | 22.52 | 22.33 | 21.09 | 21.14 | 21.68 | 21.73 | 21.08 | 21.41 | 21.89 | 21.97 | 21.60 |
| AMOT | 38.47 | 34.91 | 29.33 | 31.48 | 30.19 | 30.80 | 30.13 | 28.51 | 26.74 | 26.11 | 26.41 |
| ANG | 26.57 | 26.77 | 23.23 | 25.09 | 23.58 | 23.14 | 22.36 | 23.09 | 23.88 | 23.28 | 23.39 |
| ANGPT1 | 29.46 | 29.36 | 26.90 | 27.31 | 27.11 | 26.57 | 25.65 | 25.68 | 23.13 | 23.34 | 23.35 |
| ANGPT2 | 26.93 | 27.94 | 25.44 | 25.26 | 26.11 | 25.78 | 25.00 | 25.13 | 22.65 | 22.35 | 22.82 |
| ANGPTL1 | 25.74 | 25.66 | 24.98 | 25.09 | 26.42 | 24.26 | 23.82 | 24.02 | 22.56 | 22.68 | 22.46 |
| BAI1 | 32.43 | 35.44 | 28.04 | 29.29 | 28.17 | 26.31 | 25.05 | 24.96 | 24.80 | 24.51 | 24.15 |
| BMP2 | 23.05 | 23.24 | 23.33 | 24.02 | 23.86 | 21.52 | 20.66 | 21.55 | 25.87 | 25.25 | 25.50 |
| BTG1 | 17.81 | 17.20 | 16.98 | 18.30 | 18.10 | 17.10 | 16.82 | 17.58 | 18.29 | 18.20 | 18.23 |
| CCL15 | 39.22 | Undet. | 39.93 | Undet. | Undet. | 27.07 | 25.83 | 26.11 | 26.75 | 25.80 | 26.05 |
| CCL2 | 33.46 | 33.10 | 26.09 | 27.44 | 27.37 | 22.83 | 22.14 | 22.08 | 26.05 | 25.05 | 24.79 |
| CD55 | 19.47 | 18.62 | 20.74 | 20.60 | 21.32 | 16.14 | 15.77 | 16.50 | 21.39 | 21.39 | 21.80 |
| CD59 | 18.52 | 18.01 | 17.11 | 18.06 | 17.88 | 18.18 | 17.24 | 17.92 | 18.78 | 18.40 | 18.40 |
| CHGA | 31.54 | 32.01 | 30.43 | 30.74 | 32.08 | 30.45 | 28.58 | 29.20 | 22.46 | 22.48 | 22.49 |
| COL18A1 | 26.07 | 25.58 | 23.31 | 24.07 | 24.27 | 23.33 | 22.56 | 23.11 | 21.34 | 21.15 | 21.16 |
| COL4A3 | 25.77 | 25.73 | 29.00 | 28.73 | 29.08 | 24.15 | 23.65 | 24.30 | 24.23 | 24.60 | 24.68 |
| CSF3 | 34.40 | 30.94 | 23.95 | 21.31 | 22.47 | 31.21 | 31.03 | 30.08 | 30.19 | 29.65 | 29.89 |
| CXCL10 | Undet. | 32.24 | 20.71 | 22.07 | 21.57 | 29.09 | 27.43 | 27.35 | 24.91 | 25.12 | 25.08 |
| CXCL11 | 31.66 | Undet. | 21.32 | 22.08 | 21.64 | 26.97 | 26.42 | 26.57 | 24.24 | 25.14 | 25.32 |
| CXCL12 | 30.50 | 28.60 | 28.31 | 28.35 | 27.75 | 28.09 | 27.16 | 27.08 | 26.31 | 25.01 | 24.58 |
| CXCL13 | 39.56 | 36.29 | 29.24 | 31.52 | 30.13 | 30.04 | 29.18 | 27.90 | 25.82 | 25.12 | 24.93 |
| CXCL14 | 35.12 | 33.85 | 26.88 | 29.56 | 28.33 | 28.44 | 28.31 | 27.26 | 24.84 | 24.35 | 24.40 |
| CXCL2 | 27.32 | 25.50 | 20.70 | 20.35 | 20.99 | 21.07 | 20.33 | 20.88 | 25.82 | 25.99 | 26.03 |
| CXCL3 | 28.15 | 26.15 | 20.85 | 20.45 | 21.34 | 21.58 | 20.84 | 21.24 | 24.05 | 24.36 | 24.45 |

| | H1993 T653 | H1993 T449 | H1975 T314 | H1975 T453 | H1975 T671 | H2073 449 | H2073 370 | H2073 266 | Calu-6 265 | Calu-6 270 | Calu-6 397 |
|---|---|---|---|---|---|---|---|---|---|---|---|
| CXCL5 | 36.36 | 31.32 | 21.30 | 21.07 | 21.51 | 31.11 | 31.01 | 29.43 | 25.71 | 26.10 | 26.21 |
| CXCL6 | 35.27 | 36.49 | 19.69 | 20.15 | 20.33 | 31.30 | 30.06 | 29.32 | 25.39 | 25.14 | 25.13 |
| CXCL9 | 39.29 | 37.35 | 26.03 | 27.24 | 27.65 | 35.22 | Undet. | 30.96 | 25.64 | 25.80 | 25.92 |
| TYMP | 23.03 | 21.35 | 20.10 | 20.58 | 20.81 | 21.29 | 20.25 | 20.70 | 24.01 | 24.06 | 23.82 |
| EDIL3 | 25.15 | 25.80 | 20.50 | 20.85 | 21.70 | 23.04 | 22.42 | 23.19 | 24.02 | 24.76 | 24.58 |
| EREG | 20.33 | 20.45 | 21.35 | 20.11 | 21.34 | 20.07 | 19.55 | 20.01 | 21.76 | 21.38 | 21.11 |
| FGF1 | 29.34 | 29.59 | 25.35 | 25.81 | 25.65 | 26.40 | 26.02 | 25.52 | 23.92 | 24.05 | 23.62 |
| FGF13 | 33.45 | 31.02 | 25.07 | 25.24 | 25.66 | 28.09 | 29.15 | 28.41 | 20.46 | 21.08 | 20.82 |
| FGF2 | 25.39 | 24.80 | 24.63 | 24.61 | 24.98 | 22.50 | 22.27 | 22.67 | 22.51 | 22.41 | 23.05 |
| FGFBP1 | 23.82 | 22.14 | 25.29 | 23.30 | 25.22 | 22.73 | 22.17 | 22.79 | 27.04 | 26.90 | 26.59 |
| FIGF | 28.06 | 29.02 | 29.31 | 28.96 | 29.16 | 27.20 | 26.93 | 27.43 | 26.08 | 26.03 | 26.24 |
| FN1 | 15.89 | 15.51 | 14.10 | 15.11 | 14.82 | 20.73 | 20.96 | 21.18 | 18.16 | 17.19 | 17.82 |
| FST | 25.11 | 23.59 | 22.92 | 21.31 | 23.50 | 19.78 | 19.28 | 20.13 | 19.79 | 20.10 | 20.31 |
| GRN | 21.13 | 20.06 | 19.20 | 20.20 | 19.79 | 19.95 | 19.43 | 20.12 | 21.28 | 21.06 | 21.20 |
| GRP | Undet. | 31.71 | Undet. | Undet. | 31.40 | 34.16 | 31.55 | 29.05 | 25.99 | 26.38 | 26.58 |
| HGF | 30.08 | 32.01 | 26.89 | 27.46 | 27.21 | 25.56 | 25.45 | 26.03 | 23.81 | 24.40 | 24.34 |
| IFNA1 | 29.38 | 29.02 | 26.71 | 26.12 | 28.07 | 26.34 | 25.63 | 25.59 | 25.73 | 25.42 | 25.40 |
| IFNB1 | 32.57 | 33.26 | 28.45 | 28.69 | 28.54 | 30.73 | 28.40 | 27.22 | 26.81 | 26.03 | 25.81 |
| IFNG | 28.45 | 28.57 | 30.85 | 31.04 | 30.90 | 28.19 | 26.99 | 26.17 | 24.36 | 24.72 | 24.82 |
| IL10 | 33.20 | 33.57 | 29.97 | 34.70 | 30.19 | 29.95 | 29.46 | 28.41 | 26.07 | 25.73 | 25.89 |
| IL12A | 28.61 | 27.02 | 25.63 | 24.63 | 25.37 | 25.97 | 25.21 | 25.15 | 24.31 | 24.04 | 23.98 |
| IL12B | 31.24 | 30.07 | 29.77 | 30.55 | 29.96 | 30.59 | 29.66 | 27.86 | 25.18 | 25.65 | 25.70 |
| IL17F | 34.31 | 31.94 | 31.92 | 33.20 | 31.34 | 30.55 | 28.52 | 27.24 | 26.35 | 25.33 | 25.14 |
| IL6 | 27.07 | 27.30 | 19.99 | 19.65 | 20.20 | 24.32 | 23.33 | 23.91 | 25.59 | 26.24 | 26.09 |

| | H1993 T653 | H1993 T449 | H1975 T314 | H1975 T453 | H1975 T671 | H2073 449 | H2073 370 | H2073 266 | Calu-6 265 | Calu-6 270 | Calu-6 397 |
|---|---|---|---|---|---|---|---|---|---|---|---|
| IL8 | 24.17 | 22.13 | 17.10 | 17.89 | 18.05 | 19.86 | 19.16 | 19.54 | 23.30 | 22.83 | 22.96 |
| KITLG | 24.70 | 24.63 | 21.45 | 21.88 | 22.67 | 23.00 | 22.42 | 23.10 | 23.23 | 23.54 | 23.81 |
| KLK3 | 34.56 | 34.07 | 33.27 | 34.67 | 35.19 | 32.91 | 31.66 | 31.03 | 28.74 | 27.82 | 27.52 |
| LEP | 39.64 | 38.47 | 30.12 | 29.41 | 30.15 | 30.36 | 28.41 | 29.06 | 26.53 | 25.79 | 25.96 |
| MDK | 24.26 | 22.70 | 21.95 | 23.02 | 22.27 | 22.14 | 21.16 | 21.24 | 17.88 | 17.50 | 18.16 |
| FOXO4 | 28.22 | 27.06 | 26.14 | 26.98 | 26.28 | 26.08 | 25.18 | 25.65 | 25.71 | 25.51 | 25.01 |
| NPPB | 33.45 | 32.03 | 31.00 | 31.84 | 31.17 | 27.02 | 27.39 | 27.66 | 27.09 | 26.04 | 25.62 |
| NPR1 | 24.63 | 23.87 | 30.36 | 30.68 | 30.48 | 30.21 | 30.39 | 30.00 | 29.20 | 28.78 | 29.11 |
| PDGFB | 22.62 | 21.96 | 19.47 | 20.40 | 20.53 | 25.24 | 24.44 | 24.71 | 21.86 | 22.37 | 22.01 |
| PDGFD | 28.56 | 28.24 | 27.36 | 27.03 | 27.06 | 28.06 | 27.14 | 27.47 | 25.95 | 26.57 | 26.30 |
| PF4 | Undet. | 37.48 | 31.48 | 37.69 | 31.21 | 29.92 | 30.17 | 28.75 | 26.63 | 26.17 | 25.88 |
| PGF | 32.01 | 34.96 | 24.74 | 25.49 | 25.59 | 29.76 | 29.17 | 29.30 | 22.17 | 22.65 | 22.25 |
| PLG | Undet. | Undet. | 31.61 | 33.06 | 32.47 | 29.50 | 28.30 | 27.50 | 26.89 | 26.32 | 26.05 |
| PPBP | 36.00 | 27.83 | 28.77 | 29.20 | 28.39 | 23.13 | 22.63 | 23.01 | 25.24 | 25.62 | 25.64 |
| PRL | 37.74 | 31.46 | 29.97 | 29.74 | 30.34 | 27.18 | 27.07 | 26.44 | 22.84 | 21.67 | 21.90 |
| PROK1 | 32.27 | 32.35 | 31.80 | 32.10 | 31.94 | 31.50 | 30.76 | 30.44 | 28.56 | 28.09 | 28.32 |
| PTN | 28.85 | 29.71 | 24.87 | 25.51 | 26.22 | 23.72 | 23.07 | 23.33 | 23.88 | 24.01 | 22.68 |
| RHOB | 16.71 | 16.65 | 17.21 | 18.04 | 18.15 | 17.05 | 16.98 | 17.27 | 19.15 | 19.13 | 19.04 |
| RNH1 | 20.21 | 19.62 | 19.62 | 19.67 | 20.00 | 20.01 | 19.41 | 19.91 | 20.07 | 19.97 | 20.13 |
| RUNX1 | 22.08 | 21.65 | 19.82 | 20.16 | 20.32 | 20.53 | 20.20 | 20.34 | 19.67 | 19.45 | 19.47 |
| SERPINC1 | 29.06 | 29.37 | 30.15 | 29.38 | 30.72 | 27.29 | 26.68 | 26.23 | 24.85 | 25.31 | 25.33 |
| SERPINE1 | 18.31 | 18.64 | 15.34 | 16.80 | 16.15 | 22.51 | 22.05 | 21.86 | 24.01 | 23.43 | 23.43 |
| SERPINF1 | 25.17 | 25.26 | 22.78 | 22.33 | 23.10 | 25.18 | 24.26 | 24.62 | 17.41 | 17.00 | 17.20 |
| SPINK5 | 25.84 | 24.95 | 22.93 | 23.20 | 23.60 | 26.86 | 25.64 | 25.41 | 23.13 | 23.18 | 23.11 |

| | H1993 T653 | H1993 T449 | H1975 T314 | H1975 T453 | H1975 T671 | H2073 449 | H2073 370 | H2073 266 | Calu-6 265 | Calu-6 270 | Calu-6 397 |
|---|---|---|---|---|---|---|---|---|---|---|---|
| STAB1 | 26.63 | 25.27 | 25.79 | 26.05 | 25.49 | 25.06 | 24.77 | 25.09 | 25.58 | 25.20 | 25.34 |
| TGFA | 23.57 | 22.56 | 18.90 | 19.49 | 19.58 | 21.54 | 20.98 | 21.42 | 21.75 | 21.13 | 21.20 |
| TGFB1 | 22.59 | 21.98 | 20.10 | 20.93 | 20.72 | 20.73 | 20.60 | 21.05 | 18.90 | 18.71 | 19.05 |
| THBS1 | 20.02 | 19.77 | 16.28 | 16.63 | 17.31 | 19.45 | 19.33 | 19.76 | 22.09 | 21.48 | 21.75 |
| TIE1 | 34.81 | 32.75 | 32.47 | 32.76 | 32.57 | 31.95 | 31.96 | 31.30 | 30.32 | 29.46 | 29.40 |
| TIMP1 | 19.42 | 18.82 | 17.09 | 17.16 | 17.92 | 16.92 | 16.47 | 16.93 | 17.78 | 17.45 | 17.89 |
| TIMP2 | 19.17 | 18.31 | 20.59 | 21.78 | 21.28 | 21.40 | 20.99 | 21.34 | 20.41 | 20.36 | 20.67 |
| TIMP3 | 32.15 | 36.23 | 33.95 | 31.28 | 31.38 | 30.09 | 28.34 | 28.63 | 27.06 | 26.32 | 26.83 |
| TNF | 27.23 | 27.30 | 23.09 | 23.29 | 23.39 | 29.16 | 27.98 | 27.30 | 27.34 | 25.76 | 25.49 |
| TNNI2 | 29.55 | 29.28 | 23.92 | 24.29 | 24.30 | 24.09 | 23.44 | 23.15 | 25.23 | 24.46 | 24.24 |
| TNNI3 | 23.91 | 23.11 | 20.70 | 20.83 | 21.06 | 21.04 | 20.31 | 20.56 | 22.09 | 22.01 | 21.91 |
| VEGFA | 20.15 | 20.52 | 18.30 | 19.50 | 19.20 | 19.93 | 19.07 | 19.53 | 23.20 | 22.24 | 22.14 |
| B2M | 18.46 | 18.16 | 14.27 | 15.14 | 15.42 | 15.87 | 14.79 | 14.18 | 16.15 | 16.03 | 16.04 |
| HPRT1 | 20.95 | 20.95 | 19.53 | 19.45 | 20.03 | 20.04 | 19.78 | 19.99 | 19.05 | 19.22 | 19.13 |
| RPL13A | 17.07 | 16.18 | 18.33 | 18.36 | 18.79 | 17.20 | 16.77 | 17.59 | 15.08 | 14.95 | 15.01 |
| GAPDH | 14.99 | 14.40 | 13.80 | 13.97 | 14.28 | 14.27 | 13.86 | 14.10 | 13.02 | 12.87 | 12.74 |
| ACTB | 14.77 | 13.74 | 12.62 | 12.28 | 13.14 | 14.48 | 14.18 | 14.55 | 13.63 | 13.72 | 13.37 |
| HGDC | 38.26 | 32.54 | 31.07 | 32.53 | 29.58 | 29.75 | 27.82 | 27.84 | 25.11 | 24.96 | 24.82 |
| RTC | 19.97 | 19.55 | 19.46 | 19.31 | 18.70 | 19.33 | 19.09 | 19.09 | 19.49 | 19.56 | 19.64 |
| RTC | 19.91 | 19.47 | 19.06 | 19.18 | 19.03 | 19.23 | 19.16 | 19.11 | 19.48 | 19.63 | 19.55 |
| RTC | 19.93 | 19.28 | 19.07 | 19.30 | 18.79 | 19.27 | 19.12 | 19.14 | 19.47 | 19.47 | 19.51 |
| PPC | 13.94 | 13.72 | 13.82 | 13.77 | 13.73 | 13.86 | 13.83 | 14.06 | 13.77 | 13.79 | 13.90 |
| PPC | 14.03 | 13.82 | 13.84 | 13.88 | 13.86 | 13.89 | 13.73 | 13.73 | 13.80 | 20.67 | 14.03 |
| PPC | 14.04 | 14.56 | 13.96 | 13.87 | 13.77 | 13.98 | 13.93 | 14.01 | 13.94 | 13.74 | 13.83 |

| | Calu-3 674 | Calu-3 719 | Calu-3 724 | A549 216 | A549 222 | A549 224 | H1155 872 | H1155 786 | H1395 914 | H1395 971 | H1395 958 |
|---|---|---|---|---|---|---|---|---|---|---|---|
| AGGF1 | 20.61 | 21.21 | 21.07 | 22.50 | 21.16 | 21.85 | 20.89 | 20.68 | 21.72 | 21.17 | 21.47 |
| AMOT | 24.11 | 24.61 | 24.28 | 23.51 | 25.89 | 25.82 | 27.34 | 25.44 | 26.55 | 26.48 | 26.57 |
| ANG | 22.89 | 23.26 | 23.08 | 22.01 | 20.56 | 20.69 | 24.40 | 23.90 | 20.94 | 20.01 | 20.10 |
| ANGPT1 | 23.94 | 24.40 | 25.04 | 21.74 | 24.05 | 24.03 | 27.36 | 24.75 | 24.44 | 24.30 | 23.99 |
| ANGPT2 | 24.60 | 25.03 | 24.58 | 22.79 | 24.38 | 24.31 | 24.70 | 24.10 | 24.50 | 24.13 | 24.26 |
| ANGPTL1 | 24.08 | 24.46 | 24.77 | 22.47 | 23.55 | 23.30 | 25.32 | 24.36 | 23.45 | 23.41 | 23.54 |
| BAI1 | 29.59 | 29.85 | 29.56 | 22.14 | 23.32 | 23.67 | 20.76 | 20.25 | 25.11 | 25.07 | 25.15 |
| BMP2 | 24.53 | 24.23 | 24.42 | 23.17 | 25.15 | 26.12 | 34.23 | 26.13 | 23.65 | 23.11 | 23.45 |
| BTG1 | 17.02 | 18.01 | 17.95 | 20.62 | 17.09 | 18.12 | 20.27 | 20.05 | 17.35 | 17.16 | 17.25 |
| CCL15 | 29.20 | 30.15 | 30.65 | 21.53 | 23.41 | 23.63 | 29.59 | 24.50 | 24.32 | 24.36 | 24.18 |
| CCL2 | 23.83 | 25.15 | 23.74 | 21.66 | 20.11 | 22.05 | 23.37 | 21.00 | 24.02 | 23.60 | 23.99 |
| CD55 | 19.91 | 20.07 | 20.44 | 21.67 | 18.25 | 18.79 | 21.66 | 21.53 | 16.71 | 16.25 | 17.14 |
| CD59 | 15.91 | 16.68 | 16.50 | 22.20 | 19.17 | 19.98 | 20.74 | 20.21 | 19.16 | 18.89 | 19.04 |
| CHGA | 31.46 | 30.60 | 30.64 | 23.33 | 25.91 | 26.24 | 21.94 | 21.11 | 26.41 | 26.11 | 26.33 |
| COL18A1 | 20.25 | 20.65 | 20.45 | 23.89 | 22.69 | 23.89 | 24.16 | 23.72 | 26.01 | 25.84 | 26.08 |
| COL4A3 | 22.85 | 23.06 | 23.48 | 21.97 | 21.72 | 21.85 | 29.29 | 25.22 | 24.46 | 24.11 | 24.15 |
| CSF3 | 30.44 | 30.21 | 30.28 | 24.29 | 27.21 | 27.27 | 31.69 | 27.54 | 27.34 | 27.31 | 27.11 |
| CXCL10 | 24.36 | 25.60 | 25.70 | 23.06 | 25.13 | 25.04 | 27.63 | 25.64 | 24.78 | 25.26 | 25.47 |
| CXCL11 | 24.42 | 25.08 | 26.34 | 22.56 | 25.07 | 24.93 | 29.08 | 26.04 | 24.23 | 24.84 | 25.24 |
| CXCL12 | 28.06 | 27.91 | 28.25 | 23.47 | 25.50 | 25.85 | 26.73 | 25.23 | 26.05 | 25.93 | 26.11 |
| CXCL13 | 29.31 | 31.36 | 32.26 | 23.72 | 25.31 | 25.99 | 26.77 | 26.48 | 25.90 | 26.24 | 25.90 |
| CXCL14 | 25.59 | 26.28 | 28.21 | 21.50 | 24.05 | 24.47 | 30.86 | 24.55 | 21.99 | 20.32 | 21.04 |
| CXCL2 | 19.54 | 21.28 | 21.16 | 23.35 | 20.75 | 21.17 | 29.40 | 26.61 | 22.02 | 20.71 | 22.41 |
| CXCL3 | 19.83 | 21.09 | 20.58 | 23.01 | 21.20 | 22.01 | 28.70 | 25.90 | 23.81 | 23.56 | 24.19 |

| | Calu-3 674 | Calu-3 719 | Calu-3 724 | A549 216 | A549 222 | A549 224 | H1155 872 | H1155 786 | H1395 914 | H1395 971 | H1395 958 |
|---|---|---|---|---|---|---|---|---|---|---|---|
| CXCL5 | 16.29 | 17.27 | 17.01 | 22.08 | 18.34 | 19.31 | 28.51 | 25.16 | 21.30 | 20.51 | 21.03 |
| CXCL6 | 17.77 | 18.46 | 18.22 | 23.20 | 25.53 | 25.67 | 30.72 | 26.56 | 25.11 | 25.60 | 25.52 |
| CXCL9 | Undet. | 31.02 | 31.78 | 22.62 | 25.10 | 25.08 | 30.35 | 26.03 | 24.96 | 25.08 | 25.44 |
| TYMP | 22.18 | 22.53 | 22.14 | 23.65 | 21.67 | 22.42 | 24.18 | 23.68 | 20.72 | 20.37 | 20.91 |
| EDIL3 | 23.07 | 23.09 | 23.87 | 22.02 | 23.47 | 24.00 | 27.24 | 25.03 | 21.10 | 20.27 | 21.06 |
| EREG | 16.65 | 17.87 | 18.19 | 22.65 | 21.59 | 22.46 | 28.15 | 26.04 | 21.19 | 20.59 | 20.82 |
| FGF1 | 27.30 | 26.96 | 27.51 | 22.33 | 24.16 | 24.26 | 24.81 | 24.16 | 24.59 | 24.93 | 24.62 |
| FGF13 | 29.70 | 29.44 | 29.90 | 22.94 | 25.23 | 26.10 | 24.89 | 24.63 | 24.52 | 23.98 | 24.24 |
| FGF2 | 19.77 | 20.10 | 20.26 | 22.66 | 21.59 | 22.51 | 22.42 | 22.19 | 23.26 | 22.59 | 22.68 |
| FGFBP1 | 24.71 | 24.84 | 25.01 | 23.01 | 24.79 | 25.60 | 32.01 | 25.78 | 25.50 | 25.51 | 25.51 |
| FIGF | 27.32 | 28.39 | 28.02 | 22.85 | 24.93 | 24.57 | 26.51 | 24.99 | 25.53 | 25.18 | 25.68 |
| FN1 | 16.98 | 17.49 | 17.27 | 22.37 | 16.90 | 18.51 | 26.58 | 24.64 | 19.94 | 19.38 | 19.99 |
| FST | 24.41 | 26.02 | 25.15 | 22.93 | 20.24 | 20.87 | 28.62 | 25.40 | 20.13 | 19.52 | 19.82 |
| GRN | 19.42 | 19.94 | 19.69 | 23.23 | 20.74 | 22.00 | 22.36 | 21.80 | 20.10 | 19.14 | 19.18 |
| GRP | 31.81 | 32.21 | Undet. | 23.53 | 26.09 | 25.76 | 30.45 | 26.05 | 25.51 | 25.67 | 26.19 |
| HGF | 30.27 | 29.89 | Undet. | 22.25 | 23.53 | 24.11 | 28.61 | 25.55 | 23.08 | 22.21 | 22.65 |
| IFNA1 | 24.70 | 24.82 | 26.03 | 23.02 | 25.02 | 24.98 | 29.36 | 25.07 | 25.36 | 25.33 | 25.64 |
| IFNB1 | 27.88 | 28.67 | 29.21 | 24.04 | 26.00 | 26.01 | 27.90 | 27.16 | 26.34 | 26.32 | 26.70 |
| IFNG | 34.55 | 31.10 | Undet. | 22.26 | 24.78 | 24.83 | 29.65 | 25.36 | 24.19 | 24.70 | 24.74 |
| IL10 | 30.43 | 31.60 | 32.08 | 22.35 | 24.78 | 24.79 | 28.95 | 25.45 | 24.55 | 24.84 | 24.72 |
| IL12A | 26.08 | 26.55 | 26.90 | 22.53 | 23.51 | 23.61 | 25.24 | 24.83 | 24.30 | 24.50 | 24.43 |
| IL12B | 35.02 | 31.16 | 34.20 | 22.11 | 24.90 | 25.03 | 29.22 | 25.22 | 24.41 | 24.91 | 24.73 |
| IL17F | 31.12 | 30.57 | 31.17 | 23.18 | 25.28 | 25.63 | 29.72 | 25.86 | 25.36 | 25.34 | 25.69 |
| IL6 | 21.13 | 22.09 | 22.64 | 22.51 | 22.33 | 23.13 | 30.36 | 25.69 | 21.36 | 21.55 | 21.38 |

| | Calu-3 674 | Calu-3 719 | Calu-3 724 | A549 216 | A549 222 | A549 224 | H1155 872 | H1155 786 | H1395 914 | H1395 971 | H1395 958 |
|---|---|---|---|---|---|---|---|---|---|---|---|
| IL8 | 17.00 | 18.50 | 18.80 | 21.78 | 19.75 | 20.10 | 25.11 | 23.52 | 20.71 | 20.02 | 20.20 |
| KITLG | 22.28 | 23.33 | 22.67 | 22.47 | 22.81 | 23.07 | 23.03 | 22.29 | 22.09 | 21.53 | 22.04 |
| KLK3 | 34.67 | 34.19 | 33.80 | 24.25 | 27.30 | 26.94 | 31.53 | 27.20 | 27.17 | 27.42 | 27.31 |
| LEP | 31.29 | 31.38 | 30.66 | 22.36 | 25.15 | 25.08 | 29.54 | 25.47 | 25.11 | 25.26 | 25.32 |
| MDK | 22.15 | 23.00 | 22.69 | 24.01 | 24.08 | 24.23 | 18.54 | 18.24 | 26.22 | 26.21 | 26.05 |
| FOXO4 | 23.59 | 24.47 | 23.72 | 23.43 | 24.84 | 25.00 | 25.00 | 24.15 | 25.14 | 25.00 | 25.03 |
| NPPB | 30.81 | 30.82 | 30.94 | 23.65 | 26.12 | 26.11 | 28.35 | 25.77 | 26.33 | 26.22 | 26.14 |
| NPR1 | 31.41 | 33.84 | 32.28 | 24.30 | 27.26 | 27.26 | 30.16 | 27.32 | 27.03 | 26.85 | 27.04 |
| PDGFB | 21.86 | 21.88 | 22.16 | 23.71 | 22.08 | 23.55 | 24.29 | 24.33 | 25.28 | 25.47 | 25.71 |
| PDGFD | 23.10 | 23.84 | 23.28 | 23.22 | 23.04 | 23.32 | 28.97 | 25.96 | 23.02 | 21.93 | 21.89 |
| PF4 | 24.11 | 24.31 | 24.46 | 23.16 | 25.52 | 25.88 | 29.21 | 26.86 | 25.44 | 25.09 | 25.09 |
| PGF | 30.82 | 31.24 | 30.99 | 26.11 | 28.20 | 28.37 | 23.95 | 24.11 | 28.85 | 28.21 | 28.21 |
| PLG | 32.70 | 31.76 | 31.66 | 24.25 | 26.33 | 26.29 | 28.41 | 26.26 | 26.88 | 26.80 | 27.04 |
| PPBP | 27.84 | 29.75 | 30.37 | 23.03 | 24.78 | 25.00 | 28.94 | 26.14 | 24.91 | 25.09 | 25.48 |
| PRL | 29.19 | 31.54 | 30.82 | 22.70 | 25.06 | 25.27 | 24.14 | 24.08 | 24.83 | 25.04 | 25.01 |
| PROK1 | 32.35 | 32.36 | 32.85 | 24.27 | 26.55 | 26.66 | 31.04 | 27.06 | 27.02 | 26.35 | 26.84 |
| PTN | 22.19 | 23.96 | 22.34 | 22.48 | 24.65 | 24.75 | 21.31 | 21.11 | 23.93 | 24.19 | 23.63 |
| RHOB | 16.01 | 17.16 | 16.65 | 21.74 | 17.85 | 18.24 | 19.20 | 18.98 | 19.03 | 19.16 | 18.96 |
| RNH1 | 19.93 | 20.14 | 20.27 | 22.83 | 20.05 | 20.99 | 19.64 | 19.19 | 19.92 | 19.25 | 19.28 |
| RUNX1 | 20.02 | 20.47 | 20.44 | 23.44 | 21.09 | 22.16 | 26.40 | 25.09 | 21.11 | 20.75 | 21.18 |
| SERPINC1 | 28.44 | 29.20 | 29.89 | 22.32 | 24.78 | 25.04 | 27.94 | 25.31 | 24.53 | 24.61 | 24.85 |
| SERPINE1 | 22.47 | 23.21 | 23.52 | 22.60 | 19.82 | 21.93 | 26.57 | 25.04 | 23.76 | 24.24 | 24.09 |
| SERPINF1 | 25.74 | 25.44 | 25.84 | 22.09 | 23.48 | 23.75 | 23.16 | 23.09 | 24.17 | 23.91 | 23.92 |
| SPINK5 | 27.21 | 27.25 | 27.27 | 23.01 | 24.80 | 25.29 | 28.28 | 25.93 | 23.50 | 22.92 | 23.06 |

| | Calu-3 674 | Calu-3 719 | Calu-3 724 | A549 216 | A549 222 | A549 224 | H1155 872 | H1155 786 | H1395 914 | H1395 971 | H1395 958 |
|---|---|---|---|---|---|---|---|---|---|---|---|
| STAB1 | 24.61 | 24.84 | 25.31 | 23.05 | 24.37 | 24.68 | 26.47 | 24.78 | 25.28 | 24.99 | 24.70 |
| TGFA | 20.24 | 21.10 | 21.03 | 22.02 | 23.13 | 24.02 | 25.06 | 23.76 | 24.22 | 24.19 | 24.31 |
| TGFB1 | 19.65 | 20.16 | 19.95 | 22.11 | 21.02 | 22.03 | 21.64 | 21.01 | 24.21 | 24.33 | 24.09 |
| THBS1 | 16.11 | 16.39 | 16.66 | 23.32 | 20.56 | 22.18 | 25.83 | 26.01 | 22.38 | 22.15 | 22.61 |
| TIE1 | 33.00 | 34.51 | 34.01 | 25.33 | 28.08 | 28.08 | 34.04 | 28.06 | 28.88 | 29.07 | 28.51 |
| TIMP1 | 16.94 | 17.35 | 17.66 | 22.16 | 18.37 | 19.25 | 18.43 | 18.11 | 18.38 | 17.81 | 17.82 |
| TIMP2 | 19.18 | 19.90 | 19.82 | 22.07 | 21.04 | 22.59 | 20.11 | 19.89 | 23.01 | 22.34 | 22.49 |
| TIMP3 | 29.77 | 30.36 | Undet. | 22.62 | 25.13 | 25.34 | 30.15 | 25.55 | 25.19 | 25.21 | 25.38 |
| TNF | 24.68 | 26.02 | 25.36 | 23.83 | 25.24 | 25.74 | 24.44 | 23.25 | 25.96 | 26.09 | 26.04 |
| TNNI2 | 24.12 | 23.83 | 23.90 | 22.42 | 23.99 | 23.82 | 27.36 | 24.28 | 25.07 | 25.08 | 25.29 |
| TNNI3 | 24.91 | 25.15 | 24.85 | 22.45 | 24.55 | 24.62 | 21.39 | 21.27 | 22.22 | 22.08 | 21.79 |
| VEGFA | 18.30 | 18.29 | 18.56 | 22.60 | 20.59 | 20.65 | 19.89 | 20.08 | 18.25 | 18.23 | 18.21 |
| B2M | 15.22 | 16.14 | 15.89 | 20.74 | 17.05 | 17.66 | 15.20 | 15.02 | 15.63 | 14.72 | 14.97 |
| HPRT1 | 19.38 | 19.64 | 20.00 | 22.99 | 20.17 | 20.93 | 18.14 | 18.13 | 21.93 | 21.07 | 21.25 |
| RPL13A | 17.28 | 18.13 | 18.08 | 19.12 | 16.20 | 16.18 | 18.09 | 18.01 | 16.12 | 15.52 | 15.81 |
| GAPDH | 14.45 | 14.70 | 14.48 | 18.02 | 13.46 | 14.15 | 13.62 | 13.55 | 13.60 | 13.24 | 13.07 |
| ACTB | 12.87 | 13.43 | 13.31 | 19.89 | 14.25 | 15.62 | 13.17 | 12.91 | 15.59 | 14.94 | 15.05 |
| HGDC | 29.74 | 30.53 | 29.65 | 23.14 | 24.90 | 25.05 | 27.42 | 25.73 | 25.14 | 25.27 | 25.52 |
| RTC | 18.73 | 19.25 | 19.07 | 20.29 | 19.15 | 19.31 | 18.83 | 19.11 | 19.31 | 19.19 | 19.29 |
| RTC | 18.75 | 19.24 | 19.13 | 20.15 | 19.16 | 19.39 | 18.92 | 19.12 | 19.33 | 19.21 | 19.23 |
| RTC | 18.63 | 19.16 | 19.02 | 20.20 | 19.24 | 19.29 | 18.87 | 19.09 | 19.34 | 19.18 | 19.20 |
| PPC | 13.67 | 13.80 | 13.78 | 13.88 | 13.89 | 13.91 | 13.96 | 24.26 | 13.76 | 13.80 | 13.87 |
| PPC | 13.68 | 13.77 | 13.59 | 13.88 | 13.81 | 14.01 | 14.00 | 13.73 | 13.74 | 13.84 | 13.80 |
| PPC | 13.93 | 13.94 | 13.89 | 14.10 | 14.01 | 13.88 | 13.99 | 13.75 | 13.83 | 13.97 | 13.94 |

## Appendix C: List of MILLIPLEX MAP cytokine panels

| Human Cytokines | Gene Name | Gene.ID |
|---|---|---|
| EGF | EGF | 1950 |
| Eotaxin | CCL11 | 6356 |
| FGF-2 | FGF2 | 2247 |
| Flt-3L | FLT3L | 2323 |
| Fractalkine | CX3CL1 | 6376 |
| G-CSF | CSF3 | 1440 |
| GM-CSF | CSF2 | 1437 |
| GRO | CXCL1 | 2919 |
| IFN-2α | IFNA2 | 3440 |
| IFN-γ | IFNγ | 3458 |
| IL-1α | IL1A | 3552 |
| IL-1β | IL1B | 3553 |
| IL-1ra | IL1RA | 3557 |
| IL-2 | IL2 | 3558 |
| IL-3 | IL3 | 3562 |
| IL-4 | IL4 | 3565 |
| IL-5 | IL5 | 3567 |
| IL-6 | IL6 | 3569 |
| IL-7 | IL7 | 3574 |
| IL-8 | IL8 | 3576 |
| IL-9 | IL9 | 3578 |
| IL-10 | IL10 | 3586 |
| IL-12p40 | IL12B | 3593 |
| IL-12p70 | IL12B | 3593 |
| IL-13 | IL13 | 3596 |
| IL-15 | IL15 | 3600 |
| IL-17 | IL17 | 3605 |
| IP-10 | CXCL10 | 3627 |
| MCP-1 | CCL2 | 6347 |
| MCP-3 | CCL7 | 6354 |
| MDC | CCL22 | 6367 |
| MIP-1α | CCL3 | 6348 |
| MIP-1β | CCL4 | 6351 |
| sCD40L | CD40LG | 959 |
| sIL-2Ra | IL2RA | 3559 |
| TGF-α | TGFA | 7039 |
| TNF-α | TNF | 7124 |
| TNF-β | LTA | 4049 |
| VEGF | VEGFA | 7422 |

| Mouse Cytokines | Gene Name | Gene.ID |
|---|---|---|
| Eotaxin | CCL11 | 20292 |
| G-CSF | CSF3 | 12985 |
| GM-CSF | CSF2 | 12981 |
| IFN-γ | IGN-γ | 15978 |
| IL-1α | IL-1α | 16175 |
| MCSF | CSF1 | 12977 |
| IL-1β | IL-1β | 16176 |
| IL-2 | IL-2 | 16183 |
| IL-3 | IL-3 | 16187 |
| IL-4 | IL-4 | 16189 |
| IL-5 | IL-5 | 16191 |
| IL-6 | IL-6 | 16193 |
| IL-7 | IL-7 | 16196 |
| IL-10 | IL-10 | 16153 |
| IL-12p40 | IL-12b | 16160 |
| IL-13 | IL-13 | 16163 |
| IL-15 | IL-15 | 16168 |
| IL-17 | IL-17a | 16171 |
| IP-10 | CXCL10 | 15945 |
| MIP2 | CXCL2 | 20310 |
| KC | CXCL10 | 14825 |
| LIF | LIF | 16876 |
| LIX | CXCL5 | 20311 |
| MCP1 | CCL2 | 20296 |
| MIP-1α | CCL3 | 20302 |
| MIP-1β | CCL4 | 20303 |
| MIG | CXCL9 | 17329 |
| RANTES | CCL5 | 20304 |
| TNF-α | TNF | 21926 |
| IL-12p70 | IL12B | 16160 |
| VEGF | VEGFA | 22339 |
| IL-9 | IL-9 | 16198 |

# Appendix D: MILLIPLEX MAP raw human cytokine values

| | EGF pg/mL | Eotaxin pg/mL | FGF2 pg/mL | Flt-3L pg/mL | Fractalkine pg/mL | G-CSF pg/mL | GM-CSF pg/mL | GRO pg/mL | IFN-2a pg/mL | IFN-g pg/mL |
|---|---|---|---|---|---|---|---|---|---|---|
| H2073 XTL 449 | 2.24 | 0.62 | 655.27 | 4.95 | 58.02 | 10.21 | 4.77 | 437.99 | 9.82 | 2.72 |
| H2073 XTL 370 | 0.35 | 3.10 | 385.02 | 3.21 | 47.26 | 11.73 | 5.17 | 361.08 | 13.12 | 2.06 |
| H2073 XTL 266 | 6.22 | 6.26 | 612.19 | 4.95 | 139.72 | 20.04 | 7.40 | 522.59 | 25.48 | 3.06 |
| H2073 r84 394 | 1.09 | 4.47 | 648.99 | 4.95 | 63.27 | 15.53 | 4.82 | 398.32 | 11.24 | 2.23 |
| H2073 r84 389 | 3.41 | 4.37 | 662.81 | 4.95 | 68.39 | 9.82 | 4.28 | 465.38 | 8.39 | 2.56 |
| H2073 r84 395 | 2.39 | 6.13 | 455.68 | 5.78 | 78.63 | 10.71 | 8.82 | 760.11 | 9.34 | 2.98 |
| H2073 bev 363 | 0.00 | 0.00 | 464.99 | 2.32 | 36.24 | 11.60 | 2.25 | 131.94 | 9.80 | 1.32 |
| H2073 bev 368 | 1.60 | 1.23 | 554.75 | 4.95 | 52.64 | 7.43 | 4.77 | 498.19 | 7.91 | 2.63 |
| H2073 bev 435 | 0.35 | 1.03 | 672.05 | 4.95 | 68.39 | 18.51 | 4.87 | 519.44 | 11.65 | 2.55 |
| H1993 XTL T444 | 3.65 | 7.77 | 715.44 | 4.04 | 135.33 | 47.83 | 8.58 | 8.78 | 19.54 | 4.30 |
| H1993 XTL T653 | 3.13 | 4.93 | 613.85 | 5.12 | 54.21 | 21.21 | 12.36 | 18.88 | 24.11 | 5.87 |
| H1993 XTL T449 | 2.27 | 4.09 | 95.11 | 3.01 | 54.21 | 36.18 | 11.63 | 24.39 | 11.69 | 3.69 |
| H1993 r84 T446 | 3.81 | 7.52 | 535.10 | 6.96 | 151.42 | 30.58 | 12.01 | 5.45 | 18.07 | 5.03 |
| H1993 r84 T652 | 2.59 | 7.09 | 666.66 | 4.04 | 69.69 | 30.30 | 7.82 | 14.83 | 15.72 | 4.66 |
| H1993 r84 T481 | 1.45 | 4.26 | 483.67 | 5.12 | 117.83 | 30.58 | 10.48 | 7.83 | 12.98 | 4.53 |
| H1993 bev T442 | 2.74 | 6.19 | 686.19 | 6.29 | 118.30 | 36.50 | 13.50 | 12.22 | 14.80 | 5.75 |
| H1993 bev T663 | 3.86 | 5.44 | 670.08 | 6.87 | 134.63 | 39.89 | 11.63 | 12.45 | 21.00 | 7.16 |
| H1993 bev T487 | 2.97 | 7.11 | 620.08 | 3.49 | 151.42 | 43.31 | 10.49 | 12.45 | 21.98 | 6.13 |
| H1975 XTL T453 | 4.04 | 7.94 | 706.25 | 17.53 | 414.17 | 8809.81 | 1028.90 | 6278.73 | 23.98 | 13.27 |
| H1975 XTL T314 | 2.48 | 4.49 | 1446.32 | 5.12 | 236.88 | 440.31 | 283.23 | 917.66 | 10.81 | 5.03 |
| H1975 XTL T671 | 1.81 | 2.45 | 736.82 | 2.96 | 69.69 | 461.58 | 166.85 | 172.99 | 8.32 | 2.73 |
| H1975 r84 T451 | 3.97 | 11.27 | 771.26 | 9.95 | 270.94 | 1086.10 | 1329.74 | 1260.25 | 14.39 | 8.43 |
| H1975 r84 T461 | 3.08 | 4.75 | 1435.34 | 5.12 | 168.46 | 37.15 | 184.95 | 615.77 | 10.81 | 4.03 |
| H1975 r84 T668 | 3.90 | 14.00 | 191.87 | 14.97 | 338.73 | 1520.29 | 1628.46 | 2521.06 | 28.09 | 8.93 |
| H1975 bev T462 | 3.37 | 7.95 | 1188.14 | 5.96 | 219.76 | 75.86 | 249.90 | 173.09 | 10.81 | 5.99 |
| H1975 bev T464 | 4.03 | 5.87 | 805.73 | 8.69 | 253.95 | 280.96 | 852.22 | 2685.62 | 14.33 | 7.62 |
| H1975 bev T491 | 3.87 | 5.56 | 1063.64 | 6.29 | 254.01 | 88.19 | 348.00 | 523.26 | 9.99 | 4.78 |
| H1155 XTL 786 | 0.00 | 0.00 | 286.97 | 3.21 | 16.64 | 3.43 | 1.52 | 7.95 | 5.06 | 1.60 |
| H1155 XTL 787 | 0.35 | 0.00 | 320.82 | 3.21 | 41.75 | 4.84 | 1.61 | 7.95 | 5.06 | 2.06 |
| H1155 XTL 791 | 1.44 | 0.00 | 594.44 | 1.42 | 68.52 | 4.84 | 1.61 | 10.04 | 6.48 | 1.48 |
| H1155 r84 779 | 0.00 | 0.00 | 306.09 | 1.42 | 25.05 | 3.32 | 1.18 | 3.20 | 3.66 | 1.19 |
| H1155 r84 781 | 0.00 | 0.00 | 118.04 | 1.42 | 19.45 | 5.81 | 1.26 | 3.20 | 4.12 | 1.05 |
| H1155 r84 783 | 1.09 | 0.00 | 296.08 | 2.32 | 19.45 | 4.72 | 1.09 | 5.58 | 4.12 | 1.32 |
| H1155 bev 782 | 0.00 | 0.00 | 138.68 | 1.42 | 19.45 | 5.32 | 1.18 | 0.00 | 3.21 | 1.19 |
| H1155 bev 785 | 0.00 | 0.00 | 228.26 | 2.76 | 25.05 | 4.60 | 1.39 | 3.20 | 4.12 | 1.46 |
| H1155 bev 797 | 0.00 | 0.00 | 280.79 | 2.32 | 47.26 | 5.32 | 1.52 | 3.20 | 5.06 | 1.19 |

| | EGF pg/mL | Eotaxin pg/mL | FGF2 pg/mL | Flt-3L pg/mL | Fractalkine pg/mL | G-CSF pg/mL | GM-CSF pg/mL | GRO pg/mL | IFN-2a pg/mL | IFN-g pg/mL |
|---|---|---|---|---|---|---|---|---|---|---|
| H1395 XTL 972 | 0.00 | 0.00 | 313.31 | 3.21 | 36.24 | 7.30 | 3.39 | 79.28 | 6.96 | 2.73 |
| H1395 XTL 956 | 0.00 | 0.00 | 301.93 | 2.32 | 30.65 | 6.80 | 3.20 | 83.77 | 7.43 | 1.60 |
| H1395 XTL 958 | 0.00 | 0.00 | 193.51 | 2.32 | 25.05 | 4.60 | 3.20 | 63.50 | 6.48 | 1.90 |
| H1395 r84 970 | 0.35 | 0.00 | 188.04 | 3.21 | 25.05 | 6.80 | 3.88 | 71.34 | 6.48 | 2.22 |
| H1395 r84 963 | 0.00 | 0.00 | 317.05 | 2.32 | 30.65 | 7.55 | 3.69 | 84.04 | 7.43 | 1.90 |
| H1395 r84 923 | 0.00 | 0.00 | 252.17 | 1.42 | 3.31 | 5.45 | 2.06 | 45.24 | 5.53 | 1.32 |
| H1395 bev 967 | 0.00 | 0.00 | 405.65 | 1.42 | 25.05 | 8.30 | 1.88 | 14.02 | 6.96 | 1.46 |
| H1395 bev 968 | 0.00 | 0.16 | 335.28 | 3.21 | 36.24 | 8.81 | 2.16 | 10.79 | 6.72 | 2.08 |
| H1395 bev 955 | 0.00 | 0.00 | 372.57 | 3.21 | 25.05 | 9.57 | 2.43 | 74.52 | 7.19 | 1.75 |
| A549 XTL 216 | 0.00 | 0.00 | 754.23 | 2.32 | 47.26 | 7.55 | 2.63 | 112.97 | 4.58 | 1.05 |
| A549 XTL 222 | 1.47 | 2.40 | 708.32 | 3.21 | 36.24 | 8.81 | 2.62 | 85.38 | 6.48 | 1.07 |
| A549 XTL 224 | 0.00 | 0.00 | 566.21 | 2.32 | 57.89 | 16.91 | 2.34 | 41.40 | 6.96 | 1.19 |
| A549 r84 225 | 0.35 | 0.62 | 722.56 | 1.42 | 36.24 | 12.36 | 2.16 | 30.91 | 6.01 | 1.33 |
| A549 r84 246 | 0.00 | 0.00 | 1221.89 | 1.16 | 25.05 | 6.30 | 2.53 | 114.57 | 4.58 | 0.81 |
| A549 r84 298 | 0.00 | 0.00 | 722.87 | 2.32 | 19.45 | 13.63 | 3.10 | 179.12 | 5.06 | 1.33 |
| A549 bev 214 | 0.00 | 0.00 | 1124.65 | 3.21 | 25.05 | 5.57 | 2.96 | 113.01 | 5.06 | 1.75 |
| A549 bev 282 | 0.00 | 6.25 | 697.03 | 3.21 | 41.75 | 13.12 | 5.68 | 234.57 | 7.91 | 2.22 |
| A549 bev 300 | 0.00 | 0.00 | 769.18 | 1.42 | 22.26 | 5.81 | 1.61 | 33.48 | 4.12 | 1.07 |
| Calu-3 XTL 674 | 3.55 | 4.36 | 8456.80 | 7.52 | 254.01 | 15.41 | 20.73 | 3602.93 | 19.05 | 9.97 |
| Calu-3 XTL 707 | 3.23 | 7.47 | 8953.38 | 13.72 | 691.06 | 26.43 | 32.99 | 3375.13 | 22.07 | 10.81 |
| Calu-3 XTL 719 | 4.16 | 6.64 | 8341.51 | 16.25 | 405.87 | 25.50 | 27.91 | 4919.87 | 26.01 | 11.00 |
| Calu-3 r84 716 | 5.55 | 6.69 | 6268.76 | 9.91 | 211.17 | 23.06 | 20.38 | 2382.18 | 17.14 | 7.47 |
| Calu-3 r84 717 | 4.50 | 7.10 | 5214.66 | 14.37 | 262.46 | 23.04 | 21.08 | 4787.72 | 22.98 | 8.91 |
| Calu-3 r84 718 | 3.48 | 5.67 | 5700.85 | 12.43 | 219.79 | 21.23 | 19.31 | 3060.17 | 20.11 | 6.41 |
| Calu-3 bev 534 | 3.82 | 6.43 | 6436.48 | 9.95 | 330.51 | 25.18 | 22.99 | 3088.22 | 21.98 | 7.64 |
| Calu-3 bev 701 | 4.30 | 7.66 | 7519.35 | 14.34 | 288.07 | 22.75 | 22.81 | 3427.92 | 20.50 | 10.46 |
| Calu-3 bev 712 | 5.20 | 7.55 | 5903.83 | 13.07 | 245.45 | 23.64 | 20.91 | 3535.66 | 17.14 | 8.62 |
| Calu-6 XTL 388 | 2.97 | 4.63 | 4315.70 | 8.78 | 134.63 | 25.82 | 17.87 | 22.97 | 22.48 | 4.94 |
| Calu-6 XTL 393 | 1.97 | 2.85 | 2141.96 | 6.29 | 109.59 | 16.83 | 22.64 | 43.42 | 11.66 | 3.83 |
| Calu-6 XTL 397 | 2.30 | 3.39 | 802.56 | 2.07 | 26.36 | 25.49 | 57.66 | 17.44 | 10.40 | 4.03 |
| Calu-6 r84 271 | 1.61 | 3.59 | 1002.85 | 4.04 | 26.36 | 13.76 | 19.67 | 25.83 | 12.11 | 4.53 |
| Calu-6 r84 274 | 3.66 | 4.25 | 1914.83 | 4.04 | 134.63 | 26.78 | 18.24 | 23.06 | 13.53 | 5.87 |
| Calu-6 r84 384 | 4.65 | 7.51 | 1204.38 | 4.04 | 101.50 | 21.82 | 44.80 | 20.21 | 16.18 | 6.13 |
| Calu-6 bev 247 | 6.14 | 4.75 | 3193.06 | 6.29 | 142.98 | 24.57 | 13.12 | 28.68 | 13.42 | 5.71 |
| Calu-6 bev 365 | 3.64 | 5.57 | 2635.37 | 3.15 | 101.50 | 23.35 | 34.86 | 12.45 | 11.24 | 4.28 |
| Calu-6 bev 387 | 3.87 | 4.46 | 1273.31 | 3.49 | 93.26 | 18.27 | 33.13 | 31.71 | 18.20 | 4.80 |

| | IL-1a pg/mL | IL-1b pg/mL | IL-1ra pg/mL | IL-2 pg/mL | IL-3 pg/mL | IL-4 pg/mL | IL-5 pg/mL | IL-6 pg/mL | IL-7 pg/mL | IL-8 pg/mL |
|---|---|---|---|---|---|---|---|---|---|---|
| H2073 XTL 449 | 7.06 | 1.34 | 897.69 | 1.87 | 1.26 | 5.04 | 0.27 | 36.86 | 6.82 | 34.32 |
| H2073 XTL 370 | 6.30 | 1.47 | 528.71 | 1.87 | 0.00 | 6.87 | 0.75 | 42.73 | 6.41 | 42.11 |
| H2073 XTL 266 | 8.28 | 1.47 | 695.90 | 1.87 | 0.01 | 4.18 | 0.30 | 85.45 | 11.23 | 53.54 |
| H2073 r84 394 | 9.22 | 1.09 | 605.76 | 1.38 | 0.00 | 3.76 | 0.24 | 40.45 | 7.42 | 33.24 |
| H2073 r84 389 | 7.36 | 1.22 | 688.38 | 1.69 | 3.14 | 4.60 | 0.21 | 57.03 | 8.22 | 50.78 |
| H2073 r84 395 | 9.98 | 1.35 | 901.42 | 2.15 | 0.20 | 4.83 | 0.31 | 111.84 | 8.61 | 80.56 |
| H2073 bev 363 | 2.80 | 0.85 | 251.58 | 1.09 | 0.00 | 1.72 | 0.21 | 18.55 | 4.99 | 18.94 |
| H2073 bev 368 | 9.97 | 1.34 | 998.36 | 1.91 | 0.00 | 3.35 | 0.21 | 51.75 | 5.81 | 47.41 |
| H2073 bev 435 | 8.90 | 1.47 | 949.98 | 2.05 | 0.00 | 4.17 | 0.31 | 53.83 | 7.22 | 50.93 |
| H1993 XTL T444 | 3.87 | 3.56 | 424.34 | 3.33 | 2.27 | 7.28 | 0.80 | 18.86 | 11.96 | 8.50 |
| H1993 XTL T653 | 4.44 | 3.07 | 464.14 | 2.93 | 1.21 | 5.89 | 0.63 | 62.79 | 13.13 | 29.70 |
| H1993 XTL T449 | 4.79 | 2.95 | 273.51 | 3.42 | 1.60 | 4.18 | 0.63 | 73.22 | 9.97 | 40.31 |
| H1993 r84 T446 | 3.69 | 3.32 | 322.73 | 3.58 | 1.38 | 4.37 | 0.63 | 100.26 | 13.13 | 23.13 |
| H1993 r84 T652 | 4.66 | 2.37 | 306.87 | 3.08 | 1.37 | 3.85 | 0.46 | 29.14 | 12.46 | 13.03 |
| H1993 r84 T481 | 3.69 | 2.61 | 940.17 | 3.08 | 0.57 | 6.57 | 0.32 | 42.55 | 12.96 | 17.19 |
| H1993 bev T442 | 4.23 | 2.95 | 710.96 | 3.00 | 2.06 | 4.54 | 1.07 | 58.23 | 15.50 | 29.36 |
| H1993 bev T663 | 3.52 | 3.34 | 560.92 | 4.27 | 4.89 | 7.90 | 0.80 | 50.15 | 15.33 | 26.93 |
| H1993 bev T487 | 3.87 | 3.07 | 573.29 | 3.68 | 2.06 | 7.44 | 0.46 | 21.67 | 13.97 | 21.08 |
| H1975 XTL T453 | 1557.41 | 13.91 | 126.37 | 5.15 | 0.75 | 10.27 | 1.93 | 4417.86 | 13.30 | 1304.36 |
| H1975 XTL T314 | 274.24 | 3.07 | 105.67 | 3.08 | 0.70 | 2.85 | 0.80 | 462.63 | 11.62 | 127.49 |
| H1975 XTL T671 | 62.68 | 2.37 | 9.99 | 2.76 | 0.28 | 0.52 | 0.63 | 150.27 | 7.39 | 23.64 |
| H1975 r84 T451 | 143.04 | 4.41 | 23.15 | 3.59 | 0.95 | 6.96 | 1.55 | 4127.50 | 16.69 | 520.85 |
| H1975 r84 T461 | 165.42 | 2.59 | 46.35 | 2.60 | 0.77 | 5.30 | 0.80 | 248.90 | 8.67 | 117.15 |
| H1975 r84 T668 | 163.68 | 3.95 | 11.32 | 3.58 | 1.31 | 11.26 | 1.36 | 4567.90 | 14.65 | 869.87 |
| H1975 bev T462 | 117.94 | 2.16 | 18.75 | 2.60 | 1.19 | 8.17 | 0.80 | 575.38 | 11.96 | 99.51 |
| H1975 bev T464 | 200.17 | 3.96 | 71.49 | 3.42 | 0.80 | 4.80 | 1.16 | 1975.09 | 11.63 | 704.36 |
| H1975 bev T491 | 157.08 | 3.32 | 71.49 | 2.92 | 0.58 | 4.33 | 0.98 | 559.21 | 11.79 | 187.90 |
| H1155 XTL 786 | 1.14 | 0.74 | 0.59 | 0.70 | 0.00 | 2.31 | 0.21 | 0.00 | 3.19 | 7.48 |
| H1155 XTL 787 | 0.70 | 0.85 | 0.46 | 0.57 | 0.00 | 2.06 | 0.13 | 0.00 | 4.59 | 6.81 |
| H1155 XTL 791 | 0.91 | 0.74 | 0.46 | 0.57 | 0.00 | 2.96 | 0.18 | 0.01 | 5.80 | 11.48 |
| H1155 r84 779 | 0.51 | 0.53 | 0.46 | 0.50 | 0.00 | 1.90 | 0.18 | 0.00 | 2.80 | 4.93 |
| H1155 r84 781 | 1.61 | 0.63 | 0.73 | 0.70 | 0.00 | 2.80 | 0.21 | 0.00 | 3.19 | 5.84 |
| H1155 r84 783 | 0.80 | 0.63 | 0.28 | 0.57 | 0.00 | 2.43 | 0.13 | 0.00 | 3.19 | 1.81 |
| H1155 bev 782 | 0.51 | 0.43 | 0.28 | 0.50 | 0.00 | 1.90 | 0.11 | 0.00 | 3.58 | 6.48 |
| H1155 bev 785 | 0.81 | 0.85 | 0.46 | 0.63 | 0.00 | 2.60 | 0.13 | 0.00 | 3.78 | 4.57 |
| H1155 bev 797 | 1.14 | 0.53 | 0.46 | 0.57 | 0.00 | 2.59 | 0.18 | 0.00 | 4.59 | 3.59 |

| | IL-1a pg/mL | IL-1b pg/mL | IL-1ra pg/mL | IL-2 pg/mL | IL-3 pg/mL | IL-4 pg/mL | IL-5 pg/mL | IL-6 pg/mL | IL-7 pg/mL | IL-8 pg/mL |
|---|---|---|---|---|---|---|---|---|---|---|
| H1395 XTL 972 | 8.82 | 0.85 | 12.33 | 0.70 | 0.00 | 2.04 | 0.24 | 300.60 | 7.02 | 33.50 |
| H1395 XTL 956 | 4.65 | 0.85 | 4.14 | 0.78 | 0.00 | 2.22 | 0.16 | 154.05 | 7.02 | 23.24 |
| H1395 XTL 958 | 8.28 | 0.85 | 12.87 | 0.63 | 0.00 | 1.90 | 0.18 | 253.93 | 6.41 | 49.84 |
| H1395 r84 970 | 3.78 | 0.85 | 10.71 | 0.97 | 0.00 | 2.96 | 0.24 | 325.07 | 7.02 | 40.93 |
| H1395 r84 963 | 11.75 | 1.09 | 12.87 | 0.70 | 0.00 | 2.22 | 0.18 | 232.57 | 7.42 | 39.00 |
| H1395 r84 923 | 2.39 | 0.64 | 2.84 | 0.57 | 0.00 | 1.27 | 0.13 | 91.08 | 4.79 | 23.04 |
| H1395 bev 967 | 1.13 | 0.63 | 2.04 | 0.63 | 0.00 | 2.59 | 0.16 | 36.04 | 7.42 | 4.70 |
| H1395 bev 968 | 1.04 | 0.64 | 2.46 | 0.65 | 0.00 | 2.08 | 0.19 | 21.64 | 7.32 | 2.45 |
| H1395 bev 955 | 6.07 | 0.85 | 8.08 | 0.57 | 0.00 | 2.06 | 0.18 | 174.74 | 8.02 | 20.61 |
| A549 XTL 216 | 17.22 | 0.63 | 7.06 | 0.77 | 0.00 | 2.15 | 0.16 | 38.68 | 5.60 | 31.77 |
| A549 XTL 222 | 5.70 | 0.74 | 2.46 | 0.70 | 0.00 | 2.60 | 0.18 | 55.98 | 5.60 | 17.16 |
| A549 XTL 224 | 3.94 | 0.63 | 0.73 | 0.78 | 0.00 | 2.63 | 0.13 | 19.94 | 7.82 | 9.08 |
| A549 r84 225 | 5.10 | 0.74 | 0.73 | 0.70 | 0.00 | 2.27 | 0.13 | 25.11 | 6.21 | 6.69 |
| A549 r84 246 | 7.52 | 0.43 | 47.96 | 0.64 | 0.00 | 1.09 | 0.11 | 55.31 | 4.99 | 16.72 |
| A549 r84 298 | 5.70 | 0.74 | 10.18 | 0.77 | 0.00 | 1.72 | 0.18 | 64.71 | 5.20 | 28.00 |
| A549 bev 214 | 25.08 | 0.63 | 2.04 | 0.63 | 0.00 | 2.06 | 0.18 | 41.91 | 3.59 | 19.53 |
| A549 bev 282 | 13.91 | 0.85 | 4.14 | 0.77 | 0.00 | 2.40 | 0.20 | 157.95 | 6.21 | 47.67 |
| A549 bev 300 | 3.78 | 0.43 | 0.46 | 0.50 | 0.00 | 1.31 | 0.11 | 28.37 | 4.39 | 7.14 |
| Calu-3 XTL 674 | 8.26 | 4.63 | 5179.29 | 6.62 | 2.01 | 6.75 | 1.55 | 561.81 | 11.79 | 202.44 |
| Calu-3 XTL 707 | 11.47 | 4.62 | 7384.36 | 7.37 | 1.68 | 10.07 | 1.94 | 1326.62 | 12.96 | 229.13 |
| Calu-3 XTL 719 | 22.16 | 4.90 | 8064.78 | 7.47 | 2.03 | 10.74 | 1.26 | 544.92 | 13.64 | 347.04 |
| Calu-3 r84 716 | 7.69 | 4.37 | 6674.18 | 6.82 | 2.15 | 9.02 | 1.76 | 213.18 | 12.63 | 90.01 |
| Calu-3 r84 717 | 13.51 | 5.04 | 9993.83 | 7.56 | 2.68 | 10.76 | 1.07 | 226.91 | 11.96 | 347.35 |
| Calu-3 r84 718 | 10.25 | 3.82 | 6594.92 | 5.89 | 1.46 | 6.84 | 1.55 | 204.18 | 9.66 | 213.80 |
| Calu-3 bev 534 | 11.23 | 5.04 | 9810.48 | 8.05 | 1.63 | 14.59 | 0.63 | 222.98 | 11.96 | 103.43 |
| Calu-3 bev 701 | 13.78 | 4.63 | 9830.10 | 7.19 | 2.38 | 6.98 | 1.16 | 286.27 | 10.96 | 166.62 |
| Calu-3 bev 712 | 15.00 | 4.62 | 7483.68 | 8.52 | 2.74 | 9.26 | 1.36 | 197.61 | 13.47 | 255.06 |
| Calu-6 XTL 388 | 7.47 | 2.72 | 2.49 | 2.31 | 1.33 | 3.01 | 0.63 | 1.94 | 10.14 | 12.39 |
| Calu-6 XTL 393 | 11.60 | 2.15 | 1.49 | 2.44 | 0.95 | 3.85 | 0.46 | 3.14 | 9.32 | 41.20 |
| Calu-6 XTL 397 | 9.30 | 2.83 | 2.06 | 2.28 | 1.34 | 2.44 | 0.46 | 3.81 | 7.39 | 19.66 |
| Calu-6 r84 271 | 5.18 | 2.72 | 1.72 | 2.44 | 0.87 | 2.26 | 0.32 | 3.14 | 7.08 | 26.52 |
| Calu-6 r84 274 | 6.09 | 3.34 | 2.57 | 2.47 | 2.64 | 4.22 | 0.63 | 2.90 | 9.32 | 20.96 |
| Calu-6 r84 384 | 16.48 | 3.08 | 3.01 | 3.08 | 3.20 | 5.73 | 0.71 | 2.77 | 11.96 | 16.99 |
| Calu-6 bev 247 | 5.12 | 2.83 | 3.81 | 3.41 | 3.16 | 8.35 | 0.89 | 1.47 | 9.64 | 6.93 |
| Calu-6 bev 365 | 13.65 | 2.83 | 2.49 | 2.60 | 2.91 | 7.21 | 0.32 | 1.53 | 10.63 | 15.24 |
| Calu-6 bev 387 | 8.38 | 2.97 | 1.28 | 2.28 | 1.85 | 3.92 | 0.54 | 2.47 | 9.64 | 20.70 |

| | IL-9 pg/mL | IL-10 pg/mL | IL-12p40 pg/mL | IL-12p70 pg/mL | IL-13 pg/mL | IL-15 pg/mL | IL-17 pg/mL | IP-10 pg/mL | MCP-1 pg/mL | MCP-3 pg/mL |
|---|---|---|---|---|---|---|---|---|---|---|
| H2073 XTL 449 | 0 | 8.52 | 9.18 | 3.08 | 209.45 | 11.805 | 2.31 | 20.4 | 79.295 | 12.82 |
| H2073 XTL 370 | 0 | 5.76 | 7.895 | 3.08 | 9.27 | 7.83 | 2.51 | 21.01 | 81.23 | 10.01 |
| H2073 XTL 266 | 0.64 | 6.13 | 11.795 | 4.44 | 9.495 | 12.02 | 2.51 | 19.15 | 155.4 | 12.17 |
| H2073 r84 394 | 0 | 5.975 | 9.57 | 3.41 | 5.985 | 9.855 | 2.05 | 18.55 | 66.32 | 8.53 |
| H2073 r84 389 | 0 | 6.575 | 8.775 | 3.245 | 4.085 | 13.18 | 2.38 | 19.105 | 97.2 | 8.32 |
| H2073 r84 395 | 0 | 8.52 | 13.23 | 3.76 | 4.995 | 15.05 | 2.245 | 23.345 | 157.07 | 11.49 |
| H2073 bev 363 | 0 | 2.515 | 6.27 | 2.275 | 4.665 | 4.155 | 1.735 | 14.69 | 20.51 | 6.84 |
| H2073 bev 368 | 0 | 7.92 | 10.45 | 2.915 | 3.07 | 13.615 | 1.985 | 19.79 | 102.485 | 10.01 |
| H2073 bev 435 | 0 | 7.62 | 8.775 | 3.58 | 37.635 | 12.6 | 2.05 | 16.645 | 87.565 | 10.01 |
| H1993 XTL T444 | 1.22 | 5.345 | 15.835 | 17.22 | 9.69 | 37.875 | 6.29 | 20.85 | 29.515 | 6.22 |
| H1993 XTL T653 | 0.59 | 6.655 | 14.865 | 11.455 | 14.935 | 55.345 | 5.77 | 22.975 | 23.69 | 4.39 |
| H1993 XTL T449 | 1.08 | 4.72 | 7.47 | 9.06 | 5.225 | 33.425 | 5.395 | 21.175 | 26.89 | 3.165 |
| H1993 r84 T446 | 1.06 | 4.72 | 15.88 | 9.315 | 8.39 | 72.635 | 5.525 | 21.735 | 23.69 | 4.72 |
| H1993 r84 T652 | 1.185 | 4.72 | 7.99 | 12.615 | 10.195 | 30.76 | 6.32 | 19.49 | 7.53 | 4.8 |
| H1993 r84 T481 | 0.745 | 8.745 | 6.04 | 23.92 | 8.295 | 73.65 | 5.525 | 19.665 | 21.065 | 6.57 |
| H1993 bev T442 | 0.76 | 8.045 | 11.49 | 16.505 | 7.515 | 60.01 | 4.83 | 22.9 | 34.97 | 6.22 |
| H1993 bev T663 | 0.985 | 6.67 | 12.18 | 14.18 | 10.84 | 53.86 | 5.145 | 22.315 | 15.06 | 6.935 |
| H1993 bev T487 | 0.855 | 7 | 10.615 | 20.645 | 9.505 | 52.685 | 7.045 | 28.775 | 15.06 | 4.085 |
| H1975 XTL T453 | 0.625 | 9.1 | 30.81 | 13.925 | 15.03 | 15.365 | 7.805 | 1080.415 | 51.445 | 10.32 |
| H1975 XTL T314 | 0.375 | 4.115 | 7.605 | 5.505 | 6.99 | 13.4 | 5.64 | 466.475 | 60.15 | 6.935 |
| H1975 XTL T671 | 0.65 | 2.7 | 7.47 | 3.41 | 4.795 | 4.515 | 3.62 | 44.435 | 22.575 | 4.72 |
| H1975 r84 T451 | 0.275 | 6.99 | 17.115 | 16.275 | 6.67 | 18.67 | 6.915 | 765.37 | 147.81 | 9.07 |
| H1975 r84 T461 | 0.54 | 4.115 | 10.835 | 4.42 | 3.425 | 12.66 | 4.89 | 1052.225 | 39.85 | 6.15 |
| H1975 r84 T668 | 0.32 | 5.825 | 19.515 | 14.855 | 7.14 | 22.615 | 6.095 | 1082.53 | 91.26 | 10.32 |
| H1975 bev T462 | 0.675 | 2.72 | 13.65 | 6.655 | 7.045 | 10.36 | 4.845 | 194.605 | 49.045 | 6.22 |
| H1975 bev T464 | 0.42 | 5.345 | 16.46 | 8.65 | 5.4 | 23.79 | 6.435 | 1542.88 | 105.945 | 7.32 |
| H1975 bev T491 | 0.52 | 5.03 | 10.835 | 6.24 | 7.245 | 16.295 | 5.265 | 632.705 | 63.83 | 6.935 |
| H1155 XTL 786 | 0 | 0.86 | 3.965 | 1.965 | 1.14 | 0.695 | 1.8 | 19.69 | 281.57 | 6.84 |
| H1155 XTL 787 | 0 | 0.75 | 3.965 | 2.43 | 1.23 | 0.79 | 1.86 | 18.55 | 319.505 | 10.01 |
| H1155 XTL 791 | 0 | 0.975 | 6.27 | 2.275 | 1.985 | 0.695 | 1.73 | 22.195 | 221.48 | 6.84 |
| H1155 r84 779 | 0 | 0.86 | 2.615 | 1.81 | 0.97 | 0.6 | 1.55 | 16 | 85.375 | 3.04 |
| H1155 r84 781 | 0 | 0.86 | 4.735 | 2.12 | 1.32 | 0.695 | 1.735 | 17.275 | 152.185 | 3.04 |
| H1155 r84 783 | 0 | 0.75 | 3.965 | 2.275 | 1.14 | 0.695 | 1.735 | 12.67 | 66.59 | 5.15 |
| H1155 bev 782 | 0 | 0.86 | 2.085 | 2.12 | 1.145 | 0.695 | 1.55 | 15.99 | 157.22 | 5.15 |
| H1155 bev 785 | 0 | 0.975 | 4.68 | 2.275 | 1.32 | 0.79 | 1.795 | 20.4 | 96.445 | 6.84 |
| H1155 bev 797 | 0 | 0.86 | 3.33 | 2.59 | 1.505 | 0.61 | 1.855 | 20.38 | 98.86 | 3.04 |

| | IL-9 pg/mL | IL-10 pg/mL | IL-12p40 pg/mL | IL-12p70 pg/mL | IL-13 pg/mL | IL-15 pg/mL | IL-17 pg/mL | IP-10 pg/mL | MCP-1 pg/mL | MCP-3 pg/mL |
|---|---|---|---|---|---|---|---|---|---|---|
| H1395 XTL 972 | 0 | 1.455 | 5.45 | 7.05 | 1.89 | 24.025 | 1.985 | 15.345 | 22.26 | 6.84 |
| H1395 XTL 956 | 0 | 1.09 | 4.1 | 5.505 | 2.18 | 19.21 | 1.61 | 13.995 | 12.87 | 5.15 |
| H1395 XTL 958 | 0 | 1.21 | 3.965 | 3.245 | 1.79 | 23.18 | 1.73 | 9.885 | 22.235 | 5.15 |
| H1395 r84 970 | 0 | 1.33 | 7.04 | 3.92 | 2.18 | 24.17 | 1.79 | 15.345 | 35.345 | 6.84 |
| H1395 r84 963 | 0 | 1.21 | 7.04 | 6.225 | 4.175 | 25.435 | 1.79 | 14.02 | 20.66 | 6.84 |
| H1395 r84 923 | 0 | 0.86 | 2.615 | 2.43 | 1.06 | 19.92 | 1.31 | 9.885 | 12.37 | 3.04 |
| H1395 bev 967 | 0 | 0.86 | 2.615 | 4.09 | 3.74 | 25.44 | 1.49 | 12.67 | 38.385 | 3.04 |
| H1395 bev 968 | 0 | 1.095 | 4.1 | 5.235 | 2.745 | 21.34 | 1.92 | 13.23 | 32.855 | 3.04 |
| H1395 bev 955 | 0 | 1.09 | 4.39 | 4.615 | 1.885 | 38.7 | 1.61 | 11.99 | 29.495 | 0.93 |
| A549 XTL 216 | 0 | 0.975 | 2.615 | 1.81 | 1.32 | 7.4 | 1.55 | 10.6 | 192.11 | 5.15 |
| A549 XTL 222 | 0 | 0.975 | 4.735 | 2.755 | 2.08 | 6.4 | 1.43 | 13.34 | 243.5 | 6.84 |
| A549 XTL 224 | 0 | 1.09 | 1.45 | 2.435 | 4.94 | 5.975 | 1.31 | 11.975 | 107.2 | 5.15 |
| A549 r84 225 | 0 | 0.86 | 4.735 | 3.245 | 3.005 | 6.685 | 1.55 | 11.975 | 143.5 | 3.04 |
| A549 r84 246 | 0 | 0.975 | 0.545 | 2.12 | 1.505 | 14.045 | 1.14 | 7.705 | 88.69 | 3.04 |
| A549 r84 298 | 0 | 1.09 | 2.8 | 3.245 | 1.79 | 12.24 | 1.49 | 12.645 | 160.58 | 6.03 |
| A549 bev 214 | 0 | 0.975 | 3.33 | 1.965 | 1.5 | 5.55 | 1.61 | 12.67 | 335.675 | 5.15 |
| A549 bev 282 | 0 | 1.21 | 6.22 | 3.585 | 1.985 | 10.285 | 1.61 | 13.3 | 558.11 | 8.53 |
| A549 bev 300 | 0 | 0.75 | 1.075 | 2.755 | 1.69 | 6.825 | 1.31 | 7.72 | 127.835 | 3.04 |
| Calu-3 XTL 674 | 1.095 | 22.405 | 26.33 | 12.325 | 8.09 | 14.3 | 9.515 | 34.3 | 41.84 | 8.135 |
| Calu-3 XTL 707 | 0.86 | 28.165 | 33.815 | 13.92 | 10.31 | 12.075 | 7.035 | 54.29 | 131.36 | 9.64 |
| Calu-3 XTL 719 | 1.015 | 36.96 | 31.885 | 14.855 | 14.92 | 11.635 | 6.485 | 48.985 | 63.765 | 12.175 |
| Calu-3 r84 716 | 0.965 | 26.135 | 24.29 | 9.48 | 8.985 | 9.525 | 8.025 | 39.955 | 66.95 | 8.135 |
| Calu-3 r84 717 | 1.035 | 37.895 | 17.715 | 14.385 | 8.99 | 12.075 | 7.66 | 39.325 | 64.38 | 10.765 |
| Calu-3 r84 718 | 0.9 | 28.61 | 14.17 | 13.475 | 10.19 | 9.27 | 5.145 | 35.565 | 54.875 | 8.135 |
| Calu-3 bev 534 | 1.03 | 34.215 | 26.33 | 10.345 | 8.005 | 12.51 | 6.89 | 36.165 | 47.41 | 10.32 |
| Calu-3 bev 701 | 1.28 | 44.94 | 23.78 | 14.17 | 9.38 | 10.925 | 8.62 | 41.29 | 38.75 | 12.275 |
| Calu-3 bev 712 | 1.245 | 35.54 | 21.77 | 13.945 | 10.415 | 10.64 | 6.29 | 31.805 | 43.83 | 9.945 |
| Calu-6 XTL 388 | 0.265 | 3.97 | 8.025 | 5.895 | 9.49 | 3.565 | 4.795 | 26.425 | 23.69 | 6.15 |
| Calu-6 XTL 393 | 0.39 | 3.535 | 4.565 | 9.925 | 6.11 | 3.055 | 4.905 | 20.625 | 52.18 | 6.15 |
| Calu-6 XTL 397 | 0.58 | 2.975 | 8.545 | 12.565 | 5.495 | 3.345 | 5.03 | 16.255 | 58.995 | 3.755 |
| Calu-6 r84 271 | 0.465 | 2.7 | 3.345 | 8.64 | 5.05 | 2.95 | 4.67 | 19.545 | 64.805 | 5.105 |
| Calu-6 r84 274 | 0.64 | 3.82 | 12.705 | 10.615 | 5.755 | 3.455 | 6.38 | 20.85 | 79.955 | 5.435 |
| Calu-6 r84 384 | 1.37 | 3.535 | 14.94 | 14.02 | 6.76 | 3.87 | 5.485 | 30.05 | 35.34 | 4.72 |
| Calu-6 bev 247 | 0.775 | 3.985 | 25.29 | 16.04 | 5.94 | 3.25 | 8.065 | 22.315 | 30.09 | 6.935 |
| Calu-6 bev 365 | 0.68 | 3.395 | 17.805 | 13.3 | 6.67 | 4.29 | 7.095 | 25.22 | 24.935 | 6.935 |
| Calu-6 bev 387 | 0.715 | 3.535 | 13.395 | 8.88 | 5.755 | 3.475 | 5.97 | 24.32 | 50.545 | 4.72 |

| | MDC pg/mL | MIP-1a pg/mL | MIP-1b pg/mL | sCD40L pg/mL | sIL-2Ra pg/mL | TGF-a pg/mL | TNF-a pg/mL | TNF-b pg/mL | VEGF pg/mL |
|---|---|---|---|---|---|---|---|---|---|
| H2073 XTL 449 | 75.89 | 1.24 | 4.95 | 4.74 | 12.035 | 3.265 | 0.95 | 1.715 | 284.11 |
| H2073 XTL 370 | 111.67 | 0.87 | 3.21 | 2.32 | 10.83 | 2.385 | 1.02 | 1.58 | 299.61 |
| H2073 XTL 266 | 61.37 | 1.975 | 5.81 | 3.23 | 20.77 | 2.485 | 1.16 | 3.7 | 109.74 |
| H2073 r84 394 | 79.865 | 2.285 | 4.95 | 2.775 | 10.385 | 2.52 | 0.83 | 1.715 | 584.56 |
| H2073 r84 389 | 99.115 | 2.94 | 4.08 | 2.775 | 12.34 | 2.925 | 0.785 | 2.145 | 866.655 |
| H2073 r84 395 | 82.42 | 4.78 | 5.81 | 3.725 | 14.155 | 4.635 | 0.99 | 1.86 | 564.63 |
| H2073 bev 363 | 30.8 | 0 | 3.21 | 2.32 | 5.945 | 1.31 | 0.745 | 1.195 | 58.915 |
| H2073 bev 368 | 137.475 | 0 | 5.81 | 2.775 | 10.535 | 3.54 | 0.92 | 1.58 | 122.535 |
| H2073 bev 435 | 130.515 | 0 | 4.95 | 3.475 | 16.605 | 2.655 | 0.875 | 2.59 | 121.66 |
| H1993 XTL T444 | 19.07 | 3.625 | 4.345 | 8.91 | 18.18 | 3.96 | 2.84 | 2.91 | 1420.475 |
| H1993 XTL T653 | 14.2 | 2.89 | 4.72 | 8.91 | 16.76 | 4.33 | 2.845 | 3.075 | 5048.275 |
| H1993 XTL T449 | 28.4 | 1.965 | 4.54 | 5.09 | 15.16 | 6.45 | 3.075 | 2.68 | 714.375 |
| H1993 r84 T446 | 37.25 | 2.965 | 5.985 | 8.91 | 18.305 | 5.58 | 2.845 | 2.91 | 3426.465 |
| H1993 r84 T652 | 28.4 | 1.445 | 5.545 | 11.32 | 20.64 | 4.7 | 2.48 | 2.455 | 1014.16 |
| H1993 r84 T481 | 21.69 | 0.82 | 4.72 | 6.81 | 24.42 | 9.97 | 2.57 | 2.84 | 2234.895 |
| H1993 bev T442 | 28.4 | 3.37 | 4.345 | 12.62 | 27.88 | 9.985 | 3.265 | 3.415 | 179.655 |
| H1993 bev T663 | 14.98 | 5.595 | 4.1 | 16.08 | 29.095 | 7.295 | 2.895 | 3.68 | 145.395 |
| H1993 bev T487 | 33.96 | 3.225 | 5.585 | 11.01 | 25.31 | 11.47 | 3.035 | 3.5 | 276.34 |
| H1975 XTL T453 | 92.86 | 2.89 | 10.75 | 36.28 | 21.985 | 29.16 | 40.54 | 4.53 | 1098.71 |
| H1975 XTL T314 | 97.565 | 1.12 | 5.21 | 13.42 | 13.39 | 19.955 | 9.375 | 3.415 | 766.755 |
| H1975 XTL T671 | 42.12 | 1.2 | 4.345 | 8.91 | 2.21 | 13.445 | 5.12 | 2.455 | 455.99 |
| H1975 r84 T451 | 95.875 | 2.71 | 8.29 | 26.92 | 17.78 | 23.695 | 21.42 | 3.595 | 4140.315 |
| H1975 r84 T461 | 92.86 | 1.165 | 5.12 | 13.42 | 12.525 | 26.62 | 4.655 | 3.24 | 1651.815 |
| H1975 r84 T668 | 73.825 | 1.795 | 8.8 | 23.2 | 15.16 | 26.62 | 25.03 | 3.25 | 4092.25 |
| H1975 bev T462 | 64.19 | 1.05 | 5.985 | 5.09 | 16.62 | 25.4 | 10.695 | 3.34 | 242.175 |
| H1975 bev T464 | 175.76 | 1.565 | 7.795 | 24.035 | 19.18 | 44.87 | 15.48 | 3.96 | 903.31 |
| H1975 bev T491 | 120.08 | 1.065 | 6.85 | 15.83 | 15.67 | 31.03 | 8.905 | 3.24 | 473.415 |
| H1155 XTL 786 | 6.89 | 0 | 1.46 | 1.55 | 7.595 | 0.905 | 5.295 | 0.73 | 58.915 |
| H1155 XTL 787 | 17.62 | 0 | 1.46 | 1.72 | 9.935 | 1.015 | 7.295 | 0.955 | 148.135 |
| H1155 XTL 791 | 18.92 | 0 | 3.21 | 1.905 | 8.755 | 0.905 | 4.2 | 1.015 | 257.625 |
| H1155 r84 779 | 6.89 | 0 | 1.46 | 1.135 | 7.31 | 0.765 | 1.85 | 0.73 | 266.625 |
| H1155 r84 781 | 5.065 | 0 | 1.46 | 1.135 | 8.61 | 0.85 | 2.185 | 0.84 | 220.61 |
| H1155 r84 783 | 8.565 | 0 | 2.335 | 1.905 | 9.195 | 0.96 | 2.885 | 0.84 | 135.21 |
| H1155 bev 782 | 3.24 | 0 | 1.46 | 1.135 | 7.31 | 0.64 | 2.185 | 0.635 | 89.195 |
| H1155 bev 785 | 6.89 | 0 | 1.605 | 1.305 | 8.17 | 0.905 | 2.415 | 1.01 | 64.125 |
| H1155 bev 797 | 10.12 | 0 | 0.73 | 0.78 | 9.345 | 0.795 | 2.53 | 0.62 | 86.38 |

| | MDC pg/mL | MIP-1a pg/mL | MIP-1b pg/mL | sCD40L pg/mL | sIL-2Ra pg/mL | TGF-a pg/mL | TNF-a pg/mL | TNF-b pg/mL | VEGF pg/mL |
|---|---|---|---|---|---|---|---|---|---|
| H1395 XTL 972 | 6.89 | 0 | 3.21 | 1.49 | 9.79 | 1.015 | 0.615 | 0.955 | 2627.26 |
| H1395 XTL 956 | 3.24 | 0 | 1.46 | 1.49 | 7.595 | 0.85 | 0.615 | 0.73 | 2813.845 |
| H1395 XTL 958 | 6.89 | 0 | 1.46 | 1.49 | 6.75 | 0.85 | 0.57 | 0.955 | 5746.075 |
| H1395 r84 970 | 8.565 | 0 | 4.08 | 1.49 | 7.595 | 0.85 | 0.615 | 0.73 | 764.72 |
| H1395 r84 963 | 5.065 | 0 | 2.335 | 1.905 | 7.025 | 0.795 | 0.655 | 0.955 | 936.965 |
| H1395 r84 923 | 3.24 | 0 | 0 | 0.78 | 6.18 | 0.69 | 0.535 | 0.62 | 954.11 |
| H1395 bev 967 | 3.24 | 0 | 1.46 | 1.135 | 6.475 | 0.74 | 0.66 | 0.62 | 213.96 |
| H1395 bev 968 | 5.065 | 0 | 1.605 | 1.49 | 7.885 | 0.695 | 0.655 | 0.845 | 142.96 |
| H1395 bev 955 | 3.24 | 0 | 0.73 | 1.135 | 7.31 | 0.745 | 0.615 | 0.62 | 166.345 |
| A549 XTL 216 | 3.24 | 0 | 2.335 | 1.49 | 7.31 | 1.07 | 1.015 | 0.62 | 174.075 |
| A549 XTL 222 | 3.24 | 0 | 1.46 | 1.49 | 5.92 | 0.85 | 0.57 | 0.73 | 249.595 |
| A549 XTL 224 | 3.24 | 0 | 1.045 | 1.49 | 5.635 | 0.905 | 0.57 | 0.73 | 139.675 |
| A549 r84 225 | 3.445 | 0 | 0.73 | 1.905 | 6.495 | 0.85 | 0.615 | 0.73 | 138.56 |
| A549 r84 246 | 3.445 | 0 | 0 | 1.55 | 4.27 | 1.22 | 0.5 | 0.525 | 111.35 |
| A549 r84 298 | 5.065 | 0 | 1.46 | 1.905 | 5.345 | 1.015 | 0.615 | 0.525 | 155.55 |
| A549 bev 214 | 3.24 | 0 | 1.46 | 2.32 | 5.62 | 1.015 | 0.66 | 0.73 | 180.965 |
| A549 bev 282 | 5.065 | 0 | 2.335 | 1.905 | 6.895 | 1.07 | 0.745 | 1.07 | 361.465 |
| A549 bev 300 | 3.24 | 0 | 1.46 | 0.78 | 5.345 | 0.745 | 0.535 | 0.35 | 146.075 |
| Calu-3 XTL 674 | 76.115 | 2.275 | 10.75 | 39.65 | 39.645 | 16.545 | 4.91 | 3.68 | 888.91 |
| Calu-3 XTL 707 | 115.61 | 1.97 | 11.81 | 49.98 | 31.26 | 23.305 | 6.63 | 4.63 | 483.86 |
| Calu-3 XTL 719 | 127.185 | 5.35 | 9.325 | 37.875 | 32.155 | 19.265 | 5.65 | 4.16 | 1708.72 |
| Calu-3 r84 716 | 78.25 | 5.535 | 9.745 | 47.985 | 27.9 | 15.105 | 4.295 | 4.14 | 871.235 |
| Calu-3 r84 717 | 90.285 | 4.9 | 13.555 | 30.33 | 32.465 | 20.88 | 7.86 | 4.43 | 1699.19 |
| Calu-3 r84 718 | 80.245 | 1.385 | 8.74 | 27.1 | 26.46 | 17.33 | 6.135 | 3.95 | 997.215 |
| Calu-3 bev 534 | 82.24 | 3.39 | 9.745 | 33.7 | 33.55 | 18.075 | 4.1 | 4.07 | 491.61 |
| Calu-3 bev 701 | 92.94 | 4.99 | 14.065 | 36.28 | 37.7 | 20.06 | 4.305 | 4.85 | 596.995 |
| Calu-3 bev 712 | 77.7 | 6.47 | 9.745 | 41.245 | 29.835 | 19.15 | 5.22 | 3.985 | 693.23 |
| Calu-6 XTL 388 | 25.405 | 1.93 | 5.21 | 8.91 | 18.825 | 24.01 | 2.75 | 3.505 | 279.295 |
| Calu-6 XTL 393 | 9.09 | 1.305 | 3.995 | 8.91 | 18.225 | 11.325 | 2.985 | 2.61 | 164.115 |
| Calu-6 XTL 397 | 28.4 | 0.825 | 3.57 | 6.81 | 20.3 | 19.495 | 2.665 | 3.16 | 88.79 |
| Calu-6 r84 271 | 21.69 | 0.475 | 3.57 | 7.995 | 20.865 | 7.62 | 2.57 | 2.775 | 120.27 |
| Calu-6 r84 274 | 14.2 | 3.15 | 4.42 | 21.15 | 17.59 | 11.275 | 2.98 | 3.075 | 193.27 |
| Calu-6 r84 384 | 7.49 | 4.175 | 3.675 | 12.18 | 20.37 | 12.475 | 2.75 | 3.885 | 557.27 |
| Calu-6 bev 247 | 18.695 | 5.23 | 8.36 | 17.5 | 30.915 | 19.265 | 2.935 | 3.77 | 74.865 |
| Calu-6 bev 365 | 28.4 | 4.045 | 5.985 | 11.01 | 21.96 | 11.76 | 2.985 | 2.92 | 170.18 |
| Calu-6 bev 387 | 21.69 | 1.505 | 6.85 | 8.91 | 16.33 | 12.34 | 2.57 | 3.16 | 174.91 |

# Appendix E: MILLIPLEX MAP raw mouse cytokine values

| | Eotaxin pg/mL | G-CSF pg/mL | GM-CSF pg/mL | IFN-γ pg/mL | IL-1α pg/mL | MCSF pg/mL | IL-1β pg/mL | IL-2 pg/mL | IL-3 pg/mL | IL-4 pg/mL | IL-5 pg/mL |
|---|---|---|---|---|---|---|---|---|---|---|---|
| H2073 XTL 449 | 17.05 | 2.54 | 11 | 5.29 | 7.28 | 1.52 | 4.69 | 2.57 | 0.94 | 3.41 | 0.76 |
| H2073 XTL 370 | 22.67 | 2.38 | 9.05 | 0.95 | 10.56 | 1.33 | 2.56 | 3.27 | 0.98 | 1.95 | 0.76 |
| H2073 XTL 266 | 16.8 | 57.24 | 10.03 | 44.56 | 59.73 | 1.15 | 2.56 | 6.14 | 0.47 | 2.54 | 0.39 |
| H2073 r84 394 | 22.52 | 1.76 | 7.1 | 10.62 | 15.48 | 0.22 | 0.66 | 4.33 | 0.37 | 1.91 | 0.36 |
| H2073 r84 389 | 23.8 | 1.33 | 5.14 | 0 | 5.9 | 0.65 | 0.66 | 1.75 | 0.37 | 2.52 | 0.3 |
| H2073 r84 395 | 16.29 | 42.48 | 9.05 | 2.36 | 21.33 | 2.14 | 1.32 | 2.8 | 0.47 | 2.86 | 0.29 |
| H2073 bev 363 | 28.08 | 0.71 | 7.1 | 2.36 | 23.85 | 0.1 | 0.66 | 3.01 | 0.37 | 0.75 | 0.36 |
| H2073 bev 368 | 39.7 | 1.24 | 7.1 | 0 | 6 | 0.36 | 1.32 | 1.83 | 0.4 | 2.79 | 0.3 |
| H2073 bev 435 | 31.85 | 0.67 | 7.1 | 25.65 | 25.24 | 0.1 | 0.66 | 3.11 | 0.31 | 3.61 | 0.29 |
| H1993 XTL T444 | 17.93 | 10.07 | 2.11 | 3.22 | 0 | 2.72 | 4.5 | 4.05 | 1.57 | 1.34 | 1.63 |
| H1993 XTL T653 | 14.05 | 3.87 | 2.87 | 2.81 | 0 | 1.53 | 3.295 | 1.97 | 1.08 | 0.91 | 0.89 |
| H1993 XTL T449 | 16.64 | 1152.27 | 4.76 | 1.94 | 52.48 | 43.08 | 23.82 | 1.49 | 0.82 | 0.54 | 0.81 |
| H1993 r84 T446 | 9.69 | 5.23 | 3.82 | 0.73 | 0 | 1.04 | 2.09 | 1.45 | 1.11 | 1.92 | 1.24 |
| H1993 r84 T652 | 16.45 | 6.47 | 4.9 | 0.4 | 0 | 1.61 | 3.295 | 2.86 | 1.37 | 2.28 | 1.06 |
| H1993 r84 T481 | 15.36 | 38.85 | 5.84 | 0.04 | 0.88 | 6.4 | 2.09 | 2.35 | 0.99 | 2.17 | 0.65 |
| H1993 bev T442 | 15.24 | 2.53 | 1.71 | 0 | 0 | 1.04 | 1.25 | 2.18 | 0.65 | 1.4 | 0.33 |
| H1993 bev T663 | 19.19 | 4.17 | 1.71 | 2.13 | 0 | 1.44 | 3.295 | 2.94 | 0.86 | 2.5 | 0.89 |
| H1993 bev T487 | 41.37 | 7.22 | 3.06 | 1.65 | 1.79 | 3.12 | 4.5 | 3.03 | 1.35 | 2.71 | 1.06 |
| H1975 XTL T453 | 29.75 | 829.85 | 2.11 | 4.17 | 8.52 | 5.96 | 8.86 | 3.81 | 0.95 | 4.25 | 0.57 |
| H1975 XTL T314 | 44.92 | 26.08 | 3.06 | 2.97 | 0.75 | 3.63 | 4.5 | 4.21 | 1.29 | 6.09 | 1.06 |
| H1975 XTL T671 | 30.28 | 38.92 | 1.35 | 0 | 0.89 | 2.82 | 5.91 | 0.37 | 1.32 | 2 | 0.89 |
| H1975 r84 T451 | 17.23 | 163.63 | 3.06 | 0.75 | 7.08 | 7.5 | 5.91 | 2.57 | 1.38 | 3.25 | 0.73 |
| H1975 r84 T461 | 46.38 | 11.35 | 2.11 | 1.25 | 6.15 | 1.36 | 2.09 | 3.93 | 0.69 | 4.56 | 0.44 |
| H1975 r84 T668 | 5.97 | 236.6 | 2.38 | 0.1 | 4.07 | 6.62 | 5.91 | 2.78 | 0.97 | 1.78 | 0.73 |
| H1975 bev T462 | 30.43 | 27.93 | 2.11 | 3.78 | 7.63 | 3.02 | 2.09 | 3.2 | 1.5 | 3.09 | 1.15 |
| H1975 bev T464 | 34.24 | 52.26 | 3.06 | 3.01 | 7.43 | 4.78 | 4.5 | 2.27 | 1.28 | 10.15 | 0.89 |
| H1975 bev T491 | 39.14 | 21.95 | 0.84 | 11.37 | 11.37 | 4.67 | 4.5 | 1.49 | 0.9 | 7.87 | 0.89 |
| H1155 XTL 786 | 21.29 | 2.54 | 6.12 | 0 | 0 | 0.77 | 16.74 | 2.23 | 0.42 | 8.89 | 0.67 |
| H1155 XTL 787 | 23.01 | 14.77 | 5.14 | 0 | 0.64 | 1.52 | 26.45 | 2.03 | 0.43 | 18.03 | 0.52 |
| H1155 XTL 791 | 35.22 | 2.92 | 5.14 | 0 | 0 | 0.1 | 26.45 | 3.51 | 0.24 | 4.49 | 0.43 |
| H1155 r84 779 | 20.36 | 3.09 | 3.21 | 0 | 0 | 0.07 | 20.01 | 3.38 | 0.2 | 17.98 | 0.43 |
| H1155 r84 781 | 17.05 | 6.79 | 2.29 | 0 | 0.18 | 0.17 | 11.82 | 3.35 | 0.22 | 3.04 | 0.23 |
| H1155 r84 783 | 6.5 | 8.61 | 4.17 | 0 | 7.78 | 1.52 | 20.01 | 2.23 | 0.64 | 9.87 | 0.58 |
| H1155 bev 782 | 19.32 | 8.54 | 8.08 | 0 | 0 | 0.53 | 5.44 | 3.58 | 0.38 | 7.32 | 0.5 |
| H1155 bev 785 | 18.51 | 4.64 | 5.14 | 0 | 0 | 0.36 | 10.19 | 3.38 | 0.22 | 10.84 | 0.59 |
| H1155 bev 797 | 33.16 | 4.58 | 7.1 | 0 | 5.03 | 1.34 | 15.1 | 3.43 | 0.25 | 14.01 | 0.36 |

| | Eotaxin pg/mL | G-CSF pg/mL | GM-CSF pg/mL | IFN-γ pg/mL | IL-1α pg/mL | MCSF pg/mL | IL-1β pg/mL | IL-2 pg/mL | IL-3 pg/mL | IL-4 pg/mL | IL-5 pg/mL |
|---|---|---|---|---|---|---|---|---|---|---|---|
| H1395 XTL 972 | 5 | 0.86 | 7.1 | 0 | 0 | 0.02 | 0.66 | 27.79 | 0.52 | 7.87 | 0.47 |
| H1395 XTL 956 | 5.47 | 0.46 | 6.12 | 0 | 2.41 | 0.22 | 0.66 | 29.49 | 0.36 | 4.29 | 0.32 |
| H1395 XTL 958 | 4.9 | 1.71 | 7.1 | 0 | 0.87 | 0.36 | 1.91 | 36.75 | 0.32 | 7.3 | 0.5 |
| H1395 r84 970 | 5.05 | 2.62 | 3.21 | 0 | 1.3 | 0.27 | 0.78 | 18.49 | 0.37 | 1.74 | 0.23 |
| H1395 r84 963 | 5.41 | 1.88 | 1.36 | 0 | 0 | 0.02 | 0.66 | 26.18 | 0.47 | 7.45 | 0.58 |
| H1395 r84 923 | 1.73 | 1.38 | 9.05 | 0 | 0 | 0 | 3.95 | 36.08 | 0.54 | 6.81 | 0.46 |
| H1395 bev 967 | 9.12 | 1.86 | 11.96 | 0 | 0.39 | 0.07 | 3.24 | 25.56 | 0.5 | 6.7 | 0.58 |
| H1395 bev 968 | 17.56 | 1.56 | 14.82 | 0 | 20.48 | 1.03 | 1.32 | 25.39 | 0.67 | 8.14 | 0.39 |
| H1395 bev 955 | 9.31 | 4.18 | 11 | 0 | 0.13 | 0 | 1.98 | 30.17 | 0.25 | 9.69 | 0.63 |
| A549 XTL 216 | 12.6 | 16.04 | 1.36 | 0 | 10.36 | 0.31 | 1.91 | 2.54 | 0.13 | 0.25 | 0.1 |
| A549 XTL 222 | 15.51 | 0.94 | 6.12 | 0 | 0 | 0.5 | 0.66 | 1.43 | 0.26 | 0.26 | 0.17 |
| A549 XTL 224 | 29.54 | 12.86 | 5.14 | 0 | 4.55 | 1.15 | 6.99 | 4.15 | 0.37 | 0.31 | 0.23 |
| A549 r84 225 | 35.9 | 5.97 | 10.03 | 0 | 0.46 | 0.48 | 0.66 | 2.7 | 0.54 | 0.37 | 0.29 |
| A549 r84 246 | 21.84 | 2.7 | 11.96 | 0 | 4.74 | 5.07 | 6.99 | 3.01 | 0.37 | 0.54 | 0.29 |
| A549 r84 298 | 18.05 | 4.95 | 9.05 | 0 | 0 | 0.36 | 0.78 | 2.78 | 0.5 | 0.29 | 0.35 |
| A549 bev 214 | 37.94 | 1.31 | 3.21 | 0 | 0 | 1.15 | 6.99 | 1.51 | 0.28 | 0.29 | 0.36 |
| A549 bev 282 | 35.8 | 2.62 | 8.08 | 0 | 0 | 0.48 | 1.32 | 1.29 | 0.37 | 0.32 | 0.32 |
| A549 bev 300 | 33.32 | 4.92 | 3.21 | 0 | 0 | 0.07 | 2.56 | 1.98 | 0.07 | 0.79 | 0.18 |
| Calu-3 XTL 674 | 20.34 | 2.48 | 1.6 | 0.19 | 0 | 2.63 | 3.295 | 1.49 | 0.73 | 0.64 | 0.89 |
| Calu-3 XTL 707 | 29.31 | 4.71 | 3.82 | 0.49 | 0 | 5.31 | 3.295 | 2.94 | 1.56 | 1.73 | 1.24 |
| Calu-3 XTL 719 | 34.91 | 3.89 | 2.11 | 1.91 | 0 | 2.63 | 3.295 | 3.36 | 0.9 | 0.65 | 0.73 |
| Calu-3 r84 716 | 51.58 | 5.38 | 0.84 | 0 | 0 | 4.04 | 2.09 | 2.01 | 0.86 | 0.75 | 0.57 |
| Calu-3 r84 717 | 33.23 | 4.28 | 0.33 | 0 | 0 | 1.88 | 1.25 | 1.02 | 0.53 | 0.54 | 0.65 |
| Calu-3 r84 718 | 33.59 | 5.26 | 5.32 | 1.8 | 0 | 4.25 | 2.09 | 2.57 | 1.32 | 1.26 | 1.06 |
| Calu-3 bev 534 | 41.29 | 12.16 | 2.11 | 0.23 | 0 | 6.18 | 2.66 | 1.49 | 1.04 | 0.64 | 0.73 |
| Calu-3 bev 701 | 34.06 | 1.69 | 0.84 | 0 | 0 | 2.53 | 3.295 | 0.98 | 0.73 | 0.62 | 0.57 |
| Calu-3 bev 712 | 35.06 | 2.51 | 0.68 | 0 | 0 | 2.34 | 2.09 | 1.62 | 0.74 | 0.75 | 0.57 |
| Calu-6 XTL 388 | 16.13 | 28.33 | 1.35 | 4.49 | 0.04 | 2.06 | 22.1 | 4.92 | 1.18 | 2.11 | 1.06 |
| Calu-6 XTL 393 | 19.71 | 12.13 | 1.06 | 0.38 | 0 | 0.96 | 16.98 | 2.01 | 0.99 | 3.38 | 0.57 |
| Calu-6 XTL 397 | 3.13 | 33.87 | 0.84 | 0.66 | 0 | 2.25 | 4.5 | 1.54 | 1.2 | 2.17 | 0.73 |
| Calu-6 r84 271 | 22.61 | 13.89 | 1.47 | 1.01 | 0 | 2.15 | 12.02 | 3.2 | 1.3 | 4.14 | 1.43 |
| Calu-6 r84 274 | 36.33 | 21.33 | 2.11 | 0.3 | 0 | 3.22 | 12.82 | 3.03 | 1.48 | 4.55 | 0.57 |
| Calu-6 r84 384 | 22.01 | 55.36 | 1.47 | 0.15 | 0 | 1.88 | 8.25 | 2.1 | 0.73 | 3.49 | 0.65 |
| Calu-6 bev 247 | 11.35 | 20.35 | 5.84 | 0.29 | 0 | 0.96 | 9.07 | 1.45 | 1 | 2.52 | 0.73 |
| Calu-6 bev 365 | 14.87 | 22.67 | 2.11 | 0.58 | 0 | 1.7 | 9.615 | 1.97 | 1.33 | 3.44 | 1.63 |
| Calu-6 bev 387 | 16.01 | 33.76 | 0.84 | 0.73 | 0 | 1.97 | 7.45 | 2.69 | 1.04 | 2.99 | 1.15 |

| | IL-6 pg/mL | IL-7 pg/mL | IL-9 pg/mL | IL-10 pg/mL | IL-12p40 pg/mL | IL-12p70 pg/mL | IL-13 pg/mL | IL-15 pg/mL | IL-17 pg/mL | IP-10 pg/mL | MIP2 pg/mL |
|---|---|---|---|---|---|---|---|---|---|---|---|
| H2073 XTL 449 | 4.12 | 3.53 | 78.03 | 2.73 | 2.53 | 23.46 | 0 | 4.44 | 0.66 | 19.8 | 10.85 |
| H2073 XTL 370 | 6.65 | 2.67 | 2.51 | 2.07 | 0.47 | 18.27 | 0 | 0.07 | 0.71 | 17.16 | 8.27 |
| H2073 XTL 266 | 15.82 | 1.97 | 0 | 1.72 | 0.67 | 19.71 | 56.59 | 9.94 | 0.76 | 22.56 | 101.78 |
| H2073 r84 394 | 4.7 | 1.05 | 0 | 1.05 | 0 | 14.3 | 0 | 0 | 0.33 | 14.83 | 5.87 |
| H2073 r84 389 | 2.81 | 1.05 | 169.48 | 1.16 | 0.22 | 15.43 | 0 | 0 | 0.34 | 31.7 | 8.27 |
| H2073 r84 395 | 20.39 | 1.8 | 0 | 1.72 | 0.43 | 16.56 | 0 | 3.87 | 0.37 | 18.87 | 42.46 |
| H2073 bev 363 | 1.79 | 1.21 | 0 | 0.78 | 0.11 | 12.07 | 0 | 0 | 0.37 | 11.83 | 9.54 |
| H2073 bev 368 | 1.69 | 1.1 | 8.46 | 0.85 | 0.11 | 15.99 | 0 | 0 | 0.22 | 24.13 | 7.04 |
| H2073 bev 435 | 2.12 | 0.58 | 253.84 | 1.47 | 0.03 | 14.3 | 0 | 0 | 0.34 | 24.31 | 5.87 |
| H1993 XTL T444 | 3.61 | 4.03 | 23.69 | 3.98 | 2.13 | 37.28 | 0 | 6.48 | 0.82 | 18.5 | 10.17 |
| H1993 XTL T653 | 4.94 | 3.07 | 0 | 1.82 | 1.15 | 31.66 | 0 | 0.75 | 0.27 | 34.24 | 13.08 |
| H1993 XTL T449 | 56.54 | 2.52 | 0 | 1.99 | 1.28 | 22.51 | 0 | 1.17 | 0.49 | 29.6 | 925.86 |
| H1993 r84 T446 | 6.72 | 2.88 | 16.43 | 1.57 | 1.83 | 37.28 | 0 | 1.4 | 0.33 | 13.65 | 12.64 |
| H1993 r84 T652 | 3.17 | 5.05 | 12.55 | 3.51 | 2.82 | 41.42 | 4.15 | 4.26 | 0.7 | 14.56 | 10.17 |
| H1993 r84 T481 | 7.67 | 3.84 | 0 | 1.05 | 3.04 | 42.33 | 0 | 2.46 | 0.49 | 36.73 | 13.94 |
| H1993 bev T442 | 2.79 | 1 | 1.51 | 1.31 | 1.12 | 19.09 | 0 | 0 | 0.14 | 18.88 | 7.33 |
| H1993 bev T663 | 4.12 | 1.83 | 4 | 1.61 | 1.83 | 33.07 | 0 | 0.59 | 0.36 | 24.98 | 8.56 |
| H1993 bev T487 | 4.18 | 3.84 | 0 | 2.28 | 3.15 | 34.48 | 3.27 | 5.89 | 0.74 | 52.36 | 6.61 |
| H1975 XTL T453 | 56.96 | 2 | 0 | 0.65 | 1.64 | 29.28 | 0 | 0.66 | 0.4 | 24.85 | 1688.27 |
| H1975 XTL T314 | 19.13 | 3.25 | 225.51 | 2.17 | 3.87 | 36.82 | 0 | 3.6 | 0.65 | 31.23 | 18.03 |
| H1975 XTL T671 | 19.96 | 3.07 | 0 | 0.37 | 2.61 | 14.66 | 0 | 1.93 | 0.32 | 8.06 | 11.99 |
| H1975 r84 T451 | 14.86 | 3.07 | 0 | 1.17 | 3.74 | 30.23 | 0 | 7.47 | 0.6 | 19.32 | 239.64 |
| H1975 r84 T461 | 14.72 | 1.51 | 81.64 | 0.37 | 1.4 | 28.32 | 0 | 0 | 0.27 | 48.96 | 8.22 |
| H1975 r84 T668 | 22.61 | 1.67 | 0 | 0.85 | 2.14 | 21.53 | 0 | 0.59 | 0.39 | 15.41 | 426.27 |
| H1975 bev T462 | 19.61 | 3.84 | 0 | 1.69 | 3.97 | 47.72 | 0 | 14.44 | 0.55 | 25.67 | 36.59 |
| H1975 bev T464 | 26.73 | 2.7 | 0 | 1.17 | 2.58 | 36.82 | 0 | 3.79 | 0.76 | 59.15 | 32.48 |
| H1975 bev T491 | 17.47 | 2.34 | 0 | 1.73 | 1.29 | 33.07 | 0 | 3.79 | 0.49 | 53.12 | 11 |
| H1155 XTL 786 | 5.61 | 2.14 | 0 | 1.94 | 1.6 | 18.85 | 0 | 0.77 | 0.67 | 28.32 | 6.45 |
| H1155 XTL 787 | 12.75 | 1.72 | 0 | 1.9 | 0.95 | 17.7 | 0 | 1.62 | 1.32 | 14.48 | 5.87 |
| H1155 XTL 791 | 12.39 | 2.69 | 0 | 1.47 | 0.29 | 26.94 | 0 | 0.82 | 1.65 | 6.34 | 9.54 |
| H1155 r84 779 | 13.15 | 0.51 | 0 | 1.22 | 0.22 | 18.85 | 0 | 0 | 0.49 | 3.84 | 4.75 |
| H1155 r84 781 | 17.85 | 1.81 | 0 | 0.39 | 0.67 | 21.44 | 0 | 0 | 0.63 | 4.25 | 7.65 |
| H1155 r84 783 | 32.28 | 2.06 | 0 | 1.98 | 0 | 21.72 | 0 | 5.56 | 0.57 | 5.81 | 7.65 |
| H1155 bev 782 | 6.92 | 0.9 | 0 | 1.62 | 0.85 | 19.13 | 0 | 0 | 1.13 | 4.72 | 10.85 |
| H1155 bev 785 | 5.79 | 1.15 | 0 | 1.69 | 0.1 | 15.99 | 0 | 0.13 | 0.66 | 7.96 | 5.87 |
| H1155 bev 797 | 4.62 | 1.34 | 0 | 2.49 | 0.01 | 21.44 | 0 | 0.77 | 0.97 | 33.72 | 8.27 |

| | IL-6 pg/mL | IL-7 pg/mL | IL-9 pg/mL | IL-10 pg/mL | IL-12p40 pg/mL | IL-12p70 pg/mL | IL-13 pg/mL | IL-15 pg/mL | IL-17 pg/mL | IP-10 pg/mL | MIP2 pg/mL |
|---|---|---|---|---|---|---|---|---|---|---|---|
| H1395 XTL 972 | 2.52 | 1.98 | 0 | 0.52 | 0.15 | 24.04 | 0 | 0.07 | 0.45 | 26.07 | 5.87 |
| H1395 XTL 956 | 2.63 | 1.65 | 0 | 1.05 | 0.67 | 23.17 | 0 | 0 | 0.38 | 20.08 | 4.75 |
| H1395 XTL 958 | 2.19 | 1.4 | 0 | 1.94 | 0.36 | 24.62 | 0 | 0.07 | 0.45 | 36.66 | 4.75 |
| H1395 r84 970 | 3.47 | 2.06 | 0 | 1.11 | 0 | 25.2 | 0 | 0 | 0.37 | 23.73 | 7.04 |
| H1395 r84 963 | 10.85 | 1.83 | 0 | 1.27 | 0.43 | 25.78 | 0 | 0 | 0.3 | 25.41 | 9.54 |
| H1395 r84 923 | 1.75 | 2.14 | 0 | 1.36 | 0.11 | 28.1 | 0 | 0.07 | 0.33 | 17.63 | 2.75 |
| H1395 bev 967 | 3.59 | 1.92 | 0 | 0.69 | 1.04 | 25.49 | 0 | 0 | 0.39 | 19.24 | 9.54 |
| H1395 bev 968 | 1.95 | 2.18 | 0 | 1.72 | 2.15 | 26.36 | 0 | 9.37 | 0.41 | 18.72 | 10.85 |
| H1395 bev 955 | 1.46 | 1.47 | 0 | 0.71 | 0 | 25.49 | 0 | 0 | 0.41 | 20.08 | 4.75 |
| A549 XTL 216 | 6.1 | 0.07 | 0 | 0 | 0.22 | 10.71 | 0 | 0 | 0.23 | 3.53 | 14.95 |
| A549 XTL 222 | 8.32 | 0.23 | 201.05 | 0.17 | 0.51 | 14.02 | 0 | 0 | 0.33 | 2.73 | 4.75 |
| A549 XTL 224 | 22.26 | 0.4 | 461.55 | 0.75 | 0 | 13.74 | 0 | 0 | 0.53 | 5.24 | 4.75 |
| A549 r84 225 | 18.38 | 1.03 | 235.22 | 0.77 | 0 | 15.99 | 0 | 0 | 0.2 | 3.58 | 8.9 |
| A549 r84 246 | 5.09 | 0.9 | 501.75 | 0.17 | 0.86 | 19.99 | 0 | 2.3 | 0.41 | 7.55 | 5.3 |
| A549 r84 298 | 6.24 | 1.38 | 796.63 | 0.52 | 1.91 | 17.7 | 0 | 2.21 | 0.23 | 4.25 | 4.22 |
| A549 bev 214 | 7.62 | 1.05 | 591.5 | 0.32 | 0.67 | 16.56 | 0 | 0 | 0.49 | 4.35 | 4.75 |
| A549 bev 282 | 30.74 | 0.73 | 195.82 | 0.26 | 0 | 13.46 | 0 | 0 | 0.17 | 5.34 | 1.96 |
| A549 bev 300 | 4.37 | 0.1 | 200.42 | 0.04 | 0 | 13.18 | 0 | 0.82 | 0.19 | 4.3 | 2.44 |
| Calu-3 XTL 674 | 6.53 | 1.21 | 0 | 0.7 | 0.51 | 26.39 | 0 | 0 | 0.4 | 33.9 | 11 |
| Calu-3 XTL 707 | 9.88 | 2.34 | 0.11 | 1.05 | 1.15 | 34.02 | 0 | 0 | 1.24 | 38.77 | 13.94 |
| Calu-3 XTL 719 | 9.88 | 2 | 0 | 0.77 | 0.87 | 28.32 | 0 | 0.07 | 0.27 | 32.22 | 10.04 |
| Calu-3 r84 716 | 7.41 | 1.51 | 0.15 | 0.53 | 1.38 | 27.36 | 0 | 0 | 0.22 | 14.1 | 12.19 |
| Calu-3 r84 717 | 8.7 | 1.07 | 0 | 0.95 | 0.75 | 25.91 | 0 | 0 | 0.4 | 20.94 | 13.94 |
| Calu-3 r84 718 | 6.65 | 2.61 | 3.5 | 1.17 | 2.15 | 38.67 | 0 | 4.13 | 0.6 | 27.87 | 15.96 |
| Calu-3 bev 534 | 14.17 | 2 | 0 | 0.48 | 2.15 | 34.02 | 0 | 3.79 | 0.4 | 22.44 | 12.19 |
| Calu-3 bev 701 | 9.68 | 1.21 | 0 | 0.19 | 1.28 | 30.23 | 0 | 0 | 0.45 | 38.11 | 3.17 |
| Calu-3 bev 712 | 10.14 | 1.36 | 0.2 | 0.37 | 0.52 | 22.51 | 0 | 0 | 0.23 | 23.33 | 3.56 |
| Calu-6 XTL 388 | 5.54 | 3.35 | 0 | 1.17 | 3.6 | 38.67 | 0 | 0.97 | 0.84 | 9.12 | 15.96 |
| Calu-6 XTL 393 | 10.8 | 1.75 | 0 | 0.55 | 1.03 | 27.36 | 0 | 0 | 0.26 | 6.38 | 14.01 |
| Calu-6 XTL 397 | 5.91 | 1.75 | 0 | 0.37 | 1.29 | 28.32 | 0 | 0 | 0.34 | 3.81 | 0.72 |
| Calu-6 r84 271 | 7.28 | 5.05 | 0 | 2.79 | 4.38 | 34.48 | 0 | 5.93 | 0.72 | 7.91 | 18.03 |
| Calu-6 r84 274 | 15.2 | 3.07 | 0 | 2.05 | 2.27 | 39.59 | 0 | 4.52 | 0.27 | 17.72 | 12.19 |
| Calu-6 r84 384 | 13.76 | 1.92 | 0 | 0.42 | 1.15 | 30.23 | 0 | 0 | 0.4 | 7.33 | 8.22 |
| Calu-6 bev 247 | 4.12 | 2.34 | 0 | 0.33 | 2.42 | 36.82 | 0 | 0.59 | 0.53 | 6.8 | 6.39 |
| Calu-6 bev 365 | 7.6 | 2.79 | 0 | 1.82 | 2.29 | 38.67 | 0 | 2.46 | 0.77 | 9.43 | 10.17 |
| Calu-6 bev 387 | 13.22 | 2.52 | 0 | 1.73 | 3.25 | 37.28 | 0 | 1.18 | 0.4 | 8.28 | 11.99 |

| | KC pg/mL | LIF pg/mL | LIX pg/mL | MCP1 pg/mL | MIP-1α pg/mL | MIP-1β pg/mL | MIG pg/mL | RANTES pg/mL | TNF-α pg/mL | VEGF pg/mL |
|---|---|---|---|---|---|---|---|---|---|---|
| H2073 XTL 449 | 6.59 | 1.07 | 0 | 5.42 | 42.64 | 13.16 | 117.21 | 8.6 | 0.77 | 14.71 |
| H2073 XTL 370 | 4.44 | 1.4 | 0 | 7.76 | 14.23 | 0 | 95.34 | 6.24 | 1.11 | 23.29 |
| H2073 XTL 266 | 28.32 | 0.46 | 30.2 | 7.76 | 96.13 | 0 | 104.48 | 7.61 | 1.11 | 4.74 |
| H2073 r84 394 | 4.76 | 0.03 | 0 | 5.42 | 19.08 | 0 | 106.31 | 8.02 | 0.77 | 24.81 |
| H2073 r84 389 | 4.28 | 0.12 | 0 | 5.48 | 4.5 | 0 | 835.9 | 8.78 | 0.17 | 31.26 |
| H2073 r84 395 | 17.84 | 0.55 | 0 | 4.3 | 19.46 | 0 | 84.32 | 7.01 | 0.77 | 21.61 |
| H2073 bev 363 | 1.59 | 0 | 0 | 4.3 | 23.65 | 0 | 42.19 | 10.84 | 0.53 | 5.63 |
| H2073 bev 368 | 4.71 | 0.03 | 0 | 3.19 | 9.73 | 0 | 75.12 | 5.34 | 0.46 | 16.85 |
| H2073 bev 435 | 5.86 | 0 | 0 | 6.59 | 28.88 | 0 | 100.83 | 8.75 | 0.62 | 19.92 |
| H1993 XTL T444 | 6.03 | 2.23 | 0 | 8.45 | 30.58 | 6.2 | 279.86 | 2.24 | 2.02 | 12.97 |
| H1993 XTL T653 | 3.24 | 1.71 | 0 | 7.4 | 16.4 | 3.02 | 973.41 | 1.22 | 1.65 | 23.47 |
| H1993 XTL T449 | 63.33 | 2.17 | 6.28 | 10.53 | 75.61 | 24.17 | 361.8 | 5.53 | 9.25 | 8.15 |
| H1993 r84 T446 | 3.24 | 1.88 | 0 | 6.36 | 16.4 | 1.09 | 722.24 | 0.38 | 1.48 | 20.66 |
| H1993 r84 T652 | 2.39 | 2.31 | 0 | 8.45 | 30.58 | 13.68 | 281.75 | 0.78 | 1.74 | 11.69 |
| H1993 r84 T481 | 7.96 | 2.06 | 0 | 8.45 | 32.33 | 3.63 | 339.63 | 0.46 | 1.65 | 23.49 |
| H1993 bev T442 | 1.56 | 1.01 | 0 | 4.23 | 19.96 | 0 | 293.96 | 0 | 0.83 | 16.22 |
| H1993 bev T663 | 3.43 | 1.28 | 0 | 5.32 | 19.96 | 0 | 345.88 | 0.88 | 1.22 | 17.19 |
| H1993 bev T487 | 5.94 | 2.89 | 0 | 11.56 | 34.08 | 5.08 | 499.07 | 2.62 | 2.1 | 25.54 |
| H1975 XTL T453 | 98.24 | 1.68 | 0 | 12.59 | 638.99 | 14.42 | 87.57 | 1.8 | 2.94 | 22.13 |
| H1975 XTL T314 | 19.04 | 1.98 | 0 | 20.6 | 34.08 | 7.02 | 139.52 | 3.59 | 1.5 | 16.56 |
| H1975 XTL T671 | 7.67 | 1.22 | 0 | 12.59 | 12.85 | 0 | 12.15 | 0.78 | 1.14 | 10.69 |
| H1975 r84 T451 | 30.22 | 3.07 | 0 | 16.65 | 57.87 | 1.76 | 128.46 | 1.4 | 2.38 | 52.07 |
| H1975 r84 T461 | 12.9 | 0.98 | 0 | 16.65 | 12.85 | 0 | 203.17 | 5.23 | 1.66 | 24.28 |
| H1975 r84 T668 | 58.58 | 3.24 | 0 | 14.63 | 95.52 | 1.76 | 121.76 | 2.04 | 2.11 | 57.37 |
| H1975 bev T462 | 13.8 | 2.89 | 0 | 8.45 | 30.58 | 5.12 | 135.11 | 2.67 | 1.83 | 15.07 |
| H1975 bev T464 | 30.07 | 2.02 | 0 | 16.65 | 34.08 | 3.63 | 260.76 | 6.07 | 1.83 | 39.64 |
| H1975 bev T491 | 14.07 | 1.25 | 0 | 12.59 | 14.62 | 0 | 223.43 | 12.2 | 1.48 | 22.65 |
| H1155 XTL 786 | 3.91 | 0.47 | 0 | 6.59 | 0 | 0 | 72.36 | 1.35 | 0.79 | 8.5 |
| H1155 XTL 787 | 6.7 | 0.45 | 0 | 3.88 | 0 | 0 | 53.07 | 1.39 | 0.46 | 10.48 |
| H1155 XTL 791 | 6.92 | 0.28 | 0 | 2.2 | 9.73 | 0 | 22.99 | 1.42 | 0.61 | 20.25 |
| H1155 r84 779 | 5.2 | 0.74 | 0 | 1.6 | 0 | 0 | 5.19 | 1.3 | 0.66 | 22.74 |
| H1155 r84 781 | 7.38 | 0.95 | 0 | 2.74 | 0 | 0 | 14.93 | 1.59 | 1.02 | 13.84 |
| H1155 r84 783 | 13.69 | 0.84 | 0 | 2.2 | 9.73 | 0 | 11.91 | 1.41 | 1.11 | 10.05 |
| H1155 bev 782 | 5.92 | 0.1 | 0 | 6.02 | 9.73 | 0 | 24.67 | 2.11 | 0.69 | 22.44 |
| H1155 bev 785 | 3.19 | 0.18 | 0 | 4.48 | 0 | 0 | 36.83 | 1.94 | 0.31 | 20.42 |
| H1155 bev 797 | 4.07 | 0.14 | 0 | 6.59 | 0 | 0 | 316.59 | 3.56 | 0.46 | 20.55 |

| | KC pg/mL | LIF pg/mL | LIX pg/mL | MCP1 pg/mL | MIP-1α pg/mL | MIP-1β pg/mL | MIG pg/mL | RANTES pg/mL | TNF-α pg/mL | VEGF pg/mL |
|---|---|---|---|---|---|---|---|---|---|---|
| H1395 XTL 972 | 2.7 | 0.14 | 0 | 0.6 | 9 | 0 | 21.33 | 4.11 | 0.77 | 144.95 |
| H1395 XTL 956 | 2.27 | 0.06 | 0 | 3.88 | 0 | 0 | 16.49 | 4.23 | 0.05 | 132.44 |
| H1395 XTL 958 | 2.99 | 0.07 | 0 | 6 | 4.5 | 0 | 46.7 | 5.11 | 0.79 | 227.71 |
| H1395 r84 970 | 2.41 | 0.44 | 0 | 5.48 | 9.73 | 0 | 29.8 | 3.22 | 0.69 | 23.61 |
| H1395 r84 963 | 2.79 | 0.2 | 0 | 2.2 | 9.73 | 0 | 11.18 | 3.86 | 0.33 | 33.95 |
| H1395 r84 923 | 2.31 | 0.1 | 0 | 0.6 | 0 | 0 | 4.04 | 3.09 | 0.94 | 30.21 |
| H1395 bev 967 | 1.56 | 0.08 | 0 | 4.08 | 9.73 | 3.5 | 6.41 | 4 | 0.46 | 64.38 |
| H1395 bev 968 | 2.6 | 0.05 | 0 | 3.74 | 4.5 | 0 | 42.19 | 3.92 | 0.39 | 43.8 |
| H1395 bev 955 | 2.36 | 0.03 | 0 | 2.71 | 9 | 0.76 | 9.06 | 4.11 | 0.77 | 41.82 |
| A549 XTL 216 | 5.14 | 0.9 | 0 | 2.71 | 0 | 0 | 7.71 | 1.29 | 0.62 | 18.47 |
| A549 XTL 222 | 0.96 | 0.44 | 0 | 4.3 | 0 | 0 | 4.6 | 1.38 | 0.61 | 31.68 |
| A549 XTL 224 | 1.68 | 1.38 | 0 | 0.6 | 0 | 0 | 19.69 | 2.43 | 1.45 | 18.99 |
| A549 r84 225 | 1.47 | 1.07 | 0 | 3.31 | 0 | 0 | 7.71 | 1.96 | 0.46 | 15.11 |
| A549 r84 246 | 2.27 | 1.95 | 0 | 0.6 | 0 | 0 | 22.15 | 1.54 | 0.94 | 14.19 |
| A549 r84 298 | 2.22 | 2.75 | 0 | 3.31 | 14.58 | 0 | 2.03 | 1.33 | 0.79 | 17.25 |
| A549 bev 214 | 2.5 | 1.98 | 0 | 0.2 | 0 | 0 | 5.19 | 1.41 | 0.61 | 27.54 |
| A549 bev 282 | 2.41 | 7.11 | 0 | 2.67 | 0 | 0 | 11.18 | 1.59 | 0.46 | 55.28 |
| A549 bev 300 | 1.29 | 0.01 | 0 | 0.6 | 0 | 0 | 5.19 | 1.2 | 0.3 | 27.84 |
| Calu-3 XTL 674 | 15.41 | 2.52 | 0 | 8.45 | 18.18 | 0 | 108.22 | 0.29 | 1.48 | 24.07 |
| Calu-3 XTL 707 | 10.23 | 3.84 | 0 | 11.56 | 23.52 | 0 | 283.64 | 0.59 | 2.02 | 20.71 |
| Calu-3 XTL 719 | 9.76 | 5.79 | 0 | 8.45 | 12.85 | 0 | 142.81 | 1.28 | 1.83 | 35.99 |
| Calu-3 r84 716 | 3.05 | 3.63 | 0 | 8.45 | 12.85 | 0 | 73.61 | 0 | 1.66 | 24.85 |
| Calu-3 r84 717 | 10.04 | 3.91 | 0 | 9.49 | 19.96 | 0 | 61.9 | 0 | 1.48 | 41.4 |
| Calu-3 r84 718 | 6.61 | 4.71 | 0 | 12.59 | 34.08 | 17.2 | 80.6 | 0.36 | 2.03 | 32.07 |
| Calu-3 bev 534 | 5.16 | 7.06 | 0 | 8.45 | 41.01 | 5.39 | 54.86 | 0 | 1.65 | 18.13 |
| Calu-3 bev 701 | 7.48 | 3.84 | 0 | 10.53 | 18.18 | 0 | 169.79 | 0 | 1.14 | 25.6 |
| Calu-3 bev 712 | 7 | 5.91 | 0 | 10.53 | 12.85 | 0 | 72.44 | 0 | 1.14 | 27.87 |
| Calu-6 XTL 388 | 7 | 1.88 | 0 | 4.23 | 34.08 | 3.81 | 59.55 | 1.66 | 1.39 | 9.94 |
| Calu-6 XTL 393 | 7.96 | 1.58 | 0 | 6.36 | 4.12 | 0 | 22.67 | 0 | 1.22 | 8.36 |
| Calu-6 XTL 397 | 25.42 | 1.97 | 0 | 6.36 | 12.85 | 0 | 16.23 | 0 | 1.48 | 3.55 |
| Calu-6 r84 271 | 5.36 | 2.54 | 0 | 17.65 | 30.58 | 11.83 | 61.9 | 0.26 | 1.83 | 6.37 |
| Calu-6 r84 274 | 8.05 | 1.68 | 0 | 5.32 | 19.96 | 5.74 | 109.36 | 1.75 | 1.66 | 9.79 |
| Calu-6 r84 384 | 21.05 | 2.13 | 0 | 14.63 | 9.31 | 0 | 66.59 | 0.78 | 1.3 | 24.95 |
| Calu-6 bev 247 | 2.29 | 1.58 | 0 | 2.33 | 28.82 | 0 | 13.15 | 0 | 1.48 | 2.71 |
| Calu-6 bev 365 | 6.71 | 2.67 | 0 | 6.36 | 27.06 | 9.42 | 33.91 | 0.66 | 1.83 | 17.04 |
| Calu-6 bev 387 | 13.08 | 2.02 | 0 | 6.36 | 23.52 | 3.18 | 57.2 | 0.78 | 2.57 | 12.94 |

# Appendix F: Reverse-phase protein array bevacizumab resistant versus sensitive fold changes in expression

| Name | Fold Δ |
|---|---|
| Axl | 2.36 |
| Insulin-like growth factor-binding protein 2 (IGFRBP2) | 2.00 |
| Src | 1.72 |
| Protein kinase C α (PKCα) | 1.65 |
| Retinoblastoma (Rb) | 1.62 |
| Insulin-like growth factor receptor 1 (IGFR1) | 1.57 |
| Phospho-retinoblastoma (pRb) (S807 811) | 1.55 |
| Epidermal growth factor receptor (EGFR) | 1.51 |
| Phospho-checkpoint homolog 1 (pChk1) | 1.41 |
| Phospho-eukaryotic translation initiation factor 4E binding protein 1 (p4EBP1) (T37/46) | 1.35 |
| Phospho-eukaryotic translation initiation factor 4E binding protein 1 (p4EBP1) (S65) | 1.31 |
| Tumor protein p53 binding protein 1 (TP53BP1) | 1.29 |
| Ku80 | 1.28 |
| Cyclin D1 | 1.27 |
| Phospho-acetyl-CoA carboxylase (pACC) (S79) | 1.25 |
| Phospho-protein kinase C α (pPKCα) (S657) | 1.25 |
| phospho-β-Catenin (S33) | 1.23 |
| Phospho-AMP-activated protein kinase α (pAMPKα) (T172) | 1.23 |
| Ribosomal protein S6 | 1.21 |
| Tafazzin (TAZ) | 1.17 |
| Cyclin B1 | 1.15 |
| NF-κB (p65) | 1.15 |
| Patched (PTCH) | 1.14 |
| Phospho-BCL2-associated agonist of cell death (pBAD) (S112) | 1.14 |
| Insulin receptor substrate 1 (IRS1) | 1.13 |
| B-cell CLL/lymphoma (BCL) | 1.12 |
| BCL2-associate X protein (BAX) | 1.11 |
| Fanconi anemia, complementation group D2 (FANCD2) | 1.08 |
| Phospho-eukaryotic translation initiation factor 4E binding protein 1 (p4EBP1) (T70) | 1.07 |
| Phospho-BCL2-associated agonist of cell death (pBAD) S155 | 1.07 |
| Acetyl-CoA carboxylase 1 (ACC1) | 1.06 |

| Name | Fold Δ |
|---|---|
| AKT | 1.06 |
| Eukaryotic translation initiation factor 4E (eIF4E) | 1.06 |
| PI3K p85 | 1.04 |
| Phospho-MEK1/2 (S217/221) | 1.04 |
| p16 INK4a | 1.03 |
| PTEN | 1.02 |
| β-Catenin | 1.02 |
| Phospho-cMyc (T58) | 1.01 |
| Phospho-cMyc (T58) | 1.01 |
| Phospho-checkpoint homolog (pChk2) (T68) | 1.00 |
| Focal adhesion kinase (FAK) | 1.00 |
| Breast cancer 2, early onset (BRCA2) | 1.00 |
| Phospho-S6 (S240/244) | 1.00 |
| RAD50 | 1.00 |
| p38 (T180/Y182) | 0.99 |
| Mammalian target of rapamycin (mTOR) | 0.99 |
| Phospho-Src (Y527) | 0.99 |
| MutS homolog 2 (MSH2) | 0.99 |
| Checkpoint homolog 1 (Chk1) | 0.99 |
| Notch3 | 0.98 |
| Smad3 | 0.98 |
| MEK1 | 0.98 |
| PI3K (p110a) | 0.98 |
| RAB25 | 0.98 |
| RAD51 | 0.98 |
| cRaf | 0.97 |
| Phospho-signal transducer and activator of transcription 5 (pSTAT5) (Y694) | 0.97 |
| Phospho-glycogen synthase kinase 3 α/β (pGSK3α/β) (S21/9) | 0.97 |
| Proliferating cell nuclear antigen (PCNA) | 0.97 |
| Phospho-Src (Y416) | 0.96 |
| Phospho-AKT (T308) | 0.96 |

| Name | Fold Δ |
|---|---|
| Phospho-ERK1/2 (T202/Y204) | 0.96 |
| Phospho-pyruvate dehydrogenase kinase, isozyme 1 (pPDK1) (S241) | 0.96 |
| E-Cadherin | 0.96 |
| X-linked inhibitor of apoptosis (XIAP) | 0.96 |
| p21 | 0.96 |
| Excision repair cross-complementing rodent repair deficiency, complementation group 1 (ERCC1) | 0.95 |
| E2F transcription factor 1 (E2F1) | 0.95 |
| B-cell leukemia/lymphoma 2 (BCL2) | 0.94 |
| Phospho-ataxia telangiectasia and Rad3 related (pATR) (S428) | 0.94 |
| Phospho-S6 (S235/236) | 0.94 |
| Caspase 3 | 0.93 |
| Phospho-p70S6K | 0.93 |
| Signal transducer and activator of transcription 5 (STAT5) | 0.92 |
| Caspase 7 | 0.92 |
| Phospho-estrogen receptor (pER) (S118) | 0.92 |
| Enhancer of zeste homolog 2 (EZH2) | 0.92 |
| N-Cadherin | 0.91 |
| Eukaryotic translation initiation factor 4E binding protein 1 (4EBP1) | 0.91 |
| Meiotic recombination 11 (MRE11) | 0.91 |
| Phospho-cJUN (S73) | 0.91 |
| p90RSK | 0.90 |
| X-ray repair complementing defective repair in chinese hampster cells 1 (XRCC1) | 0.90 |
| DNA-PKcs | 0.90 |
| Phospho-EIK1 (S383) | 0.90 |
| Glycogen synthase kinase 3β (GSK3β) | 0.89 |
| Phospho-AKT (S473) | 0.89 |
| Nuclear receptor coactivator 3 (AIB-1, NCOA3) | 0.89 |
| Tuberous sclerosis 2 (TSC2) | 0.89 |
| Phospho-p90RSK (T359) | 0.88 |
| Cleaved PARP | 0.87 |
| Uncleaved PARP | 0.87 |
| Phospho-EGFR (Y1173) | 0.86 |

| Name | Fold Δ |
|---|---|
| Ataxia telangiectasia mutated (ATM) | 0.86 |
| COX2 | 0.86 |
| LKB1 | 0.85 |
| Thymidilate Synthase | 0.85 |
| X14.3.3.Zeta | 0.85 |
| Carbonic anhydrase IX (CA IX) | 0.84 |
| Fibronectin | 0.83 |
| cMyc | 0.83 |
| ATM protein kinase | 0.83 |
| Checkpoint homolog 2 (Chk2) | 0.82 |
| Phospho-Epidermal growth factor receptor (pEGFR) (Y992) | 0.82 |
| BCL2-like 11 (BIM) | 0.81 |
| Ataxia telangiectasia and Rad3 related (ATR) | 0.80 |
| p38 | 0.80 |
| Phospho-mitogen-activated protein kinase (pMAPK) (T202/Y204) | 0.80 |
| Collagen VI | 0.78 |
| Phospho-signal transducer and activator of transcription 3 (pStat3) (Y705) | 0.77 |
| p70S6K | 0.77 |
| MET | 0.76 |
| Phospho-HER2 (Y1248) | 0.75 |
| CD31 | 0.73 |
| Mitogen-activated protein kinase 9 (JNK2) | 0.73 |
| Metastasis associated in colon cancer 1 (MACC1) | 0.72 |
| Vascular endothelial growth factor receptor 2 (VEGFR2) | 0.72 |
| MEK2 | 0.70 |
| Phospho-Axl | 0.69 |
| Caveolin | 0.63 |
| Cyclin E1 | 0.59 |
| c-Kit | 0.59 |
| p53 | 0.54 |
| Phospho-MET (Y1234/1235) | 0.50 |

# BIBLIOGRAPHY


Aase, K., von Euler, G., Li, X., Ponten, A., Thoren, P., Cao, R., Cao, Y., Olofsson, B., Gebre-Medhin, S., Pekny, M., *et al.* (2001). Vascular endothelial growth factor-B-deficient mice display an atrial conduction defect. Circulation *104*, 358-364.

Adjei, A.A., Mandrekar, S.J., Dy, G.K., Molina, J.R., Gandara, D.R., Ziegler, K.L., Stella, P.J., Rowland, K.M., Jr., Schild, S.E., and Zinner, R.G. (2010). Phase II trial of pemetrexed plus bevacizumab for second-line therapy of patients with advanced non-small-cell lung cancer: NCCTG and SWOG study N0426. J Clin Oncol *28*, 614-619.

Aguirre, A.J., Bardeesy, N., Sinha, M., Lopez, L., Tuveson, D.A., Horner, J., Redston, M.S., and DePinho, R.A. (2003). Activated Kras and Ink4a/Arf deficiency cooperate to produce metastatic pancreatic ductal adenocarcinoma. Genes Dev *17*, 3112-3126.

Ahmad, S., Hewett, P.W., Wang, P., Al-Ani, B., Cudmore, M., Fujisawa, T., Haigh, J.J., le Noble, F., Wang, L., Mukhopadhyay, D., *et al.* (2006). Direct evidence for endothelial vascular endothelial growth factor receptor-1 function in nitric oxide-mediated angiogenesis. Circ Res *99*, 715-722.

Akeson, A.L., Greenberg, J.M., Cameron, J.E., Thompson, F.Y., Brooks, S.K., Wiginton, D., and Whitsett, J.A. (2003). Temporal and spatial regulation of VEGF-A controls vascular patterning in the embryonic lung. Dev Biol *264*, 443-455.

Albain, K.S., Crowley, J.J., Turrisi, A.T., 3rd, Gandara, D.R., Farrar, W.B., Clark, J.I., Beasley, K.R., and Livingston, R.B. (2002). Concurrent cisplatin, etoposide, and chest radiotherapy in pathologic stage IIIB non-small-cell lung cancer: a Southwest Oncology Group phase II study, SWOG 9019. J Clin Oncol *20*, 3454-3460.

Alberg, A.J., Brock, M.V., and Samet, J.M. (2005). Epidemiology of lung cancer: looking to the future. J Clin Oncol *23*, 3175-3185.

Alberola, V., Camps, C., Provencio, M., Isla, D., Rosell, R., Vadell, C., Bover, I., Ruiz-Casado, A., Azagra, P., Jimenez, U., *et al.* (2003). Cisplatin plus gemcitabine versus a cisplatin-based triplet versus nonplatinum sequential doublets in advanced non-small-cell lung cancer: a Spanish Lung Cancer Group phase III randomized trial. J Clin Oncol *21*, 3207-3213.

Albuquerque, R.J., Hayashi, T., Cho, W.G., Kleinman, M.E., Dridi, S., Takeda, A., Baffi, J.Z., Yamada, K., Kaneko, H., Green, M.G., *et al.* (2009). Alternatively spliced vascular endothelial growth factor receptor-2 is an essential endogenous inhibitor of lymphatic vessel growth. Nat Med *15*, 1023-1030.

Allavena, P., Germano, G., Marchesi, F., and Mantovani, A. (2011). Chemokines in cancer related inflammation. Exp Cell Res *317*, 664-673.

Allport, J.R., and Weissleder, R. (2003). Murine Lewis lung carcinoma-derived endothelium expresses markers of endothelial activation and requires tumor-specific extracellular matrix in vitro. Neoplasia *5*, 205-217.

Alon, T., Hemo, I., Itin, A., Pe'er, J., Stone, J., and Keshet, E. (1995). Vascular endothelial growth factor acts as a survival factor for newly formed retinal vessels and has implications for retinopathy of prematurity. Nat Med *1*, 1024-1028.

Altorki, N., Lane, M.E., Bauer, T., Lee, P.C., Guarino, M.J., Pass, H., Felip, E., Peylan-Ramu, N., Gurpide, A., Grannis, F.W., *et al.* (2010). Phase II proof-of-concept study of pazopanib monotherapy in treatment-naive patients with stage I/II resectable non-small-cell lung cancer. J Clin Oncol *28*, 3131-3137.

Annabi, B., Naud, E., Lee, Y.T., Eliopoulos, N., and Galipeau, J. (2004). Vascular progenitors derived from murine bone marrow stromal cells are regulated by fibroblast growth factor and are avidly recruited by vascularizing tumors. J Cell Biochem *91*, 1146-1158.

Autiero, M., Waltenberger, J., Communi, D., Kranz, A., Moons, L., Lambrechts, D., Kroll, J., Plaisance, S., De Mol, M., Bono, F., *et al.* (2003). Role of PlGF in the intra- and intermolecular cross talk between the VEGF receptors Flt1 and Flk1. Nat Med *9*, 936-943.

Baar, J., Silverman, P., Lyons, J., Fu, P., Abdul-Karim, F., Ziats, N., Wasman, J., Hartman, P., Jesberger, J., Dumadag, L., *et al.* (2009). A vasculature-targeting regimen of preoperative docetaxel with or without bevacizumab for locally advanced breast cancer: impact on angiogenic biomarkers. Clin Cancer Res *15*, 3583-3590.

Badar, F., Meerza, F., Khokhar, R.A., Ali, F.A., Irfan, N., Kamran, S., Shahid, N., and Mahmood, S. (2006). Characteristics of lung cancer patients--the Shaukat Khanum Memorial experience. Asian Pac J Cancer Prev *7*, 245-248.

Bais, C., Wu, X., Yao, J., Yang, S., Crawford, Y., McCutcheon, K., Tan, C., Kolumam, G., Vernes, J.M., Eastham-Anderson, J., *et al.* (2010). PlGF blockade does not inhibit angiogenesis during primary tumor growth. Cell *141*, 166-177.

Baldwin, M.E., Halford, M.M., Roufail, S., Williams, R.A., Hibbs, M.L., Grail, D., Kubo, H., Stacker, S.A., and Achen, M.G. (2005). Vascular endothelial growth factor D is dispensable for development of the lymphatic system. Mol Cell Biol *25*, 2441-2449.

Bang, Y., Kwak, E.L., Shaw, A., and al., e. (2010). Clinical activity of the oral ALK inhibitor PF-02341066 in ALK-positive patients with non-small cell lung cancer (NSCLC) [abstract]. J Clin Oncol *28*, 6S.

Barleon, B., Sozzani, S., Zhou, D., Weich, H.A., Mantovani, A., and Marme, D. (1996). Migration of human monocytes in response to vascular endothelial growth factor (VEGF) is mediated via the VEGF receptor flt-1. Blood *87*, 3336-3343.

Batchelor, T.T., Sorensen, A.G., di Tomaso, E., Zhang, W.T., Duda, D.G., Cohen, K.S., Kozak, K.R., Cahill, D.P., Chen, P.J., Zhu, M., *et al.* (2007). AZD2171, a pan-VEGF receptor tyrosine kinase inhibitor, normalizes tumor vasculature and alleviates edema in glioblastoma patients. Cancer Cell *11*, 83-95.

Batevik, R., Grong, K., Segadal, L., and Stangeland, L. (2005). The female gender has a positive effect on survival independent of background life expectancy following surgical resection of primary non-small cell lung cancer: a study of absolute and relative survival over 15 years. Lung Cancer *47*, 173-181.

Belani, C.P., Choy, H., Bonomi, P., Scott, C., Travis, P., Haluschak, J., and Curran, W.J., Jr. (2005a). Combined chemoradiotherapy regimens of paclitaxel and carboplatin for locally advanced non-small-cell lung cancer: a randomized phase II locally advanced multi-modality protocol. J Clin Oncol *23*, 5883-5891.

Belani, C.P., Lee, J.S., Socinski, M.A., Robert, F., Waterhouse, D., Rowland, K., Ansari, R., Lilenbaum, R., and Natale, R.B. (2005b). Randomized phase III trial comparing cisplatin-etoposide to carboplatin-paclitaxel in advanced or metastatic non-small cell lung cancer. Ann Oncol *16*, 1069-1075.

Bergers, G., Brekken, R., McMahon, G., Vu, T.H., Itoh, T., Tamaki, K., Tanzawa, K., Thorpe, P., Itohara, S., Werb, Z., *et al.* (2000). Matrix metalloproteinase-9 triggers the angiogenic switch during carcinogenesis. Nat Cell Biol *2*, 737-744.

Bergers, G., and Hanahan, D. (2008). Modes of resistance to anti-angiogenic therapy. Nat Rev Cancer *8*, 592-603.

Bernatchez, P.N., Soker, S., and Sirois, M.G. (1999). Vascular endothelial growth factor effect on endothelial cell proliferation, migration, and platelet-activating factor synthesis is Flk-1-dependent. J Biol Chem *274*, 31047-31054.

Blackhall, F., Ranson, M., and Thatcher, N. (2006). Where next for gefitinib in patients with lung cancer? Lancet Oncol *7*, 499-507.

Blau, H.M., and Banfi, A. (2001). The well-tempered vessel. Nat Med *7*, 532-534.

Boffetta, P. (2006). Human cancer from environmental pollutants: the epidemiological evidence. Mutat Res *608*, 157-162.

Bonner, J.A., Harari, P.M., Giralt, J., Azarnia, N., Shin, D.M., Cohen, R.B., Jones, C.U., Sur, R., Raben, D., Jassem, J., *et al.* (2006). Radiotherapy plus cetuximab for squamous-cell carcinoma of the head and neck. N Engl J Med *354*, 567-578.

Borgstrom, P., Bourdon, M.A., Hillan, K.J., Sriramarao, P., and Ferrara, N. (1998). Neutralizing anti-vascular endothelial growth factor antibody completely inhibits angiogenesis and growth of human prostate carcinoma micro tumors in vivo. Prostate *35*, 1-10.

Brambilla, E., Travis, W.D., Colby, T.V., Corrin, B., and Shimosato, Y. (2001). The new World Health Organization classification of lung tumours. Eur Respir J *18*, 1059-1068.

Bray, F., Tyczynski, J.E., and Parkin, D.M. (2004). Going up or coming down? The changing phases of the lung cancer epidemic from 1967 to 1999 in the 15 European Union countries. Eur J Cancer *40*, 96-125.

Bray, F.I., and Weiderpass, E. (2010). Lung cancer mortality trends in 36 European countries: secular trends and birth cohort patterns by sex and region 1970-2007. Int J Cancer *126*, 1454-1466.

Brekken, R.A., Huang, X., King, S.W., and Thorpe, P.E. (1998). Vascular endothelial growth factor as a marker of tumor endothelium. Cancer Res *58*, 1952-1959.

Brekken, R.A., Overholser, J.P., Stastny, V.A., Waltenberger, J., Minna, J.D., and Thorpe, P.E. (2000). Selective inhibition of vascular endothelial growth factor (VEGF) receptor 2 (KDR/Flk-1) activity by a monoclonal anti-VEGF antibody blocks tumor growth in mice. Cancer Res *60*, 5117-5124.

Brostjan, C., Gebhardt, K., Gruenberger, B., Steinrueck, V., Zommer, H., Freudenthaler, H., Roka, S., and Gruenberger, T. (2008). Neoadjuvant treatment of colorectal cancer with bevacizumab: the perioperative angiogenic balance is sensitive to systemic thrombospondin-1 levels. Clin Cancer Res *14*, 2065-2074.

Brown, K. (1992). Respiratory Health Effects of Passive Smoking: Lung Cancer and Other Disorders. In, S. Beyard, J. Jinot, and A.M. Koppikar, eds. (Washington DC, USA, Environmental Protection Agency), pp. 1-29.

Bruns, C.J., Shrader, M., Harbison, M.T., Portera, C., Solorzano, C.C., Jauch, K.W., Hicklin, D.J., Radinsky, R., and Ellis, L.M. (2002). Effect of the vascular endothelial growth factor receptor-2 antibody DC101 plus gemcitabine on growth, metastasis and angiogenesis of human pancreatic cancer growing orthotopically in nude mice. Int J Cancer *102*, 101-108.

Bunn, P.A., Jr. (2002). Chemotherapy for advanced non-small-cell lung cancer: who, what, when, why? J Clin Oncol *20*, 23S-33S.

Bussolati, B., Bruno, S., Grange, C., Ferrando, U., and Camussi, G. (2008). Identification of a tumor-initiating stem cell population in human renal carcinomas. FASEB J *22*, 3696-3705.

Bussolati, B., Dunk, C., Grohman, M., Kontos, C.D., Mason, J., and Ahmed, A. (2001). Vascular endothelial growth factor receptor-1 modulates vascular endothelial growth factor-mediated angiogenesis via nitric oxide. Am J Pathol *159*, 993-1008.

Cao, Y., Ji, W.R., Qi, P., and Rosin, A. (1997). Placenta growth factor: identification and characterization of a novel isoform generated by RNA alternative splicing. Biochem Biophys Res Commun *235*, 493-498.

Carmeliet, P. (2005). VEGF as a key mediator of angiogenesis in cancer. Oncology *69 Suppl 3*, 4-10.

Carmeliet, P., and Jain, R.K. (2000). Angiogenesis in cancer and other diseases. Nature *407*, 249-257.

Carmeliet, P., Moons, L., Luttun, A., Vincenti, V., Compernolle, V., De Mol, M., Wu, Y., Bono, F., Devy, L., Beck, H., *et al.* (2001). Synergism between vascular

endothelial growth factor and placental growth factor contributes to angiogenesis and plasma extravasation in pathological conditions. Nat Med *7*, 575-583.

Casanovas, O., Hicklin, D.J., Bergers, G., and Hanahan, D. (2005). Drug resistance by evasion of antiangiogenic targeting of VEGF signaling in late-stage pancreatic islet tumors. Cancer Cell *8*, 299-309.

Cascone, T., Herynk, M.H., Xu, L., Du, Z., Kadara, H., Nilsson, M.B., Oborn, C.J., Park, Y.Y., Erez, B., Jacoby, J.J., *et al.* (2011). Upregulated stromal EGFR and vascular remodeling in mouse xenograft models of angiogenesis inhibitor-resistant human lung adenocarcinoma. J Clin Invest *121*, 1313-1328.

Cerfolio, R.J., Bryant, A.S., Scott, E., Sharma, M., Robert, F., Spencer, S.A., and Garver, R.I. (2006). Women with pathologic stage I, II, and III non-small cell lung cancer have better survival than men. Chest *130*, 1796-1802.

Chen, H., Chedotal, A., He, Z., Goodman, C.S., and Tessier-Lavigne, M. (1997). Neuropilin-2, a novel member of the neuropilin family, is a high affinity receptor for the semaphorins Sema E and Sema IV but not Sema III. Neuron *19*, 547-559.

Chen, H.X., and Cleck, J.N. (2009). Adverse effects of anticancer agents that target the VEGF pathway. Nat Rev Clin Oncol *6*, 465-477.

Chen, J., Imanaka, N., and Griffin, J.D. (2010). Hypoxia potentiates Notch signaling in breast cancer leading to decreased E-cadherin expression and increased cell migration and invasion. Br J Cancer *102*, 351-360.

Choueiri, T.K. (2008). Axitinib, a novel anti-angiogenic drug with promising activity in various solid tumors. Curr Opin Investig Drugs *9*, 658-671.

Choueiri, T.K., Regan, M.M., Rosenberg, J.E., Oh, W.K., Clement, J., Amato, A.M., McDermott, D., Cho, D.C., Atkins, M.B., and Signoretti, S. (2010). Carbonic anhydrase IX and pathological features as predictors of outcome in patients with metastatic clear-cell renal cell carcinoma receiving vascular endothelial growth factor-targeted therapy. BJU Int *106*, 772-778.

Ciardiello, F., Caputo, R., Damiano, V., Troiani, T., Vitagliano, D., Carlomagno, F., Veneziani, B.M., Fontanini, G., Bianco, A.R., and Tortora, G. (2003). Antitumor effects of ZD6474, a small molecule vascular endothelial growth factor receptor tyrosine kinase inhibitor, with additional activity against epidermal growth factor receptor tyrosine kinase. Clin Cancer Res *9*, 1546-1556.

Ciardiello, F., and Tortora, G. (2008). EGFR antagonists in cancer treatment. N Engl J Med *358*, 1160-1174.

Conejo-Garcia, J.R., Buckanovich, R.J., Benencia, F., Courreges, M.C., Rubin, S.C., Carroll, R.G., and Coukos, G. (2005). Vascular leukocytes contribute to tumor vascularization. Blood *105*, 679-681.

Cote, M.L., Kardia, S.L., Wenzlaff, A.S., Ruckdeschel, J.C., and Schwartz, A.G. (2005). Risk of lung cancer among white and black relatives of individuals with early-onset lung cancer. JAMA *293*, 3036-3042.

Curran, W., Scott, C., Langer, C.J., and al, e. (2000). Phase III comparison of sequential vs concurrent chemoradiation for patients (Pts) with unresected stage III non-small cell lung cancer (NSCLC): initial report of Radiation Therapy Oncology Group (RTOG) 9410 [abstract]. Proc Am Soc Clin Oncol *19*, 484a.

Cursiefen, C., Chen, L., Borges, L.P., Jackson, D., Cao, J., Radziejewski, C., D'Amore, P.A., Dana, M.R., Wiegand, S.J., and Streilein, J.W. (2004). VEGF-A stimulates lymphangiogenesis and hemangiogenesis in inflammatory neovascularization via macrophage recruitment. J Clin Invest *113*, 1040-1050.

de Vries, C., Escobedo, J.A., Ueno, H., Houck, K., Ferrara, N., and Williams, L.T. (1992). The fms-like tyrosine kinase, a receptor for vascular endothelial growth factor. Science *255*, 989-991.

Denduluri, N., Yang, S.X., Berman, A.W., Nguyen, D., Liewehr, D.J., Steinberg, S.M., and Swain, S.M. (2008). Circulating biomarkers of bevacizumab activity in patients with breast cancer. Cancer Biol Ther *7*, 15-20.

DePrimo, S.E., and Bello, C. (2007). Surrogate biomarkers in evaluating response to anti-angiogenic agents: focus on sunitinib. Ann Oncol *18 Suppl 10*, x11-19.

Dillman, R.O., Seagren, S.L., Propert, K.J., Guerra, J., Eaton, W.L., Perry, M.C., Carey, R.W., Frei, E.F., 3rd, and Green, M.R. (1990). A randomized trial of induction chemotherapy plus high-dose radiation versus radiation alone in stage III non-small-cell lung cancer. N Engl J Med *323*, 940-945.

Dineen, S.P., Lynn, K.D., Holloway, S.E., Miller, A.F., Sullivan, J.P., Shames, D.S., Beck, A.W., Barnett, C.C., Fleming, J.B., and Brekken, R.A. (2008). Vascular endothelial growth factor receptor 2 mediates macrophage infiltration into orthotopic pancreatic tumors in mice. Cancer Res *68*, 4340-4346.

Dowlati, A., Robertson, K., Radivoyevitch, T., Waas, J., Ziats, N.P., Hartman, P., Abdul-Karim, F.W., Wasman, J.K., Jesberger, J., Lewin, J., *et al.* (2005). Novel Phase I dose de-escalation design trial to determine the biological modulatory dose of the antiangiogenic agent SU5416. Clin Cancer Res *11*, 7938-7944.

Downward, J. (2003). Targeting RAS signalling pathways in cancer therapy. Nat Rev Cancer *3*, 11-22.

Drevs, J., Siegert, P., Medinger, M., Mross, K., Strecker, R., Zirrgiebel, U., Harder, J., Blum, H., Robertson, J., Jurgensmeier, J.M., *et al.* (2007). Phase I clinical study of AZD2171, an oral vascular endothelial growth factor signaling inhibitor, in patients with advanced solid tumors. J Clin Oncol *25*, 3045-3054.

Dumont, D.J., Jussila, L., Taipale, J., Lymboussaki, A., Mustonen, T., Pajusola, K., Breitman, M., and Alitalo, K. (1998). Cardiovascular failure in mouse embryos deficient in VEGF receptor-3. Science *282*, 946-949.

Dvorak, H.F. (2005). Angiogenesis: update 2005. J Thromb Haemost *3*, 1835-1842.

Eberhard, D.A., Johnson, B.E., Amler, L.C., Goddard, A.D., Heldens, S.L., Herbst, R.S., Ince, W.L., Janne, P.A., Januario, T., Johnson, D.H., *et al.* (2005).

Mutations in the epidermal growth factor receptor and in KRAS are predictive and prognostic indicators in patients with non-small-cell lung cancer treated with chemotherapy alone and in combination with erlotinib. J Clin Oncol *23*, 5900-5909.

Ebos, J.M., Bocci, G., Man, S., Thorpe, P.E., Hicklin, D.J., Zhou, D., Jia, X., and Kerbel, R.S. (2004). A naturally occurring soluble form of vascular endothelial growth factor receptor 2 detected in mouse and human plasma. Mol Cancer Res *2*, 315-326.

Ebos, J.M., Lee, C.R., Christensen, J.G., Mutsaers, A.J., and Kerbel, R.S. (2007). Multiple circulating proangiogenic factors induced by sunitinib malate are tumor-independent and correlate with antitumor efficacy. Proc Natl Acad Sci U S A *104*, 17069-17074.

Ebos, J.M., Lee, C.R., Cruz-Munoz, W., Bjarnason, G.A., Christensen, J.G., and Kerbel, R.S. (2009). Accelerated metastasis after short-term treatment with a potent inhibitor of tumor angiogenesis. Cancer Cell *15*, 232-239.

Eriksson, A., Cao, R., Pawliuk, R., Berg, S.M., Tsang, M., Zhou, D., Fleet, C., Tritsaris, K., Dissing, S., Leboulch, P., *et al.* (2002). Placenta growth factor-1 antagonizes VEGF-induced angiogenesis and tumor growth by the formation of functionally inactive PlGF-1/VEGF heterodimers. Cancer Cell *1*, 99-108.

Escudier, B., Pluzanska, A., Koralewski, P., Ravaud, A., Bracarda, S., Szczylik, C., Chevreau, C., Filipek, M., Melichar, B., Bajetta, E., *et al.* (2007). Bevacizumab plus interferon alfa-2a for treatment of metastatic renal cell carcinoma: a randomised, double-blind phase III trial. Lancet *370*, 2103-2111.

Ezzati, M., Henley, S.J., Lopez, A.D., and Thun, M.J. (2005). Role of smoking in global and regional cancer epidemiology: current patterns and data needs. Int J Cancer *116*, 963-971.

Ezzati, M., and Lopez, A.D. (2003). Estimates of global mortality attributable to smoking in 2000. Lancet *362*, 847-852.

Facemire, C.S., Nixon, A.B., Griffiths, R., Hurwitz, H., and Coffman, T.M. (2009). Vascular endothelial growth factor receptor 2 controls blood pressure by regulating nitric oxide synthase expression. Hypertension *54*, 652-658.

Feld, R., Rubinstein, L.V., and Weisenberger, T.H. (1984). Sites of recurrence in resected stage I non-small-cell lung cancer: a guide for future studies. J Clin Oncol *2*, 1352-1358.

Ferrara, N. (2004). Vascular endothelial growth factor: basic science and clinical progress. Endocr Rev *25*, 581-611.

Ferrara, N., Chen, H., Davis-Smyth, T., Gerber, H.P., Nguyen, T.N., Peers, D., Chisholm, V., Hillan, K.J., and Schwall, R.H. (1998). Vascular endothelial growth factor is essential for corpus luteum angiogenesis. Nat Med *4*, 336-340.

Ferrara, N., and Henzel, W.J. (1989). Pituitary follicular cells secrete a novel heparin-binding growth factor specific for vascular endothelial cells. Biochem Biophys Res Commun *161*, 851-858.

Ferrara, N., Hillan, K.J., Gerber, H.P., and Novotny, W. (2004). Discovery and development of bevacizumab, an anti-VEGF antibody for treating cancer. Nat Rev Drug Discov *3*, 391-400.

Fischer, C., Jonckx, B., Mazzone, M., Zacchigna, S., Loges, S., Pattarini, L., Chorianopoulos, E., Liesenborghs, L., Koch, M., De Mol, M., *et al.* (2007). Anti-PlGF inhibits growth of VEGF(R)-inhibitor-resistant tumors without affecting healthy vessels. Cell *131*, 463-475.

Fisher, G.H., Wellen, S.L., Klimstra, D., Lenczowski, J.M., Tichelaar, J.W., Lizak, M.J., Whitsett, J.A., Koretsky, A., and Varmus, H.E. (2001). Induction and apoptotic regression of lung adenocarcinomas by regulation of a K-Ras transgene in the presence and absence of tumor suppressor genes. Genes Dev *15*, 3249-3262.

Fisher, T., Galanti, G., Lavie, G., Jacob-Hirsch, J., Kventsel, I., Zeligson, S., Winkler, R., Simon, A.J., Amariglio, N., Rechavi, G., *et al.* (2007). Mechanisms operative in the antitumor activity of temozolomide in glioblastoma multiforme. Cancer J *13*, 335-344.

Flaherty, K.T., Schiller, J., Schuchter, L.M., Liu, G., Tuveson, D.A., Redlinger, M., Lathia, C., Xia, C., Petrenciuc, O., Hingorani, S.R., *et al.* (2008). A phase I trial of the oral, multikinase inhibitor sorafenib in combination with carboplatin and paclitaxel. Clin Cancer Res *14*, 4836-4842.

Flaumenhaft, R., and Rifkin, D.B. (1992). The extracellular regulation of growth factor action. Mol Biol Cell *3*, 1057-1065.

Folkman, J. (1971). Tumor angiogenesis: therapeutic implications. N Engl J Med *285*, 1182-1186.

Folkman, J. (2007). Angiogenesis: an organizing principle for drug discovery? Nat Rev Drug Discov *6*, 273-286.

Fong, G.H., Rossant, J., Gertsenstein, M., and Breitman, M.L. (1995). Role of the Flt-1 receptor tyrosine kinase in regulating the assembly of vascular endothelium. Nature *376*, 66-70.

Fong, G.H., Zhang, L., Bryce, D.M., and Peng, J. (1999). Increased hemangioblast commitment, not vascular disorganization, is the primary defect in flt-1 knock-out mice. Development *126*, 3015-3025.

Friedman, H.S., Prados, M.D., Wen, P.Y., Mikkelsen, T., Schiff, D., Abrey, L.E., Yung, W.K., Paleologos, N., Nicholas, M.K., Jensen, R., *et al.* (2009). Bevacizumab alone and in combination with irinotecan in recurrent glioblastoma. J Clin Oncol *27*, 4733-4740.

Fukasawa, M., and Korc, M. (2004). Vascular endothelial growth factor-trap suppresses tumorigenicity of multiple pancreatic cancer cell lines. Clin Cancer Res *10*, 3327-3332.

Fukuoka, M., Yano, S., Giaccone, G., Tamura, T., Nakagawa, K., Douillard, J.Y., Nishiwaki, Y., Vansteenkiste, J., Kudoh, S., Rischin, D., *et al.* (2003). Multi-institutional randomized phase II trial of gefitinib for previously treated patients with advanced non-small-cell lung cancer (The IDEAL 1 Trial) [corrected]. J Clin Oncol *21*, 2237-2246.

Furuse, K., Fukuoka, M., Kawahara, M., Nishikawa, H., Takada, Y., Kudoh, S., Katagami, N., and Ariyoshi, Y. (1999). Phase III study of concurrent versus sequential thoracic radiotherapy in combination with mitomycin, vindesine, and cisplatin in unresectable stage III non-small-cell lung cancer. J Clin Oncol *17*, 2692-2699.

Galland, F., Karamysheva, A., Pebusque, M.J., Borg, J.P., Rottapel, R., Dubreuil, P., Rosnet, O., and Birnbaum, D. (1993). The FLT4 gene encodes a transmembrane tyrosine kinase related to the vascular endothelial growth factor receptor. Oncogene *8*, 1233-1240.

Gao, D., Nolan, D.J., Mellick, A.S., Bambino, K., McDonnell, K., and Mittal, V. (2008). Endothelial progenitor cells control the angiogenic switch in mouse lung metastasis. Science *319*, 195-198.

Garin, A., and Proudfoot, A.E. (2011). Chemokines as targets for therapy. Exp Cell Res *317*, 602-612.

Gazdar, A.F. (2007). DNA repair and survival in lung cancer--the two faces of Janus. N Engl J Med *356*, 771-773.

Gazdar, A.F., Girard, L., Lockwood, W.W., Lam, W.L., and Minna, J.D. (2010). Lung cancer cell lines as tools for biomedical discovery and research. J Natl Cancer Inst *102*, 1310-1321.

Gerber, H.-P., Wu, X., Yu, L., Wiesmann, C., Liang, X.H., Lee, C.V., Fuh, G., Olsson, C., Damico, L., Xie, D., Meng, Y.G., Gutierrez, J., Corpuz, R., Li, B., Hall, L., Rangell, L., Ferrando, R., Lowman, H., Peale, F., Ferrara, N. (2007). Mice expressing a humanized form of VEGF-A may provide insights into the safety and efficacy of anti-VEGF antibodies. PNAS *104*, 3478-3484.

Gerber, H.P., Kowalski, J., Sherman, D., Eberhard, D.A., and Ferrara, N. (2000). Complete inhibition of rhabdomyosarcoma xenograft growth and neovascularization requires blockade of both tumor and host vascular endothelial growth factor. Cancer Res *60*, 6253-6258.

Gerber, H.P., Malik, A.K., Solar, G.P., Sherman, D., Liang, X.H., Meng, G., Hong, K., Marsters, J.C., and Ferrara, N. (2002). VEGF regulates haematopoietic stem cell survival by an internal autocrine loop mechanism. Nature *417*, 954-958.

Gerber, H.P., McMurtrey, A., Kowalski, J., Yan, M., Keyt, B.A., Dixit, V., and Ferrara, N. (1998). Vascular endothelial growth factor regulates endothelial cell survival through the phosphatidylinositol 3'-kinase/Akt signal transduction pathway. Requirement for Flk-1/KDR activation. J Biol Chem *273*, 30336-30343.

Gerber, H.P., Vu, T.H., Ryan, A.M., Kowalski, J., Werb, Z., and Ferrara, N. (1999). VEGF couples hypertrophic cartilage remodeling, ossification and angiogenesis during endochondral bone formation. Nat Med *5*, 623-628.

Gerber, H.P., Wu, X., Yu, L., Wiesmann, C., Liang, X.H., Lee, C.V., Fuh, G., Olsson, C., Damico, L., Xie, D., *et al.* (2007). Mice expressing a humanized form of VEGF-A may provide insights into the safety and efficacy of anti-VEGF antibodies. Proc Natl Acad Sci U S A *104*, 3478-3483.

Gerger, A., LaBonte, M., and Lenz, H.J. (2011). Molecular predictors of response to antiangiogenesis therapies. Cancer J *17*, 134-141.

Gerwins, P., Skoldenberg, E., and Claesson-Welsh, L. (2000). Function of fibroblast growth factors and vascular endothelial growth factors and their receptors in angiogenesis. Crit Rev Oncol Hematol *34*, 185-194.

Giaccone, G., Herbst, R.S., Manegold, C., Scagliotti, G., Rosell, R., Miller, V., Natale, R.B., Schiller, J.H., Von Pawel, J., Pluzanska, A., *et al.* (2004). Gefitinib in combination with gemcitabine and cisplatin in advanced non-small-cell lung cancer: a phase III trial--INTACT 1. J Clin Oncol *22*, 777-784.

Giantonio, B.J., Catalano, P.J., Meropol, N.J., O'Dwyer, P.J., Mitchell, E.P., Alberts, S.R., Schwartz, M.A., and Benson, A.B., 3rd (2007). Bevacizumab in combination with oxaliplatin, fluorouracil, and leucovorin (FOLFOX4) for previously treated metastatic colorectal cancer: results from the Eastern Cooperative Oncology Group Study E3200. J Clin Oncol *25*, 1539-1544.

Giger, R.J., Cloutier, J.F., Sahay, A., Prinjha, R.K., Levengood, D.V., Moore, S.E., Pickering, S., Simmons, D., Rastan, S., Walsh, F.S., *et al.* (2000). Neuropilin-2 is required in vivo for selective axon guidance responses to secreted semaphorins. Neuron *25*, 29-41.

Gjerdrum, C., Tiron, C., Hoiby, T., Stefansson, I., Haugen, H., Sandal, T., Collett, K., Li, S., McCormack, E., Gjertsen, B.T., *et al.* (2010). Axl is an essential epithelial-to-mesenchymal transition-induced regulator of breast cancer metastasis and patient survival. Proc Natl Acad Sci U S A *107*, 1124-1129.

Gluzman-Poltorak, Z., Cohen, T., Herzog, Y., and Neufeld, G. (2000). Neuropilin-2 is a receptor for the vascular endothelial growth factor (VEGF) forms VEGF-145 and VEGF-165 [corrected]. J Biol Chem *275*, 18040-18045.

Gordon, M.S., Margolin, K., Talpaz, M., Sledge, G.W., Jr., Holmgren, E., Benjamin, R., Stalter, S., Shak, S., and Adelman, D. (2001). Phase I safety and pharmacokinetic study of recombinant human anti-vascular endothelial growth factor in patients with advanced cancer. J Clin Oncol *19*, 843-850.

Goss, G.D., Arnold, A., Shepherd, F.A., Dediu, M., Ciuleanu, T.E., Fenton, D., Zukin, M., Walde, D., Laberge, F., Vincent, M.D., *et al.* (2010). Randomized, double-blind trial of carboplatin and paclitaxel with either daily oral cediranib or placebo in advanced non-small-cell lung cancer: NCIC clinical trials group BR24 study. J Clin Oncol *28*, 49-55.

Govindan, R., Page, N., Morgensztern, D., Read, W., Tierney, R., Vlahiotis, A., Spitznagel, E.L., and Piccirillo, J. (2006). Changing epidemiology of small-cell lung cancer in the United States over the last 30 years: analysis of the surveillance, epidemiologic, and end results database. J Clin Oncol *24*, 4539-4544.

Grivennikov, S.I., Greten, F.R., and Karin, M. (2010). Immunity, inflammation, and cancer. Cell *140*, 883-899.

Grothey, A., and Galanis, E. (2009). Targeting angiogenesis: progress with anti-VEGF treatment with large molecules. Nat Rev Clin Oncol *6*, 507-518.

Hainsworth, J., and Herbst, R. (2008). A phase III, multicenter, placebo-controlled, double-blind, randomized clinical trial to evaluate the efficacy of bevacizumab (Avastin) in combination iwth erlotinib (Tarceva) compared with erlotinib alone in treatment of advance non-small cell lung cacner after failure of standard first-line chemotherapy (BETA). J Thorac Oncol *3*, 1487.

Hanahan, D., and Folkman, J. (1996). Patterns and emerging mechanisms of the angiogenic switch during tumorigenesis. Cell *86*, 353-364.

Hanahan, D., and Weinberg, R.A. (2000). The hallmarks of cancer. Cell *100*, 57-70.

Hanna, N., Bunn, P.A., Jr., Langer, C., Einhorn, L., Guthrie, T., Jr., Beck, T., Ansari, R., Ellis, P., Byrne, M., Morrison, M., *et al.* (2006a). Randomized phase III trial comparing irinotecan/cisplatin with etoposide/cisplatin in patients with previously untreated extensive-stage disease small-cell lung cancer. J Clin Oncol *24*, 2038-2043.

Hanna, N., Lilenbaum, R., Ansari, R., Lynch, T., Govindan, R., Janne, P.A., and Bonomi, P. (2006b). Phase II trial of cetuximab in patients with previously treated non-small-cell lung cancer. J Clin Oncol *24*, 5253-5258.

Harichand-Herdt, S., and Ramalingam, S.S. (2009). Gender-associated differences in lung cancer: clinical characteristics and treatment outcomes in women. Semin Oncol *36*, 572-580.

Harris, J.E. (1983). Cigarette smoking among successive birth cohorts of men and women in the United States during 1900-80. J Natl Cancer Inst *71*, 473-479.

Hasselbalch, B., Eriksen, J.G., Broholm, H., Christensen, I.J., Grunnet, K., Horsman, M.R., Poulsen, H.S., Stockhausen, M.T., and Lassen, U. (2010). Prospective evaluation of angiogenic, hypoxic and EGFR-related biomarkers in recurrent glioblastoma multiforme treated with cetuximab, bevacizumab and irinotecan. APMIS *118*, 585-594.

Hattori, K., Heissig, B., Wu, Y., Dias, S., Tejada, R., Ferris, B., Hicklin, D.J., Zhu, Z., Bohlen, P., Witte, L., *et al.* (2002). Placental growth factor reconstitutes hematopoiesis by recruiting VEGFR1(+) stem cells from bone-marrow microenvironment. Nat Med *8*, 841-849.

Hecht, S.S. (2003). Tobacco carcinogens, their biomarkers and tobacco-induced cancer. Nat Rev Cancer *3*, 733-744.

Herbst, R.S., Giaccone, G., Schiller, J.H., Natale, R.B., Miller, V., Manegold, C., Scagliotti, G., Rosell, R., Oliff, I., Reeves, J.A., *et al.* (2004). Gefitinib in combination with paclitaxel and carboplatin in advanced non-small-cell lung cancer: a phase III trial--INTACT 2. J Clin Oncol *22*, 785-794.

Herbst, R.S., Heymach, J.V., and Lippman, S.M. (2008). Lung cancer. N Engl J Med *359*, 1367-1380.

Herbst, R.S., O'Neill, V.J., Fehrenbacher, L., Belani, C.P., Bonomi, P.D., Hart, L., Melnyk, O., Ramies, D., Lin, M., and Sandler, A. (2007). Phase II study of efficacy and safety of bevacizumab in combination with chemotherapy or erlotinib compared with chemotherapy alone for treatment of recurrent or refractory non small-cell lung cancer. J Clin Oncol *25*, 4743-4750.

Herbst, R.S., Prager, D., Hermann, R., Fehrenbacher, L., Johnson, B.E., Sandler, A., Kris, M.G., Tran, H.T., Klein, P., Li, X., *et al.* (2005). TRIBUTE: a phase III trial of erlotinib hydrochloride (OSI-774) combined with carboplatin and paclitaxel chemotherapy in advanced non-small-cell lung cancer. J Clin Oncol *23*, 5892-5899.

Herbst, R.S., Sun, Y., Eberhardt, W.E., Germonpre, P., Saijo, N., Zhou, C., Wang, J., Li, L., Kabbinavar, F., Ichinose, Y., *et al.* (2010). Vandetanib plus docetaxel

versus docetaxel as second-line treatment for patients with advanced non-small-cell lung cancer (ZODIAC): a double-blind, randomised, phase 3 trial. Lancet Oncol *11*, 619-626.

Hida, K., Hida, Y., and Shindoh, M. (2008). Understanding tumor endothelial cell abnormalities to develop ideal anti-angiogenic therapies. Cancer Sci *99*, 459-466.

Hirakawa, S., Kodama, S., Kunstfeld, R., Kajiya, K., Brown, L.F., and Detmar, M. (2005). VEGF-A induces tumor and sentinel lymph node lymphangiogenesis and promotes lymphatic metastasis. J Exp Med *201*, 1089-1099.

Hiratsuka, S., Minowa, O., Kuno, J., Noda, T., and Shibuya, M. (1998). Flt-1 lacking the tyrosine kinase domain is sufficient for normal development and angiogenesis in mice. Proc Natl Acad Sci U S A *95*, 9349-9354.

Hiratsuka, S., Nakamura, K., Iwai, S., Murakami, M., Itoh, T., Kijima, H., Shipley, J.M., Senior, R.M., and Shibuya, M. (2002). MMP9 induction by vascular endothelial growth factor receptor-1 is involved in lung-specific metastasis. Cancer Cell *2*, 289-300.

Hirsch, F.R., Varella-Garcia, M., Bunn, P.A., Jr., Di Maria, M.V., Veve, R., Bremmes, R.M., Baron, A.E., Zeng, C., and Franklin, W.A. (2003). Epidermal growth factor receptor in non-small-cell lung carcinomas: correlation between gene copy number and protein expression and impact on prognosis. J Clin Oncol *21*, 3798-3807.

Hoeben, A., Landuyt, B., Highley, M.S., Wildiers, H., Van Oosterom, A.T., and De Bruijn, E.A. (2004). Vascular endothelial growth factor and angiogenesis. Pharmacol Rev *56*, 549-580.

Hoffman, P.C., Mauer, A.M., and Vokes, E.E. (2000). Lung cancer. Lancet *355*, 479-485.

Holash, J., Davis, S., Papadopoulos, N., Croll, S.D., Ho, L., Russell, M., Boland, P., Leidich, R., Hylton, D., Burova, E., *et al.* (2002). VEGF-Trap: a VEGF

blocker with potent antitumor effects. Proc Natl Acad Sci U S A *99*, 11393-11398.

Holland, S.J., Pan, A., Franci, C., Hu, Y., Chang, B., Li, W., Duan, M., Torneros, A., Yu, J., Heckrodt, T.J., *et al.* (2010). R428, a selective small molecule inhibitor of Axl kinase, blocks tumor spread and prolongs survival in models of metastatic breast cancer. Cancer Res *70*, 1544-1554.

Holloway, S.E., Beck, A.W., Shivakumar, L., Shih, J., Fleming, J.B., and Brekken, R.A. (2006). Selective blockade of vascular endothelial growth factor receptor 2 with an antibody against tumor-derived vascular endothelial growth factor controls the growth of human pancreatic adenocarcinoma xenografts. Ann Surg Oncol *13*, 1145-1155.

Horn, L., and Pao, W. (2009). EML4-ALK: honing in on a new target in non-small-cell lung cancer. J Clin Oncol *27*, 4232-4235.

Houck, K.A., Ferrara, N., Winer, J., Cachianes, G., Li, B., and Leung, D.W. (1991). The vascular endothelial growth factor family: identification of a fourth molecular species and characterization of alternative splicing of RNA. Mol Endocrinol *5*, 1806-1814.

Houck, K.A., Leung, D.W., Rowland, A.M., Winer, J., and Ferrara, N. (1992). Dual regulation of vascular endothelial growth factor bioavailability by genetic and proteolytic mechanisms. J Biol Chem *267*, 26031-26037.

Hu, L., Hofmann, J., Holash, J., Yancopoulos, G.D., Sood, A.K., and Jaffe, R.B. (2005). Vascular endothelial growth factor trap combined with paclitaxel strikingly inhibits tumor and ascites, prolonging survival in a human ovarian cancer model. Clin Cancer Res *11*, 6966-6971.

Huang, J., Frischer, J.S., Serur, A., Kadenhe, A., Yokoi, A., McCrudden, K.W., New, T., O'Toole, K., Zabski, S., Rudge, J.S., *et al.* (2003). Regression of established tumors and metastases by potent vascular endothelial growth factor blockade. Proc Natl Acad Sci U S A *100*, 7785-7790.

Huang, X., Gottstein, C., Brekken, R.A., and Thorpe, P.E. (1998). Expression of soluble VEGF receptor 2 and characterization of its binding by surface plasmon resonance. Biochem Biophys Res Commun *252*, 643-648.

Hurwitz, H., Fehrenbacher, L., Novotny, W., Cartwright, T., Hainsworth, J., Heim, W., Berlin, J., Baron, A., Griffing, S., Holmgren, E., *et al.* (2004). Bevacizumab plus irinotecan, fluorouracil, and leucovorin for metastatic colorectal cancer. N Engl J Med *350*, 2335-2342.

Hutson, T.E. (2011). Targeted therapies for the treatment of metastatic renal cell carcinoma: clinical evidence. Oncologist *16 Suppl 2*, 14-22.

Inukai, M., Toyooka, S., Ito, S., Asano, H., Ichihara, S., Soh, J., Suehisa, H., Ouchida, M., Aoe, K., Aoe, M., *et al.* (2006). Presence of epidermal growth factor receptor gene T790M mutation as a minor clone in non-small cell lung cancer. Cancer Res *66*, 7854-7858.

Jain, R.K. (2001). Normalizing tumor vasculature with anti-angiogenic therapy: a new paradigm for combination therapy. Nat Med *7*, 987-989.

Jain, R.K. (2003). Molecular regulation of vessel maturation. Nat Med *9*, 685-693.

Jain, R.K. (2005). Normalization of tumor vasculature: an emerging concept in antiangiogenic therapy. Science *307*, 58-62.

Jain, R.K., Duda, D.G., Clark, J.W., and Loeffler, J.S. (2006). Lessons from phase III clinical trials on anti-VEGF therapy for cancer. Nat Clin Pract Oncol *3*, 24-40.

Jain, R.K., Duda, D.G., Willett, C.G., Sahani, D.V., Zhu, A.X., Loeffler, J.S., Batchelor, T.T., and Sorensen, A.G. (2009). Biomarkers of response and resistance to antiangiogenic therapy. Nat Rev Clin Oncol *6*, 327-338.

Jayson, G.C., Zweit, J., Jackson, A., Mulatero, C., Julyan, P., Ranson, M., Broughton, L., Wagstaff, J., Hakannson, L., Groenewegen, G., *et al.* (2002).

Molecular imaging and biological evaluation of HuMV833 anti-VEGF antibody: implications for trial design of antiangiogenic antibodies. J Natl Cancer Inst *94*, 1484-1493.

Jemal, A., Bray, F., Center, M.M., Ferlay, J., Ward, E., and Forman, D. (2011). Global cancer statistics. CA Cancer J Clin *61*, 69-90.

Jemal, A., Center, M.M., DeSantis, C., and Ward, E.M. (2010a). Global patterns of cancer incidence and mortality rates and trends. Cancer Epidemiol Biomarkers Prev *19*, 1893-1907.

Jemal, A., Chu, K.C., and Tarone, R.E. (2001). Recent trends in lung cancer mortality in the United States. J Natl Cancer Inst *93*, 277-283.

Jemal, A., Siegel, R., Xu, J., and Ward, E. (2010b). Cancer statistics, 2010. CA Cancer J Clin *60*, 277-300.

Jemal, A., Thun, M.J., Ries, L.A., Howe, H.L., Weir, H.K., Center, M.M., Ward, E., Wu, X.C., Eheman, C., Anderson, R., *et al.* (2008). Annual report to the nation on the status of cancer, 1975-2005, featuring trends in lung cancer, tobacco use, and tobacco control. J Natl Cancer Inst *100*, 1672-1694.

Jemal, A., Ward, E., and Thun, M.J. (2005). Contemporary lung cancer trends among U.S. women. Cancer Epidemiol Biomarkers Prev *14*, 582-585.

Jindal, S.K., Malik, S.K., Dhand, R., Gujral, J.S., Malik, A.K., and Datta, B.N. (1982). Bronchogenic carcinoma in Northern India. Thorax *37*, 343-347.

Johnson, D.H., Fehrenbacher, L., Novotny, W.F., Herbst, R.S., Nemunaitis, J.J., Jablons, D.M., Langer, C.J., DeVore, R.F., 3rd, Gaudreault, J., Damico, L.A., *et al.* (2004). Randomized phase II trial comparing bevacizumab plus carboplatin and paclitaxel with carboplatin and paclitaxel alone in previously untreated locally advanced or metastatic non-small-cell lung cancer. J Clin Oncol *22*, 2184-2191.

Jubb, A.M., Hurwitz, H.I., Bai, W., Holmgren, E.B., Tobin, P., Guerrero, A.S., Kabbinavar, F., Holden, S.N., Novotny, W.F., Frantz, G.D., *et al.* (2006). Impact of vascular endothelial growth factor-A expression, thrombospondin-2 expression, and microvessel density on the treatment effect of bevacizumab in metastatic colorectal cancer. J Clin Oncol *24*, 217-227.

Kaipainen, A., Korhonen, J., Mustonen, T., van Hinsbergh, V.W., Fang, G.H., Dumont, D., Breitman, M., and Alitalo, K. (1995). Expression of the fms-like tyrosine kinase 4 gene becomes restricted to lymphatic endothelium during development. Proc Natl Acad Sci U S A *92*, 3566-3570.

Kamba, T., and McDonald, D.M. (2007). Mechanisms of adverse effects of anti-VEGF therapy for cancer. Br J Cancer *96*, 1788-1795.

Kamba, T., Tam, B.Y., Hashizume, H., Haskell, A., Sennino, B., Mancuso, M.R., Norberg, S.M., O'Brien, S.M., Davis, R.B., Gowen, L.C., *et al.* (2006). VEGF-dependent plasticity of fenestrated capillaries in the normal adult microvasculature. Am J Physiol Heart Circ Physiol *290*, H560-576.

Kaplan, R.N., Riba, R.D., Zacharoulis, S., Bramley, A.H., Vincent, L., Costa, C., MacDonald, D.D., Jin, D.K., Shido, K., Kerns, S.A., *et al.* (2005). VEGFR1-positive haematopoietic bone marrow progenitors initiate the pre-metastatic niche. Nature *438*, 820-827.

Karkkainen, M.J., Haiko, P., Sainio, K., Partanen, J., Taipale, J., Petrova, T.V., Jeltsch, M., Jackson, D.G., Talikka, M., Rauvala, H., *et al.* (2004). Vascular endothelial growth factor C is required for sprouting of the first lymphatic vessels from embryonic veins. Nat Immunol *5*, 74-80.

Karkkainen, M.J., Saaristo, A., Jussila, L., Karila, K.A., Lawrence, E.C., Pajusola, K., Bueler, H., Eichmann, A., Kauppinen, R., Kettunen, M.I., *et al.* (2001). A model for gene therapy of human hereditary lymphedema. Proc Natl Acad Sci U S A *98*, 12677-12682.

Keeley, E.C., Mehrad, B., and Strieter, R.M. (2011). Chemokines as mediators of tumor angiogenesis and neovascularization. Exp Cell Res *317*, 685-690.

Kelly, K., Chansky, K., Gaspar, L.E., Albain, K.S., Jett, J., Ung, Y.C., Lau, D.H., Crowley, J.J., and Gandara, D.R. (2008). Phase III trial of maintenance gefitinib or placebo after concurrent chemoradiotherapy and docetaxel consolidation in inoperable stage III non-small-cell lung cancer: SWOG S0023. J Clin Oncol *26*, 2450-2456.

Kelly, K., Crowley, J., Bunn, P.A., Jr., Presant, C.A., Grevstad, P.K., Moinpour, C.M., Ramsey, S.D., Wozniak, A.J., Weiss, G.R., Moore, D.F., *et al.* (2001). Randomized phase III trial of paclitaxel plus carboplatin versus vinorelbine plus cisplatin in the treatment of patients with advanced non--small-cell lung cancer: a Southwest Oncology Group trial. J Clin Oncol *19*, 3210-3218.

Kendall, R.L., and Thomas, K.A. (1993). Inhibition of vascular endothelial cell growth factor activity by an endogenously encoded soluble receptor. Proc Natl Acad Sci U S A *90*, 10705-10709.

Kerbel, R.S. (2006). Antiangiogenic therapy: a universal chemosensitization strategy for cancer? Science *312*, 1171-1175.

Keyt, B.A., Berleau, L.T., Nguyen, H.V., Chen, H., Heinsohn, H., Vandlen, R., and Ferrara, N. (1996). The carboxyl-terminal domain (111-165) of vascular endothelial growth factor is critical for its mitogenic potency. J Biol Chem *271*, 7788-7795.

Kim, E.S., Hirsh, V., Mok, T., Socinski, M.A., Gervais, R., Wu, Y.L., Li, L.Y., Watkins, C.L., Sellers, M.V., Lowe, E.S., *et al.* (2008). Gefitinib versus docetaxel in previously treated non-small-cell lung cancer (INTEREST): a randomised phase III trial. Lancet *372*, 1809-1818.

Kim, K.J., Li, B., Winer, J., Armanini, M., Gillett, N., Phillips, H.S., and Ferrara, N. (1993). Inhibition of vascular endothelial growth factor-induced angiogenesis suppresses tumour growth in vivo. Nature *362*, 841-844.

Kitsukawa, T., Shimizu, M., Sanbo, M., Hirata, T., Taniguchi, M., Bekku, Y., Yagi, T., and Fujisawa, H. (1997). Neuropilin-semaphorin III/D-mediated

chemorepulsive signals play a crucial role in peripheral nerve projection in mice. Neuron *19*, 995-1005.

Kitsukawa, T., Shimono, A., Kawakami, A., Kondoh, H., and Fujisawa, H. (1995). Overexpression of a membrane protein, neuropilin, in chimeric mice causes anomalies in the cardiovascular system, nervous system and limbs. Development *121*, 4309-4318.

Kleinerman, R.A., Wang, Z., Wang, L., Metayer, C., Zhang, S., Brenner, A.V., Xia, Y., Shang, B., and Lubin, J.H. (2002). Lung cancer and indoor exposure to coal and biomass in rural China. J Occup Environ Med *44*, 338-344.

Kobayashi, S., Boggon, T.J., Dayaram, T., Janne, P.A., Kocher, O., Meyerson, M., Johnson, B.E., Eck, M.J., Tenen, D.G., and Halmos, B. (2005). EGFR mutation and resistance of non-small-cell lung cancer to gefitinib. N Engl J Med *352*, 786-792.

Kopetz, S., Hoff, P.M., Morris, J.S., Wolff, R.A., Eng, C., Glover, K.Y., Adinin, R., Overman, M.J., Valero, V., Wen, S., *et al.* (2010). Phase II trial of infusional fluorouracil, irinotecan, and bevacizumab for metastatic colorectal cancer: efficacy and circulating angiogenic biomarkers associated with therapeutic resistance. J Clin Oncol *28*, 453-459.

Kosaka, T., Yatabe, Y., Endoh, H., Kuwano, H., Takahashi, T., and Mitsudomi, T. (2004). Mutations of the epidermal growth factor receptor gene in lung cancer: biological and clinical implications. Cancer Res *64*, 8919-8923.

Koukourakis, M.I., Papazoglou, D., Giatromanolaki, A., Bougioukas, G., Maltezos, E., and Sivridis, E. (2004). VEGF gene sequence variation defines VEGF gene expression status and angiogenic activity in non-small cell lung cancer. Lung Cancer *46*, 293-298.

Kris, M.G., Natale, R.B., Herbst, R.S., Lynch, T.J., Jr., Prager, D., Belani, C.P., Schiller, J.H., Kelly, K., Spiridonidis, H., Sandler, A., *et al.* (2003). Efficacy of gefitinib, an inhibitor of the epidermal growth factor receptor tyrosine kinase, in

symptomatic patients with non-small cell lung cancer: a randomized trial. JAMA *290*, 2149-2158.

Kumar, R., Knick, V.B., Rudolph, S.K., Johnson, J.H., Crosby, R.M., Crouthamel, M.C., Hopper, T.M., Miller, C.G., Harrington, L.E., Onori, J.A., *et al.* (2007). Pharmacokinetic-pharmacodynamic correlation from mouse to human with pazopanib, a multikinase angiogenesis inhibitor with potent antitumor and antiangiogenic activity. Mol Cancer Ther *6*, 2012-2021.

Kuwana, H., Terada, Y., Kobayashi, T., Okado, T., Penninger, J.M., Irie-Sasaki, J., Sasaki, T., and Sasaki, S. (2008). The phosphoinositide-3 kinase gamma-Akt pathway mediates renal tubular injury in cisplatin nephrotoxicity. Kidney Int *73*, 430-445.

Lam, W.K., White, N.W., and Chan-Yeung, M.M. (2004). Lung cancer epidemiology and risk factors in Asia and Africa. Int J Tuberc Lung Dis *8*, 1045-1057.

Lara, P.N., Jr., Natale, R., Crowley, J., Lenz, H.J., Redman, M.W., Carleton, J.E., Jett, J., Langer, C.J., Kuebler, J.P., Dakhil, S.R., *et al.* (2009). Phase III trial of irinotecan/cisplatin compared with etoposide/cisplatin in extensive-stage small-cell lung cancer: clinical and pharmacogenomic results from SWOG S0124. J Clin Oncol *27*, 2530-2535.

Le Calvez, F., Mukeria, A., Hunt, J.D., Kelm, O., Hung, R.J., Taniere, P., Brennan, P., Boffetta, P., Zaridze, D.G., and Hainaut, P. (2005). TP53 and KRAS mutation load and types in lung cancers in relation to tobacco smoke: distinct patterns in never, former, and current smokers. Cancer Res *65*, 5076-5083.

Le Chevalier, T., Arriagada, R., Quoix, E., Ruffie, P., Martin, M., Tarayre, M., Lacombe-Terrier, M.J., Douillard, J.Y., and Laplanche, A. (1991). Radiotherapy alone versus combined chemotherapy and radiotherapy in nonresectable non-small-cell lung cancer: first analysis of a randomized trial in 353 patients. J Natl Cancer Inst *83*, 417-423.

LeCouter, J., Moritz, D.R., Li, B., Phillips, G.L., Liang, X.H., Gerber, H.P., Hillan, K.J., and Ferrara, N. (2003). Angiogenesis-independent endothelial protection of liver: role of VEGFR-1. Science *299*, 890-893.

Lee, S., Jilani, S.M., Nikolova, G.V., Carpizo, D., and Iruela-Arispe, M.L. (2005). Processing of VEGF-A by matrix metalloproteinases regulates bioavailability and vascular patterning in tumors. J Cell Biol *169*, 681-691.

Less, J.R., Skalak, T.C., Sevick, E.M., and Jain, R.K. (1991). Microvascular architecture in a mammary carcinoma: branching patterns and vessel dimensions. Cancer Res *51*, 265-273.

Leung, D.W., Cachianes, G., Kuang, W.J., Goeddel, D.V., and Ferrara, N. (1989). Vascular endothelial growth factor is a secreted angiogenic mitogen. Science *246*, 1306-1309.

Li, Y., Ye, X., Tan, C., Hongo, J.A., Zha, J., Liu, J., Kallop, D., Ludlam, M.J., and Pei, L. (2009). Axl as a potential therapeutic target in cancer: role of Axl in tumor growth, metastasis and angiogenesis. Oncogene *28*, 3442-3455.

Liang, W.C., Wu, X., Peale, F.V., Lee, C.V., Meng, Y.G., Gutierrez, J., Fu, L., Malik, A.K., Gerber, H.P., Ferrara, N., *et al.* (2006a). Cross-species vascular endothelial growth factor (VEGF)-blocking antibodies completely inhibit the growth of human tumor xenografts and measure the contribution of stromal VEGF. J Biol Chem *281*, 951-961.

Liang, Y., Brekken, R.A., and Hyder, S.M. (2006b). Vascular endothelial growth factor induces proliferation of breast cancer cells and inhibits the anti-proliferative activity of anti-hormones. Endocr Relat Cancer *13*, 905-919.

Lilenbaum, R.C., Herndon, J.E., 2nd, List, M.A., Desch, C., Watson, D.M., Miller, A.A., Graziano, S.L., Perry, M.C., Saville, W., Chahinian, P., *et al.* (2005). Single-agent versus combination chemotherapy in advanced non-small-cell lung cancer: the cancer and leukemia group B (study 9730). J Clin Oncol *23*, 190-196.

Lin, Y.S., Nguyen, C., Mendoza, J.L., Escandon, E., Fei, D., Meng, Y.G., and Modi, N.B. (1999). Preclinical pharmacokinetics, interspecies scaling, and tissue distribution of a humanized monoclonal antibody against vascular endothelial growth factor. J Pharmacol Exp Ther *288*, 371-378.

Linger, R.M., Keating, A.K., Earp, H.S., and Graham, D.K. (2008). TAM receptor tyrosine kinases: biologic functions, signaling, and potential therapeutic targeting in human cancer. Adv Cancer Res *100*, 35-83.

LoRusso, P.M., Heath, E., Valdivieso, M., Pilar, M., and al., E. (2006). Phase I evaluation of AZD2171, a highly potent and selective inhibitor of VEGFR signaling, in combination with selected chemotherapy regimens in patients with advanced solid tumors. J Clin Oncol *24*, Abstract 3034.

Loupakis, F., Falcone, A., Masi, G., Fioravanti, A., Kerbel, R.S., Del Tacca, M., and Bocci, G. (2007). Vascular endothelial growth factor levels in immunodepleted plasma of cancer patients as a possible pharmacodynamic marker for bevacizumab activity. J Clin Oncol *25*, 1816-1818.

Lu, D., Jimenez, X., Zhang, H., Bohlen, P., Witte, L., and Zhu, Z. (2002). Selection of high affinity human neutralizing antibodies to VEGFR2 from a large antibody phage display library for antiangiogenesis therapy. Int J Cancer *97*, 393-399.

Lu, D., Shen, J., Vil, M.D., Zhang, H., Jimenez, X., Bohlen, P., Witte, L., and Zhu, Z. (2003). Tailoring in vitro selection for a picomolar affinity human antibody directed against vascular endothelial growth factor receptor 2 for enhanced neutralizing activity. J Biol Chem *278*, 43496-43507.

Lucio-Eterovic, A.K., Piao, Y., and de Groot, J.F. (2009). Mediators of glioblastoma resistance and invasion during antivascular endothelial growth factor therapy. Clin Cancer Res *15*, 4589-4599.

Ludwig, J.A., and Weinstein, J.N. (2005). Biomarkers in cancer staging, prognosis and treatment selection. Nat Rev Cancer *5*, 845-856.

Luo, Y., He, D.L., Ning, L., Shen, S.L., Li, L., Li, X., Zhau, H.E., and Chung, L.W. (2006). Over-expression of hypoxia-inducible factor-1alpha increases the invasive potency of LNCaP cells in vitro. BJU Int *98*, 1315-1319.

Luttun, A., Tjwa, M., Moons, L., Wu, Y., Angelillo-Scherrer, A., Liao, F., Nagy, J.A., Hooper, A., Priller, J., De Klerck, B., *et al.* (2002). Revascularization of ischemic tissues by PlGF treatment, and inhibition of tumor angiogenesis, arthritis and atherosclerosis by anti-Flt1. Nat Med *8*, 831-840.

Lyden, D., Hattori, K., Dias, S., Costa, C., Blaikie, P., Butros, L., Chadburn, A., Heissig, B., Marks, W., Witte, L., *et al.* (2001). Impaired recruitment of bone-marrow-derived endothelial and hematopoietic precursor cells blocks tumor angiogenesis and growth. Nat Med *7*, 1194-1201.

Lymboussaki, A., Olofsson, B., Eriksson, U., and Alitalo, K. (1999). Vascular endothelial growth factor (VEGF) and VEGF-C show overlapping binding sites in embryonic endothelia and distinct sites in differentiated adult endothelia. Circ Res *85*, 992-999.

Lynch, T.J., Bell, D.W., Sordella, R., Gurubhagavatula, S., Okimoto, R.A., Brannigan, B.W., Harris, P.L., Haserlat, S.M., Supko, J.G., Haluska, F.G., *et al.* (2004). Activating mutations in the epidermal growth factor receptor underlying responsiveness of non-small-cell lung cancer to gefitinib. N Engl J Med *350*, 2129-2139.

Maemondo, M., Inoue, A., Kobayashi, K., Sugawara, S., Oizumi, S., Isobe, H., Gemma, A., Harada, M., Yoshizawa, H., Kinoshita, I., *et al.* (2010). Gefitinib or chemotherapy for non-small-cell lung cancer with mutated EGFR. N Engl J Med *362*, 2380-2388.

Maglione, D., Guerriero, V., Viglietto, G., Delli-Bovi, P., and Persico, M.G. (1991). Isolation of a human placenta cDNA coding for a protein related to the vascular permeability factor. Proc Natl Acad Sci U S A *88*, 9267-9271.

Majka, S., Fox, K., McGuire, B., Crossno, J., Jr., McGuire, P., and Izzo, A. (2006). Pleiotropic role of VEGF-A in regulating fetal pulmonary mesenchymal cell turnover. Am J Physiol Lung Cell Mol Physiol *290*, L1183-1192.

Makinen, T., Olofsson, B., Karpanen, T., Hellman, U., Soker, S., Klagsbrun, M., Eriksson, U., and Alitalo, K. (1999). Differential binding of vascular endothelial growth factor B splice and proteolytic isoforms to neuropilin-1. J Biol Chem *274*, 21217-21222.

Mamluk, R., Gechtman, Z., Kutcher, M.E., Gasiunas, N., Gallagher, J., and Klagsbrun, M. (2002). Neuropilin-1 binds vascular endothelial growth factor 165, placenta growth factor-2, and heparin via its b1b2 domain. J Biol Chem *277*, 24818-24825.

Margolin, K., Gordon, M.S., Holmgren, E., Gaudreault, J., Novotny, W., Fyfe, G., Adelman, D., Stalter, S., and Breed, J. (2001). Phase Ib trial of intravenous recombinant humanized monoclonal antibody to vascular endothelial growth factor in combination with chemotherapy in patients with advanced cancer: pharmacologic and long-term safety data. J Clin Oncol *19*, 851-856.

Martin, L.P., Kozloff, M.F., Krzakowski, M., Samuel, T.A., and al., E. (2009). Axitinib (AG-013736; AG) combined with chemotherapy in patients (pts) with advanced non-small cell lung cancer (NSCLC) and other solid tumors. J Clin Oncol *27*, Abstract 3559.

Mascaux, C., Iannino, N., Martin, B., Paesmans, M., Berghmans, T., Dusart, M., Haller, A., Lothaire, P., Meert, A.P., Noel, S., *et al.* (2005). The role of RAS oncogene in survival of patients with lung cancer: a systematic review of the literature with meta-analysis. Br J Cancer *92*, 131-139.

Matakidou, A., Eisen, T., and Houlston, R.S. (2005). Systematic review of the relationship between family history and lung cancer risk. Br J Cancer *93*, 825-833.

Melnyk, O., Shuman, M.A., and Kim, K.J. (1996). Vascular endothelial growth factor promotes tumor dissemination by a mechanism distinct from its effect on primary tumor growth. Cancer Res *56*, 921-924.

Miao, H.Q., Hu, K., Jimenez, X., Navarro, E., Zhang, H., Lu, D., Ludwig, D.L., Balderes, P., and Zhu, Z. (2006). Potent neutralization of VEGF biological activities with a fully human antibody Fab fragment directed against VEGF receptor 2. Biochem Biophys Res Commun *345*, 438-445.

Migdal, M., Huppertz, B., Tessler, S., Comforti, A., Shibuya, M., Reich, R., Baumann, H., and Neufeld, G. (1998). Neuropilin-1 is a placenta growth factor-2 receptor. J Biol Chem *273*, 22272-22278.

Mignatti, P., and Rifkin, D.B. (1993). Biology and biochemistry of proteinases in tumor invasion. Physiol Rev *73*, 161-195.

Millauer, B., Wizigmann-Voos, S., Schnurch, H., Martinez, R., Moller, N.P., Risau, W., and Ullrich, A. (1993). High affinity VEGF binding and developmental expression suggest Flk-1 as a major regulator of vasculogenesis and angiogenesis. Cell *72*, 835-846.

Miller, K., Wang, M., Gralow, J., Dickler, M., Cobleigh, M., Perez, E.A., Shenkier, T., Cella, D., and Davidson, N.E. (2007). Paclitaxel plus bevacizumab versus paclitaxel alone for metastatic breast cancer. N Engl J Med *357*, 2666-2676.

Miller, K.D., Chap, L.I., Holmes, F.A., Cobleigh, M.A., Marcom, P.K., Fehrenbacher, L., Dickler, M., Overmoyer, B.A., Reimann, J.D., Sing, A.P., *et al.* (2005). Randomized phase III trial of capecitabine compared with bevacizumab plus capecitabine in patients with previously treated metastatic breast cancer. J Clin Oncol *23*, 792-799.

Miller, V.A., O'Connor, P., Soh, C., and al., E. (2009). A randomized, double-blind, placebo-controlled, phase IIIb trial (ATLAS) comparing bevacizumab (B) therapy with or without erlotinib (E) after completion of chemotherapy with B for

first-line treatment of locally advanced, recurrent, or metastatic non-small cell lung cancer (NSCLC). J Clin Oncol *27*, Abstract 8002.

Mills, C.N., Joshi, S.S., and Niles, R.M. (2009). Expression and function of hypoxia inducible factor-1 alpha in human melanoma under non-hypoxic conditions. Mol Cancer *8*, 104.

Mitchell, D.C., and Bryan, B.A. (2010). Anti-angiogenic therapy: adapting strategies to overcome resistant tumors. J Cell Biochem *111*, 543-553.

Mitsudomi, T., Morita, S., Yatabe, Y., Negoro, S., Okamoto, I., Tsurutani, J., Seto, T., Satouchi, M., Tada, H., Hirashima, T., *et al.* (2010). Gefitinib versus cisplatin plus docetaxel in patients with non-small-cell lung cancer harbouring mutations of the epidermal growth factor receptor (WJTOG3405): an open label, randomised phase 3 trial. Lancet Oncol *11*, 121-128.

Mok, T.S., Wu, Y.L., Thongprasert, S., Yang, C.H., Chu, D.T., Saijo, N., Sunpaweravong, P., Han, B., Margono, B., Ichinose, Y., *et al.* (2009). Gefitinib or carboplatin-paclitaxel in pulmonary adenocarcinoma. N Engl J Med *361*, 947-957.

Motzer, R.J., Michaelson, M.D., Redman, B.G., Hudes, G.R., Wilding, G., Figlin, R.A., Ginsberg, M.S., Kim, S.T., Baum, C.M., DePrimo, S.E., *et al.* (2006). Activity of SU11248, a multitargeted inhibitor of vascular endothelial growth factor receptor and platelet-derived growth factor receptor, in patients with metastatic renal cell carcinoma. J Clin Oncol *24*, 16-24.

Mukohara, T., Engelman, J.A., Hanna, N.H., Yeap, B.Y., Kobayashi, S., Lindeman, N., Halmos, B., Pearlberg, J., Tsuchihashi, Z., Cantley, L.C., *et al.* (2005). Differential effects of gefitinib and cetuximab on non-small-cell lung cancers bearing epidermal growth factor receptor mutations. J Natl Cancer Inst *97*, 1185-1194.

Muller, Y.A., Chen, Y., Christinger, H.W., Li, B., Cunningham, B.C., Lowman, H.B., and de Vos, A.M. (1998). VEGF and the Fab fragment of a humanized

neutralizing antibody: crystal structure of the complex at 2.4 A resolution and mutational analysis of the interface. Structure *6*, 1153-1167.

Muller, Y.A., Li, B., Christinger, H.W., Wells, J.A., Cunningham, B.C., and de Vos, A.M. (1997). Vascular endothelial growth factor: crystal structure and functional mapping of the kinase domain receptor binding site. Proc Natl Acad Sci U S A *94*, 7192-7197.

Murdoch, C., Muthana, M., Coffelt, S.B., and Lewis, C.E. (2008). The role of myeloid cells in the promotion of tumour angiogenesis. Nat Rev Cancer *8*, 618-631.

Murukesh, N., Dive, C., and Jayson, G.C. (2010). Biomarkers of angiogenesis and their role in the development of VEGF inhibitors. Br J Cancer *102*, 8-18.

Nanjundan, M., Byers, L.A., Carey, M.S., Siwak, D.R., Raso, M.G., Diao, L., Wang, J., Coombes, K.R., Roth, J.A., Mills, G.B., *et al.* (2010). Proteomic profiling identifies pathways dysregulated in non-small cell lung cancer and an inverse association of AMPK and adhesion pathways with recurrence. J Thorac Oncol *5*, 1894-1904.

Nardo, G., Favaro, E., Curtarello, M., Moserle, L., Zulato, E., Persano, L., Rossi, E., Esposito, G., Crescenzi, M., Casanovas, O., *et al.* (2011). Glycolytic Phenotype and AMP Kinase Modify the Pathologic Response of Tumor Xenografts to VEGF Neutralization. Cancer Res *71*, 4214-4225.

Natale, R.B., Bodkin, D., Govindan, R., Sleckman, B.G., Rizvi, N.A., Capo, A., Germonpre, P., Eberhardt, W.E., Stockman, P.K., Kennedy, S.J., *et al.* (2009). Vandetanib versus gefitinib in patients with advanced non-small-cell lung cancer: results from a two-part, double-blind, randomized phase ii study. J Clin Oncol *27*, 2523-2529.

NationalCancerInstitute (2011). Bevacizumab in NSCLC Clinical Trials Search Results.

Nguyen, D.X., Bos, P.D., and Massague, J. (2009). Metastasis: from dissemination to organ-specific colonization. Nat Rev Cancer *9*, 274-284.

Nicholson, R.I., Gee, J.M., and Harper, M.E. (2001). EGFR and cancer prognosis. Eur J Cancer *37 Suppl 4*, S9-15.

Nikolinakos, P., and Heymach, J.V. (2008). The tyrosine kinase inhibitor cediranib for non-small cell lung cancer and other thoracic malignancies. J Thorac Oncol *3*, S131-134.

Noguchi, M. (2010). Stepwise progression of pulmonary adenocarcinoma--clinical and molecular implications. Cancer Metastasis Rev *29*, 15-21.

Nolan, D.J., Ciarrocchi, A., Mellick, A.S., Jaggi, J.S., Bambino, K., Gupta, S., Heikamp, E., McDevitt, M.R., Scheinberg, D.A., Benezra, R., *et al.* (2007). Bone marrow-derived endothelial progenitor cells are a major determinant of nascent tumor neovascularization. Genes Dev *21*, 1546-1558.

Norden, A.D., Young, G.S., Setayesh, K., Muzikansky, A., Klufas, R., Ross, G.L., Ciampa, A.S., Ebbeling, L.G., Levy, B., Drappatz, J., *et al.* (2008). Bevacizumab for recurrent malignant gliomas: efficacy, toxicity, and patterns of recurrence. Neurology *70*, 779-787.

Novello, S., Scagliotti, G.V., Rosell, R., Socinski, M.A., Brahmer, J., Atkins, J., Pallares, C., Burgess, R., Tye, L., Selaru, P., *et al.* (2009). Phase II study of continuous daily sunitinib dosing in patients with previously treated advanced non-small cell lung cancer. Br J Cancer *101*, 1543-1548.

Nozaki, M., Sakurai, E., Raisler, B.J., Baffi, J.Z., Witta, J., Ogura, Y., Brekken, R.A., Sage, E.H., Ambati, B.K., and Ambati, J. (2006). Loss of SPARC-mediated VEGFR-1 suppression after injury reveals a novel antiangiogenic activity of VEGF-A. J Clin Invest *116*, 422-429.

NSCLCCollaborativeGroup (1995). Chemotherapy in non-small cell lung cancer: a meta-analysis using updated data on individual patients from 52 randomised

clinical trials. Non-small Cell Lung Cancer Collaborative Group. BMJ *311*, 899-909.

O'Callaghan, D.S., O'Donnell, D., O'Connell, F., and O'Byrne, K.J. (2010). The role of inflammation in the pathogenesis of non-small cell lung cancer. J Thorac Oncol *5*, 2024-2036.

Ohe, Y., Ohashi, Y., Kubota, K., Tamura, T., Nakagawa, K., Negoro, S., Nishiwaki, Y., Saijo, N., Ariyoshi, Y., and Fukuoka, M. (2007). Randomized phase III study of cisplatin plus irinotecan versus carboplatin plus paclitaxel, cisplatin plus gemcitabine, and cisplatin plus vinorelbine for advanced non-small-cell lung cancer: Four-Arm Cooperative Study in Japan. Ann Oncol *18*, 317-323.

Ohsaki, Y., Tanno, S., Fujita, Y., Toyoshima, E., Fujiuchi, S., Nishigaki, Y., Ishida, S., Nagase, A., Miyokawa, N., Hirata, S., *et al.* (2000). Epidermal growth factor receptor expression correlates with poor prognosis in non-small cell lung cancer patients with p53 overexpression. Oncol Rep *7*, 603-607.

Olofsson, B., Korpelainen, E., Pepper, M.S., Mandriota, S.J., Aase, K., Kumar, V., Gunji, Y., Jeltsch, M.M., Shibuya, M., Alitalo, K., *et al.* (1998). Vascular endothelial growth factor B (VEGF-B) binds to VEGF receptor-1 and regulates plasminogen activator activity in endothelial cells. Proc Natl Acad Sci U S A *95*, 11709-11714.

Olofsson, B., Pajusola, K., von Euler, G., Chilov, D., Alitalo, K., and Eriksson, U. (1996). Genomic organization of the mouse and human genes for vascular endothelial growth factor B (VEGF-B) and characterization of a second splice isoform. J Biol Chem *271*, 19310-19317.

Olsson, A.K., Dimberg, A., Kreuger, J., and Claesson-Welsh, L. (2006). VEGF receptor signalling - in control of vascular function. Nat Rev Mol Cell Biol *7*, 359-371.

Paez-Ribes, M., Allen, E., Hudock, J., Takeda, T., Okuyama, H., Vinals, F., Inoue, M., Bergers, G., Hanahan, D., and Casanovas, O. (2009). Antiangiogenic

therapy elicits malignant progression of tumors to increased local invasion and distant metastasis. Cancer Cell *15*, 220-231.

Paez, J.G., Janne, P.A., Lee, J.C., Tracy, S., Greulich, H., Gabriel, S., Herman, P., Kaye, F.J., Lindeman, N., Boggon, T.J., *et al.* (2004). EGFR mutations in lung cancer: correlation with clinical response to gefitinib therapy. Science *304*, 1497-1500.

Pajusola, K., Aprelikova, O., Korhonen, J., Kaipainen, A., Pertovaara, L., Alitalo, R., and Alitalo, K. (1992). FLT4 receptor tyrosine kinase contains seven immunoglobulin-like loops and is expressed in multiple human tissues and cell lines. Cancer Res *52*, 5738-5743.

Pandya, K.J., Dahlberg, S., Hidalgo, M., Cohen, R.B., Lee, M.W., Schiller, J.H., and Johnson, D.H. (2007). A randomized, phase II trial of two dose levels of temsirolimus (CCI-779) in patients with extensive-stage small-cell lung cancer who have responding or stable disease after induction chemotherapy: a trial of the Eastern Cooperative Oncology Group (E1500). J Thorac Oncol *2*, 1036-1041.

Pao, W., and Girard, N. (2011). New driver mutations in non-small-cell lung cancer. Lancet Oncol *12*, 175-180.

Pao, W., Miller, V.A., Politi, K.A., Riely, G.J., Somwar, R., Zakowski, M.F., Kris, M.G., and Varmus, H. (2005a). Acquired resistance of lung adenocarcinomas to gefitinib or erlotinib is associated with a second mutation in the EGFR kinase domain. PLoS Med *2*, e73.

Pao, W., Wang, T.Y., Riely, G.J., Miller, V.A., Pan, Q., Ladanyi, M., Zakowski, M.F., Heelan, R.T., Kris, M.G., and Varmus, H.E. (2005b). KRAS mutations and primary resistance of lung adenocarcinomas to gefitinib or erlotinib. PLoS Med *2*, e17.

Park, J.E., Chen, H.H., Winer, J., Houck, K.A., and Ferrara, N. (1994). Placenta growth factor. Potentiation of vascular endothelial growth factor bioactivity, in vitro and in vivo, and high affinity binding to Flt-1 but not to Flk-1/KDR. J Biol Chem *269*, 25646-25654.

Park, J.E., Keller, G.A., and Ferrara, N. (1993). The vascular endothelial growth factor (VEGF) isoforms: differential deposition into the subepithelial extracellular matrix and bioactivity of extracellular matrix-bound VEGF. Mol Biol Cell *4*, 1317-1326.

Parkin, D.M., Bray, F., Ferlay, J., and Pisani, P. (2005). Global cancer statistics, 2002. CA Cancer J Clin *55*, 74-108.

Parkin, D.M., Pisani, P., and Ferlay, J. (1993). Estimates of the worldwide incidence of eighteen major cancers in 1985. Int J Cancer *54*, 594-606.

Patel, J.D., Bonomi, P., Socinski, M.A., Govindan, R., Hong, S., Obasaju, C., Pennella, E.J., Girvan, A.C., and Guba, S.C. (2009a). Treatment rationale and study design for the pointbreak study: a randomized, open-label phase III study of pemetrexed/carboplatin/bevacizumab followed by maintenance pemetrexed/bevacizumab versus paclitaxel/carboplatin/bevacizumab followed by maintenance bevacizumab in patients with stage IIIB or IV nonsquamous non-small-cell lung cancer. Clin Lung Cancer *10*, 252-256.

Patel, J.D., Hensing, T.A., Rademaker, A., Hart, E.M., Blum, M.G., Milton, D.T., and Bonomi, P.D. (2009b). Phase II study of pemetrexed and carboplatin plus bevacizumab with maintenance pemetrexed and bevacizumab as first-line therapy for nonsquamous non-small-cell lung cancer. J Clin Oncol *27*, 3284-3289.

Pennathur, A., Luketich, J.D., Abbas, G., Chen, M., Fernando, H.C., Gooding, W.E., Schuchert, M.J., Gilbert, S., Christie, N.A., and Landreneau, R.J. (2007). Radiofrequency ablation for the treatment of stage I non-small cell lung cancer in high-risk patients. J Thorac Cardiovasc Surg *134*, 857-864.

Pepper, M.S. (2001). Extracellular proteolysis and angiogenesis. Thromb Haemost *86*, 346-355.

Perez-Soler, R., Chachoua, A., Hammond, L.A., Rowinsky, E.K., Huberman, M., Karp, D., Rigas, J., Clark, G.M., Santabarbara, P., and Bonomi, P. (2004). Determinants of tumor response and survival with erlotinib in patients with non--small-cell lung cancer. J Clin Oncol *22*, 3238-3247.

Perez, C.A., Stanley, K., Rubin, P., Kramer, S., Brady, L., Perez-Tamayo, R., Brown, G.S., Concannon, J., Rotman, M., and Seydel, H.G. (1980). A prospective randomized study of various irradiation doses and fractionation schedules in the treatment of inoperable non-oat-cell carcinoma of the lung. Preliminary report by the Radiation Therapy Oncology Group. Cancer *45*, 2744-2753.

Peto, R., Lopez, A.D., Bereham, J., and Thun, M. (2006). Mortality From Smoking in Developed Countries 1950-2000 (Available at: http://www.ctsu.ox.ac.uk/~tobacco/SMK_All_PAGES.pdf. International Union Against Cancer (UICC). Geneva: Switzerland

).

Pham, D., Kris, M.G., Riely, G.J., Sarkaria, I.S., McDonough, T., Chuai, S., Venkatraman, E.S., Miller, V.A., Ladanyi, M., Pao, W., *et al.* (2006). Use of cigarette-smoking history to estimate the likelihood of mutations in epidermal growth factor receptor gene exons 19 and 21 in lung adenocarcinomas. J Clin Oncol *24*, 1700-1704.

Pomyje, J., Zivny, J., Sefc, L., Plasilova, M., Pytlik, R., and Necas, E. (2003). Expression of genes regulating angiogenesis in human circulating hematopoietic cord blood CD34+/CD133+ cells. Eur J Haematol *70*, 143-150.

PORTMeta-analysisTrialistsGroup (1998). Postoperative radiotherapy in non-small-cell lung cancer: systematic review and meta-analysis of individual patient data from nine randomised controlled trials. PORT Meta-analysis Trialists Group. Lancet *352*, 257-263.

Posey, J.A., Ng, T.C., Yang, B., Khazaeli, M.B., Carpenter, M.D., Fox, F., Needle, M., Waksal, H., and LoBuglio, A.F. (2003). A phase I study of anti-kinase insert domain-containing receptor antibody, IMC-1C11, in patients with liver metastases from colorectal carcinoma. Clin Cancer Res *9*, 1323-1332.

Presta, L.G., Chen, H., O'Connor, S.J., Chisholm, V., Meng, Y.G., Krummen, L., Winkler, M., and Ferrara, N. (1997). Humanization of an anti-vascular endothelial growth factor monoclonal antibody for the therapy of solid tumors and other disorders. Cancer Res *57*, 4593-4599.

Prevention, C.f.D.C.a. (2007). Best Practices for Comprehensive Tobacco Control Programs-2007 (Atlanta, GA, US Department of Health and Human Services, Centers for Disease Control and Prevention, National Center for Chronic Disease Prevention and Health Promotion, Office on Smoking and Health).

Prewett, M., Huber, J., Li, Y., Santiago, A., O'Connor, W., King, K., Overholser, J., Hooper, A., Pytowski, B., Witte, L., *et al.* (1999). Antivascular endothelial growth factor receptor (fetal liver kinase 1) monoclonal antibody inhibits tumor angiogenesis and growth of several mouse and human tumors. Cancer Res *59*, 5209-5218.

Putnam, E.A., Yen, N., Gallick, G.E., Steck, P.A., Fang, K., Akpakip, B., Gazdar, A.F., and Roth, J.A. (1992). Autocrine growth stimulation by transforming growth factor-alpha in human non-small cell lung cancer. Surg Oncol *1*, 49-60.

Quinn, T.P., Peters, K.G., De Vries, C., Ferrara, N., and Williams, L.T. (1993). Fetal liver kinase 1 is a receptor for vascular endothelial growth factor and is selectively expressed in vascular endothelium. Proc Natl Acad Sci U S A *90*, 7533-7537.

Ramalingam, S., and Belani, C.P. (2004). State-of-the-art chemotherapy for advanced non-small cell lung cancer. Semin Oncol *31*, 68-74.

Ramalingam, S.S., and Belani, C.P. (2010). Antiangiogenic agents in the treatment of nonsmall cell lung cancer: reality and hope. Curr Opin Oncol *22*, 79-85.

Ramalingam, S.S., Owonikoko, T.K., and Khuri, F.R. (2011). Lung cancer: New biological insights and recent therapeutic advances. CA Cancer J Clin *61*, 91-112.

Ran, S., Huang, X., Downes, A., and Thorpe, P.E. (2003). Evaluation of novel antimouse VEGFR2 antibodies as potential antiangiogenic or vascular targeting agents for tumor therapy. Neoplasia *5*, 297-307.

Rapp, E., Pater, J.L., Willan, A., Cormier, Y., Murray, N., Evans, W.K., Hodson, D.I., Clark, D.A., Feld, R., Arnold, A.M., *et al.* (1988). Chemotherapy can prolong survival in patients with advanced non-small-cell lung cancer--report of a Canadian multicenter randomized trial. J Clin Oncol *6*, 633-641.

Raymond, E., Dahan, L., Raoul, J.L., Bang, Y.J., Borbath, I., Lombard-Bohas, C., Valle, J., Metrakos, P., Smith, D., Vinik, A., *et al.* (2011). Sunitinib malate for the treatment of pancreatic neuroendocrine tumors. N Engl J Med *364*, 501-513.

Reck, M., Frickhofen, N., Cedres, S., Gatzemeier, U., Heigener, D., Fuhr, H.G., Thall, A., Lanzalone, S., Stephenson, P., Ruiz-Garcia, A., *et al.* (2010). Sunitinib in combination with gemcitabine plus cisplatin for advanced non-small cell lung cancer: a phase I dose-escalation study. Lung Cancer *70*, 180-187.

Reck, M., von Pawel, J., Zatloukal, P., Ramlau, R., Gorbounova, V., Hirsh, V., Leighl, N., Mezger, J., Archer, V., Moore, N., *et al.* (2009). Phase III trial of cisplatin plus gemcitabine with either placebo or bevacizumab as first-line therapy for nonsquamous non-small-cell lung cancer: AVAil. J Clin Oncol *27*, 1227-1234.

Relf, M., LeJeune, S., Scott, P.A., Fox, S., Smith, K., Leek, R., Moghaddam, A., Whitehouse, R., Bicknell, R., and Harris, A.L. (1997). Expression of the angiogenic factors vascular endothelial cell growth factor, acidic and basic fibroblast growth factor, tumor growth factor beta-1, platelet-derived endothelial cell growth factor, placenta growth factor, and pleiotrophin in human primary breast cancer and its relation to angiogenesis. Cancer Res *57*, 963-969.

Ricci-Vitiani, L., Pallini, R., Biffoni, M., Todaro, M., Invernici, G., Cenci, T., Maira, G., Parati, E.A., Stassi, G., Larocca, L.M., *et al.* (2010). Tumour vascularization via endothelial differentiation of glioblastoma stem-like cells. Nature *468*, 824-828.

Riely, G.J., Kris, M.G., Rosenbaum, D., Marks, J., Li, A., Chitale, D.A., Nafa, K., Riedel, E.R., Hsu, M., Pao, W., *et al.* (2008). Frequency and distinctive spectrum of KRAS mutations in never smokers with lung adenocarcinoma. Clin Cancer Res *14*, 5731-5734.

Rini, B.I., Halabi, S., Rosenberg, J.E., Stadler, W.M., Vaena, D.A., Ou, S.S., Archer, L., Atkins, J.N., Picus, J., Czaykowski, P., *et al.* (2008). Bevacizumab plus interferon alfa compared with interferon alfa monotherapy in patients with metastatic renal cell carcinoma: CALGB 90206. J Clin Oncol *26*, 5422-5428.

Robert, F., Sandler, A., Schiller, J.H., Liu, G., Harper, K., Verkh, L., Huang, X., Ilagan, J., Tye, L., Chao, R., *et al.* (2010). Sunitinib in combination with docetaxel in patients with advanced solid tumors: a phase I dose-escalation study. Cancer Chemother Pharmacol *66*, 669-680.

Roberts, D.M., Kearney, J.B., Johnson, J.H., Rosenberg, M.P., Kumar, R., and Bautch, V.L. (2004). The vascular endothelial growth factor (VEGF) receptor Flt-1 (VEGFR-1) modulates Flk-1 (VEGFR-2) signaling during blood vessel formation. Am J Pathol *164*, 1531-1535.

Robinson, C.J., and Stringer, S.E. (2001). The splice variants of vascular endothelial growth factor (VEGF) and their receptors. J Cell Sci *114*, 853-865.

Rocchigiani, M., Lestingi, M., Luddi, A., Orlandini, M., Franco, B., Rossi, E., Ballabio, A., Zuffardi, O., and Oliviero, S. (1998). Human FIGF: cloning, gene structure, and mapping to chromosome Xp22.1 between the PIGA and the GRPR genes. Genomics *47*, 207-216.

Rockwell, P., Neufeld, G., Glassman, A., Caron, D., and Goldstein, N. (1995). *In vitro* neutralization of vascular endothelial growth factor activation of Flk-1 by a monoclonal antibody. Mol Cell Differ *3*, 91-109.

Roland, C.L., Dineen, S.P., Lynn, K.D., Sullivan, L.A., Dellinger, M.T., Sadegh, L., Sullivan, J.P., Shames, D.S., and Brekken, R.A. (2009a). Inhibition of vascular endothelial growth factor reduces angiogenesis and modulates immune cell infiltration of orthotopic breast cancer xenografts. Mol Cancer Ther *8*, 1761-1771.

Roland, C.L., Lynn, K.D., Toombs, J.E., Dineen, S.P., Udugamasooriya, D.G., and Brekken, R.A. (2009b). Cytokine levels correlate with immune cell infiltration after anti-VEGF therapy in preclinical mouse models of breast cancer. PLoS One *4*, e7669.

Roodhart, J.M., Langenberg, M.H., Witteveen, E., and Voest, E.E. (2008). The molecular basis of class side effects due to treatment with inhibitors of the VEGF/VEGFR pathway. Curr Clin Pharmacol *3*, 132-143.

Rosell, R., Moran, T., Queralt, C., Porta, R., Cardenal, F., Camps, C., Majem, M., Lopez-Vivanco, G., Isla, D., Provencio, M., *et al.* (2009). Screening for epidermal growth factor receptor mutations in lung cancer. N Engl J Med *361*, 958-967.

Roskoski, R., Jr. (2007a). Sunitinib: a VEGF and PDGF receptor protein kinase and angiogenesis inhibitor. Biochem Biophys Res Commun *356*, 323-328.

Roskoski, R., Jr. (2007b). Vascular endothelial growth factor (VEGF) signaling in tumor progression. Crit Rev Oncol Hematol *62*, 179-213.

Rudin, C.M., Salgia, R., Wang, X., Hodgson, L.D., Masters, G.A., Green, M., and Vokes, E.E. (2008). Randomized phase II Study of carboplatin and etoposide with or without the bcl-2 antisense oligonucleotide oblimersen for extensive-stage small-cell lung cancer: CALGB 30103. J Clin Oncol *26*, 870-876.

Rugo, H.S., Herbst, R.S., Liu, G., Park, J.W., Kies, M.S., Steinfeldt, H.M., Pithavala, Y.K., Reich, S.D., Freddo, J.L., and Wilding, G. (2005). Phase I trial of the oral antiangiogenesis agent AG-013736 in patients with advanced solid tumors: pharmacokinetic and clinical results. J Clin Oncol *23*, 5474-5483.

Rusch, V., Baselga, J., Cordon-Cardo, C., Orazem, J., Zaman, M., Hoda, S., McIntosh, J., Kurie, J., and Dmitrovsky, E. (1993). Differential expression of the epidermal growth factor receptor and its ligands in primary non-small cell lung cancers and adjacent benign lung. Cancer Res *53*, 2379-2385.

Saharinen, P., Tammela, T., Karkkainen, M.J., and Alitalo, K. (2004). Lymphatic vasculature: development, molecular regulation and role in tumor metastasis and inflammation. Trends Immunol *25*, 387-395.

Sandler, A., Gray, R., Perry, M.C., Brahmer, J., Schiller, J.H., Dowlati, A., Lilenbaum, R., and Johnson, D.H. (2006). Paclitaxel-carboplatin alone or with bevacizumab for non-small-cell lung cancer. N Engl J Med *355*, 2542-2550.

Sandler, A.B., Nemunaitis, J., Denham, C., von Pawel, J., Cormier, Y., Gatzemeier, U., Mattson, K., Manegold, C., Palmer, M.C., Gregor, A., *et al.* (2000). Phase III trial of gemcitabine plus cisplatin versus cisplatin alone in patients with locally advanced or metastatic non-small-cell lung cancer. J Clin Oncol *18*, 122-130.

Scagliotti, G., Novello, S., von Pawel, J., Reck, M., Pereira, J.R., Thomas, M., Abrao Miziara, J.E., Balint, B., De Marinis, F., Keller, A., *et al.* (2010). Phase III study of carboplatin and paclitaxel alone or with sorafenib in advanced non-small-cell lung cancer. J Clin Oncol *28*, 1835-1842.

Schiller, J.H., Harrington, D., Belani, C.P., Langer, C., Sandler, A., Krook, J., Zhu, J., and Johnson, D.H. (2002). Comparison of four chemotherapy regimens for advanced non-small-cell lung cancer. N Engl J Med *346*, 92-98.

Schiller, J.H., Larson, T., Ou, S.H., Limentani, S., Sandler, A., Vokes, E., Kim, S., Liau, K., Bycott, P., Olszanski, A.J., *et al.* (2009). Efficacy and safety of axitinib in patients with advanced non-small-cell lung cancer: results from a phase II study. J Clin Oncol *27*, 3836-3841.

Schneider, B.P., Wang, M., Radovich, M., Sledge, G.W., Badve, S., Thor, A., Flockhart, D.A., Hancock, B., Davidson, N., Gralow, J., *et al.* (2008). Association of vascular endothelial growth factor and vascular endothelial growth factor receptor-2 genetic polymorphisms with outcome in a trial of paclitaxel compared with paclitaxel plus bevacizumab in advanced breast cancer: ECOG 2100. J Clin Oncol *26*, 4672-4678.

Scolnik, P.A. (2009). mAbs: a business perspective. MAbs *1*, 179-184.

Senger, D.R., Connolly, D.T., Van de Water, L., Feder, J., and Dvorak, H.F. (1990). Purification and NH2-terminal amino acid sequence of guinea pig tumor-secreted vascular permeability factor. Cancer Res *50*, 1774-1778.

Sengupta, S., and Harris, C.C. (2005). p53: traffic cop at the crossroads of DNA repair and recombination. Nat Rev Mol Cell Biol *6*, 44-55.

Sequist, L.V., Bell, D.W., Lynch, T.J., and Haber, D.A. (2007). Molecular predictors of response to epidermal growth factor receptor antagonists in non-small-cell lung cancer. J Clin Oncol *25*, 587-595.

Sessa, C., Guibal, A., Del Conte, G., and Ruegg, C. (2008). Biomarkers of angiogenesis for the development of antiangiogenic therapies in oncology: tools or decorations? Nat Clin Pract Oncol *5*, 378-391.

Shaheen, R.M., Tseng, W.W., Vellagas, R., Liu, W., Ahmad, S.A., Jung, Y.D., Reinmuth, N., Drazan, K.E., Bucana, C.D., Hicklin, D.J., *et al.* (2001). Effects of an antibody to vascular endothelial growth factor receptor-2 on survival, tumor vascularity, and apoptosis in a murine model of colon carcinomatosis. Int J Oncol *18*, 221-226.

Shaked, Y., Ciarrocchi, A., Franco, M., Lee, C.R., Man, S., Cheung, A.M., Hicklin, D.J., Chaplin, D., Foster, F.S., Benezra, R., *et al.* (2006). Therapy-induced acute recruitment of circulating endothelial progenitor cells to tumors. Science *313*, 1785-1787.

Shaked, Y., and Kerbel, R.S. (2007). Antiangiogenic strategies on defense: on the possibility of blocking rebounds by the tumor vasculature after chemotherapy. Cancer Res *67*, 7055-7058.

Shalaby, F., Rossant, J., Yamaguchi, T.P., Gertsenstein, M., Wu, X.F., Breitman, M.L., and Schuh, A.C. (1995). Failure of blood-island formation and vasculogenesis in Flk-1-deficient mice. Nature *376*, 62-66.

Sharma, S.V., Bell, D.W., Settleman, J., and Haber, D.A. (2007). Epidermal growth factor receptor mutations in lung cancer. Nat Rev Cancer *7*, 169-181.

Shaw, A.T., Yeap, B.Y., Mino-Kenudson, M., Digumarthy, S.R., Costa, D.B., Heist, R.S., Solomon, B., Stubbs, H., Admane, S., McDermott, U., *et al.* (2009).

Clinical features and outcome of patients with non-small-cell lung cancer who harbor EML4-ALK. J Clin Oncol *27*, 4247-4253.

Shepherd, F.A., Rodrigues Pereira, J., Ciuleanu, T., Tan, E.H., Hirsh, V., Thongprasert, S., Campos, D., Maoleekoonpiroj, S., Smylie, M., Martins, R., *et al.* (2005). Erlotinib in previously treated non-small-cell lung cancer. N Engl J Med *353*, 123-132.

Shibuya, M., and Claesson-Welsh, L. (2006). Signal transduction by VEGF receptors in regulation of angiogenesis and lymphangiogenesis. Exp Cell Res *312*, 549-560.

Shibuya, M., Yamaguchi, S., Yamane, A., Ikeda, T., Tojo, A., Matsushime, H., and Sato, M. (1990). Nucleotide sequence and expression of a novel human receptor-type tyrosine kinase gene (flt) closely related to the fms family. Oncogene *5*, 519-524.

Shieh, Y.S., Lai, C.Y., Kao, Y.R., Shiah, S.G., Chu, Y.W., Lee, H.S., and Wu, C.W. (2005). Expression of axl in lung adenocarcinoma and correlation with tumor progression. Neoplasia *7*, 1058-1064.

Shigematsu, H., and Gazdar, A.F. (2006). Somatic mutations of epidermal growth factor receptor signaling pathway in lung cancers. Int J Cancer *118*, 257-262.

Shigematsu, H., Lin, L., Takahashi, T., Nomura, M., Suzuki, M., Wistuba, II, Fong, K.M., Lee, H., Toyooka, S., Shimizu, N., *et al.* (2005). Clinical and biological features associated with epidermal growth factor receptor gene mutations in lung cancers. J Natl Cancer Inst *97*, 339-346.

Siddiqui, F., Bae, K., Langer, C.J., Coyne, J.C., Gamerman, V., Komaki, R., Choy, H., Curran, W.J., Watkins-Bruner, D., and Movsas, B. (2010). The influence of gender, race, and marital status on survival in lung cancer patients: analysis of Radiation Therapy Oncology Group trials. J Thorac Oncol *5*, 631-639.

Skobe, M., Rockwell, P., Goldstein, N., Vosseler, S., and Fusenig, N.E. (1997). Halting angiogenesis suppresses carcinoma cell invasion. Nat Med *3*, 1222-1227.

Slotman, B., Faivre-Finn, C., Kramer, G., Rankin, E., Snee, M., Hatton, M., Postmus, P., Collette, L., Musat, E., and Senan, S. (2007). Prophylactic cranial irradiation in extensive small-cell lung cancer. N Engl J Med *357*, 664-672.

Socinski, M.A. (2008). The current status and evolving role of sunitinib in non-small cell lung cancer. J Thorac Oncol *3*, S119-123.

Socinski, M.A., Novello, S., Brahmer, J.R., Rosell, R., Sanchez, J.M., Belani, C.P., Govindan, R., Atkins, J.N., Gillenwater, H.H., Pallares, C., *et al.* (2008). Multicenter, phase II trial of sunitinib in previously treated, advanced non-small-cell lung cancer. J Clin Oncol *26*, 650-656.

Soda, M., Choi, Y.L., Enomoto, M., Takada, S., Yamashita, Y., Ishikawa, S., Fujiwara, S., Watanabe, H., Kurashina, K., Hatanaka, H., *et al.* (2007). Identification of the transforming EML4-ALK fusion gene in non-small-cell lung cancer. Nature *448*, 561-566.

Soda, M., Takada, S., Takeuchi, K., Choi, Y.L., Enomoto, M., Ueno, T., Haruta, H., Hamada, T., Yamashita, Y., Ishikawa, Y., *et al.* (2008). A mouse model for EML4-ALK-positive lung cancer. Proc Natl Acad Sci U S A *105*, 19893-19897.

Soker, S., Takashima, S., Miao, H.Q., Neufeld, G., and Klagsbrun, M. (1998). Neuropilin-1 is expressed by endothelial and tumor cells as an isoform-specific receptor for vascular endothelial growth factor. Cell *92*, 735-745.

Stacker, S.A., Stenvers, K., Caesar, C., Vitali, A., Domagala, T., Nice, E., Roufail, S., Simpson, R.J., Moritz, R., Karpanen, T., *et al.* (1999). Biosynthesis of vascular endothelial growth factor-D involves proteolytic processing which generates non-covalent homodimers. J Biol Chem *274*, 32127-32136.

Stayner, L., Bena, J., Sasco, A.J., Smith, R., Steenland, K., Kreuzer, M., and Straif, K. (2007). Lung cancer risk and workplace exposure to environmental tobacco smoke. Am J Public Health *97*, 545-551.

Stephan, S., Datta, K., Wang, E., Li, J., Brekken, R.A., Parangi, S., Thorpe, P.E., and Mukhopadhyay, D. (2004). Effect of rapamycin alone and in combination with antiangiogenesis therapy in an orthotopic model of human pancreatic cancer. Clin Cancer Res *10*, 6993-7000.

Sternberg, C.N., Davis, I.D., Mardiak, J., Szczylik, C., Lee, E., Wagstaff, J., Barrios, C.H., Salman, P., Gladkov, O.A., Kavina, A., *et al.* (2010). Pazopanib in locally advanced or metastatic renal cell carcinoma: results of a randomized phase III trial. J Clin Oncol *28*, 1061-1068.

Stinchcombe, T.E., and Socinski, M.A. (2009). Current treatments for advanced stage non-small cell lung cancer. Proc Am Thorac Soc *6*, 233-241.

Subramanian, J., and Govindan, R. (2007). Lung cancer in never smokers: a review. J Clin Oncol *25*, 561-570.

Sullivan, L.A., and Brekken, R.A. (2010). The VEGF family in cancer and antibody-based strategies for their inhibition. MAbs *2*.

Sullivan, L.A., Carbon, J.G., Roland, C.L., Toombs, J.E., Nyquist-Andersen, M., Kavlie, A., Schlunegger, K., Richardson, J.A., and Brekken, R.A. (2010). r84, a novel therapeutic antibody against mouse and human VEGF with potent anti-tumor activity and limited toxicity induction. PLoS One *5*, e12031.

Sun, S., Schiller, J.H., and Gazdar, A.F. (2007). Lung cancer in never smokers--a different disease. Nat Rev Cancer *7*, 778-790.

Takagi, S., Kasuya, Y., Shimizu, M., Matsuura, T., Tsuboi, M., Kawakami, A., and Fujisawa, H. (1995). Expression of a cell adhesion molecule, neuropilin, in the developing chick nervous system. Dev Biol *170*, 207-222.

Takahashi, T., Yamaguchi, S., Chida, K., and Shibuya, M. (2001). A single autophosphorylation site on KDR/Flk-1 is essential for VEGF-A-dependent activation of PLC-gamma and DNA synthesis in vascular endothelial cells. EMBO J *20*, 2768-2778.

Takashima, S., Kitakaze, M., Asakura, M., Asanuma, H., Sanada, S., Tashiro, F., Niwa, H., Miyazaki Ji, J., Hirota, S., Kitamura, Y., *et al.* (2002). Targeting of both mouse neuropilin-1 and neuropilin-2 genes severely impairs developmental yolk sac and embryonic angiogenesis. Proc Natl Acad Sci U S A *99*, 3657-3662.

Tam, I.Y., Chung, L.P., Suen, W.S., Wang, E., Wong, M.C., Ho, K.K., Lam, W.K., Chiu, S.W., Girard, L., Minna, J.D., *et al.* (2006). Distinct epidermal growth factor receptor and KRAS mutation patterns in non-small cell lung cancer patients with different tobacco exposure and clinicopathologic features. Clin Cancer Res *12*, 1647-1653.

Terman, B.I., Dougher-Vermazen, M., Carrion, M.E., Dimitrov, D., Armellino, D.C., Gospodarowicz, D., and Bohlen, P. (1992). Identification of the KDR tyrosine kinase as a receptor for vascular endothelial cell growth factor. Biochem Biophys Res Commun *187*, 1579-1586.

Thatcher, N., Chang, A., Parikh, P., Rodrigues Pereira, J., Ciuleanu, T., von Pawel, J., Thongprasert, S., Tan, E.H., Pemberton, K., Archer, V., *et al.* (2005). Gefitinib plus best supportive care in previously treated patients with refractory advanced non-small-cell lung cancer: results from a randomised, placebo-controlled, multicentre study (Iressa Survival Evaluation in Lung Cancer). Lancet *366*, 1527-1537.

Timmerman, R., Paulus, R., Galvin, J., Michalski, J., Straube, W., Bradley, J., Fakiris, A., Bezjak, A., Videtic, G., Johnstone, D., *et al.* (2010). Stereotactic body radiation therapy for inoperable early stage lung cancer. JAMA *303*, 1070-1076.

Tischer, E., Mitchell, R., Hartman, T., Silva, M., Gospodarowicz, D., Fiddes, J.C., and Abraham, J.A. (1991). The human gene for vascular endothelial growth factor. Multiple protein forms are encoded through alternative exon splicing. J Biol Chem *266*, 11947-11954.

Toh, C.K., Gao, F., Lim, W.T., Leong, S.S., Fong, K.W., Yap, S.P., Hsu, A.A., Eng, P., Koong, H.N., Thirugnanam, A., *et al.* (2006). Never-smokers with lung cancer: epidemiologic evidence of a distinct disease entity. J Clin Oncol *24*, 2245-2251.

Tonra, J.R., and Hicklin, D.J. (2007). Targeting the vascular endothelial growth factor pathway in the treatment of human malignancy. Immunol Invest *36*, 3-23.

Twombly, R. (2011). Avastin's uncertain future in breast cancer treatment. J Natl Cancer Inst *103*, 458-460.

Ulahannan, S.V., and Brahmer, J.R. (2011). Antiangiogenic agents in combination with chemotherapy in patients with advanced non-small cell lung cancer. Cancer Invest *29*, 325-337.

Vahakangas, K.H., Bennett, W.P., Castren, K., Welsh, J.A., Khan, M.A., Blomeke, B., Alavanja, M.C., and Harris, C.C. (2001). p53 and K-ras mutations in lung cancers from former and never-smoking women. Cancer Res *61*, 4350-4356.

Vineis, P., Alavanja, M., Buffler, P., Fontham, E., Franceschi, S., Gao, Y.T., Gupta, P.C., Hackshaw, A., Matos, E., Samet, J., *et al.* (2004). Tobacco and cancer: recent epidemiological evidence. J Natl Cancer Inst *96*, 99-106.

Visbal, A.L., Williams, B.A., Nichols, F.C., 3rd, Marks, R.S., Jett, J.R., Aubry, M.C., Edell, E.S., Wampfler, J.A., Molina, J.R., and Yang, P. (2004). Gender differences in non-small-cell lung cancer survival: an analysis of 4,618 patients diagnosed between 1997 and 2002. Ann Thorac Surg *78*, 209-215; discussion 215.

Voelkel, N.F., Vandivier, R.W., and Tuder, R.M. (2006). Vascular endothelial growth factor in the lung. Am J Physiol Lung Cell Mol Physiol *290*, L209-221.

Vredenburgh, J.J., Desjardins, A., Reardon, D.A., and Friedman, H.S. (2009). Experience with irinotecan for the treatment of malignant glioma. Neuro Oncol *11*, 80-91.

Wakelee, H.A., Chang, E.T., Gomez, S.L., Keegan, T.H., Feskanich, D., Clarke, C.A., Holmberg, L., Yong, L.C., Kolonel, L.N., Gould, M.K., *et al.* (2007). Lung cancer incidence in never smokers. J Clin Oncol *25*, 472-478.

Waltenberger, J., Claesson-Welsh, L., Siegbahn, A., Shibuya, M., and Heldin, C.H. (1994). Different signal transduction properties of KDR and Flt1, two receptors for vascular endothelial growth factor. J Biol Chem *269*, 26988-26995.

Wang, R., Chadalavada, K., Wilshire, J., Kowalik, U., Hovinga, K.E., Geber, A., Fligelman, B., Leversha, M., Brennan, C., and Tabar, V. (2010). Glioblastoma stem-like cells give rise to tumour endothelium. Nature *468*, 829-833.

Warren, R.S., Yuan, H., Matli, M.R., Gillett, N.A., and Ferrara, N. (1995). Regulation by vascular endothelial growth factor of human colon cancer tumorigenesis in a mouse model of experimental liver metastasis. J Clin Invest *95*, 1789-1797.

Webb, J.D., and Simon, M.C. (2010). Novel insights into the molecular origins and treatment of lung cancer. Cell Cycle *9*, 4098-4105.

Wedge, S.R., Kendrew, J., Hennequin, L.F., Valentine, P.J., Barry, S.T., Brave, S.R., Smith, N.R., James, N.H., Dukes, M., Curwen, J.O., *et al.* (2005). AZD2171: a highly potent, orally bioavailable, vascular endothelial growth factor receptor-2 tyrosine kinase inhibitor for the treatment of cancer. Cancer Res *65*, 4389-4400.

Wedge, S.R., Ogilvie, D.J., Dukes, M., Kendrew, J., Chester, R., Jackson, J.A., Boffey, S.J., Valentine, P.J., Curwen, J.O., Musgrove, H.L., *et al.* (2002). ZD6474 inhibits vascular endothelial growth factor signaling, angiogenesis, and tumor growth following oral administration. Cancer Res *62*, 4645-4655.

Weinstein, I.B. (2002). Cancer. Addiction to oncogenes--the Achilles heal of cancer. Science *297*, 63-64.

Whitehurst, B., Flister, M.J., Bagaitkar, J., Volk, L., Bivens, C.M., Pickett, B., Castro-Rivera, E., Brekken, R.A., Gerard, R.D., and Ran, S. (2007). Anti-VEGF-A therapy reduces lymphatic vessel density and expression of VEGFR-3 in an orthotopic breast tumor model. Int J Cancer *121*, 2181-2191.

Wiesmann, C., Fuh, G., Christinger, H.W., Eigenbrot, C., Wells, J.A., and de Vos, A.M. (1997). Crystal structure at 1.7 A resolution of VEGF in complex with domain 2 of the Flt-1 receptor. Cell *91*, 695-704.

Wilhelm, S.M., Adnane, L., Newell, P., Villanueva, A., Llovet, J.M., and Lynch, M. (2008). Preclinical overview of sorafenib, a multikinase inhibitor that targets both Raf and VEGF and PDGF receptor tyrosine kinase signaling. Mol Cancer Ther *7*, 3129-3140.

Wilhelm, S.M., Carter, C., Tang, L., Wilkie, D., McNabola, A., Rong, H., Chen, C., Zhang, X., Vincent, P., McHugh, M., *et al.* (2004). BAY 43-9006 exhibits broad spectrum oral antitumor activity and targets the RAF/MEK/ERK pathway and receptor tyrosine kinases involved in tumor progression and angiogenesis. Cancer Res *64*, 7099-7109.

Willett, C.G., Duda, D.G., di Tomaso, E., Boucher, Y., Ancukiewicz, M., Sahani, D.V., Lahdenranta, J., Chung, D.C., Fischman, A.J., Lauwers, G.Y., *et al.* (2009). Efficacy, safety, and biomarkers of neoadjuvant bevacizumab, radiation therapy, and fluorouracil in rectal cancer: a multidisciplinary phase II study. J Clin Oncol *27*, 3020-3026.

Wimmel, A., Glitz, D., Kraus, A., Roeder, J., and Schuermann, M. (2001). Axl receptor tyrosine kinase expression in human lung cancer cell lines correlates with cellular adhesion. Eur J Cancer *37*, 2264-2274.

Wozniak, A.J., Crowley, J.J., Balcerzak, S.P., Weiss, G.R., Spiridonidis, C.H., Baker, L.H., Albain, K.S., Kelly, K., Taylor, S.A., Gandara, D.R., *et al.* (1998). Randomized trial comparing cisplatin with cisplatin plus vinorelbine in the

treatment of advanced non-small-cell lung cancer: a Southwest Oncology Group study. J Clin Oncol *16*, 2459-2465.

Wu-Williams, A.H., Dai, X.D., Blot, W., Xu, Z.Y., Sun, X.W., Xiao, H.P., Stone, B.J., Yu, S.F., Feng, Y.P., Ershow, A.G., *et al.* (1990). Lung cancer among women in north-east China. Br J Cancer *62*, 982-987.

Wu, Y., Hooper, A.T., Zhong, Z., Witte, L., Bohlen, P., Rafii, S., and Hicklin, D.J. (2006a). The vascular endothelial growth factor receptor (VEGFR-1) supports growth and survival of human breast carcinoma. Int J Cancer *119*, 1519-1529.

Wu, Y., Zhong, Z., Huber, J., Bassi, R., Finnerty, B., Corcoran, E., Li, H., Navarro, E., Balderes, P., Jimenez, X., *et al.* (2006b). Anti-vascular endothelial growth factor receptor-1 antagonist antibody as a therapeutic agent for cancer. Clin Cancer Res *12*, 6573-6584.

Xu, L., Cochran, D.M., Tong, R.T., Winkler, F., Kashiwagi, S., Jain, R.K., and Fukumura, D. (2006). Placenta growth factor overexpression inhibits tumor growth, angiogenesis, and metastasis by depleting vascular endothelial growth factor homodimers in orthotopic mouse models. Cancer Res *66*, 3971-3977.

Xu, Z.Y., Blot, W.J., Xiao, H.P., Wu, A., Feng, Y.P., Stone, B.J., Sun, J., Ershow, A.G., Henderson, B.E., and Fraumeni, J.F., Jr. (1989). Smoking, air pollution, and the high rates of lung cancer in Shenyang, China. J Natl Cancer Inst *81*, 1800-1806.

Yamamoto, N., Tamura, T., Yamada, K., Yamada, Y., Nokihara, H., Fujiwara, Y., Takahashi, T., Murakami, H., Boku, N., Yamazaki, K., *et al.* (2009). Phase I, dose escalation and pharmacokinetic study of cediranib (RECENTIN), a highly potent and selective VEGFR signaling inhibitor, in Japanese patients with advanced solid tumors. Cancer Chemother Pharmacol *64*, 1165-1172.

Yamazaki, M., Nakamura, K., Mizukami, Y., Ii, M., Sasajima, J., Sugiyama, Y., Nishikawa, T., Nakano, Y., Yanagawa, N., Sato, K., *et al.* (2008). Sonic hedgehog

derived from human pancreatic cancer cells augments angiogenic function of endothelial progenitor cells. Cancer Sci *99*, 1131-1138.

Yan, L., Hsu, K., and Beckman, R.A. (2008). Antibody-based therapy for solid tumors. Cancer J *14*, 178-183.

Yang, S.X., Steinberg, S.M., Nguyen, D., Wu, T.D., Modrusan, Z., and Swain, S.M. (2008). Gene expression profile and angiogenic marker correlates with response to neoadjuvant bevacizumab followed by bevacizumab plus chemotherapy in breast cancer. Clin Cancer Res *14*, 5893-5899.

Yang, W., Ahn, H., Hinrichs, M., Torry, R.J., and Torry, D.S. (2003). Evidence of a novel isoform of placenta growth factor (PlGF-4) expressed in human trophoblast and endothelial cells. J Reprod Immunol *60*, 53-60.

Ye, X., Li, Y., Stawicki, S., Couto, S., Eastham-Anderson, J., Kallop, D., Weimer, R., Wu, Y., and Pei, L. (2010). An anti-Axl monoclonal antibody attenuates xenograft tumor growth and enhances the effect of multiple anticancer therapies. Oncogene *29*, 5254-5264.

Youlden, D.R., Cramb, S.M., and Baade, P.D. (2008). The International Epidemiology of Lung Cancer: geographical distribution and secular trends. J Thorac Oncol *3*, 819-831.

Yuan, L., Moyon, D., Pardanaud, L., Breant, C., Karkkainen, M.J., Alitalo, K., and Eichmann, A. (2002). Abnormal lymphatic vessel development in neuropilin 2 mutant mice. Development *129*, 4797-4806.

Zhang, L., Yu, D., Hicklin, D.J., Hannay, J.A., Ellis, L.M., and Pollock, R.E. (2002a). Combined anti-fetal liver kinase 1 monoclonal antibody and continuous low-dose doxorubicin inhibits angiogenesis and growth of human soft tissue sarcoma xenografts by induction of endothelial cell apoptosis. Cancer Res *62*, 2034-2042.

Zhang, S., Zhang, D., and Sun, B. (2007). Vasculogenic mimicry: current status and future prospects. Cancer Lett *254*, 157-164.

Zhang, W., Ran, S., Sambade, M., Huang, X., and Thorpe, P.E. (2002b). A monoclonal antibody that blocks VEGF binding to VEGFR2 (KDR/Flk-1) inhibits vascular expression of Flk-1 and tumor growth in an orthotopic human breast cancer model. Angiogenesis *5*, 35-44.

Zhu, Z., Hattori, K., Zhang, H., Jimenez, X., Ludwig, D.L., Dias, S., Kussie, P., Koo, H., Kim, H.J., Lu, D., *et al.* (2003). Inhibition of human leukemia in an animal model with human antibodies directed against vascular endothelial growth factor receptor 2. Correlation between antibody affinity and biological activity. Leukemia *17*, 604-611.

Zhu, Z., Rockwell, P., Lu, D., Kotanides, H., Pytowski, B., Hicklin, D.J., Bohlen, P., and Witte, L. (1998). Inhibition of vascular endothelial growth factor-induced receptor activation with anti-kinase insert domain-containing receptor single-chain antibodies from a phage display library. Cancer Res *58*, 3209-3214.

Zhu, Z., and Witte, L. (1999). Inhibition of tumor growth and metastasis by targeting tumor-associated angiogenesis with antagonists to the receptors of vascular endothelial growth factor. Invest New Drugs *17*, 195-212.